

Manufacture and Use of Solid Petroleum Pitch

Harold Beuther
Richard G. Goldthwait

Gulf Research & Development Company
Pittsburgh, Pennsylvania

INTRODUCTION

For many years there has been a continuing effort in the petroleum industry to increase the amount of distillate products obtained from crude oil. This effort has been motivated by the higher value of distillate oils and the poor economics of adding these higher value distillate oils to viscous residues to make them marketable as fuels. During the past decade some progress has been made on this problem. The residues from certain crudes can be processed effectively by thermal visbreaking to increase substantially the yields of distillate oils. The residues from any crude can be processed either by coking to make largely distillate oils and coke or by hydrodesulfurization to remove sulfur as well as to convert any required amount of the asphalt. In addition, many refiners today gain distillate yield by burning viscous residual oils as refinery fuel to avoid the blending-off of lighter oils required in the marketing of No. 6 Fuel Oil. The production and burning of solid petroleum pitch goes one step further than the use of a viscous residue. By concentrating further the heavy residual oils that the refiner now burns, additional distillate oil is removed and the asphaltic portion is converted to a hard, brittle solid which can be handled and burned as a solid fuel. There are several potential advantages in going to this added degree of reduction of petroleum residues. (1) A solid fuel can be stored and transported more easily than viscous fuel which requires heating to keep it pumpable when the fuel use is beyond the immediate refinery area. (2) The reduced yield of residual fuel when making a solid pitch results in a higher yield of more valuable distillate oil. While this distillate oil is "dirty" by normal standards for distillate stocks, improved refining techniques in modifications to catalytic cracking and in hydrocracking will now readily accept such oils as charge stocks. (3) The processing required to produce a solid petroleum pitch is more simple and less costly than is required for either coking or hydrodesulfurization.

DESCRIPTION OF SOLID PETROLEUM PITCH

Solid petroleum pitch is an asphalt concentrate from crude oil where enough oil has been removed from the asphalt to produce a high melting point, coal-like solid. This material is brittle and easily pulverized; it can be stored outside without fusing or agglomerating and makes an excellent solid fuel having considerable less ash and more BTU'S per pound than coal. Table I gives a brief summary of the physical properties of petroleum pitch compared to bituminous coal, a coal tar pitch and petroleum coke. Although not shown in this table, petroleum pitch is more similar to certain natural occurring bitumens, such as gilsonite than it is to coke, coal or coal tar pitch. Petroleum pitch differs from coal and petroleum coke in that it has a melting or softening point. This softening point is high enough, however, (about 350°F.) to allow pitch to be stored in 40-foot piles at 170°F. without the agglomeration of particles.

Needless to say, the advantage for producing a solid petroleum pitch from a crude oil will vary widely and will be most advantageous to those refiners having high asphalt-content crudes and in a depressed marketing area for residual fuel oils. In looking to the future, the need for such a process is expected to increase when our fuel economy must rely more heavily on low-gravity crudes, tar sands, and low grade hydrocarbon deposits.

Table I

PROPERTIES OF VARIOUS CARBONACEOUS SOLIDS

	<u>Petroleum Pitch</u>	<u>Typical Bituminous Coal</u>	<u>Coal Tar Pitch</u>	<u>Petroleum Coke (Delayed)</u>
Specific Gravity	1.05-1.15	-	1.20-1.30	1.28-1.42
Softening Point: °F.	300-400	-	110-320	none
Solubility in Benzene: %	75-99	-	45-75	-
Volatile Matter: %	50-70	34	40-50	8-17
Heating Matter: BTU/Lb.	16,500-17,600	14,400	-	14,600-16,000

MANUFACTURE OF SOLID PETROLEUM PITCH

It can be seen from the volatile content in Table I that petroleum pitch is a concentrate of the asphaltic material in crude. By removing or eliminating oil which is included with normal vacuum reduced crudes, a pitch can be produced whose asphaltene concentration is sufficiently high to impart hardness properties, which permit satisfactory handling, storing, grinding and burning as a solid fuel. For certain crudes which have very hard asphalts, it is possible to produce solid petroleum pitch by simply increasing the severity of normal refinery vacuum distillation¹ by 50° to 100°F. (corrected to 760 mm. Hg). Certain Mississippi and Venezuelan Crudes are of this type. Such crudes are generally low in API gravity and sufficiently high in viscosity to meet the No. 6 Fuel Oil specification upon removal of a few per cent of gasoline. Baxterville Crude, for instance, can be distilled to produce 5% gasoline with the remaining 95% being a heavy fuel oil. By a combination of atmospheric and vacuum distillations (the latter carried out at 1070°F. corrected to 760 mm. Hg), there is obtained from this crude 5% of gasoline, 24% of furnace oil, 46% of fair-quality catalytic cracking charge stock, and 26% of a 360°F. softening point pitch. A simplified flow diagram for one of several possible methods for carrying out this operation is given in Figure 1. By varying the severity of distillation, pitches of varying softening point can be obtained; however, higher softening point pitches are more difficult and costly to produce and the resulting gas oils are of higher carbon residues and metal contents. As will be discussed later, it is believed that pitches of 350°F. minimum softening point can be handled and burned in most burners designed for either coal or heavy fuel oil with but minor modifications, and it is entirely possible that lower softening point (275°-325°F.) pitches can be handled and burned in specially-designed equipment. Yields and inspection data for pitch and catalytic cracking charge stock produced at three severities of vacuum reduction from Baxterville Crude are given in Table II.

The use of vacuum distillation to produce pitch is limited to crudes containing asphalts of very low oil content (hard asphalts). For other crudes it is necessary to remove a portion of the oil from the asphalt by cracking. Thermal visbreaking of

Table II

YIELDS AND INSPECTIONS OF PITCHES AND CATALYTIC CRACKING STOCKS
FROM SEVERAL SEVERITIES OF VACUUM REDUCING BAXTERVILLE CRUDE

	Mild Vacuum Reduction	Moderately Severe Vacuum Reduction ^a	Severe Vacuum Reduction
Pitch			
Yield: % by Vol. of Crude	33.5	25.7	17.9
Ring and Ball Softening Point: °F.	275	360	441
Catalytic Cracking Charge Stock			
Yield: % by Vol. of Crude	37.7	45.5	53.8
Carbon Residue, Conradson: %	0.64	1.58	3.32
Vanadium: PPM	0.13	0.70	3.40
Flash Temperature, ^b Corrected to 760 Mm. Hg: °F.	969	1068	1201

^a Recommended reduction to produce a solid fuel.

^b When charging a gasoline-free Baxterville Crude to vacuum tower.

the normal vacuum residue from many crudes concentrates the asphaltenes by "cracking out" the oil so it can readily be removed by atmospheric distillation.² Here again, when producing pitch by visbreaking, the asphalt charge to the visbreaker must be relatively hard, preferably above 160°F. softening point; otherwise a very severe visbreaking operation is necessary or the subsequent distillation must be carried out under vacuum. A typical operation to produce pitch from a 12.5% reduced Eastern Venezuela Crude (165°F. softening point) requires single-pass visbreaking at furnace conditions of 915°F. outlet temperature and 200 psig. pressure. Operating conditions in this range are practical for heavy vacuum reduced crudes³ as evidenced by several visbreaking operations for conventional purposes now carried out in Gulf's refineries. By visbreaking a 5.2 °API vacuum reduced Eastern Venezuela Crude and distilling the visbreaker residue, the following yields of products are obtained: 13.3% gasoline and naphtha, 13.3% furnace oil, 15.6% catalytic cracking charge stock, 12.2% fuel oil, and 45.3% pitch. The inspections of the distillate products are similar to products obtained from delayed coking and are given in Table III. The process flow, which is shown diagrammatically in Figure 2, is typical of thermal visbreaking except for the handling of the visbreaking effluent. The visbreaker effluent is distilled at atmospheric pressure in the presence of 5 to 40 pounds of steam per barrel of charge to obtain an approximately 350°F. softening point pitch and a cracking stock, as well as lighter distillates. A more severe visbreaking operation would reduce the steam requirements.

Most Venezuelan Crudes and domestic crudes containing hard asphalts such as East Texas, California, etc., are very readily processed by visbreaking to produce solid pitch. Crudes with softer asphalts require more severe visbreaking and distillations conditions than those given above for the Eastern Venezuela residue, and high softening petroleum pitches have been prepared from Kuwait, West Texas, and Mid Continent Crudes. •⁵

Table III

PRODUCTION OF PITCH BY THERMAL VISBREAKING
FOLLOWED BY ATMOSPHERIC REDUCTION
OF REDUCED EASTERN VENEZUELAN CRUDE

300° F. End Point Gasoline (10 RVP)	
Yields: % by Vol.	8.0
Sulfur: %	0.61
Research Octane No., +3 Cc. TEL	85.6
300°-400° F. Naphtha	
Yield: % by Vol.	5.3
Furnace Oil Fraction	
Yield: % by Vol.	13.3
Sulfur: %	1.83
Gravity: °API	31.2
Characterization Factor	11.34
Catalytic Charge Stock	
Yield: % by Vol.	15.6
Sulfur: %	2.02
Characterization Factor	11.62
Carbon Residue	0.8
Heavy Gas Oil	
Yield: % by Vol.	12.2
Carbon Residue, Conradson: %	13.9
Pitch	
Yield: % by Vol.	45.3
Softening Point: °F.	364

In the manufacture of pitch, it is necessary to provide a means of cooling and solidifying the pitch after removal from the atmospheric or vacuum distillation column. The most practical means for most locations is through the use of a continuous moving stainless steel belt. The hot pitch from the distillation column is poured continuously onto the belt, which is cooled from beneath by water and may be cooled with auxiliary water sprays on top. Pitch produced by this manner consists of flakes about one-quarter inch thick which break at random into pieces one to six inches across. The pitch readily separates from the stainless steel belt upon cooling because of its different coefficient of expansion. A photograph of pitch produced in this manner is shown in Figure 3. Such material is quite brittle and breaks readily upon handling. With handling there is produced only a very small amount of fines which are not troublesome. There are other methods which may be more desirable in certain locations for cooling and solidifying the hot liquid pitch. These include the use of large cooling pits into which the pitch is pumped as a hot liquid and allowed to cool slowly in the atmosphere in a large mass. When solid, the pitch is then broken up and moved with power shovels. Hot liquid pitch also may be solidified by spraying into water or steam, or it may be solidified on a water-cooled rotary drum. From our experience, however, the simplest and most convenient method is that of the continuous moving belt.

USES OF PETROLEUM PITCH

Because of the large quantities of crudes and residues processed in the petroleum industry, any scheme for producing solid petroleum pitch which would be effective in improving the ratio of distillate to residual oils would produce so much pitch that a fuel market must be considered as its primary use. Thus, it was on the basis of a fuel market that economics and process developments were carried out. Even a small unit charging 5000 barrels per day of Eastern Venezuela residue would produce 430 tons per day of pitch. In considering the use of petroleum pitch as a fuel it was necessary to determine the minimum softening point that would allow transportation, storage and grinding in hot weather without the pitch becoming tacky or plastic and possibly fusing. It was found that these properties of pitch depended on the crude source and method of production. For a typical pitch from Eastern Venezuela Crude, it was found that a 350°F. ring and ball softening point was sufficiently high to prevent fusion at temperatures and pressures which would be encountered under almost any circumstance. Figure 4 presents a plot of incipient fusion temperature of Eastern Venezuela pitch as a function of pitch softening point when under a pressure equivalent to 40 feet of pitch. This incipient fusion temperature is the temperature at which particles first adhere to one another but readily break apart with slight handling. From this plot it can be seen that a 350°F. softening point pitch only begins to fuse at 170°F. at these conditions. It is not until temperatures of about 15°F. higher that fusion becomes serious and permanent. Thus, an Eastern Venezuelan pitch of 350°F. softening point can be stored in piles 40 feet high at 170°F. before any evidence of particle adherence occurs. Obviously, lower softening point pitches would be satisfactory in locations with lower ambient temperatures. The burning characteristics of 350°F. softening point pitch have been evaluated in a two-foot diameter Babcock and Wilcox experimental cyclone furnace.⁶

Several modifications were made to the normal operation of the cyclone furnace.

1. Cold air was used in pulverizing and charging the pitch so it would not melt before entering the furnace.
2. An ash with a suitable fusion temperature was added to the pitch to form a fluid slag coating on the walls of the cyclone.

The ash which was added was from the burning of coal and the quantity, 5%, was chosen arbitrarily. This quantity could have undoubtedly been reduced or the slag could have been recycled if no such material were continuously available. The burning characteristics of the pitch were excellent in every respect. The flame was stable and clean, the appearance of the stack was excellent, and the oxygen content of the flue gas was 2% indicating about 10% excess air. There were no problems with ignition, dust carryover, or flame propagation. There was no build up of slag in the combustion chamber, and the burner itself was clean with no build up of pitch. The carbon loss to the stack was below that obtained with coal firing, which is in the range of one pound per 1000 pounds of flue gas. During the test, no particular effort was made to control the grinding of the pitch or the size of the slag particles. The pitch was ground in a hammermill and found to crush more readily than coal. About twice the percentage passing through a 200-mesh screen was obtained from pitch than from coal using the same crushing equipment. Based on the observations of these test runs, the furnace equipment manufacturer believes that petroleum pitch is a suitable fuel for a cyclone furnace and that it can be fired without difficulty, provided the minor modification to the furnace mentioned previously are made. In comparison with bituminous coal, petroleum pitch has a number of distinct advantages for use as a boiler fuel. It is much easier to pulverize, requiring lower power and maintenance costs; it requires a reduced capital cost by eliminating the requirements for fly-ash removal equipment; and it has excellent ignition and burning properties and a high BTU content.

There are many other interesting and potential uses for petroleum pitch other than that of fuel. A summary in Table IV gives properties of several pitches. Petroleum pitch as was mentioned earlier is somewhat similar to certain natural bitumens occurring in the western part of the United States. Petroleum pitch is potentially cheaper and undoubtedly could be used for many of the applications now requiring the naturally occurring bitumens. Petroleum pitch can be used satisfactorily as a binder for carbonaceous materials, although for this purpose it is not quite as good as coal tar pitch because of its higher volatile content. Another use for pitch is in beneficiation of non-coking coals when added in amounts of 10% to 20%. Various pitches have also been tested for many other lower volume uses.

PROPERTIES OF DISTILLATE PRODUCTS FROM PITCH MANUFACTURE

The economic advantage to the petroleum industry in making pitch is that of obtaining additional yields of gasoline, furnace oil, and catalytic cracking charge stock and decreased yields of No. 6 Fuel Oil.

When producing pitch by vacuum distillation, all distillate oils are straight run stocks and require further treatment only when the crude is high in nitrogen or sulfur content or when the heavy gas oil contains more metals or a higher carbon residue than is desired for catalytic cracking. Data from Baxterville Crude indicate that the entire gas oil fraction from producing a 360°F. softening point pitch is satisfactory as a catalytic cracking stock but that the furnace oil requires desulfurization to meet present day sulfur specifications.

When producing pitch by visbreaking followed by distillation, the resulting gasoline and furnace oil fractions require further treatment because of their poor stability, high sulfur content, and the low octane number of the gasoline. A large portion of the gas oil fraction can be catalytically cracked without a pretreatment, but treating the entire gas oil fraction with hydrogen greatly increases the amount of oil available for catalytic cracking. Inspections of distillate fractions from several crudes when making pitch by visbreaking followed by distillation are given in Table V. Many of these distillate fractions have been catalytically treated with hydrogen in the laboratory and all have shown considerable improvement. For example, a pretreated naphtha had a naphthene content slightly higher than that of straight run Kuwait naphtha and was shown to be a better reformer charge stock. The furnace oil fractions were easily treated with hydrogen to produce premium No. 2 Fuel Oils. The heavy gas oils, either treated or untreated, were found to be not quite as good as straight run oils for use as cracking stocks. A comparison of the the inspections and cracking characteristics of these stocks is given in Table VI.

ECONOMICS

The economics of producing solid petroleum pitch can vary widely depending upon the crude source, the refinery location and the availability of idle thermal cracking equipment. Illustrative economic studies showed a payout time after income tax of 5.6 years for making pitch from Baxterville Crude by vacuum distillation when assuming a value of \$8 per ton for pitch. This value for pitch is conservative since on a BTU basis one ton of petroleum pitch (17,000 BTU per pound) is equivalent to about one and one-third tons of bituminous coal (14,000 BTU per pound). A payout time of 3.4 years was obtained for making pitch by visbreaking a vacuum reduced Eastern Venezuela Crude and then distilling the visbreaker residue. If idle thermal cracking equipment were available, this payout time would be even lower. This latter payout is quite attractive, but in each case both economics and an adequate and permanent market must be developed.

Table IV

PHYSICAL PROPERTIES OF PITCHES

Crude Source	Yield: % by Vol. of Crude	Baxterville	Eastern Venezuela	Kuwait
Inspection:	33.5	25.7	3.9	4.3
Gravity, Solid State	1.103	1.099	1.124	1.196
Sp. Gr., 77°/77°F.	275	360	426	415
Ring and Ball	23	4	1	---
Softening Point: °F.	---	0.07	---	1.46
Penetration, ASTM D 5-49	36.5	43.5	53.7	63.2
210°F., 100 G., 5 Sec.	65.5	60.8	51.8	41.0
Sediment: %	34.5	39.1	47.7	58.9
ASTM D 473-48	0.0	0.1	0.5	0.1
Carbon Residue, Conradson: %	0.3	0.4	1.3	0.7
Proximate Analysis, Dry Basis: %	4.8	5.0	3.2	7.6
Volatile Carbon	8.6	8.8	8.6	6.6
Fixed Carbon	84.8	85.8	86.0	84.1
Ash	1.5	0.0	0.3	1.0
Analysis, Ultimate: % by Wt.	---	0.08	0.52	0.14
Nitrogen	0.13	0.08	0.11	---
Sulfur	17.400	17.170	17.170	16.400
Hydrogen	114.6	111.0	84.0	348.0
Carbon	53.2	64.2	212.0	99.5
Undetermined	1.7	2.6	---	---
Ash as Oxide: %	45.0	56.0	51.0	224.0
Insoluble in Trichloroethylene: % by Wt.	---	---	---	---
Heating Value, BTU/lb.	---	---	---	---
Metals: PPM	---	---	---	---
Vanadium	---	---	---	---
Nickel	---	---	---	---
Copper	---	---	---	---
Iron	---	---	---	---

Table V

DISTILLATE OILS FROM VISBREAKING TO MAKE PITCH

<u>Reduced Crude Charge</u>	<u>Baxterville</u>	<u>Western Venezuela</u>	<u>Eastern Venezuela</u>	<u>Kuwait</u>
<u>Charge Stock</u>				
% of Crude	33.3	46.4	11.5	14.4
Softening Point: °F.	280	162	180	165
Carbon Residue: %	34.9	25.1	26.5	27.7
<u>300°F. E.P. Gasoline</u>				
Yield, % by Vol.	1.9	10.1	8.8	11.2
Gravity: °API	58.4	63.2	63.5	64.3
Sulfur, L: %	0.88	0.84	0.72	0.93
Research Method: Octane No.				
Clear	68.0	79.0	77.9	73.0
+3 Cc. TEL	76.2	87.2	85.6	80.3
<u>Naphtha</u>				
Yield, % by Vol.	2.4	6.7	5.3	6.5
Gravity: °API	44.8	44.1	44.8	44.7
Sulfur, L: %	1.17	1.34	—	1.30
Research Method: Octane No.				
Clear	49.2	60.8	55.7	51.8
+3 Cc. TEL	57.2	70.2	65.8	60.6
Characterization Factor	11.70	11.60	11.67	11.66
<u>Furnace Oil</u>				
Yield, % by Vol.	5.5	14.7	13.3	14.5
Gravity: °API	30.5	29.6	31.2	27.9
Sulfur, Braun-Shell: %	2.57	2.34	1.83	3.47
Aniline Point: °F.	129	118	129	114
Characterization Factor	11.50	11.39	11.52	11.25
<u>Cracking Stock</u>				
Yield, % by Vol.				
670°F. IBP Gas Oil	7.1	19.3	18.1	14.9
Gravity: °API	19.1	15.5	19.0	13.0
Sulfur, Braun-Shell: %	3.36	2.94	2.11	5.20
Sediment: %				
ASTM D 473-48	0.02	<0.01	<0.01	0.01
Carbon Residue, Conradson: %	0.7	1.03	1.12	1.04
Ash, Humber: %	0.0004	0.0002	0.0057	0.0004
Metals: PPM				
Vanadium	0.02	0.08	0.03	0.03
Nickel	0.08	0.05	0.07	0.05
Characterization Factor	11.53	11.33	11.55	11.05
<u>Heavy Gas Oil</u>				
Yield, % by Vol.	2.9	9.3	9.7	12.7
Gravity: °API	10.0	7.1	8.5	1.0
Sulfur, Braun-Shell: %	3.61	2.96	2.34	6.12
Carbon Residue, Conradson: %	14.1	13.4	16.5	16.6
Characterization Factor	11.30	11.18	11.30	10.66

Table VI

CATALYTIC CRACKING CHARACTERISTICS OF
VIRGIN, CATALYTIC AND VISBREAKER GAS OILS

	<u>Virgin Kuwait Gas Oil</u>	<u>Kuwait Heavy Catalytic Gas Oil</u>	<u>Gas Oil From Visbreaking to Make Pitch</u>
Charge Stock Properties			
Gravity: °API	22.2	17.7	18.1
Sulfur: %	3.06	3.36	4.14
Carbon Residue: %	0.73	0.11	1.45
Vanadium, PPM	0.56	—	0.34
Characterization Factor	11.76	11.10	11.46
Conversion: % by Volume	53.8	34.2	43.3
Yields: % by Volume			
Depropanized Gasoline	49.1	25.6	35.0
Light Catalytic Gas Oil	20.7	18.7	20.4
Heavy Catalytic Gas Oil	25.5	47.1	36.3
Goke	5.2	6.6	6.6
Gasoline: Coke Ratio	9.5	3.9	5.2

REFERENCES

1. H. Beuther, W. C. Offutt and P. Siecke, June 18, 1957, U. S. Patent 2,796,388.
2. H. Beuther and R. G. Goldthwait, U. S. Patent 2,850,436.
3. H. Beuther, R. G. Goldthwait, and W. C. Offutt, Oil and Gas Journal, Vol. 57, No. 46, pp. 151-157, November 9, 1959.
4. H. Beuther, W. C. Offutt, and P. Siecke, U. S. Patent 2,847,359.
5. R. G. Goldthwait and W. R. Lehrian, U. S. Patent 2,944,958.
6. Watts, G. A. and Sage, W. L. Mechanical Engineering, Vol. 78, pp. 823-827, September, 1956.

FIGURE 1
PRODUCTION OF PITCH BY VACUUM REDUCTION

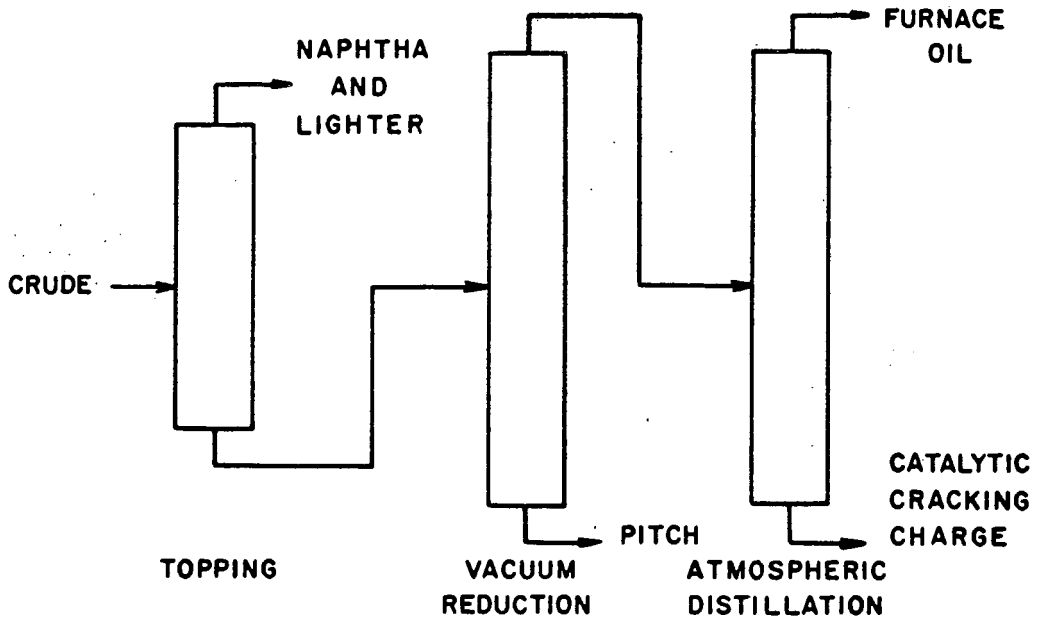


FIGURE 2
PRODUCTION OF PITCH BY VISBREAKING

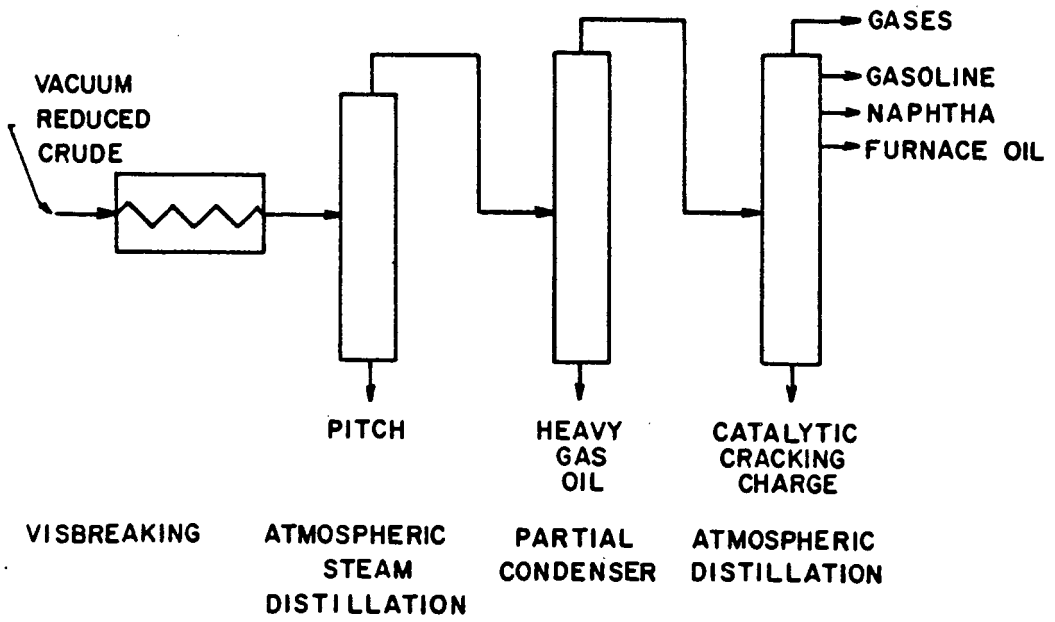
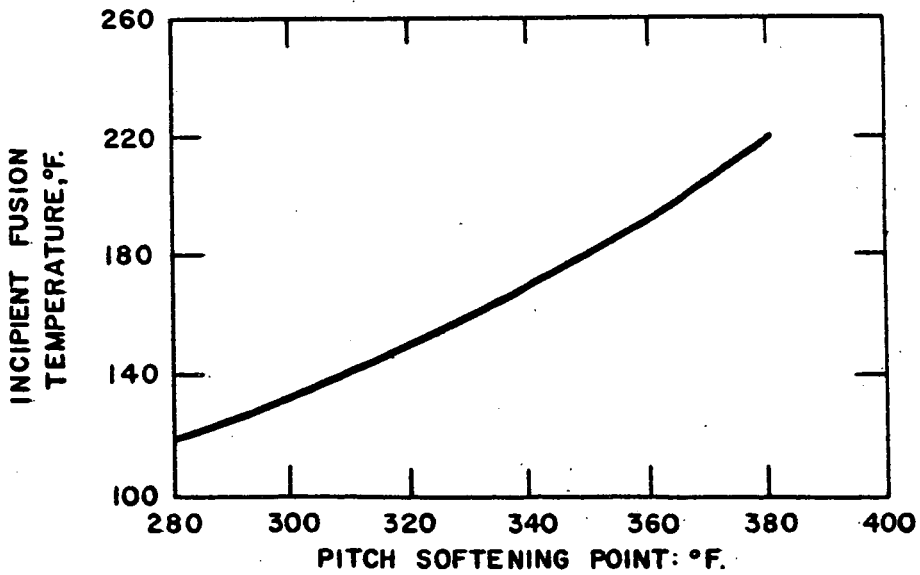




Figure 3
PETROLEUM PITCH PRODUCED BY COOLING ON A STAINLESS STEEL BELT

FIGURE 4
INCIPIENT FUSION POINT OF EASTERN VENEZUELA PITCH



STRUCTURE DETERMINATION OF RESINS FROM PITCH OF
LOW-TEMPERATURE TAR BY COMBINED PYROLYSIS
AND GAS-LIQUID CHROMATOGRAPHY

Clarence Karr, Jr., Joseph R. Comberiat, and Patricia A. Estep

U. S. Department of the Interior, Bureau of Mines,
Morgantown Coal Research Center, Morgantown, W. Va.

This report is the second by this laboratory on investigations of the composition of the resins from pitch in connection with the Federal Bureau of Mines' research on the nature of coal and its products. The first report concerned the structure determination of resins by ring analysis and spectral characterization¹. The present work involves structure determination of resins from pitch of low-temperature tar by combined pyrolysis and gas-liquid chromatography.

Pyrolysis or thermal degradation of complex substances is one of the oldest methods of structure determination. Gas-liquid chromatography makes it possible to isolate the pyrolysis products immediately upon formation so that they can be identified before they are lost or altered in secondary reactions. There are apparently no previous reports in the literature on structure determination of resins from pitch by pyrolysis. The characterization of low-temperature tar resins is important, however, because they are major components of the pitch, and, in the case of some bituminous tars, make up as much as half the weight of the total tar.

The conditions of pyrolysis were chosen to yield, insofar as possible, primary products that would give the maximum information about the structure of the resin. The products of greatest interest were those large enough (C_5 and greater) to yield meaningful clues to structure. The pyrolysis temperature was generally in the range 520° - $530^\circ C.$, or above the temperature at which no volatile pyrolysis products are observed, and the heating time was only a few seconds. In addition, because the sample was heated in the absence of air in a glass container, catalytic effects should have been quite low if not non-existent. Under these conditions the pyrolysis products could be considered to represent primary fragments from the resin molecule.

EXPERIMENTAL

Many pyrolysis experiments were made under a wide variety of conditions to gain some insight into the behavior of the various resins from several pitches. This report has been limited to the experimental procedures and results that are of greater interest.

Apparatus

The pyrolysis apparatus consisted of a small coil (diameter, 1/8-inch) made from a 25.5-inch length of 28-gauge nichrome wire suspended in a stainless-steel chamber connected directly to a gas-liquid chromatographic unit by a short length of 1/8-inch stainless-steel tubing, as shown in Figure 1. The chamber, the connecting tubing, and a longer preheating section of tubing were all electrically heated to approximately the same temperature, which was a few degrees below the GLC column temperature. Helium carrier gas was passed through the preheat section and the pyrolysis chamber into the column. A 30-second maximum electrical timing switch and powerstat were used to control the firing period and voltage for the pyrolysis coil. The maximum temperature obtained during firing was determined in calibration runs with a thermocouple; the helium flow and other conditions were the same as during the pyrolysis runs. This thermocouple was placed inside a glass tube, which in turn was inside the coil. The thermocouple leads passed through gas-tight fittings in the lid of the pyrolysis chamber. In addition, the maximum temperature of the coil surface itself was estimated by means of thin films of materials selected to melt at specified temperatures.

Two different columns were used in order to determine the pyrolysis products under different conditions. One column was constructed of 15 feet of 1/4-inch diameter aluminum tubing and packed with 25 weight-percent polyphenyl ether on 30 to 60 mesh firebrick. The other column consisted of a 20-foot length of 1/4-inch copper tubing filled with 75 g. packing made from 25 percent Apiezon L grease on 30 to 60 mesh firebrick. A column temperature of 220 °C. was used so that relatively high-boiling products, such as phenols and naphthalenes, would be readily detected, if present.

Gas-liquid chromatographic fractions were collected for infrared spectra. The higher boiling fractions were collected in 6-inch 18-gauge needles cooled in powdered dry ice. A U-trap of 1/4-inch aluminum tubing was required for the lower boiling fractions (below benzene) in order to have enough cooling surface to condense this material from its dilute mixture in the helium carrier gas. This U-trap could then be warmed, and the evolved gas readily condensed in a 6-inch needle. The needles were stoppered at both ends with Teflon plugs and kept in Dewar flasks filled with powdered dry ice until the infrared spectra could be obtained. To determine the spectra, each needle was given a single rinse with 15 μ l. carbon disulfide introduced into the hub end with a micro syringe. The solution was allowed to flow from the point of the needle into a 0.5 mm. ultramicrocavity cell, which was then stoppered and placed in a liquid cell holder. The cell holder in turn was placed in the 6X beam condenser in the spectrophotometer. The details of this cell holder have been described elsewhere².

Pyrolysis results

The results of the pyrolysis of the semi-solid, benzene-soluble, petroleum ether-insoluble resin from Nugget, Wyoming, subbituminous coal tar pitch may be cited as an example. The resin was pyrolyzed at about 528 °C. in a chamber preheated to 175 °C., using a sealed glass tube technique. This procedure consisted of placing about 25 mg. of the finely divided resin in a glass capillary tube that was then evacuated,

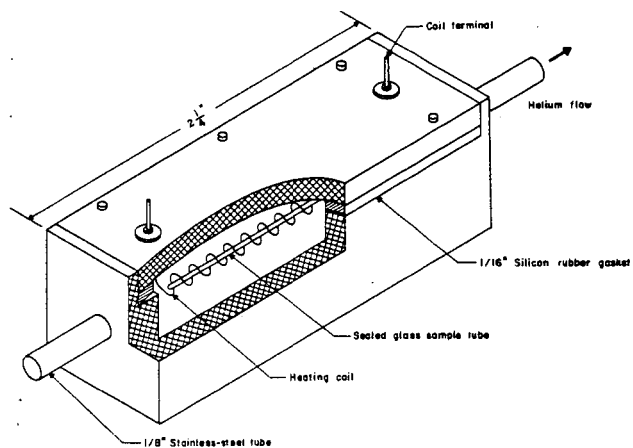


Figure 1. Pyrolysis apparatus for sealed glass tube technique.

sealed, and inserted in the coil. With this size sample and a setting of about 22.5 volts, the tube shattered at 8.4 seconds. The maximum temperature inside the glass tube after this length of time was determined from the calibration runs with a thermocouple. The volatile pyrolysis products were swept immediately and directly into the gas-liquid chromatographic column by the stream of helium. The pyrolysis residue appeared to consist of a mixture of char and an unknown amount of essentially unaltered resin.

Although the resin is subjected to a high pressure in the last few seconds before the tube shatters, this increased pressure has little apparent effect on the nature of the pyrolysis products as compared to heating a film of resin on the coil. This was shown by depositing a thin layer of the resin from solution on a coil and firing at various known maximum temperatures. At coil temperatures around 500°C., the low molecular weight resins (M, 400 to 500) simply evaporated from the coil and were deposited on the cooler walls of the pyrolysis chamber. A small peak was obtained on the chromatogram at the retention time for air, which had apparently been trapped in the semi-solid resin film. There were no other peaks, indicating that the resin had been distilled at about 500°C. without decomposition to lower boiling materials. [This suggests the possibility that at least some of the resins found in tars produced by low-temperature carbonization (500°C.) are essentially unaltered "coal molecules."] The medium molecular weight resins (M, 500 to 650) however, did not completely evaporate from the coil under these conditions, and at higher temperatures (around 530°C.), decomposition occurred. The chromatograms of these pyrolysis products were basically the same as those obtained with the sealed tube technique. The main difference between the two methods was the sharper, better resolved peaks with the sealed tube method. Pyrolysis of resins in evacuated sealed glass tubes thus had five distinct advantages: (1) no sample was lost from the pyrolysis zone by evaporation; (2) the resin was not heated on a metal surface so possible catalytic effects were avoided; (3) the pyrolysis products were swept into the gas chromatographic column during an exceedingly brief interval when the tube shattered; the resulting chromatogram had sharper and better resolved peaks; (4) the tube shattered so violently and into such small pieces that no sample remained in the pyrolysis zone; and (5) the little "spike" produced on the recording by this pressure surge was an accurate indication of zero time.

A typical chromatogram obtained with the subbituminous resin using the sealed tube technique and the Apiezon L column is shown in Figure 2. A recording with the methane peak 1 off-scale was chosen so that the minor component peak 12 would be evident. (All peaks were recorded at the same attenuation.) On other chromatograms, it was clear that peaks 4 and 5 were separate. The relative retentions of the pyrolysis products producing these peaks are compared with the relative retentions of pure compounds in Table 1. The wavelengths of some of the observed infrared absorption bands of the trapped fractions corresponding to peaks 7 through 14 are also shown in Table 1, as well as the quantities of pyrolysis products determined from corrected peak areas and spectra of trapped fractions. The identities of the pyrolysis products with relative retentions less than that for n-pentane were not considered pertinent to the present work. Nevertheless, evidence was obtained showing that peaks 1 through 4 are undoubtedly produced by the C₁ through C₄ hydrocarbons, all of which are gases. Several attempts were made to obtain evidence for pyrolysis

Table 1. Relative retentions and infrared-absorption bands of pyrolysis products

Compound	Relative retention ^a		GLC peak no.	Some observed I. R. bands, wavelength, μ	Weight percent ^b
	Pure	Pyrolysis product			
Methane	0.37	0.37	1		
		0.43	2		
		0.49	3		
		0.57	4		
1-Pentene ^c	0.60	0.59	5		9.7
2-Methyl-1-pentene ^c	0.70	0.71	6		2.7
2,2,4-Trimethylpentane	0.93	0.93	7	7.33, 7.81, 8.03, 8.32, 8.57, 10.21	24.7
Benzene	1.00	1.00	8	2.44, 3.20, 3.25, 5.12, 5.52, 9.65, 14.85	19.3
2,3,4-Trimethylpentane	1.15	1.15	9	7.25, 7.32, 8.93, 9.30, 10.07, 10.32, 10.92	26.9
2,2,4,4-Tetramethylpentane	1.23	1.23	10	8.03, 8.54, 10.28	7.0
Toluene	1.37	1.37	11	9.28, 9.71, 13.74, 14.43	3.5
2,6-Dimethyl-1,4-heptadiene ^c	1.53 ^e	1.55	12		0.5
p-Xylene)	1.92	1.93	13	8.95, 12.60 (para)	0.9
m-Xylene)				8.57, 9.13, 13.02, 14.53 (meta)	2.1
o-Xylene	2.14	2.15	14	7.22, 8.96, 9.53, 9.81, 13.46	2.7
					<u>100.0</u>

a Relative to benzene on Apiezon L grease at 220°C.

b On the basis of the total liquid pyrolysis products.

c This compound is typical of several equally likely possibilities.

d See text for discussion of olefin bands.

e Retention obtained from log retention-boiling point correlations.

products with retention times greater than that for o-xylene. However, even with the largest sample size of resin, the highest sensitivity setting of the GLC apparatus, and a more sensitive flame detector instead of a thermal conductivity detector, the recording beyond the o-xylene peak remained a straight line, including the region for higher boiling compounds such as phenol and naphthalene. Under the same conditions it was known that very small quantities of these compounds could be detected.

In addition to the infrared absorption bands listed in Table 1, there were several bands, characteristic of different types of olefins, which were readily observed. These were bands at 10.14μ and 11.06μ due to α -olefins, a band at 11.30μ due to branched (2-position) α -olefins, a band at 14.44μ due to cis-olefins, a band at 10.38μ due to trans-olefins, and a band at 12.32μ possibly due to branched internal olefins. The band at 6.1μ due to the C=C stretching vibration in olefins was detected, this being a weak band as is observed for non-conjugated compounds. No individual olefin compound could be identified with certainty. It appeared likely, however, that most of these olefins had the same highly branched carbon skeleton as the saturated hydrocarbons. This condition was verified by the complete absence of the band at 13.80μ due to the $-(CH_2)_4-$ group or larger. Conversely, the 8.57μ band for the "isopropyl" grouping of carbon atoms was frequently observed to be a major band. Bands at 7.23μ and 7.30μ also indicated the presence of the $(CH_3)_2CH-$ group.

DISCUSSION

From the large number of pyrolysis experiments that were made, it appeared from the repeated evidence of characterizing infrared absorption bands and the excellent agreement with relative retentions, that the 3 major liquid pyrolysis products of the subbituminous resin were 2,3,4-trimethylpentane, 2,2,4-trimethylpentane, and benzene, in that order of decreasing quantity. The large quantity of highly branched, relatively high carbon number (C_8) saturated hydrocarbons was of unusual interest.

As previously mentioned, it appeared reasonable to assume that, under the conditions adhered to in this work, these pyrolysis products represented primary fragments from the resin molecule. It was recognized that the actual fragments were very likely free radicals at the instant of formation, that is, that a free radical mechanism was involved in the thermal degradation around $500^\circ C$. It appears almost certain that the benzene rings found in the pyrolysis products existed as such in the resin molecule. These monocyclic aromatics (benzene, toluene, the 3 xylenes) are present in the same quantities at the threshold temperature for pyrolysis (slightly over $500^\circ C$.) as at much higher temperatures (up to about $650^\circ C$.). Non-catalytic aromatization is generally considered to become significant only for temperatures at or above about $650^\circ C$. In the absence of specific catalysts, the rate of formation of aromatics from non-aromatics at about $500^\circ C$. is presumably too slow to account for their production during the 2 or 3 seconds that the resin is heated above 300 or $400^\circ C$. DHONT has pyrolyzed a wide variety of pure compounds over "Chromosorb" at $550^\circ C$., the products being immediately analyzed by gas-liquid chromatography³. Compounds containing a benzene ring (such as benzyl alcohol) yielded benzene as a pyrolysis product. Aliphatic compounds yielded no benzene under these conditions.

From the pyrolysis results, it would appear that the resin molecule contains isolated benzene rings joined together by saturated, fused multi-ring systems with saturated bridge carbons, including quaternary carbons. From previous work on the resins as well as the non-resinous portions of the tar, it is known that the great majority of alkyl groups on aromatic rings are methyl groups, with very small amounts of ethyl and propyl groups, and negligible amounts of butyl groups. Thus alkyl groups could contribute products only to the permanent gases, in particular methane. The aliphatic compounds above C_4 in the pyrolysis products must therefore come from internal structures, that is, ring structures, rather than side chains.

A resin molecule containing as part of its structure a unit like 5,6,6a,7,8,12b-hexahydro-6,7-dimethylbenzo[c]phenanthrene could conceivably split up (with, of course, transfer of hydrogen from other structural units) to form 2,3,4-trimethylpentane, as shown in Figure 3. Only those methyl groups required for the formation of 2,3,4-trimethylpentane are shown; additional methyl groups would be present, as determined in previous work¹. One of the benzene rings in this unit could be released as such, or both benzene rings could be incorporated in the formation of the pyrolysis residue or char. The fact that the resins are rich in oxygen (10 to 15 weight-percent) whereas no oxygen-containing organic compounds could be identified in the volatile pyrolysis products would indicate that the oxygen-containing units in the resin (primarily benzene rings with phenolic hydroxyl groups) are involved in char formation. Under these circumstances, there would be a greater proportion of aliphatic compounds than aromatic compounds in the volatile products, such as was actually observed.

Although the pyrolysis results might appear unusual or unexpected, nevertheless the general structure of the resins indicated by these results is the same as that indicated by ring analysis (including ring arrangement), infrared spectra, and ultraviolet spectra¹.

REFERENCES

- 1 KARR, C., JR., COMBERIATI, J. R., and ESTEP, P. A. Fuel, Lond. 1962, 41, 167.
- 2 ESTEP, P. A., and KARR, C., JR. Applied Spectroscopy (accepted for publication).
- 3 DHONT, J. H. Nature 1961, 192, 747.

(Grateful acknowledgment is made to W. C. Warner for obtaining many of the infrared spectra in this work.)

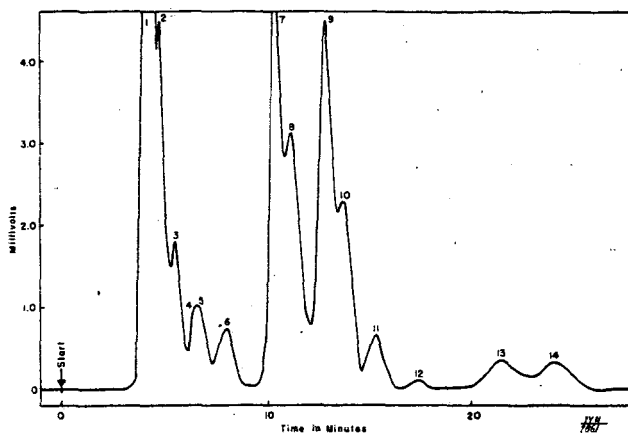


Figure 2. Chromatogram of pyrolysis products from a subbituminous resin.

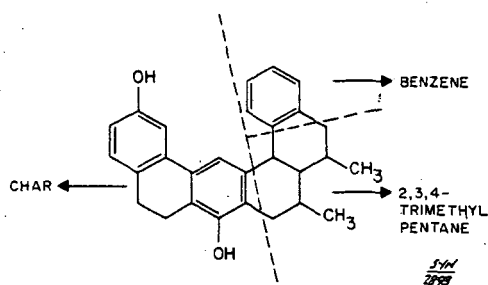


Figure 3. A representation of the pyrolysis of a hypothetical resin molecule.

THE STRUCTURE OF PETROLEUM ASPHALTENES
AS INDICATED BY PROTON MAGNETIC RESONANCE

By R. S. Winniford and M. Bersohn
California Research Corporation, Richmond, California

Introduction

Proton magnetic resonance has been used in the past to provide information on the structure of asphalt fractions. In a paper by R. B. Williams,¹ the proton magnetic resonance data are combined with infrared data to yield information suggesting the size of the clusters of aromatic rings in a number of asphalt fractions, including asphaltenes. Gardner, Hardman, Jones, and Williams² used proton magnetic resonance to provide information on the structure of thermal diffusion fractions of petroleues from an asphalt.

In the present study, the proton magnetic resonance data have been combined with other analytical data and contributions from the literature to yield information about the structures of four asphaltenes. The four asphaltenes include two asphaltenes from asphalt crude oils, an asphaltene produced by air blowing, and another produced through a cracking process.

Proton Magnetic Resonance Data

Proton magnetic resonance spectra were obtained on a Varian Model A-60 NMR spectrometer at 14,090 gauss. The solvent used was carbon disulfide. Spectra used as a basis for quantitative analysis were taken with a sweep width of 1000 cycles per second, a sweep time of 250 seconds, an RF field of 0.08 milligauss, and a filter band width of one cycle per second.

Characteristic spectra for the four asphaltenes are given in Figures 1, 2, 3, and 4. The horizontal scale of the spectra, labeled PPM, shows the "chemical shift" downfield from a reference material, tetramethylsilane, at which the various proton types appear. The magnitude of the shift is expressed in parts per million of the reference field, 14,090 gauss.

The Varian A-60 spectrometer resolves the hydrogens into four classes. These classes are methylene, methyl, benzylic, and aromatic. Aromatic protons are seen at 6.5 to 8 ppm. Benzylic protons appear at 2 to 3 ppm. The methylenic hydrogens give the tall peak at 1.2 ppm, while the methyl protons produce the peak at 0.8 ppm on the shoulder of the methylene peak.

The amplitude of the peaks is governed by the concentration of the particular hydrogen type and also by the instrument settings. Thus, it has no absolute value and the spectra have a purely arbitrary vertical scale. For the purposes of this study, only the intensity of the various peaks relative to that of the methylene peak is required.

Encl.-Tables I and II
Figures 1 through 8
(RD 622541, RD 622542,
RE 622497, RE 622498,
RD 622499, and RE 622500)

The peaks obtained were compared by planimetry. The repeatability in the area measurement obtained this way was better than 1% in the case of the large peaks. For the smallest peaks, such as that due to the aromatic proton of the asphaltene from the air-blown California residuum, the repeatability was + 6% to 8%. The peak from the aromatic proton of the Venezuelan asphaltene was too small to measure. The error in repeatability of the spectra themselves was negligible.

Figure 1 shows the spectrum of an asphaltene from a Venezuelan crude oil which is widely used for asphalt manufacture. Figure 2 is the spectrum of an asphaltene from a crude oil of the San Joaquin Valley Area in California. This oil is also widely used for asphalt manufacture. The spectrum of Figure 3 is that of an asphaltene produced by laboratory air blowing at 475° F of the residuum from the California crude oil of Figure 2. In this process, about 85% of the total asphaltenes contained in the air-blown asphalt are formed in the air-blowing process. Figure 4 shows the spectrum of the benzene soluble, heptane insoluble asphaltenes produced in cracking the California residuum of Figure 2. This cracking was done by a refinery thermal cracking unit operating at a temperature of 900° F.

Analytical data on these asphaltenes are given in Table I. It is recognized that asphaltenes are heterogeneous substances and that these data, therefore, refer to the average composition. However, it is not possible to deviate very widely from these analytical results and still have asphalt fractions which retain the solubility characteristics of the asphaltene class.³

The areas under the peaks of Figures 1, 2, 3, and 4 were measured for each of the classes of protons to give a quantitative measure of the relative amounts of each type of proton present. The base line for these areas is that of the minimum shown in the spectra between the peaks for the aromatic and benzylic protons.

The areas so obtained were all divided by the area for the methylenic protons in that particular spectrum to provide ratios between the amounts of the different proton classes present. These ratios are given in Table II.

Average Molecular Structures

Using the ratios between the four classes of hydrogens and other chemical and physical data, one can construct formulas which are consistent with these data. This has been done to provide the average molecular structures of Figures 5, 6, 7, and 8. The ratios between the hydrogen types shown on the figures are those of the molecular structures drawn. They fit as closely as was possible the data of Table II on the asphaltenes.

A brief justification for the drawing of average asphaltene molecules may be desired at this point. It is recognized that asphaltenes are a heterogeneous classification and that the possibilities for variation from molecule to molecule are almost infinite. Also, the average structure of various fractions from asphaltenes will differ. Nevertheless, there is an over-all average ring size, an average content of polar atoms, and some arrangements which are preferred over others. For the very reason that the individual molecules are different, we are forced to consider average structures. We believe that these are sufficiently helpful in giving a general idea of the nature of the species to overcome the criticism that they are only average structures.

Among the pertinent literature which is drawn upon to arrive at the structures portrayed may be cited the high mass spectrograph data of Clerc and O'Neal⁴ on

asphalt, wherein polynuclear aromatic ring systems were identified and also the work of Carlson and O'Neal⁵ on heavy petroleum compounds wherein it was deduced that the rings in these compounds were condensed together and that the aliphatic portion of the molecule was primarily one long chain. Sergienko and Pustil'nikova⁶ and Fischer and Schramm⁷ have conducted hydrogenation experiments on asphalts leading to the conclusion that sulfur and oxygen compounds form the majority of the connecting links between segments of the asphaltene molecules. Goppel and Knotnerus⁸ deduced from chemical analyses that three fifths of the bonds formed in the air-blowing process were ester bonds. Evidence that the nitrogen in asphaltenes is primarily included in the condensed ring portion of the molecule was provided by the studies of Ball, et al.⁹ Additional evidence regarding the types of oxygen containing functional groups was provided by Knotnerus.¹⁰ X-ray diffraction studies by Erdman and coworkers¹¹ indicated that the asphaltenes consisted of systems of polynuclear aromatic plates carrying side chains and connecting links of paraffinic nature. The size of the condensed ring systems in the molecules of Figures 5 through 8 is consistent with Erdman's X-ray diffraction data.¹¹

The molecular weights of the asphaltenes of this study were not determined. They are assumed to fall in the range between 2000 and 3000 molecular weight which is indicated by recent research^{12,6,7,13} on asphaltene molecular weights. In systems where association of the asphaltenes can occur, extremely high molecular weights, up to 500,000, can be obtained.¹² However, where conditions of the determination are such as will minimize asphaltene association, the values appear to fall in the vicinity of 2000 to 3000.^{6,7,13} A lower molecular weight is assumed for the cracked tar asphaltene, as it is derived by degradation of natural asphaltenes with breaking off of side chains and aliphatic connecting links between ring systems.

The air-blown asphaltene of Figure 7 is purposely shown less condensed than the natural asphaltenes (Figure 5) as the air-blown asphaltenes are made by condensation and aromatization of the smaller and less polar resin molecules. The natural asphaltenes may also polymerize; however, in the air-blown California residuum the bulk of the asphaltenes come from nonasphaltene precursors. Ester links between the segments are shown in accordance with the findings of Goppel and Knotnerus.⁸ We suspect that these ester groups arise from the rearrangement of peroxide links which formed originally through the coupling of free radicals produced by the reaction with oxygen.

The cracked tar asphaltene of Figure 8 is related to the natural asphaltene of Figure 6 and can be made from it by aromatizing portions of the ring system of Figure 6 and by breaking off aliphatic fragments from the natural asphaltene. These processes are known to occur in cracking of petroleum hydrocarbons.

A few hypothetical structures for asphaltenes have been presented in the literature. None of these is entirely consistent with the proton magnetic resonance data reported in this paper. The asphaltene drawn in a previous paper by Winniford³ contains too much benzylic hydrogen and not enough methyl hydrogen. That drawn by Carlson, et al,¹⁴ is much too low in methylene hydrogen and also has too much benzylic and not enough methyl. The structure drawn by Gardner, Hardman, Jones, and Williams² for their petroleum Fraction No. 10 is a near asphaltene in chemical composition; but its loose structure contains far too much aromatic hydrogen for an asphaltene and probably, therefore, it should be drawn as a more compactly condensed molecule. The structure drawn by Given¹⁵ for bituminous coals cannot be correct for petroleum asphaltenes as it contains far too much oxygen and shows no methyl or methylene hydrogen at all.

The chemical nature of asphaltenes can by no means be considered settled by the brief results of this study. It is not believed that large deviations from

these results on the ratios of various classes of hydrogen will be found. However, more information is needed on the nature of links between the ring systems and on the size of the ring systems. Also, the disposition of the heterocyclic atoms, oxygen, sulfur, and nitrogen should be further clarified.

Acknowledgment

The authors wish to express their appreciation to the American Bitumuls and Asphalt Company for their support of this work.

Literature Cited

1. Williams, R. B., Presented at ASTM meeting, New Orleans, February 8-9, 1957.
2. Gardner, R. A., Hardman, H. F., Jones, A. L., and Williams, R. B., J. Chem. and Engr. Data 4, 155 (1959).
3. Winniford, R. S., ASTM Special Technical Publication No. 294, p. 31 (1960).
4. Clerc, R. J. and O'Neal, M. J., Jr., Preprints, Div. Petrol. Chem., ACS, Vol. 5, A-5 (1960).
5. Carlson, E. G. and O'Neal, M. J., Jr., Presented at ASTM meeting, New Orleans, February 8-9, 1957.
6. Sergienko, S. R., and Pustil'nikova, S. D., J. Appl. Chem., USSR, Vol. 32, 2982 (1959).
7. Fischer, K. A., and Schramm, A., Fifth World Petroleum Congress (1959), Section V, Preprint 20.
8. Goppel, J. M. and Knotnerus, J., Fourth World Petroleum Congress (1955), Vol. 3, p. 399.
9. Ball, J. S., Latham, D. R., and Helm, R. V., J. Chem. Engr. Data 4, 167 (1959).
10. Knotnerus, J., J. Inst. Petrol. 42, 355 (1956).
11. Yen, T. F., Erdman, J. G., and Pollack, S. S., Anal. Chem. 33, 1587 (1961).
12. Winniford, R. S., Preprints, Div. of Petrol. Chem., ACS 5, No. 4, A-11 (1960).
13. Flinn, R. A., Beuther, H., and Schmid, B. K., Petrol. Refiner 40, Vol. 1, 139 (1961).
14. Carlson, C. S., Langer, A. W., Stewart, J., and Hill, R. M., Ind. and Eng. Chem. 50, 1067 (1958).
15. Given, P. H., Nature 184, 980 (1959).

:caf

TABLE I
ANALYTICAL DATA ON ASPHALTENES

<u>Per Cent</u>	Asphaltene			
	Venezuelan	Californian	Air-Blown Californian	Cracked Californian
Carbon	81.17	85.54	86.22	88.43
Hydrogen	7.86	8.08	8.22	6.63
Nitrogen	2.02	3.33	2.0	2.08
Sulfur	6.89	1.28	1.89	2.24
Oxygen	2.02	2.48	3.74	0.62
Carbon/Hydrogen Ratio	0.86	0.89	0.88	1.12

CALIFORNIA RESEARCH CORPORATION
RICHMOND, CALIFORNIA 4-24-62
RSW

TABLE II

RATIOS OF THE AMOUNTS OF METHYLENIC,
METHYL, BENZYLIC, AND AROMATIC PROTONS
SHOWN BY THE PMR SPECTRA

	Venezuelan	Californian	Air Blown Californian	Cracked Californian
Methylene	1.00	1.00	1.00	1.00
Methyl	0.39	0.60	0.90	0.49
Benzyllic	0.29	0.45	0.44	0.72
Aromatic	Trace	0.19	0.16	0.66

CALIFORNIA RESEARCH CORPORATION
RICHMOND, CALIFORNIA 4-24-62
RSW

FIG. 1
ASPHALTENE FROM VENEZUELAN
CRUDE OIL

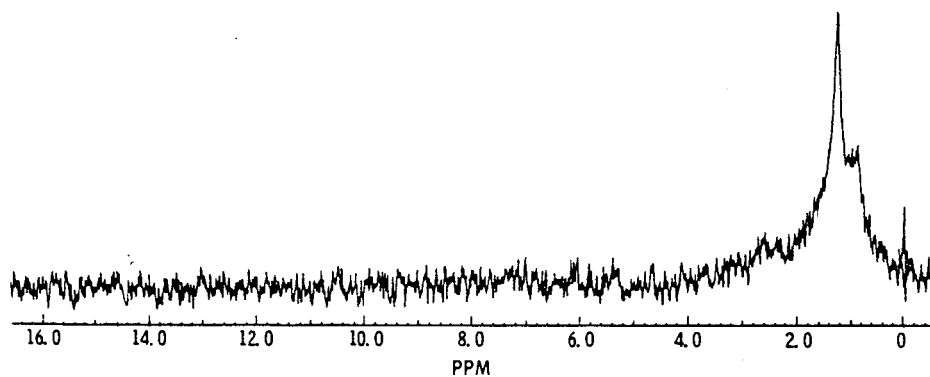
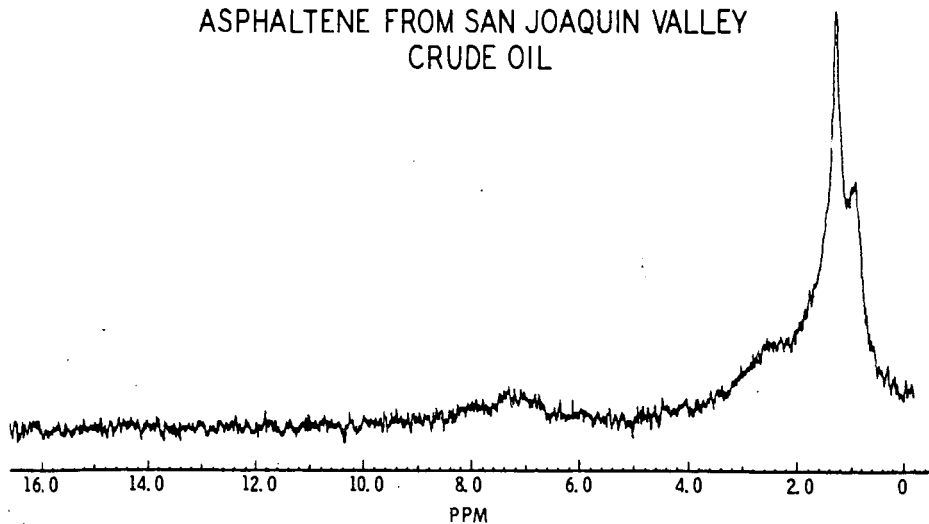


FIG. 2
ASPHALTENE FROM SAN JOAQUIN VALLEY
CRUDE OIL



3-28-62

CALIFORNIA RESEARCH
CORPORATION
RICHMOND, CALIFORNIA
RSW RD 622541

FIG. 3
ASPHALTENE FROM AIRBLOWN
SAN JOAQUIN VALLEY RESIDUUM

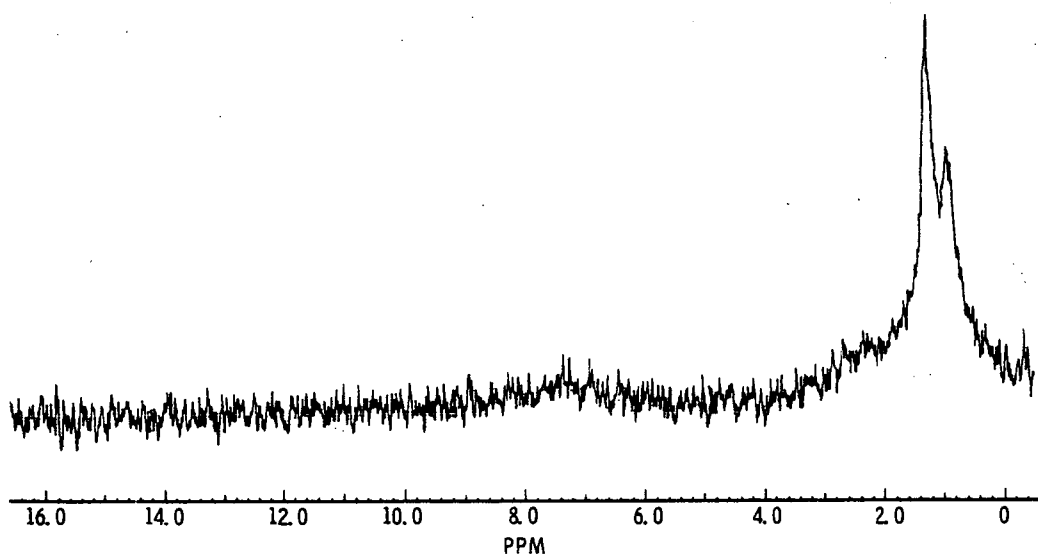
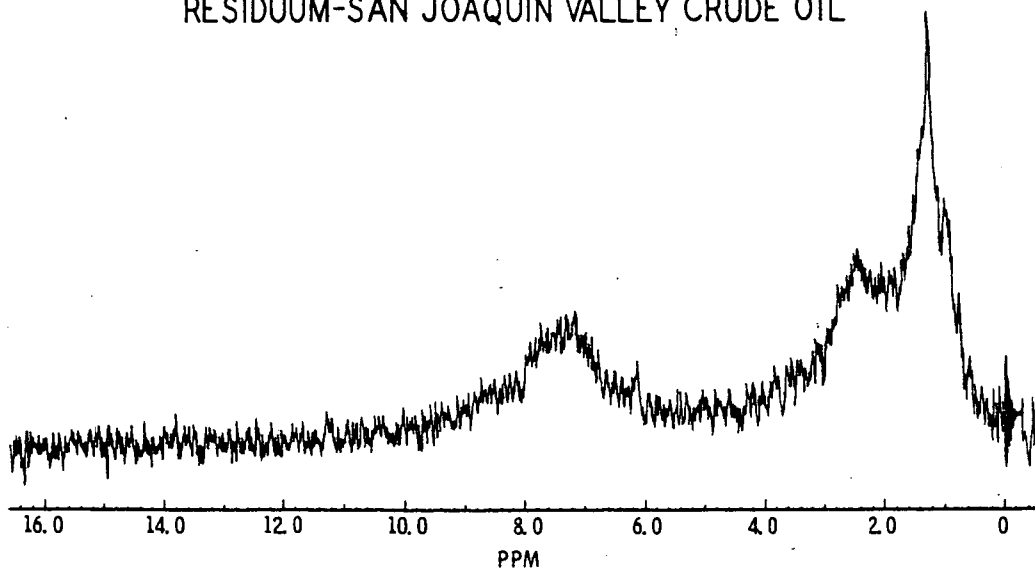


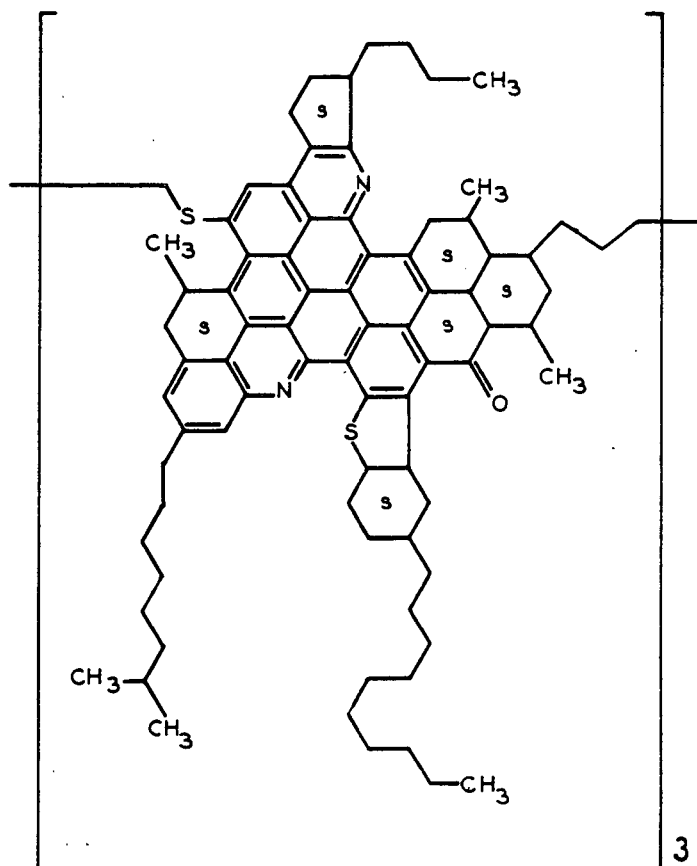
FIG. 4
ASPHALTENE FROM THERMALLY CRACKED
RESIDUUM-SAN JOAQUIN VALLEY CRUDE OIL



CALIFORNIA RESEARCH
CORPORATION
RICHMOND, CALIFORNIA

RSW RD 622542

FIG. 5
 ASPHALTENE FROM VENEZUELAN
 CRUDE OIL



$(C_{79}H_{92}N_2S_2O)_3$
 Mol Wt 3449

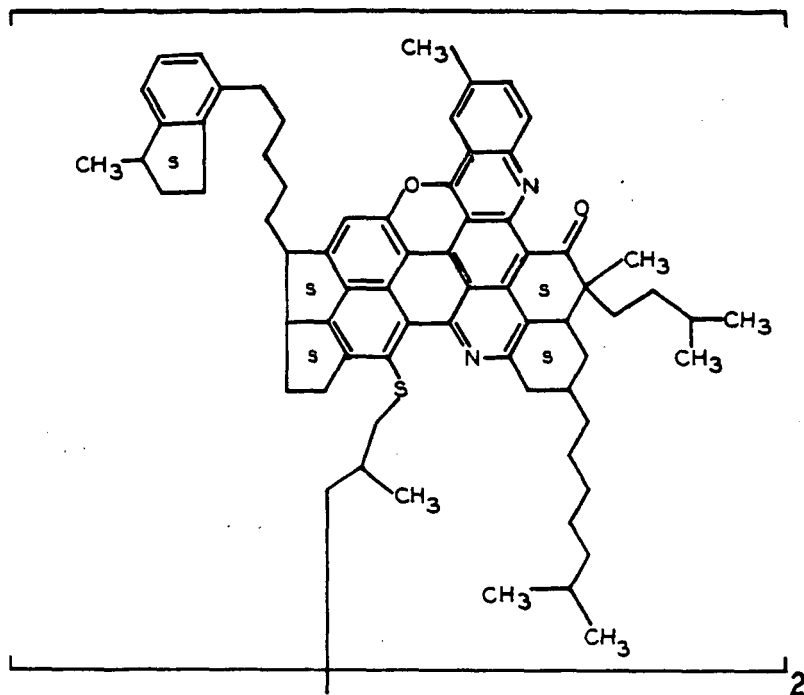
Hydrogen Distribution

Ratios	
Methylene	1.00
Methyl	0.40
Benzyllic	0.28
Aromatic	0.06

Composition

% C =	82.5
% H =	8.0
% N =	2.5
% O =	1.4
% S =	5.6
C/H Ratio =	0.86

FIG. 6
 ASPHALTENE FROM SAN JOAQUIN
 VALLEY CRUDE OIL



$(C_{70}H_{79}N_2O_2S)_2$
 Mol Weight 2024

Hydrogen Distribution
 Ratios

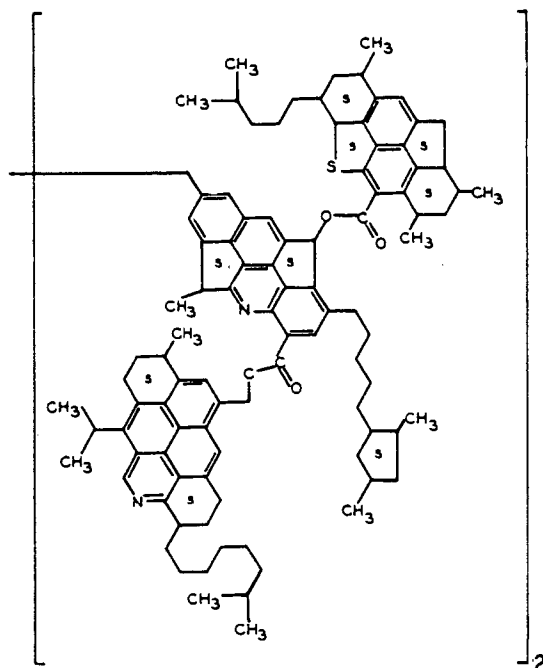
Methyl	0.58
Methylene	1.00
Benzylic	0.42
Aromatic	0.19

Composition

% C =	83.0
% H =	7.8
% N =	2.8
% O =	3.2
% S =	3.2
C/H Ratio =	0.89

CALIFORNIA RESEARCH
 CORPORATION
 RICHMOND, CALIFORNIA

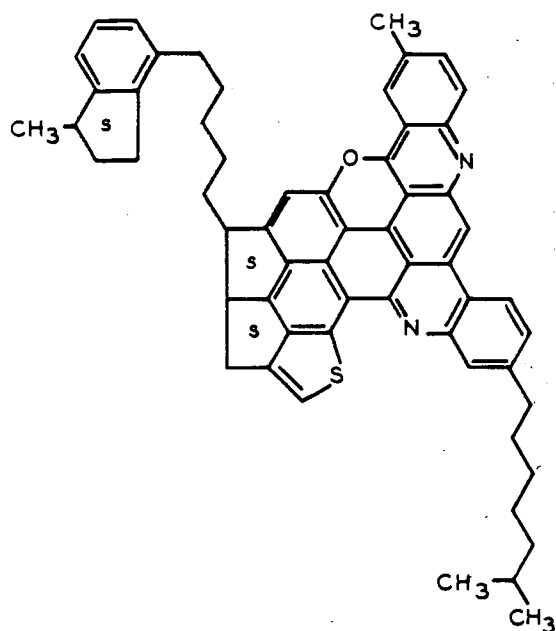
FIG. 7
 ASPHALTENE FROM AIRBLOWN SAN JOAQUIN
 VALLEY RESIDUUM



$(C_{98}H_{113}N_2O_4S)_2$
 Mol Weight 2830

Hydrogen Distribution Ratios		Composition	
Methylene	1.00	% C =	83.1
Methyl	0.89	% H =	8.1
Benzylic	0.47	% N =	2.0
Aromatic	0.18	% O =	4.5
		% S =	2.3
		C/H Ratio =	0.87

FIG. 8
 ASPHALTENE FROM THERMALLY
 CRACKED RESIDUUM-SAN JOAQUIN VALLEY
 CRUDE OIL



$C_{59}H_{54}N_2SO$
 Mol Wt 838

Hydrogen Distribution
 Ratios

Methylene	1.00
Methyl	0.47
Benzyllic	0.74
Aromatic	0.63

Composition

% C =	84.5
% H =	6.4
% N =	3.3
% S =	3.8
% O =	1.9
C/H Ratio =	1.09

PROTON MAGNETIC RESONANCE SPECTROMETRY
IN THE CHARACTERIZATION OF COAL-TAR PITCHES

C. W. DeWalt, Jr., and M. S. Morgan

Mellon Institute
Pittsburgh 13, Pennsylvania

Introduction

Coal-tar pitch is the residue, boiling at temperatures above 350° C, from the fractional distillation of coal tar. Although it constitutes about 50% of the tar yield from high-temperature carbonization in coke ovens, its chemical composition is not nearly as well known as that of many of the smaller, more-volatile fractions. Coal-tar pitch has numerous large-scale uses, some of which call for modification of the material by physical or chemical techniques. However, much of this modification is empirical to the extent that the results are measured in terms of efficacy for a specific end-use rather than in terms of change in chemical structure. Additional investigations of the chemistry of this rather intractable material are desirable toward developing new uses and placing pitch-treating procedures on a more scientific basis. With the development of proton magnetic resonance (PMR) techniques, a promising method of examining the types of hydrogen in pitches became available. Attention was therefore turned to the results which might be obtained by PMR examination of pitches.

Chemically speaking, pitch cannot be considered as a single type, but rather there are large differences between pitches, depending upon their source. Coke-oven pitches, which are of primary concern in this paper, are produced from high-rank (coking) coals at very high temperatures (1000° to 1300° C). The severe conditions control the product so that coke-oven pitches constitute a narrow class among coal-tar pitches, as indicated by Volkmann.¹ They are the most aromatic of the pitches, and a precise aromaticity determination is necessary to distinguish one from another.

The aromaticity of a pitch can be defined by two parameters. One is the ratio of the aromatic structures to the whole pitch. The other is the degree of condensation of the aromatic portion. This degree of condensation could range from the polyphenylene- to the graphite-type. Aromaticity factors can be calculated from various types of data, including density, atomic C/H ratio, and the ratio of aromatic hydrogen (Har) to total hydrogen (H). The latter is the most sensitive method for highly aromatic materials like coke-oven pitches, since the proportion of non-aromatic hydrogen atoms is greater than that of non-aromatic carbon atoms. For example, methylphenanthrene with 6.7% non-aromatic carbon atoms has 25% non-aromatic hydrogen atoms.

Considerable work has been reported toward establishing an infrared Har/H measurement,^{2,3,4,5,6} but more detailed and reliable data are reported from PMR measurements.^{2,6,7,8,9} Three types of hydrogen were estimated in pitch-like materials by PMR methods: aromatic hydrogen (Har); hydrogen on saturated carbon alpha to aromatic rings, or alpha hydrogen (H_α); and hydrogen on other saturated hydrocarbon structures, or beta hydrogen (H_β). Both Brown and Ladner² and Oth and Tschamler⁸ were able to calculate structural parameters for pitch-like materials through the use of such PMR data.

For structural analysis, Brown and Ladner's² method appeared especially suitable for adaptation to coke-oven pitch. Details of the structure of the aromatic portion of their pitch-like materials were derived by subtracting the non-aromatic atoms from the whole. This introduced an uncertainty by requiring an estimate of the H/C ratio in the substantial fraction of non-aromatic structures. Nevertheless, the parameters of their distillates proved to be functions of the ranks of the parent coals. Coke-oven pitches in this analysis should enjoy the advantage of a very low proportion of non-aromatic structures.

Rao, Murty, and Lahiri⁶ reported the use of the PMR spectrum in the characterization of the 65 weight per cent carbon disulfide-soluble fraction of a pitch that was evidently of coke-oven origin. Only 22% of the hydrogen was non-aromatic, and 70% of the non-aromatic hydrogen was of the alpha type. They concluded that the non-aromatic hydrogen was mostly present as methylene-, methyl-, and small alkyl-substituents on aromatic ring systems.

This paper describes the application of PMR spectrometric methods to the determination of certain aspects of the chemical structure of coke-oven pitches.

Experimental

A series of coke-oven pitches representing a wide range of electrode-binder properties with a narrow range of softening points and, for comparison purposes, a low-temperature-carbonization pitch from a sub-bituminous B coal were selected. The analytical data for these pitches, together with the sources and methods of preparation, are summarized in Table I.

A.C.S. reagent-grade carbon disulfide was used to prepare the pitch extracts for the PMR determinations. The internal PMR standard was Anderson Chemical Division of Stauffer Chemical Company's "pure" grade of tetramethylsilane (TMS). The reference compounds were fluorene, m.p. 114-116° C (lit., 115-116° C), and acenaphthene, m.p. 93-94° C (lit., 95° C).

Carbon Disulfide-Soluble Fractions of Pitches

The carbon disulfide-soluble PMR spectra samples were prepared in the following manner: Samples of the pitch weighing 5.00 g. and sized to pass a 20-mesh sieve were added to 50 ml. of carbon disulfide in a 250-ml. beaker with stirring. The beaker was covered with a watch glass, and the magnetic stirring was maintained for 30 minutes. After collecting the insolubles on a 60-ml., medium-porosity fritted-glass funnel and washing with 25 ml. of carbon disulfide, the solids were air-dried and weighed. The filtrate and washings were concentrated on the steam bath (in a hood) to give a 60% weight/volume (w/v) solution. Samples of this solution and of dilutions made up as needed were placed in Varian A-60 Spectrometer sample tubes, and a trace of TMS was dissolved in each sample.

Determination of PMR Spectra

The PMR spectra were recorded on a 10 in. by 20 in. record sheet using a Varian A-60 Spectrometer. The samples were spun rapidly at room temperature, and the spectra were traversed slowly (sweep time 500 sec.) from 550 to 50 cycles per second (c.p.s.) below the TMS line (the increasing-frequency convention was observed). Radio-frequency (RF) power settings were intermediate—between 0.04 and 0.20 milligauss (mG.)—and filter bandwidth was usually set at 1 c.p.s.

Determination of the Integrals of the PMR Spectra

After plotting a spectrum, the integral of the curve was recorded electronically in a 10 in. by 20 in. area of chart, using the same sample and conditions,

with the exceptions and precautions noted below (see Figure 1). Care was necessary to insure both stability of the integral and non-saturation of any of the sample protons. To avoid saturating sample protons, the RF energy was kept below a setting of about 0.4 mG., while the sweep time was set down to 50 or 100 seconds. Saturation of a particular proton would result in an area under its absorption band less than proportional to the number of protons represented. Three factors were used to obtain stable integrals. The use of only the most concentrated, the 30 and 60% w/v, solutions for integrals was important. Also, the sweep time was reduced to 50 or 100 seconds, and finally, it was sometimes advantageous to increase the RF power.

Estimation of Hydrogen Types from PMR Integrals

Quantitative estimation of the hydrogen types involved measurement of the integral heights at the following frequencies (tau values; see Figure 1): for aromatic hydrogen together with phenolic hydrogen (H_{ph}), approximately 4.5 tau; for alpha² hydrogen (H_{α²}; this is hydrogen on any carbon atom which joins two aromatic rings), 6.60 tau; for alpha hydrogen, approximately 8.1 tau; and for beta hydrogen, the end of the spectrum (about 9.2 tau). These boundary tau values were equivalent to the following frequencies in c.p.s. below TMS: about 4.5 tau, near 315 c.p.s.; 6.60 tau, 190 c.p.s. for 30% and 180 c.p.s. for 60% w/v solutions; and 8.1 tau, 110 c.p.s. for both 30 and 60% solutions. The considerations which led to the choice of these frequencies will be discussed in the following section.

PMR Frequencies (Tau Values)

The use of dissolved TMS eliminated volume susceptibility corrections¹⁰ and interference by the standard in regions where the pitch components absorbed. It did not, however, prevent anomalous aromatic medium effects¹¹ from interfering. The spectra of different concentrations of pitch fractions in carbon disulfide showed frequency differences as great as 0.40 p.p.m. (tau units). To eliminate these effects, extrapolation to infinite dilution with the internal standard was necessary. This procedure with CS₂ extracts of pitches 1 and 2 gave smooth curves and infinite dilution frequencies for various absorption components of the spectra (see Figure 2).

The use of carbon disulfide provided a pitch solvent with Van der Waals deshielding effect about the same as that of carbon tetrachloride,¹² the tau solvent. Therefore, the infinite dilution frequencies should be very nearly true tau values,¹³ in which form they are herewith reported. This was confirmed by the value of 6.68 tau thus obtained for the methylene line of acenaphthene in pitch (lit., 6.66 tau).

The choice of the frequencies listed in the preceding section to divide between the four types of hydrogen was made in the following manner: There was a broad region of zero signal between aromatic and non-aromatic bands, centering in the 4.5 tau region. The alpha² hydrogen, since it is close to two rather than one aromatic ring, is more deshielded than alpha hydrogen. Thus, the alpha² hydrogen absorption occurs at lower tau values (frequencies). The boundary was chosen just below the acenaphthene methylene peak at 6.66 tau because this is an intermediate type between alpha and alpha², although it is formally alpha hydrogen. Conservatively, then, absorption below 6.60 tau was attributed to alpha² hydrogen. The anomalous shifts due to changes in pitch concentration necessitated the use of the two frequencies. For the boundary between alpha and beta hydrogen, the spectrum of pitch 7, which showed separate absorption maxima for beta and for alpha hydrogen types, was considered (see Figure 3). The minimum between these maxima occurred at about 8.2 tau. To avoid overestimating alpha hydrogen, a value near 8.1 tau was chosen. This includes types such as durene methyl groups (7.86 tau) and excludes such types as Me₃CH (8.44 tau) and cyclohexane (8.56 tau).

Molecular Weight Determination

Molecular weight measurements were ebullioscopic with incremental addition of sample and extrapolation to infinite dilution. Solvents were benzene and freshly prepared chloroform, depending upon the solubility of the sample. Interference by foaming or incomplete solubility prevented determination of molecular weight in certain cases (see Table II).

Structural Parameters

From PMR and elementary analytical data, Brown and Ladner² were able to calculate the following average structural characteristics of their pitch-like materials:

f_a , the ratio of aromatic carbon (C_{ar}) to total carbon (C),

σ , the fraction of the total available outer-edge positions of the aromatic skeleton which is occupied by substituents, and

H_{ar}/C_{ar} , the atomic H/C ratio that the average aromatic skeleton would have if each substituent were replaced by a hydrogen atom.

Brown and Ladner developed the following equations for calculating these parameters:

$$f_a = \frac{\frac{C}{H} - \frac{H_{\alpha}^*}{x} - \frac{H_{\beta}^*}{y}}{\frac{C}{H}} \quad (1)$$

$$\sigma = \frac{\frac{H_{\alpha}^*}{x} + \frac{O}{H}}{\frac{H_{\alpha}^*}{x} + \frac{O}{H} + H_{ar}^*} \quad (2)$$

$$\frac{H_{ar}}{C_{ar}} = \frac{\frac{H_{\alpha}^*}{x} + \frac{O}{H} + H_{ar}^*}{\frac{C}{H} - \frac{H_{\alpha}^*}{x} - \frac{H_{\beta}^*}{y}} \quad (3)$$

where C/H and O/H are the atomic ratios, obtained from elementary analysis; $H_{\alpha}^* = H_{\alpha}/H$, the ratio of alpha-type hydrogen to total hydrogen obtained from PMR spectrometric analysis; $H_{\beta}^* = H_{\beta}/H$, the ratio of beta-type hydrogen to total hydrogen from PMR analysis; $x = H_{\alpha}/C_{\alpha}$ and $y = H_{\beta}/C_{\beta}$, the atomic ratios of hydrogen to carbon in the alpha and beta structures, both of which must be obtained by estimate; $H_{ar}^* = H_{ar}/H$, the ratio of aromatic hydrogen to total hydrogen obtained indirectly from PMR spectrometry with the help of elementary analysis, assuming 60% of the total oxygen to be phenolic. Since phenolic hydrogen (H_{ph}) is included in the "aromatic" hydrogen ($H_{ar} + ph$) seen in PMR spectra, H_{ar}^* was calculated by the following equation:

$$\frac{(\text{Har} + \text{ph})}{\text{H}} - 0.60 \frac{\text{O}}{\text{H}} = \frac{\text{Har}}{\text{H}} = \text{Har}^*$$

They assumed that every oxygen atom was present as a substituent on an aromatic nucleus in completing the development of the above equations.

Their method for the conversion of the hydrogen distribution in coal-like materials to carbon structure was adapted for use with coke-oven pitches. Changes were made in the assumptions and equations as described below. It is accepted that 60% of the total oxygen is phenolic, but Brown and Ladner's assumption that all of the oxygen occurred as substituents on aromatic nuclei could not be justified for coke-oven pitches. Instead, the remaining 40% oxygen is assumed to occur not as aromatic substituents but in other forms, among which heterocyclic oxygen must be included. Alpha² hydrogen is included in the equations separately as $\text{H}\alpha^2$, with $z = 2$ the estimated ratio of hydrogen to carbon in such groups, and $\text{H}\alpha^{2*} = \text{H}\alpha^2/\text{H}$. Because the predominant alkyl substituent in known coke-oven pitch components is the methyl group, the value of x (estimated H/C ratio for alpha structures) is raised from the value of 2 to 2.5. The value of $y = 2$ is retained.

Considering equation (1), a term for alpha²-type carbon is added to its numerator, the number of aromatic carbon atoms, giving $\text{C} - \text{C}\alpha^2 - \text{C}\alpha - \text{C}\beta$. The resulting equation for coke-oven pitches is the following:

$$f_a = \frac{\frac{\text{C}}{\text{H}} - \frac{\text{H}\alpha^{2*}}{2} - \frac{\text{H}\alpha^*}{2.5} - \frac{\text{H}\beta^*}{2}}{\frac{\text{C}}{\text{H}}} \quad (4)$$

Considering equation (2), it is necessary to add a term for the contribution of alpha² structures to the total number of substituents. Since each bridge represents two substituents, this added term must equal $2 \times \text{C}\alpha^2$, which is $2 \text{H}\alpha^2/z$. To replace (2) for determining the degree of substitution of coke-oven pitches, the following equation is used:

$$\sigma = \frac{\text{H}\alpha^{2*} + \frac{\text{H}\alpha^*}{2.5} + 0.6 \frac{\text{O}}{\text{H}}}{\text{H}\alpha^{2*} + \frac{\text{H}\alpha^*}{2.5} + (\text{Har} + \text{ph})^*} \quad (5)$$

Similarly, equation (3) is replaced by the following equation for the atomic C/H ratio of the hypothetical unsubstituted average aromatic nucleus of coke-oven pitches:

$$\frac{\text{Car}}{\text{Haru}} = \frac{\frac{\text{C}}{\text{H}} - \frac{\text{H}\alpha^{2*}}{2} - \frac{\text{H}\alpha^*}{2.5} - \frac{\text{H}\beta^*}{2}}{\text{H}\alpha^{2*} + \frac{\text{H}\alpha^*}{2.5} + (\text{Har} + \text{ph})^*} \quad (6)$$

This degree-of-condensation parameter is also the ratio of total aromatic carbon to aromatic edge-carbon.

Equations 4, 5, and 6 were used to calculate parameters for the carbon disulfide solubles of eight pitches and for the carbon disulfide-soluble, n-hexane-insoluble (resin) fraction of one of the coke-oven pitches. The parameters of low-temperature-carbonization pitch 7 were calculated by means of equations 1, 2, and 3. Data and results are listed in Table II.

Results and Discussion

PMR Spectra of Coke-Oven Pitches

The carbon disulfide-soluble fractions of coke-oven pitches, using the Varian A-60 Spectrometer, showed hydrogen distributions in keeping with the reputed high aromaticity of these pitches. From 80 to 90% of their hydrogen was aromatic. The higher molecular weight resin fraction of pitch 2 had an even higher (95%) aromatic hydrogen content. This is in sharp contrast with the 20% of aromatic hydrogen in the low-temperature-carbonization pitch carbon disulfide-soluble fraction.

There were only two absorption maxima in the coke-oven pitch spectra: the aromatic- and the alpha-hydrogen bands. Both indicate types closely associated with aromatic rings. Reports on other pitches^{2,3,8} have shown an additional band due to hydrogen not associated with any aromatic ring (beta hydrogen). Low-temperature-carbonization pitch 7 also fell in the latter category (see Figure 3), exhibiting two maxima in the beta hydrogen region. The total alpha and alpha² hydrogen in coke-oven pitches was never less than 79% of the non-aromatic hydrogen. Thus, only 21% of the non-aromatic and only 4.2% of the total hydrogen failed to show a close proximity to an aromatic ring.

In addition to the above considerations, which are based on tau values, there was the sensibility of the non-aromatic protons of the coke-oven pitches to the anomalous aromatic medium shifts. This is a further indication that these protons are held close to aromatic rings, since paraffins were insensitive to these effects.

Individual Components

Without fractionating the pitches, it was possible in four cases to identify acenaphthene, and in two, fluorene, as components of the pitch. There is a possibility that yet other of the more abundant components could thus be identified, since a number of sharp individual peaks appeared in each spectrum. Two factors combined to confirm the conclusions as to identity. The first factor was the identity of the peaks in question with those of the added authentic compound at one concentration. The second factor was repetition of the same results at another concentration of the pitch in the solvent. Thus, the aromatic medium effect was shown to be the same for the authentic compound and the pitch component.

Structural Parameters

A Brown-Ladner type of analysis of the PMR and elementary analytical data, together with molecular weight data, permitted the following conclusions regarding molecular structure (see Table II):

Carbon Aromaticity (f_a)

The coke-oven-pitch carbon disulfide-soluble fractions were estimated to contain only 2.5 to 5.7% non-aromatic carbon atoms ($f_a = 0.975$ to 0.943). A contrast between coke-oven pitch 2 and low-temperature-carbonization pitch 7 is available through their resin fractions, which by calculation contained 1 and 33% non-aromatic carbon ($f_a = 0.987, 0.67$), respectively.

Degree of Substitution (σ)

Only from 6 to 12 of every 100 available sites for substitution around the average nucleus were occupied by substituents in these coke-oven-pitch fractions ($\sigma = 0.063$ to 0.116). The value was 2 per 100 lower ($\sigma = 0.048$) in the larger molecular weight fraction of pitch 2. Such trends to less substitution in larger

molecules of pitch have been reported by other workers using other methods.^{14,15} Again, comparison with pitch 7 serves to emphasize the high aromaticity of the coke-oven pitches. Sixty five per cent ($\sigma = 0.65$) of the edge aromatic carbons were bonded to substituents in pitch 7 resin fraction.

C/H of the Aromatic Nucleus (Car/Haru)

The atomic C/H ratios of the average hypothetical unsubstituted aromatic nucleus (Car/Haru values) of the coke-oven pitches were, for carbon disulfide-soluble fractions, 1.5 to 1.7, and for the resin fraction of pitch 2, 1.83 (Table II). The interpretation of these numbers depends upon the molecular weight of the materials. With the molecular weights, the degree of condensation of the average aromatic nucleus was shown to be nearly linear (of the benzene-naphthalene-phenanthrene series: each ring fusion involves only two carbon atoms).

The average molecular weight of the carbon disulfide-soluble fraction was about 400. As a result, an average aromatic nucleus of 7 to 8 rings with one substituent was indicated. The resin fraction of pitch 2 with molecular weight 660 would indicate an average aromatic nucleus with near 13 rings and about 1.3 substituents.

To illustrate this, for the fractions of pitch 2, a type molecule was chosen as a possible structure for the average molecule, as shown in Table III. This suggests that the higher molecular weight fractions of coke-oven pitch, such as the C-1 sooty material, do not approach graphite in structure but may be mostly linearly condensed aromatic ring systems.

PMR Solvent

Carbon disulfide proved to be a good solvent for PMR examination of coke-oven pitches. The soluble fraction represented a large proportion—60 to 84%—of the total material. Solutions of concentrations up to 60% were readily available in this non-protonic solvent, permitting accurate quantitative work, and the infinite dilution values were very nearly true tau values.

Summary

Proton magnetic resonance spectrometry proved a useful method for the characterization of coke-oven pitch. The estimation of aromatic and three types of aliphatic hydrogen by this means made possible the formulation of a structure for the typical molecule in the carbon disulfide-soluble fraction. This was a linearly condensed aromatic nucleus with 2 to 6% of the carbon atoms occurring as substituents which were predominantly methyl groups. The average molecular weight was near 400, which was equivalent to 7 or 8 fused aromatic rings. Fluorene and acenaphthene were identified in several of the pitches. It is hoped that these methods will prove to be of value in a search for correlations between the chemical and physical properties of a coke-oven pitch and its efficacy in a particular industrial end-use.

Acknowledgement

This work was done by the Coal Chemicals Research Project, sustained by the United States Steel Corporation, to whom the authors wish to express appreciation for permission to publish the results. The authors also wish to acknowledge their indebtedness to Dr. A. A. Bothner-By, Dr. B. L. Shapiro, and Mr. F. E. Dickson of the Mellon Institute for their assistance in obtaining and interpreting the PMR spectra.

References

- (1) E. W. Volkmann, "The Structure of Coke Oven Tar," Fuel, **38**, 445-468 (1959).

- (2) J. K. Brown and W. R. Ladner, "A Study of the Hydrogen Distribution in Coal-Like Materials by High-Resolution Nuclear Magnetic Resonance Spectroscopy. II," Fuel, 39, 87-96 (1960).
- (3) M. B. Dell, "Characterization of Pitches for Carbon Anodes," Fuel, 38, 183-187 (1959).
- (4) L. J. Wood and W. G. Wilman, "Chemical Nature of Coal Tar Pitch," Proceedings: Residential Conference on Science in the Use of Coal, Sheffield, Institute of Fuel, London, 1958, pp. C10-C14.
- (5) L. J. Wood, "Chemical Constitution of Road Tars and Coal-Tar Pitches," J. Appl. Chem., 11, 130-136 (1961).
- (6) H. S. Rao, G. S. Murty, and A. Lahiri, "The Infra-Red and High-Resolution Nuclear Magnetic Resonance Spectrum of Coal Tar Pitch," Fuel, 39, 263-266 (1960).
- (7) L. M. Jackman, Applications of Nuclear Magnetic Resonance Spectroscopy in Organic Chemistry, Pergamon Press, New York City, 1959.
- (8) J. F. M. Oth and H. Tschamler, "Comparison and Interpretation of Proton Spin Resonance Measurements on a Coal Extract in the Solid State and in Solution," Fuel, 40, 119-122 (1961).
- (9) J. K. Brown, W. R. Ladner, and N. Sheppard, "A Study of the Hydrogen Distribution in Coal-Like Materials by High-Resolution Nuclear Magnetic Resonance Spectroscopy. I," Fuel, 39, 79-86 (1960).
- (10) L. M. Jackman, op. cit., pp. 41-48.
- (11) A. A. Bothner-By and R. E. Glick, "Medium Effects in the Nuclear Magnetic Resonance Spectra of Liquids. III. Aromatics," J. Chem. Phys., 26, 1651-1654 (1957).
- (12) A. A. Bothner-By, "Medium Effects in the Nuclear Magnetic Resonance Spectra of Liquids. IV. Nature of the Effects," J. Mol. Spectry., 5, 56 (1960).
- (13) See reference 7, page 47, for a definition of tau value.
- (14) H.-G. Franck, "The True Nature of Bituminous Coal Tar Pitch," Brennstoff-Chem., 36, 12-19 (1955).
- (15) C. Karr, Jr., J. R. Comberlata, and P. A. Estep, "Ring Analysis and the Spectral Characterization of Resins from Pitch of Low Temperature Tar," Fuel, 41, 167-176 (1962).

Table I

Analytical Data, Sources, and Methods of Preparing
Experimental Pitches

<u>Pitch Designation^{a)}</u>	<u>Softening Point, °C, C.I.A. ^{b)}</u>	<u>Benzene Insoluble, Wt. %</u>	<u>Quinoline Insoluble, Wt. %</u>	<u>Atomic C/H Ratio</u>
1	89.0	33.2	13.1	1.80
2	90.2	32.6	12.8	1.93
3	93.5	29.7	10.58	1.87
4	94.9	28.0	9.13	1.76
5	90.6	17.5	6.87	1.78
6	88.2	13.0	2.44	1.61
A	102.3	25.5	12.4	1.84
C	95.0	25.0	4.2	1.73
7	59.5	—	—	0.95

a) 1. Thermal treatment of a 74° C pitch at 380° C for 24 hours and back-blending with 9.1% of starting pitch. 2. Laboratory distillation of soft pitch from a production tar. 3. Laboratory distillation of 36.2 wt. % from a production tar. 4. Blend of 88.55 wt. % 105° C pitch (produced by distillation of light tar at 50 mm. to 300° C) with 11.45% of coal-tar distillate oil (boiling 230° to 270° C). 5. A production pitch after removal of n-heptane solubles. 6. Laboratory distillation of a 69° C pitch from light tar. A. Produced by plant distillation of production tar. C. Produced by adding quinoline to the parent tar of A, centrifuging this mixture to remove insolubles, and then distilling. 7. A 60° C pitch produced by blowing at 120° C a tar from low-temperature carbonization of a sub-bituminous B coal.

b) Cube-in-air method.

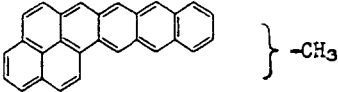
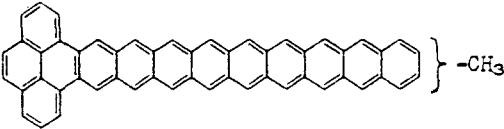
Table II
Structural Parameters of Pitch Fractions

Pitch	2	3	A	5	C	4	1	6	7	
Pitch Analysis	93.41 4.07	93.31 4.18	93.22 4.24	92.55 4.38	93.29 4.52	92.88 4.44	93.34 4.36	91.35 4.77	76.94 6.81	
N, %								1.11	0.78	
S, %								0.73	0.29	
O (diff.), %	2.52	2.51	2.54	3.07	2.19	2.68	2.30	2.04	15.18	
Solvent Fraction*	2	2 + 3	2 + 3	2 + 3	2 + 3	2 + 3	2 + 3	2 + 3	2**	
Analysis of Fraction	92.87 4.34 2.79 1.80 0.040	92.92 4.69 2.42 1.66 0.032	93.09 4.88 2.02 1.65 0.026	92.70 4.72 2.57 1.65 0.034	92.50 4.91 2.58 1.58 0.033	92.48 4.83 2.68 1.61 0.035	91.80 4.90 3.30 1.57 0.042	92.00 5.18 2.81 1.49 0.034	91.10 5.13 3.61 1.49 0.044	75.84 6.12 18.04 1.04 0.186
Molecular Weight	660	386	370	---	421	459	---	379	455	
Yield of Fraction, Wt %	21.1	69.3	73.6	80.5	70.9	70.9	66.2	83.8	7.4	
Hydrogen Distillation	0.946 0.009 0.035 0.010	0.902 0.017 0.064 0.0146	0.902 0.017 0.068 0.0126	0.892 0.019 0.075 0.0136	0.903 0.016 0.074 0.014	0.890 0.018 0.082 0.011	0.864 0.022 0.098 0.017	0.856 0.025 0.096 0.024	0.802 0.024 0.1344 0.042	0.315 -- 0.382 0.303
Structural Parameters	fa σ Car/Maru	0.987 0.048 1.83	0.974 0.063 1.65	0.972 0.074 1.71	0.972 0.069 1.62	0.971 0.077 1.66	0.963 0.093 1.64	0.958 0.091 1.55	0.943 0.116 1.60	0.670 0.65 1.20

* Solvent fraction 2 is the carbon-disulfide-soluble, n-hexane-insoluble fraction; fraction 2 + 3 is the carbon-disulfide-soluble fraction.
** The original Brown-Ladner equations were used to calculate fu, σ, and Car/Maru for this low-temperature-carbonization pitch fraction.

Table III

Correlation of Structural Parameters in Pitch Fractions
with Possible Type Molecules

PITCH #2 FRACTION or TYPE MOLECULE	PARAMETER VALUES FOR FRACTIONS AND TYPE MOLECULES				
	C/H	Mol. Wt.	fa	σ	Car/Haru
CS ₂ -Soluble Fraction	1.66	386	0.975	0.066	1.71
 (C ₂₈ H ₁₅ -CH ₃)	1.61	364	0.965	0.062	1.75
Resin Fraction	1.80	660	0.987	0.048	1.83
 (C ₅₂ H ₂₇ -CH ₃)	1.77	666	0.981	0.036	1.86

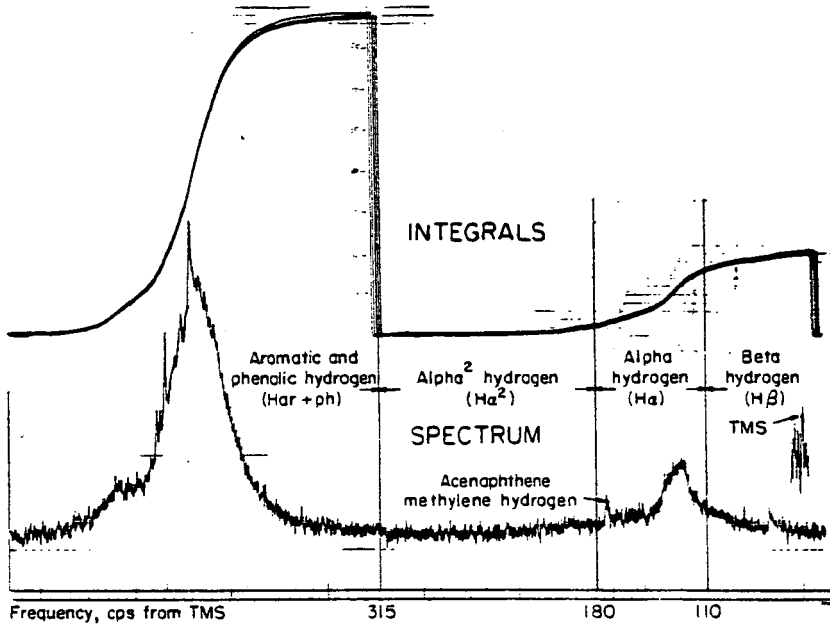


Figure 1. PMR Spectrum and Integrals: Pitch 6, Carbon Disulfide Solubles

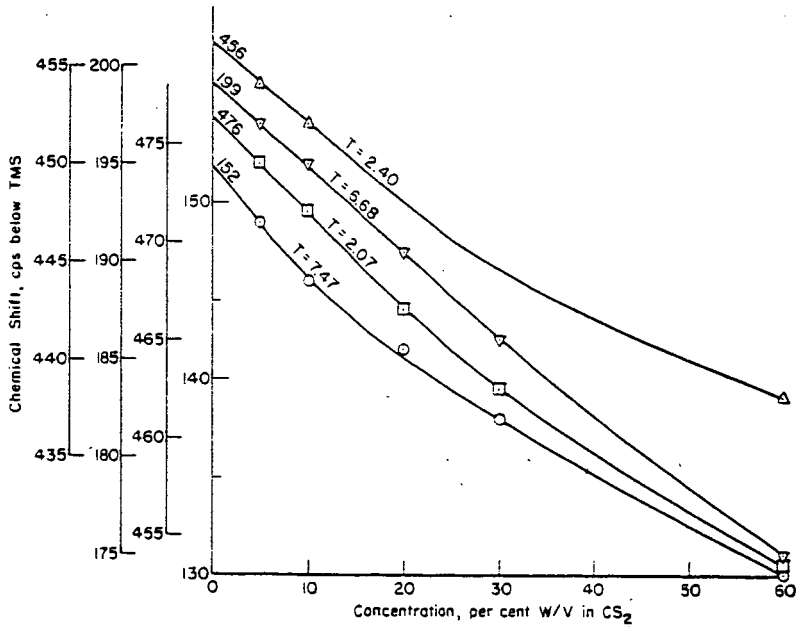


Figure 2. Extrapolation of PMR Frequencies to Infinite Dilution with an Internal Standard: Pitch 1 - CS₂ Extract

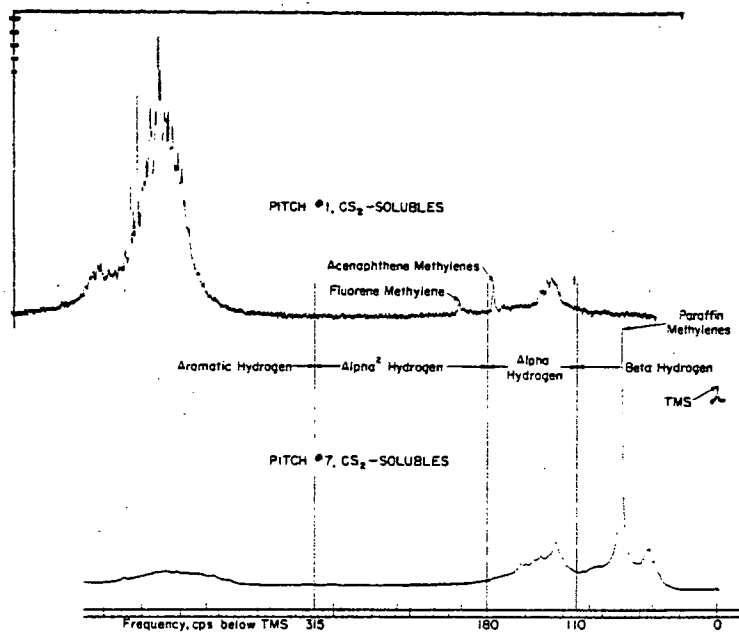


Figure 3. Comparison of PMR Spectra: Coke-Oven Pitch (No. 1) and Low-Temperature-Carbonization Pitch (No. 7); CS₂ Solubles, 60% w/v in CS₂

THE USE OF THE BRABENDER PLASTOGRAPH IN STUDYING
THE RHEOLOGY OF ELECTRODE MIXES

T. F. Eckle, A. T. Elenice, and F. A. Smith

U. S. Steel Corporation
Applied Research Laboratory
Monroeville, Pennsylvania

Introduction

The performance of the continuous, self-baking Soderberg electrode, which is widely used in the production of primary aluminum, is closely related to the rheology of the carbon mix that is added to the top of the electrode. The fluidity must be sufficient to ensure an even distribution of the mix over the top of the electrode and to permit the mix to fill voids that are created when contact studs are removed. However, separation of the binder from the aggregate or difficulty in containing the mix in the sheet metal casing may result if the mix is excessively fluid.

Some investigators have attempted to obtain mixes with proper fluidity by studying the rheology of the binders with the assumption that the rheology of the mix is a function of the rheology of the binder.¹⁾* Others have investigated the rheology of the mix itself.²⁾ The latter approach appears to be the more desirable because interactions between the binder and aggregate influence the rheological behavior of the mix.

A method in which a Brabender Plastograph is used for measuring the consistency of the Soderberg mix was described at a previous meeting of this division.³⁾ In the development of the method at the Applied Research Laboratory of the U. S. Steel Corporation, a petroleum-coke aggregate was used that had a smaller size-consist than is commonly used in plant practice. The method has been extended to include the measurement of the consistencies (rheological measurements) of Soderberg mixes containing plant-scale aggregates.

The present paper presents typical results that were obtained in an investigation to (1) use the consistencies of mixes prepared with plant-scale aggregates to predict the optimum binder content for optimum electrode properties and (2) determine the influence of temperature and time in the Soderberg electrode on the consistency of the mix.

Experimental

The two electrode binders and the plant-scale petroleum-coke aggregate used in this investigation are representative of the materials in use at a carbon-paste plant. Some of the more common properties of the two binders are shown in

* See References.

Table I. The properties of the two binders are similar; however, Pitch B contains slightly more benzene- and quinoline-insoluble matter than Pitch A. Past-plant experience has shown that subtle but significant differences exist in the performance of the two binders: pastes prepared with Pitch B required the use of more binder for optimum electrode performance than Pitch A, and the electrodes produced with Pitch B performed better than the electrodes from Pitch A.

The plant-scale petroleum-coke aggregate was graded into the seven fractions shown in Table II. The appropriate weight of each fraction, corresponding to the percentage shown, was used in each binder-aggregate mix.

The major phases of the present investigation are as follows:

1. Determination of the maximum mix consistency for optimum binder concentration and optimum electrode properties. (The two binders were used in the preparation of mixes containing from 28 to 35 percent binder).
2. Investigation of the effect of mixing temperature and holding time on the mix consistency and electrode properties.

The Brabender Plastograph, shown in Figure 1, was used to prepare Soderberg mixes and measure their consistencies. A brief description of the operation of the instrument is given below. The sigma blades in the mixing head are driven by a dynamometer, which is suspended between floating bearings. The torque produced as the blades rotate in the mix at a constant rate of shear is transmitted to the dynamometer. The dynamometer translates the torque through a series of balance levers to a direct-reading balance, which is calibrated to indicate the torque in meter-gram units. A strip chart provides a continuous record of the consistency in terms of meter-gram units. Excessive movement of the lever system is dampened by an oil dash pot.

The mixing head has a working capacity of 650 milliliters. It is heated by recirculating hot oil from a constant-temperature bath through a jacket that surrounds the mixing head. A special insulated lid, not supplied by the instrument manufacturer, minimizes the loss of heat from the head and is an indispensable aid in maintaining the mix at a uniform temperature. Through a small opening in the lid, coke additions can be made without removing the lid.

In the determination of maximum mix consistency for optimum binder concentration and optimum electrode properties, mixes containing from 28 to 34 percent of Pitch A and mixes containing from 30 to 35 percent of Pitch B were prepared at 155 C. In all tests, the weight of the mix was held constant at 700 grams.

In the preparation of a typical mix, the calculated amount of binder is added to the preheated mixing head and is allowed to melt for eight minutes. The binder is then mixed for seven minutes to permit temperature equilibration. The 0.525-inch to 3-mesh fraction (preheated to 155 C) is then added through the opening in the insulated lid. The remaining fractions are added in the order of decreasing size at 5-minute intervals. This sequence of coke additions is used to (1) permit thorough wetting of the large coke particles before the addition

of fine particles to prevent uncoated fine particles from plugging the pores of the large particles and (2) minimize preferential absorption of binder by the fine particles. Mixing is continued for 30 minutes after the addition of the last coke fraction. The torque reading, in meter-grams, at the end of this mixing period is recorded as the consistency of the mix.

The temperature in the Soderberg electrode ranges from about 950 C at the lower working face to about 150 C at the top. As the electrode is consumed, it is lowered, and the unbaked mix in the upper end of the electrode is subjected to gradually increasing temperatures. To provide an indication of the effect of increasing temperature on the consistency of the mix and on the electrode properties, four mixes were prepared at temperatures between 155 C and 225 C. The optimum concentration of Pitch A was used with the mixing procedure previously described.

In the Soderberg electrode, temperature changes occur gradually, and a given portion of the unbaked mix may be subjected to a specific temperature for a relatively long period of time. The effect of time without mixing on the consistency of the mix was determined by repeating consistency measurements on the two mixes with the optimum concentration of Pitch A at 155 C and 225 C. At the conclusion of the normal mixing time, the mixer was stopped, and the mix was maintained at the mix temperature until the consistency approached the limit-of-scale value of 1000 meter-grams or 24 hours, whichever was shorter. Consistency measurements were recorded hourly.

All mixes were packed into perforated graphite molds and baked to 1000 C at a controlled rate of temperature rise in 24 hours. The baked electrodes were then tested for crushing strength and electrical resistivity. The procedure for baking and testing specimen electrodes has been described by Jones, Simon, and Wilt.⁴⁾

Results and Discussion

The relationship between the mix consistency and electrode crushing strength at various binder concentrations is shown in Figure 2. To illustrate this relationship, the experimental data are plotted in bar-chart form. The lined bars represent the consistency of the mix at various levels of binder concentration, and the dotted bars show the crushing strength of specimen electrodes from those mixes. The number at the bottom of each bar represents the percentage of binder in the mix.

This chart indicates that the Plastograph is sufficiently sensitive to detect changes in binder concentration as small as 1 percent and that a good correlation exists between the mix consistency and the electrode crushing strength. As the percentage of binder increases within the limits shown, the consistency and crushing strength values pass through a maximum simultaneously. This relationship indicates that the mix-consistency measurement can be used to predict the optimum binder content for optimum electrode crushing strength. For Pitch A, the optimum binder content for optimum electrode crushing strength is 32 percent and for Pitch B, the optimum binder content is 34 percent. These results correlate well with carbon-paste-plant data on these two binders.

The relationship between the mix consistency and the electrical resistivity of specimen electrodes is shown in Figure 3. A good correlation also exists between these parameters. For each binder, as the consistency values pass through a maximum, the resistivity values pass through a minimum. This relationship further substantiates the premise that the mix-consistency measurement can be used to determine the optimum binder content for optimum electrode properties.

The effect of temperature on the mix consistency and electrode crushing strength is illustrated in Figure 4. The mixes, prepared with 32 percent of pitch A, show successive decreases in consistency as the temperature of the mix increases. The decreasing consistency results from increased fluidity of the binder at the higher temperatures. Simultaneously, the electrode crushing strength increases with higher mix temperatures and lower consistencies. The increase in strength is particularly pronounced between 200 C and 225 C. The higher crushing strengths apparently result from the increased fluidity of the mix. The method described here would provide a suitable means of determining the temperature susceptibility of mixes prepared with various binders.

A susceptibility index (SI) could be calculated with the following equation:

$$SI = \frac{(\text{Consistency at } 155 \text{ C}) - (\text{Consistency at } 225 \text{ C})}{\text{Consistency at } 175 \text{ C}}$$

A low value for the susceptibility index (approaching zero) is indicative of a mix that is not sensitive to temperature change, whereas a high susceptibility index would be obtained with a temperature-sensitive mix.

The effect of hold time without mixing at two temperatures on the mix consistency and electrode properties is shown in Table III. When the mix is maintained at 155 C for 7.5 hours, the mix consistency increases from 600 meter-grams to 1000 meter-grams. Substantial improvements in the electrode crushing strength and electrical resistivity are noted. Similarly, at 225 C, the mix consistency increases from 190 meter-grams to 600 meter-grams in 24 hours, with significant improvements in electrode properties. The increased consistency and improved electrode properties resulting from extended time at high temperatures may be due to an aging or curing of the binder that is initiated or accelerated by the presence of the carbon aggregate. Similar effects probably occur in the Soderberg electrode as the unbaked mix is subjected to elevated temperatures for extended periods of time.

The rheology of the mix in the upper portion of the Soderberg electrode is strongly influenced by temperature and by the length of time the mix is exposed to elevated temperatures. Increased temperature tends to decrease the mix consistency, whereas an extended holding time without mixing at elevated temperatures tends to increase the consistency. The over-all effect of both factors is to improve the electrode crushing strength and electrical resistivity.

Summary

Consistency measurements on Soderberg mixes containing a plant-scale aggregate have been made, with a Brabender Plastograph. The consistencies were

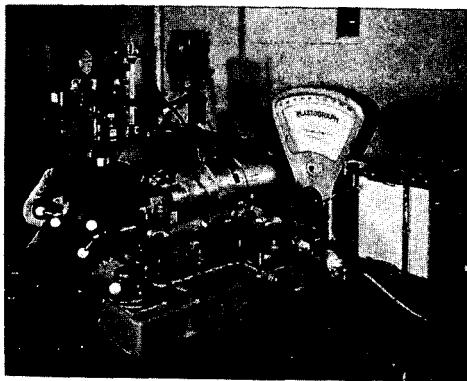
used to predict the optimum binder concentration for each of two binders. A different amount of each binder was required for optimum binder content and optimum electrode properties. This difference was verified by carbon-paste-plant data on the two binders. The effects of temperature and time on the mix consistency and electrode properties were also studied. Increased temperature tends to decrease the mix consistency, whereas consistency increases with an increase in holding time without mixing at elevated temperatures. The over-all effect of the two factors is to improve the electrode crushing strength and electrical resistivity.

Acknowledgment

The authors wish to express their appreciation to Aluminium Laboratories Limited of Canada, which supplied the samples used in this work.

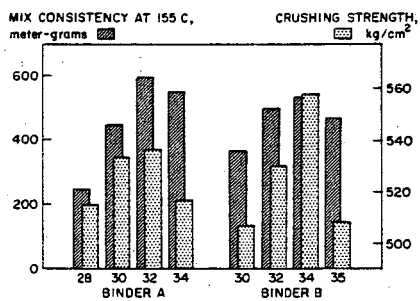
References

1. H. W. Nelson, "Viscosity Stability of Binders for Soderberg Electrodes," paper presented at New York City meeting of American Institute of Mechanical Engineers, February 18-22, 1962.
2. O. Bowitz, T. Eftestol, and R. A. Selvik, "New Methods for Testing Raw Materials for Anode Carbon Paste," paper presented at New York City meeting of American Institute of Mechanical Engineers, February 18-22, 1962.
3. F. A. Smith and A. J. Lombardo, "The Relationship Between the Consistency of the Green Electrode Mix and the Properties of Test Electrodes," paper presented at the New York City meeting of the Fuel Division of the American Chemical Society, September 11-16, 1960.
4. H. L. Jones, Jr., A. W. Simon, and M. H. Wilt, "A Laboratory Evaluation of Pitch Binders Using Compressive Strength of Test Electrodes," Journal of Chemical Engineering Data, 5, No. 1, pp. 84-87 (1960).



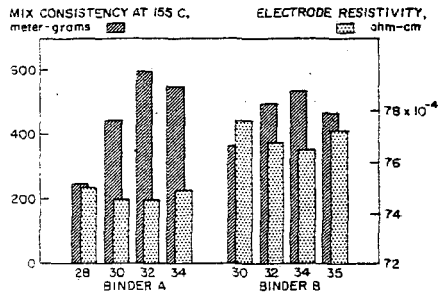
The Brabender Plastograph

Figure 1



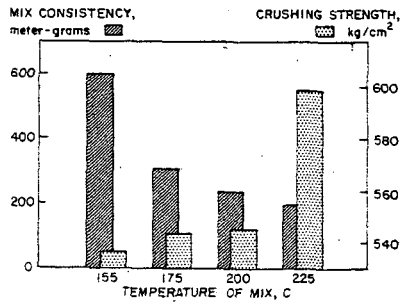
Relationship Between Mix Consistency and
Electrode Crushing Strength

Figure 2



Relationship Between Mix Consistency and Electrode Resistivity

Figure 3



Effect of Mixing Temperature on Mix Consistency and Electrode Crushing Strength

Figure 4

PROPERTIES OF PITCHES

	PITCH A	PITCH B
SOFTENING POINT (CIA), C	109.5	109.0
BENZENE INSOLUBLE, wt %	29.3	34.3
QUINOLINE INSOLUBLE, wt %	10.3	14.3
COKE VALUE (CONRADSON), wt %	58.5	58.3
SPECIFIC GRAVITY 60 F/60 F	1.32	1.29

Table I

PARTICLE-SIZE DISTRIBUTION
OF PETROLEUM-COKE

TYLER MESH SIZE	FRACTION SIZE, weight percent
-0.525 in. +3 MESH	5.0
-3 +4 MESH	5.0
-4 +10 MESH	15.0
-10 +20 MESH	10.0
-20 +48 MESH	15.0
-48 +200 MESH	20.0
-200 MESH	30.0

Table II

EFFECT OF TIME ON MIX CONSISTENCY
AND ELECTRODE PROPERTIES

TEMPERATURE, C	155		225	
	0	7.5	0	24
HOLD TIME, hours	600	1000	190	600
MIX CONSISTENCY, meter-grams	536	622	598	642
ELECTRODE STRENGTH, kg/cm ²	74.5	63.2	73.9	63.0
ELECTRODE RESISTIVITY, ohm-cm x 10 ⁻⁴				

Table III

RAPID TEST METHOD FOR THE DETERMINATION OF THE BENZENE-
AND QUINOLINE-INSOLUBLE CONTENT OF PITCHES

R. W. Domitrovic, R. M. Stickel, F. A. Smith

Applied Research Laboratory
U. S. Steel Corporation
Monroeville, Pennsylvania

Introduction

Tests to determine the amount of benzene- and quinoline-insoluble matter in pitch are widely used by producers and consumers of pitch. For example, several thousand solvent-insolubles tests are performed annually at U. S. Steel's pitch-producing facilities. The present test method for determining the benzene-insoluble content of pitch is based upon a test that was developed by the Barrett Company (presently a division of Allied Chemical Corporation).

Briefly, the Barrett procedure involves digestion of the pitch sample in toluene, filtration, and then extraction of the residue in refluxing benzene. Because of the time-consuming extraction phase, the Barrett test requires in excess of 24 hours to complete. The undesirability of lengthy analytical procedures, especially in plant control work, prompted the Applied Research Laboratory of U. S. Steel to develop a rapid benzene-insolubles test that could be completed in about 6 hours.

This paper describes the salient features of the rapid method for determining the benzene-insoluble content of pitch. A rapid method for determining quinoline insolubles is also described and discussed briefly.

Experimental Work

The Barrett method for determining benzene insolubles is an empirical method that has been used throughout the industry over a number of years and has been accepted as a more or less standard procedure. To date, no ASTM (American Society for Testing Materials) test method for benzene insolubles has been devised. In developing a rapid method, the following objectives were fixed: (1) The time required to complete the test should be 8 hours or less. (2) The values obtained by the new method should be equivalent to those obtained by the Barrett method. (3) The general principles of digestion and extraction should be retained.

The rapid benzene-insoluble test closely duplicates the Barrett method in all phases except that the size-consist of the particles in the sample is controlled and the reflux extraction apparatus and technique are changed. A number of modifications have been made in the procedure and in the design of the apparatus. These changes provide the same degree of extraction as the Barrett method but in much less time. The apparatus used in each method is shown in Figure 1. In the new method, the special extraction flask and the filter paper thimble of the Barrett test are replaced with the more modern and versatile Soxhlet extraction apparatus and Soxhlet paper extraction thimble.

Important added features of the Soxhlet extraction apparatus are shown in Figure 2. The wire spacer, which rests on the bottom of the extraction cup of the Soxhlet apparatus, positions the thimble so that the middle of the thimble is at the top of the siphon tube. This provides an adequate liquid level in the thimble and at the same time prevents loss of sample through overflow. A reflux guide, built onto the bottom of the condenser, directs all of the refluxing stream into the thimble. Without the guide, considerable solvent by-passes the thimble.

The coal-tar pitches selected for use in this study represent a wide range (15 to 35 wt %) of benzene-insoluble contents. Table I shows some of the more common properties of these pitches. Three of the pitches were obtained from tars recovered during the high-temperature carbonization of bituminous coal. The fourth pitch was produced from tar from the low-temperature carbonization of sub-bituminous coal. The table shows the benzene-insoluble content of the pitches as determined by the Barrett method.

In the new rapid method, standard sampling procedures (ASTM D 140-55 and ASTM D 346-35) are followed to insure that the portion used for analysis is representative of the pitch sample. In addition, when the pitch is sufficiently hard it is ground to pass through a U. S. No. 60 sieve and the test sample is collected from material retained on a U. S. No. 100 sieve. This is done to obtain a sample with a particle size (0.0058-in. to 0.0082-in. diameter) that will insure good solvent contact. The particles should be sufficiently small so that the solvent can be rapidly absorbed, but not so small that agglomeration or packing of fines can prevent or retard solvent contact. The sample size is adjusted to yield approximately 0.25 gram of insoluble material (usually 1 or 2 grams). The sample is weighed into a beaker and digested in 60 milliliters (ml) of toluene for 30-minutes on a steam bath. The contents of the beaker are then transferred to a 30- by 77 mm (single weight) Soxhlet extraction thimble that has been previously tared in a weighing bottle. The thimble is placed in a crucible holder over a beaker and the insoluble matter is transferred to the thimble by the use of a brush and a small amount of toluene. Figure 3 shows this operation. When the liquid portion of the suspension has passed through the thimble, the thimble is washed with benzene and then placed into a 44-mm Soxhlet apparatus for extraction. Heat is applied gradually to the flask to avoid the possibility of liquid erupting into the extraction tube. The gradual heatup period requires approximately 15 minutes and the close attention of the operator. Once the desired throughput is achieved, the test will proceed practically unattended. The extraction is conducted for a total of 4 hours with a siphoning cycle of approximately three minutes. This approximates a solvent reflux rate of about 1800 ml per hour. At the end of this period the thimble is removed, air-dried for 15 minutes, oven-dried for 30 minutes at 105 C, cooled in a desiccator, and weighed. Six hours are required to complete the determination of the amount of sample insoluble in benzene.

Results and Discussion

Several steps were involved in arriving at the proper operating conditions for the Soxhlet extractor. They were (1) determination of the permeability of the Soxhlet thimble relative to the filter-paper thimble, (2) establishment of the maximum throughput capacity for benzene in the Soxhlet apparatus, and (3) establishment of the throughput of benzene in the Barrett apparatus when operating at the recommended boilup rate.

That the Soxhlet thimble is no more permeable to the retained insoluble matter than is the filter-paper thimble was established by an experiment in which the Soxhlet thimble was used in the extraction apparatus of the Barrett method. This experiment showed that the use of the Soxhlet thimble gave results identical to those obtained in a test in which the filter-paper thimble was used.

The Soxhlet thimble was found to be capable of handling all the benzene returned to the siphon cup of the Soxhlet extraction apparatus at maximum boilup, which was 1800 ml per hour.

The average throughput of benzene in the Barrett test (about 80 drops per minute) is about 6600 ml in 24 hours. At maximum boilup, the Soxhlet apparatus required slightly less than 4 hours to reflux the same quantity of benzene.

Another matter that was considered concerned the temperatures to which the samples were subjected in the rapid test. Since the exterior of the thimble in the Soxhlet apparatus is partially immersed in the benzene condensate during a portion of the extraction cycle, it was conceivable that the condensate could lower the temperature of the contents of the thimble. In the Barrett apparatus, the thimble is constantly bathed by solvent vapors and refluxing solvent. To ascertain whether there was a temperature difference, an experiment was performed in which thermocouples were suspended in the liquid and vapor portions of the solvent in an operating Soxhlet extractor. After the first few siphon cycles, the temperature differential was within one degree Centigrade. A thermocouple was also suspended in the vapor portion of the Barrett apparatus and it was established that the vapor temperatures were the same in both apparatus.

The rapid benzene-insolubles test was performed by each of three operators, who conducted three duplicate tests on each pitch sample, to establish the repeatability of the test. The results of the tests are shown in Table II and plotted in Figure 4. The horizontal line across the center of the chart in Figure 4 represents a scale for benzene-insolubles values as determined by the Barrett test method. The points on the scale are the average of three duplicate determinations for benzene-insoluble contents of the four samples when tested by the Barrett method. The vertical scale represents the deviation, expressed in percentage of sample, from the values obtained by the Barrett method (the horizontal center line). The lines digressing from the horizontal center line represent the limits of reproducibility as established by the Barrett method. This is expressed in percentage of sample as $0.1 + 0.05 \times$ percent insoluble matter in benzene. The points above and below the center line represent the values obtained by the rapid benzene-insolubles method. The different symbols represent different operators and each point represents a mean value as determined from the values of duplicate tests; as stated before, each operator performed three duplicate tests or six tests per pitch sample, to obtain three mean values for comparison with the standard value (center line).

As may be seen on the graph, most of the values obtained by the rapid procedure fall within the limits of reproducibility set for the values by the Barrett method.

Mean and standard deviation values for each of the pitches analyzed by the rapid method are shown in Table III.

Because of the exceptionally good reproducibility and the savings in time, we feel the rapid test method for benzene insolubles is a good replacement for the Barrett test method.

Quinoline Insolubles

The less time-consuming a quality control test or specification test is, the more desirable it is. Even though the commonly used method for determining the portion of sample insoluble in quinoline requires only about 3 hours to complete, the possibility of shortening the time requirement was investigated. As in the investigation of the rapid benzene-insolubles test, the objectives included the limitation that the empirical values as obtained by the presently used procedure would be duplicated, and that the general principles of digestion and extraction should be retained.

A test meeting these requirements was developed which could be completed in less than 1 hour. The new rapid procedure differs little from the old procedure in principle. Time requirements were decreased by changing the techniques of extraction and drying.

Experimental Work

The pitch samples tested were the same as those used in the benzene-insolubles study. Also, the same techniques of sample preparation were followed.

In the rapid quinoline-insolubles test, a weighed sample of sufficient size to yield 0.1 gram of insoluble material is digested with hot (170 C) quinoline for two minutes. The digested sample is then filtered with the aid of suction, as shown in Figure 5, through a Selas crucible (fine porosity) containing a quantity of diatomaceous filter aid. When substantially all of the material has been transferred from the beaker to the crucible, the beaker is rinsed with 20 ml of hot (170 C) quinoline; this material is also transferred to the crucible. Any particles that adhere to the beaker are washed into the crucible with benzene. The filter cake in the crucible is then washed with 80 ml of benzene and then with 80 ml of acetone. After the acetone wash, the filter cake is dried while still under suction by means of a 250-watt infrared lamp mounted about 12 inches above the crucible. This operation should be conducted in a well ventilated hood, to remove the small amount of acetone vapors that are evolved. When dry (about 15 minutes), the crucible is cooled in a desiccator and weighed.

Results and Discussion

To develop a rapid quinoline-insolubles test method that would retain the basic principles of the old method, it was necessary to reduce the time requirement by altering the techniques of operation. One area studied was the conditions of digestion. It was determined that increasing the temperature of the quinoline from 80 C to 170 C and shortening the time of digestion from 20 to 2 minutes did not alter the end result. Adding an acetone wash to the procedure shortened the drying process. The acetone removes benzene, which is more difficult to vaporize, from the quinoline-insoluble matter. Subsequent removal of the acetone was quickly accomplished by the application of heat from a heat lamp. Further time savings were derived by using previously dried crucibles and filter-aid material. The sum of these time savers resulted in a rapid method that required less than 1 hour to complete as opposed to the 3 hours for the old method.

Table IV and Figure 6 show the results of rapid quinoline-insolubles tests as determined by three operators. The horizontal line across the center of the chart represents a scale for quinoline-insolubles values as determined by the old method of test. The points on the scale are the average of three sets of duplicate determinations of quinoline-insoluble contents of the four samples tested by the old method. The vertical scale represents the deviation, expressed in percentage of sample, from the values by the old method (the horizontal center line). The lines digressing from the center line represent the limits of reproducibility as established by the old method. This is expressed in percentage of sample as $0.10 + 0.02 \times$ percent insoluble matter in quinoline. The points above and below the center line represent the values obtained by the rapid quinoline-insolubles method. The different symbols represent different operators and each point represents a mean value as determined from the values of duplicate tests. Each operator performed three duplicate tests, or six tests per pitch sample, to obtain three mean values for comparison with the standard value or center line.

As was true with the benzene-insolubles values, nearly all the quinoline-insolubles values obtained by the rapid method fall within the limits of reproducibility set for the values obtainable by the old method for quinoline insolubles.

Mean and standard deviation values for each of the samples analyzed by the rapid method are shown in Table V.

Summary

Methods have been developed for the rapid determination of benzene- and quinoline-insolubles in pitches. The rapid benzene-insolubles test requires 6 hours to complete as compared to the 24 hours necessary for the generally used Barrett method. The rapid quinoline-insolubles test requires 1 hour to complete as opposed to 3 hours for the old method. Results obtained with the rapid test methods correlate well with those of the standard methods. It is hoped that the time advantages gained warrant the consideration of these rapid tests as acceptable methods for analysis of benzene- and quinoline-insoluble matter.

Table I
Properties of Pitches

	Pitch			
	A	B	C	D
Benzene Insolubles, wt %	14.73	22.57	33.94	35.42
Quinoline Insolubles, wt %	2.25	9.98	12.23	28.99
Softening Point, C	78.3	105.5	117.5	64.9
Coke Value, wt %	42.5	56.0	58.9	35.8

Table II
Results of Benzene-Insolubles Determinations

Rapid Method		Pitch, wt %							
		A		B		C		D	
Operator	Run No.								
I	1	14.17		21.72		32.60		36.09	
	2	14.26	14.22*	21.80	21.76	32.39	32.50	35.60	35.85
	3	14.50		21.61		34.62		36.01	
	4	13.85	14.18	22.46	22.04	34.39	34.56	36.10	36.06
	5	14.82		21.41		33.70		34.90	
	6	15.22	15.02	22.40	21.92	33.50	33.60	34.82	34.86
II	1	13.86		22.50		33.55		37.29	
	2	14.13	14.00	23.44	22.97	33.33	33.54	36.63	36.96
	3	13.89		21.61		33.53		36.84	
	4	13.37	13.63	21.41	21.51	33.59	33.55	36.56	36.70
	5	14.52		22.57		32.92		36.33	
	6	14.69	14.50	23.22	22.90	33.17	33.04	36.53	36.43
III	1	14.40		22.06		32.20		36.36	
	2	14.37	14.39	22.02	22.04	33.83	33.02	36.91	36.64
	3	15.40		23.38		33.77		36.19	
	4	15.31	15.35	23.64	23.51	34.24	34.00	35.83	36.01
	5	15.08		22.56		35.05		35.74	
	6	15.97	15.53	21.85	22.20	34.94	35.00	35.14	35.44
<u>Barrett Method</u>		14.73		22.57		33.94		35.42	

* Mean values

Table III

Statistical Data for the Rapid Benzene-Insolubles Test

	Pitch			
	A	B	C	D
Number of Runs	18	18	18	18
Mean	14.53	22.31	35.57	36.10
Standard Deviation	0.663	0.718	0.912	0.682

Table IV

Results of Quinoline-Insolubles DeterminationsRapid Method

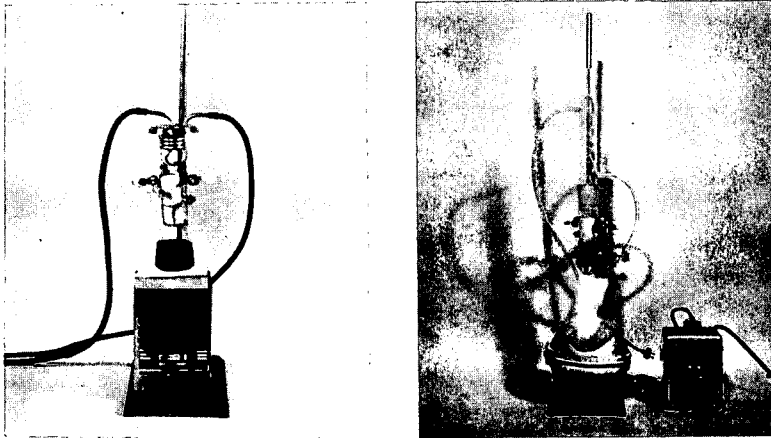
Operator	Run No.	Pitch, wt %							
		A		B		C		D	
I	1	2.20		10.21		12.16		29.46	
	2	2.22	2.21*	10.26	10.24	12.17	12.17	29.98	29.22
	3	2.31		10.23		12.20		28.07	
	4	2.33	2.32	10.23	10.23	11.99	12.10	28.41	28.24
	5	2.17		10.15		12.11		28.50	
	6	2.15	2.16	10.16	10.16	12.23	12.17	28.54	28.52
II	1	2.33		10.26		12.17		28.99	
	2	2.30	2.32	9.74	10.00	12.18	12.18	28.86	28.94
	3	2.28		10.20		12.93		28.95	
	4	2.30	2.29	10.23	10.22	12.79	12.86	28.90	28.93
	5	2.28		10.24		11.93		28.92	
	6	2.27	2.28	10.17	10.20	12.94	12.44	28.85	28.89
III	1	2.33		9.84		12.31		28.47	
	2	2.45	2.39	10.05	9.95	13.27	12.79	28.76	28.62
	3	2.22		10.13		12.13		28.64	
	4	2.35	2.29	10.11	10.12	12.69	12.41	28.79	28.72
	5	2.45		10.29		12.27		28.38	
	6	2.32	2.40	10.32	10.30	12.23	12.25	28.33	28.36
<u>Barrett Method</u>		2.25		9.98		12.23		28.99	

* Mean values

Table V

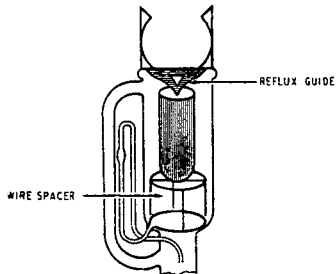
Statistical Data for the Rapid Quinoline-Insolubles Test

	Pitch			
	A	B	C	D
Number of Runs	18	18	18	18
Mean	2.29	10.16	12.38	28.71
Standard Deviation	0.081	0.150	0.377	0.325



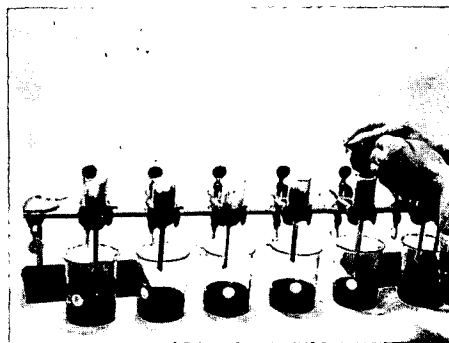
Extraction Apparatus for Benzene-Insolubles Tests

Figure 1



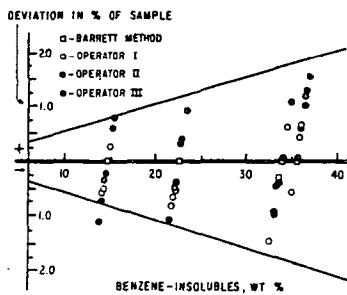
Modifications of Soxhlet Extractor
for Rapid Benzene-Insolubles Test

Figure 2



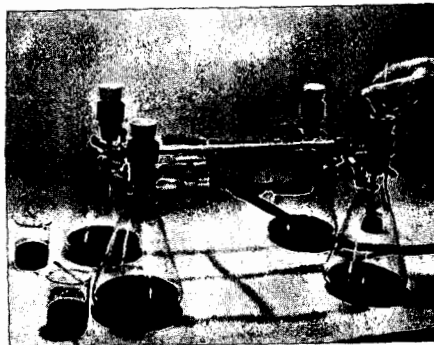
Transferring Insoluble Matter to Thimbles in
Rapid Benzene-Insolubles Test

Figure 3



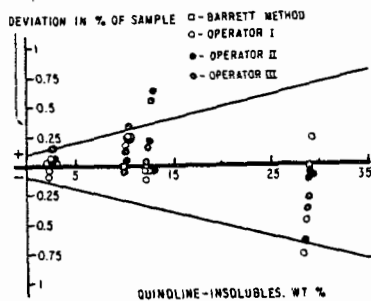
Statistical Data for Benzene-Insolubles Test

Figure 4



Quinoline-Insolubles Filtering Apparatus

Figure 5



Statistical Data for Quinoline-Insolubles Test

Figure 6

RECENT ADVANCES IN THE CHEMICAL CONSTITUTION OF COAL

B. K. Mazumdar and A. Lahiri,
Central Fuel Research Institute, Jealgora,
Dhanbad, India

The problem of chemical constitution of coal has long remained an intractable one but intensive work carried within the last decade in particular has steadily revealed important information on the structural pattern of coal. Since 1952 the concept of the structural parameters has emerged and, broadly speaking, whatever has been achieved so far mainly concerns this aspect of coal structure. By structural parameters is generally meant the state of combination of carbon, hydrogen and oxygen and their distribution in the average structural 'unit'. Such knowledge has been obtained from various physical studies e.g. x-ray¹⁻⁸, infra-red⁹⁻¹¹, nuclear magnetic resonance (n.m.r.)¹²⁻¹⁴, proton spin resonance (p.s.r.)¹⁵, electron spin resonance (e.s.r.)¹⁶⁻¹⁸ and statistical techniques¹⁹⁻²³ involving density, refraction, sound velocity, magnetic susceptibility²⁴ and other properties.

Recently a number of chemical techniques²⁵⁻⁴⁰ have been developed in these laboratories to assess the structural parameters in coal as revealed by physical measurements. In the main, these constitute oxidation, pyrolysis, and dehydrogenation and have led to important information on the state of combination of carbon and hydrogen in coal as well as on the size of the aromatic nucleus.

AROMATIC CARBON IN COAL:

Carbon is the predominant element in coal and the major part of it is believed⁴¹ to be aromatic in character.

Two chemical techniques, namely, oxidation^{25,28} and pyrolysis³¹, have been employed by the authors for the quantitative measurement of the aromatic carbon. It is believed that by these methods of treatment the non-aromatic structure is preferentially oxidized or devolatilized leaving the aromatic skeleton of coal unaffected. It may as well be that the mechanisms of oxidation or pyrolysis of coal are not as simple as that. Hence, in more recent work^{42,43} further support of the validity of the oxidation and pyrolysis techniques has been obtained by applying the methods on reduced coals. This is because in reduced coals the essential features of the original structure are believed to be retained, but the distribution of carbon and hydrogen in two forms, aromatic and non-aromatic, are altered.

A series of vitrains were reduced with lithium and ethylenediamine following the technique of I. Wender⁴⁴ and his co-workers. This treatment creates fresh hydroaromatic structure at the expense of the aromatics. The aromaticity of reduced coals can be theoretically calculated from the amount of hydrogen added during reduction provided that the aromaticity of the original coals as determined by chemical techniques are assumed to be correct. The aromaticity of the reduced coals as determined by oxidation as well as by pyrolysis studies have been found to be in excellent agreement with the theoretical values as reproduced⁴²⁻⁴³ in Tables 1, 2.

Recent physico-chemical deductions^{45,46,50,66,68} based on infra-red^{4,9} and n-m-r¹³⁻¹⁴ data especially those⁴⁵⁻⁴⁶ put forward by the authors (Table 3) also give values of aromaticity which are in good agreement with those determined by the chemical methods of oxidation and pyrolysis (Fig.1). The values of aromaticity obtained by chemical techniques can perhaps be taken to be more precise than those deduced earlier by physical techniques.

Now that a precise estimate of aromaticity is available from chemical methods, it is of interest to compare such values with those earlier assessed by a number of physical techniques. Such comparison is depicted in Fig. 2. It is found that the values of "ordered" carbon obtained by x-ray diffraction studies³ closely fall in line with the most acceptable values of aromaticity. Assessment of non-aromatic structure and hence of the aromatic by infra-red studies is rendered difficult because of the lack of precise data on extinction coefficient ratio required for computation. Thus no firm values of aromaticity could be obtained by such methods. The preferred values of aromaticity obtained by I.G.C. Dryden⁴⁷ by a study of the self-consistency between several physical techniques are about 5 to 10 per cent higher than those directly obtained by chemical studies and cannot be reconciled with the values of alicyclicity obtained by the authors³⁷. The values of aromaticity deduced by any of the statistical techniques made by van Krevelen and co-workers¹⁹⁻²³ are also 10-15 per cent higher than those obtained later by chemical techniques (Fig. 1). Their values of aromaticity can also not be reconciled with the most preferred values of alicyclicity (determined in these laboratories), because the sum of the two exceeds the total carbon in coal (Table 4). If the amount of methyl carbon is taken into consideration the discrepancy would increase still further.

It will be of interest to note that the differences between values of aromaticity obtained by different techniques are greater in the case of coals of lower rank, but they tend to narrow down for higher rank coals. This may perhaps be explained by the inherent difficulties in the accurate measurement of the physical parameters owing to the possible interference by the presence of more oxygenated groups in coals of lower rank.

NON-AROMATIC CARBON IN COAL

(a) Alicyclic Combination

Information about the disposition and character of the non-aromatic carbon in coal has recently been obtained by the authors by a series of dehydrogenation studies³²⁻⁴⁰. It has been shown that the non-aromatic structure of coal is predominantly alicyclic.

The first estimates of alicyclicity³²⁻³³ were obtained by employing Vesterberg's technique of dehydrogenation. The results so obtained were confirmed by another method of dehydrogenation with iodine. These estimates indicated that broadly 10-25 per cent of the carbon is in alicyclic combination in the bituminous range (carbon : 80-90 per cent). The alicyclicity progressively diminishes with increase in rank and is practically non-existent in the anthracite stage.

Subsequently, M.E. Peover⁴⁸ introduced the benzoquinone method of dehydrogenation and obtained much higher results. It has recently been shown by the authors³⁷ that the higher estimates of Peover may have been due to some systematic error in the polarographic determination of hydroquinone produced as a result of the dehydrogenation of coal. In fact, an investigation of the benzoquinone method in these laboratories has shown that the three methods of dehydrogenation viz. by sulphur, iodine and benzoquinone are comparable in so far as the extent of dehydrogenation possible in different ranks of coal (Table 5).

Further, the applicability of Vesterberg's technique in the dehydrogenation of coal structure has been corroborated by determination of hydroaromaticity in reduced coals. It has been found⁴⁹ that the freshly created hydroaromatic structure in the reduced coals undergoes dehydrogenation with sulphur quantitatively, apparently without any side reactions. These results are reproduced in Table 6.

Thus, the values of alicyclicity originally presented³²⁻³³ from these

laboratories in 1958 should be treated as largely correct (Fig.3)*. In fact, the amount of hydrogen which could be added to coal at any stage of reduction could be quantitatively removed⁴⁹ during dehydrogenation with sulphur (Table 6). This indicates that coal structure is perhaps unique in its chemical reactivity and that the estimates of alicyclicity obtained by treatment with sulphur are possibly the maximum values.

An immediate consequence of dehydrogenation studies has been the recognition of the fact that the sum of aromatic and alicyclic carbon appears to be virtually constant at the level of 92 per cent of the total carbon in coal, irrespective of its rank, from lignite to the highest rank bituminous coal. The same conclusion repeatedly emerged from the pyrolysis studies on dehydrogenated coals and coals pre-treated with different chemical reagents⁵⁷. The aromaticity progressively increases at the expense of the alicyclic structure, with increase in rank and this appears to be the principal mechanism⁴⁰ involved in geo-chemical metamorphism of coal in the bituminous range. The implications of this concept has been discussed elsewhere⁴⁰ and has possibly led to a better understanding of the pattern of coal structure and its variation during the genesis of coal. The physico-chemical deductions later made by A.F. Gaines⁵⁰ as well as by the present authors⁴⁵⁻⁴⁶ (Table 3) also point to this constant feature of coal structure.

(b) Aliphatic Combination

As the aromatic and alicyclic carbon constitute about 92 per cent of the total carbon in coal, the aliphatic carbon would amount to about 8 per cent. Attempts made by several workers⁵¹⁻⁵³ to estimate the methyl groups in coal by employing Kuhn-Roth reaction have indicated that hardly 3-4 per cent of the carbon is possibly present in this form. This leaves another 4 per cent of the carbon unaccounted. From certain structural considerations the present authors suggested earlier that this unaccounted carbon could also be present^{27,40} in the form of methyl groups. It is well-known that Kuhn-Roth method cannot be applied for the quantitative determination of β -methyl groups linked to aromatic structure and hence estimates of β -methyl groups by such procedure can only be minimum values.

From recent p.s.r. measurements made by Oth & Tschamler¹⁵ it appears that 30-35 per cent of hydrogen may be present as constituents of β -methyl groups in coal. This is consistent with the authors' view that about 8 per cent of carbon in coal is present as methyl groups. Recent physico-chemical deductions⁴⁵ made by the present authors also lead to a similar conclusion (Table 3).

Nevertheless, direct experimental proof for the above supposition is yet to come. In this context the question of the probable presence of angular methyl groups in coal structure cannot be disregarded in view of strong indications for the same from dehydrogenation studies³³.

* van Krevelen et al.⁵⁷ had questioned the validity of Vesterberg's technique in the selective dehydrogenation of the alicyclic structure. Further studies^{38,39} made since then indicated that side-reactions, if any, appeared to be minor and, accordingly, a revised estimate of minimum alicyclicity was presented. However in more recent studies⁴⁹ by the authors on reduced coals, it appears that, in so far as coal dehydrogenation is concerned, the Vesterberg's technique is possibly specific in the dehydrogenation of the alicyclic structure. A fuller account of the recent developments is being presented elsewhere⁴⁹.

HYDROGEN IN COAL

From chemical studies attempts have also been made to determine the different forms of hydrogen in coal, aromatic, alicyclic and aliphatic. Oxidation and pyrolysis techniques have enabled measurements of hydrogen broadly in two forms - aromatic and non-aromatic. Such measurements are not in good agreement with those assessed by infra-red studies. The discrepancy between these two sets of estimates is possibly due to inherent difficulties in the measurements of optical density and its interpretation which requires precise values for the extinction coefficient ratio. The estimates of aromatic and non-aromatic hydrogen made by the authors by oxidation and pyrolysis are mutually consistent (Fig.4). Further, it has been recently shown elsewhere⁵⁴ that the same techniques of oxidation and pyrolysis can also be successfully employed to determine the altered distribution of hydrogen in reduced coals. It may, therefore, be concluded that the variation of hydrogen in aromatic and non-aromatic form with increase in rank as determined by chemical methods by the authors can be considered the most acceptable at the moment. Such determinations were also reported by Van Krevelen⁵⁵ a few months later but only by the pyrolysis technique: his results are in agreement with the authors' values and are also shown in Fig.4. Probably re-assessment of the extinction coefficient ratio in case of infra-red results may reconcile the discrepancy between the two sets of estimates, made by physical and by chemical methods. J.K. Brown et al^{10,11} have claimed to have given support to their preferred values of extinction coefficient ratio on the basis of recent studies on coal distillates, but such vacuum distillate of coal may not represent the coal structure. It has been earlier shown³⁴ by the authors (and which has been recently confirmed⁵⁶) that such distillates primarily originate from the alicyclic structure in coal (Fig.5).

AROMATIC RING SIZE IN COAL

Coal is believed to have a polymeric or perhaps poly-condensate assemblage of structural units of varying dimensions. The measurement of the size of aromatic clusters in such structural 'units' is as important as the study of the state of combination of carbon and hydrogen. By oxidation studies the authors had also attempted an assessment of the average size of aromatic nuclei. According to the mechanism of oxidation suggested by the authors, the final oxidised residue of coal is believed to retain the aromatic skeleton of coal. Hence the atomic H/C ratio of the hypothetical unsubstituted aromatic skeleton corresponding to the oxidised coal would give a measure of the average size of the aromatic nuclei. It has been found²⁷ that the average size of aromatic nuclei does not vary much in the bituminous range (carbon: 80-90%) and is possibly constituted of 4 to 5 poly-condensed benzene rings per mean structural unit (Table 7). Earlier studies on x-ray diffraction³ and on diamagnetic susceptibility²⁴ of coals led to similar assessments. Recent measurement of electron activation energy⁵³ also support the above estimates. In view of the consistency between the physical and chemical measurements (Table 7) it may, therefore, be concluded that possibly a fair estimate of the size of the aromatic units is now available.

Mild hydrogenolysis of coal extract, residue or coal itself by B.S. Biggs⁵⁹, B.S. Biggs and J.F. Weiler⁶⁰ as well as by J. Le Claire⁶¹ had also led to the recognition (1936-37) that the 'units' of coal structure must be small in size. The isolation of dodeca- and tetradeca-hydrophenanthrene and hexadeca- and octadeca-hydrochrysene corresponding to 3-4 ring systems would now appear to be significant in the light of measurements of aromatic ring size by physical and chemical methods.

DISCUSSION

The techniques of selective oxidation and pyrolysis in conjunction with dehydrogenation studies have possibly yielded the most acceptable information on the state of combination of carbon and hydrogen as well as on the size of the aromatic nucleus. The knowledge that has been acquired is summarised in Table 8.

Perhaps the time has now come for reorientation of the studies on the consti-

tution of coal. There are still many gaps in our knowledge which have to be bridged before the macro-molecular structural pattern of coal can be precisely depicted. Such problems that remain to be solved are :

- (i) Whether coal is a polymer in the typical sense;
- (ii) If so, what is the nature of the polymer, especially the nature of linkage between the 'units' of coal structure;
- (iii) The specific sizes of the individual structural 'units' of coal, in particular, the distribution of molecular weights among such 'units' which may not be all identical.

Information on the polymeric character of coal has been forthcoming from ⁵² studies on solvent extraction and those on hydrogenolysis. R.A.Glenn and co-workers, from a study of the liquid products obtained from hydrogenolysis, were led to conclude that coal structure has possibly repetitive units just as in a typical polymer. Confirmation of this polymeric concept has also possibly emerged from the recent studies of the authors⁶³ on the reaction of permanganate on coal. It has been shown that at any stage of degradation the residual coal left over after reacting coal with either acidic or alkaline permanganate retains virtually the same physical and chemical properties as that of the original coal (Table 9). This could perhaps be explained as a case of depolymerisation of the coal structure, followed by decomposition of the fragments into water soluble products like carbon dioxide, oxalic acid and benzene polycarboxylic acids.

The next stage is obviously to have adequate information about the actual repetitive 'units'. This can only be possible by isolation of the 'units' of coal by depolymerisation and determination of molecular weights of the 'units' thus isolated.

Another equally important knowledge to be sought is about the nature of linkage between the 'units'. Little or no information is available on this aspect at the moment. Studies on the mechanism of solvolysis of coal in organic solvents and of the dispersibility of coal in alkali (especially in lower ranks of coal) may reveal useful information.

In 1957 the authors⁶⁴ had indicated that the dissolution of lignite in alkali, even at room temperature is not merely a physical process but is probably preceded by hydrolytic splitting of bonds between the 'units'. It was suggested that in lignite (and in coal) the part that gives rise to humic acid and the residual part are possibly linked by flavone or similar type of linkage (e.g. pyrone, lactone, etc.) which are susceptible to cleavage in presence of alkali. However, it is premature to conclude anything definitely but it is believed that further work on these lines and others may throw greater light on this important aspect of coal structure. A fuller knowledge of the nature of the 'unaccounted' oxygen in coal vis-a-vis the dispersibility of coals in alkali, and of the mechanism of regeneration of humic acids from mature coals, may also be of help.

Besides the above basic considerations, we have yet to know more precisely about the character of nitrogen and sulphur. They are minor elements in coal but are believed to be integral parts of the coal structure. Information on the state of nitrogen has been scanty, though, of late, it has been suggested⁶⁵ that it may be largely present as functional groups. About sulphur, our knowledge is even less exact. The states of combination of these minor elements in coal are just as important as those of carbon and hydrogen.

ACKNOWLEDGEMENT

The authors are grateful to Mr. S.Majumdar, Chief Information Officer, Central Fuel Research Institute, for many valuable suggestions and help in effective

presentation of the present review. Thanks are due to Mr. A.J. Bhattacharyya for help in literature survey and in compilation of the manuscript.

BIBLIOGRAPHY

1. NELSON, J.B. - X-ray Studies of the Ultrafine Structure of Coal - II. Atomic Distribution Function of Vitrinite from Bituminous Coals, *Fuel*, 1954, 33, 153, 381.
2. HIRSCH, P.B. - X-ray Scattering from Coals, *Proc. Roy. Soc. A.*, 1954, 226, 143.
3. HIRSCH, P.B. - Conclusions from X-ray Scattering Data on Vitrain Coals, *Proc. Sheffield Conf. on "Science in the Use of Coal"*, The Institute of Fuel, London, 1958, p.A. 29.
4. BROWN, J.K. and HIRSCH, P.B. - Recent Infra-red and X-ray Studies of Coal, *Nature*, 1955, 175, 229.
5. GARTZ, L, DIAMOND, R and HIRSCH, P.B. - New X-ray Data on Coals, *Nature*, 1956, 177, 500
6. DIAMOND, R. - X-ray Studies of Some Carbonised Coals (Ph.D. Thesis, University of Cambridge, 1956).
7. DIAMOND, R - X-ray Diffraction Data for Large Aromatic Molecules, *Acta, Cryst.* 1957, 10, 359.
8. RULAND, W. and TSCHAMLER, H., Rontgenographische Bestimmung der Aromatgrobenverteilung in einem Vitrit und Seinen Extraktionsproducten, *Brennstoff-Chemie*, 1958, 32, 363.
9. BROWN, J.K. - Infra-red Spectra of Coals, *J. Chem. Soc.(Lond.)*, 1955, 744.
10. BROWN, J.K. and LANDER, W.R. - A Study of the Hydrogen Distribution in Coal-like Materials by High-resolution Nuclear Magnetic Resonance Spectroscopy II - Comparison with Infra-red Measurement and the Conversion to Carbon Structure, *Fuel*, 1960, 39, 87.
11. BROWN, J.K., LANDER, W.R. and SHEPPARD, N. - A Study of the Hydrogen Distribution in Coal-like Materials by High-resolution Nuclear Magnetic Resonance Spectroscopy - I - The Measurement and Interpretation of the Spectra, *Fuel*, 1960, 39, 79.
12. BELL, C.L.M., RICHARDS, R.E. and YORKE, R.W. - Nuclear Magnetic Studies on Coal Structure, *Brennstoff-Chemie*, 1958, 32, 30.
13. LANDER, W.R. and STAEY, A.E. - A Proton Magnetic Resonance Study of Coals and Some Soluble Fractions of Coal, *Fuel*, 1961, 40, 295.
14. LANDER, W.R. and STAEY, A.E. - Some Discussion on Possible Coal Structures - *Fuel*, 1961, 40, 452.
15. OPH, J.F.M. and TSCHAMLER, H. - Comparison and Interpretation of Proton Spin Resonance Measurement on a Coal Extract in the Solid State and in Solution, *Fuel*, 1961, 40, 119.
16. INGRAM, D.J.E., PAPLEY, G.G., JACKSON, R., BOND, H.L. and MURNAGHAN, A.R. - Paramagnetic Resonance in Carbonaceous Solids, *Nature*, 1954, 174, 797.
17. UEBERSFELD, J., ETIENEN, A., and COMBRISON, J. - Paramagnetic Resonance, a New Property of Coal-like Materials, *Nature*, 1954, 174, 614.

18. SMIDT, J. and VAN KREVELEN, D.W. - Chemical Structure and Properties of Coal - XXIII - Electron Spin Resonance of Vitrains, Fuel, 1959, 38, 355.
19. VAN KREVELEN, D.W. and CHERMIN, H.A.G. - Chemical Structure and Properties of Coal - I : Elementary Composition and Density, Fuel, 1954, 33, 79.
20. VAN KREVELEN, D.W. and CHERMIN, H.A.G. - Chemical Structure and Properties of Coal (V) Aromaticity and Volatile Matter, Fuel, 1954, 33, 338.
21. SCHUYER, J. and VAN KREVELEN, D.W. - Chemical Structure and Properties of Coal : III - Molar Refraction, Fuel, 1954, 33, 176.
22. VAN KREVELEN, D.W. and SCHUYER, J., Chemical Structure and Properties of Coal - XII : Reevaluation of the Structural Parameters of Vitrinites, Fuel, 1957, 36, 313.
23. VAN KREVELEN, D.W., CHERMIN, H.A.G. and SCHUYER, J, Chemical Structure and Properties of Coal : XXIV - Sound Velocity and Fraction of Aromatic Carbon - Fuel, 1959, 38, 483.
24. HONDA, H and OUCHI, K, Magnetochemistry of Coal (I), Magnetic Susceptibility of Coal, Fuel, 1957, 36, 159.
25. MAZUMDAR, B.K., ANAND, K.S., ROY, S.N. and LAHIRI, A., Mechanisms der Oxydation der Kohle - Brennstoff-Chemie, 1957, 38, 305.
26. MAZUMDAR, B.K., CHAKRABARTTY, S.K. and LAHIRI, A, Aromaticity and Oxidation of Coal - J. sci. industr. Res., 1957, 16B, 275.
- 27(a). CHAKRABARTTY, S.K., MAZUMDAR, B.K., ROY, S.N. and LAHIRI, A, Strukturparameter Von Kohle and Grund Von Oxydation Versuchen - Brennstoff-Chemie, 1960, 41, 138;
- 27(b). CHAKRABARTTY, S.K., MAZUMDAR, B.K. and LAHIRI, A., Disposition of Hydrogen in Coal Structure, Fuel, 1958, 37, 498.
28. MAZUMDAR, B.K., CHAKRABARTTY, S.K., SAHA, M., ANAND, K.S. and LAHIRI, A., Further Studies on the Mechanism of Oxidation of Coal, Fuel, 1959, 38, 469.
29. MAZUMDAR, B.K., CHAKRABARTTY, S.K. and LAHIRI, A., Aromaticity of Coal : An Appraisal, Fuel, 1959, 38, 112.
30. MAZUMDAR, B.K., CHAKRABARTTY, S.K. and LAHIRI, A, Determination of Aromaticity of Coal by Oxidation, J. sci. industr. Res., 1962, 21A, 84.
31. MAZUMDAR, B.K., CHAKRABARTTY, S.K. and LAHIRI, A., Pyrolysis and Its Relation to The Structural Parameters of Coal: Proc. Symp. on the "Nature of Coal", Central Fuel Research Institute, Jealgora, India, 1959 Feb., p. 253.
32. MAZUMDAR, B.K., CHOUDHURY, S.S., CHAKRABARTTY, S.K. and LAHIRI, A., Dehydrogenation Studies on Coal : J. sci. industr. Res., 1958, 17B, 509.
33. MAZUMDAR, B.K., CHAKRABARTTY, S.K., CHOUDHURY, S.S. and LAHIRI, A., Dehydrogenation Studies on Coal, Proc. Symp. on "Nature of Coal", C.F.R.I, Jealgora, India, Feb. 1959, p.219.
34. MAZUMDAR, B.K., CHAKRABARTTY, S.K. and LAHIRI, A., Dehydrogenation and Tar Formation, Fuel, 1959, 38, 112.

35. MAZUMDAR, B.K., CHOUDHURY, S.S. and LAHIRI, A., Alicyclicity and Smoke Emission of Coal - Nature, 1959, 183, 1613.
36. MAZUMDAR, B.K., CHOWDHURY, S.S. and LAHIRI, A., Dehydrogenation of Coal by Iodine, Fuel, 1960, 39, 179.
37. MAZUMDAR, B.K. BHATTACHARYYA, A.C., GANGULY, S and LAHIRI, A., Alicyclicity of Coals : An Appraisal, Fuel, 1962, 41, 105.
38. MAZUMDAR, B.K., CHAKRABARTTY, S.K., DE, N.G., GANGULY, S. and LAHIRI, A., Further Studies on the Dehydrogenation of Coal by Sulphur, Fuel, 1962, 41, 121.
39. MAZUMDAR, B.K. DE, N.G. and LAHIRI, A., Dehydrogenation and Alicyclicity in Coals - J. sci. industr. Res., 1962, 21A, 36.
40. MAZUMDAR, B.K., CHAKRABARTTY, S.K. and LAHIRI, A., Some Aspects of the Constitution of Coal, Fuel, 1962, 41, 129.
41. BONE, W.A. and et al - Researches in the Chemistry of Coal - Proc. Roy. Soc. A., 1926, 111, 537; 1930, 127, 480; 1938, 148, 492.
42. BHATTACHARYYA, A.C., MAZUMDAR, B.K. and LAHIRI, A., Fuel, Lond, in press.
43. BHATTACHARYYA, A.C., MAZUMDAR, B.K. and LAHIRI, A., Fuel, Lond., in press.
44. REGGEL, R., RAYMOND, R.A., STEINER, W.A., FRIEDEL, R.A. and WENDER, I., Reduction of Coal by Lithium-Ethylenediamine Studies on a Series of Vitrains. Fuel, 1961, 40, 339; also, Fuel, Lond. 1958, 37, 126.
45. MAZUMDAR, B.K. and LAHIRI, A., The Probable Distribution of Carbon and Hydrogen Groupings in Coal, Fuel, 1962, in press.
46. MAZUMDAR, B.K. and LAHIRI, A., The Distribution on Non-Aromatic Group in Coal - J. sci. industr. Res., 1962, in press.
47. DRYDEN, I.G.C. , Chemical Structure of Coals : A Method for Comparing Data of Different Origins and For Testing Sets of Data for Self-consistency, Fuel, 1958, 37, 444.
48. PROVER, M.E., Dehydrogenation of Coals by p-Benzoquinone, J.C.S., 1960, 5020.
49. BHATTACHARYYA, A.C., Private Communication.
50. GAINES, A.F., The Distribution of Aliphatic Groups in Coal, Fuel, 1962, 41, 112.
51. KINNEY, C.R., The Source of Acetic Acid Obtained by Oxidation of Coal, J.A.C.S., 1947, 69, 284.
52. BROOKS, J.D., DURIE, R.A., STERNHELL, S., Chemistry of Brown Coals - III : Pyrolytic Reactions, Austr. J. Appl. Sci., 1958, 9, 303.
53. KAISER, F., RAO, H.S. and LAHIRI, A., Carbon Bound Methyl Groups in Coal, Proc. Symp. on the Nature of Coal, C.F.R.I., Jealgora, India, Feb. 1959, p.242
54. BHATTACHARYYA, A.C., MAZUMDAR, B.K. and LAHIRI, A., Fuel, Lond., in press.
- 55(a). VAN KREVELLEN, D.W., WOLFS, P.M.J., WATERMAN, H.I., Der Chemismus der Verkokung Untersucht an Polymeren Steinkohle-Modellstoffen VII, Anwendung der Gewonnenen Einsichten auf Steinkohle - Brennstoff-Chemie, 1959, 40, 371.

- 55(b). WOLFS, P.M.J., VAN KREVELEN, B.W. and WATERMAN, H.I., Chemical Structure and Properties of Coal XIV : The Carbonisation of Coal Models, Fuel, 1960, 39, 25; presented at the Third International Conference on Coal Science, Volkenberg(L), Netherlands, 27th to 30th April, 1959.
56. GANGULI, S., MAZUMDAR, B.K. and LAHIRI, A., Fuel, Lond., in press.
57. MAZUMDAR, B.K., GANGULI, S., DE, N.G. and LAHIRI, A., Action of Sulphuric and Phosphoric Acids on Coal Structure, Fuel, 1962, in press.
58. DE. RUIJTER, E. LEUPNER, R. TSCHEMLER, H., Electrical Conductivity and Aromatic Cluster Size of Coals and Coal Extracts, Fuel, 1962, 41, 118.
59. SIGES, B.S., Chemical Nature of Extracts from a Bituminous Coal, J.A.C.S., 1936, 58, 484.
60. SIGES, B.S. and WEILER, J.F., Chemical Constitution of a Bituminous Coal as Revealed by its Hydrogenation Products, J.A.C.S., 1937, 59, 369.
61. LE CLAIRE, C.D., Nature of Oils Obtained from the Hydrogenation of a Few Typical Bituminous Coal, J.A.C.S., 1941, 63, 343.
62. GLENN, R.A., Coal Hydrogenation Process Studies (IV) : Effects of Preheat on Restricted Hydrogenolysis of Pittsburg Seam Coal : Fuel, 1954, 33, 419.
63. BANERJEE, A., MAZUMDAR, B.K. and LAHIRI, A., Action of Permanganate on Coal, Nature, 1962, 267.
64. MAZUMDAR, B.K., CHAKRABARTY, S.K. and LAHIRI, A., Action of Aqueous Alkali on Lignite, J. sci. industr. Res., 1957, 16B, 519.
65. BROOKS, J.D. and SMITH, J.W., Basic Nitrogen in Coal, Austr. J. Appl. Sci., 1961, 12, 241-5.
66. EVDEN, I.G.C., Carbon-Hydrogen Groupings in Coal Molecule, Fuel, 1962, 41, 35.
67. VAN KREVELEN, D.W. GEOSKOOP, M.L., PALMEN, P.H.G., Dehydrogenation and Aromaticity of Coals, Fuel, 1959, 38, 256.
68. LADNER, W.R. and SPACCI, A.E., The Distribution of Aliphatic Groups in Coal, Fuel, 1962, 41, 114.
69. VAN KREVELEN, D.W., 'COAL' - ELSEVIER, Amsterdam, London, New York, Princeton, 1961.

.....

Table 1 - Verification⁴² of the Oxidation Technique by the Determination of the Aromaticity of Reduced Coal Samples.

Sample No. & Particulars	%Analysis of the samples, d.m.f.		C	H	O	% loss or gain on oxidation	Analysis of oxidised samples, % d.m.f.			C	COOH	COOH	Carbon in oxidized samples, gm. Total Corrected for C _{COOH} (C _{ar})	Aromaticity (C _{ar} /C)	
	C	H					C	H	O					Found	** Calculated
1. Original	85.7	5.2	6.4	--	--	-12	63.5	2.1	32.2	19.0	7.1	55.9	49.7	0.76*	--
1A. Reduced**	84.1	6.7	6.6	21	--	--	--	--	--	--	--	--	--	0.59	0.55
2. Original	89.8	4.8	2.8	--	--	+7.4	73.1	2.1	22.3	13.0	4.9	78.5	73.2	0.82	--
2C. Reduced**	86.1	7.3	4.1	35	--	-22.2	61.4	2.2	34.2	18.6	7.0	47.8	42.4	0.49	0.47

* Oxidation done at 170°C for a prolonged period until there was no further oxidation. Generally this requires 1500 to 2000 hrs. in case of vitrains.

** Theoretical aromaticity calculated on the basis of hydrogen that was added during reduction.

+ from pyrolysis; see Table 2.

** Ethylene-diamine free analysis.

Table 2 - Validity of the Pyrolysis Technique in the Determination of the Aromaticity of Coal.

Sample No. & Particulars	Analysis		Pyrolysis (600°C)			Aromaticity, $\frac{C_{ar}}{C}$		$\frac{2(R-1)}{C}$ *
	C %	H %	H/C	V %	F %	Calculated from reduction data	Statistical* method	
1. Original	85.7	5.2	0.73	26.8	73.2	--	--	0.51
1A. Reduced	84.1	6.7	0.95	48.5	51.5	0.54	0.54	-do-
1B. "	83.4	5.8	0.84	40.7	59.3	0.63	0.65	-do-
2. Original	89.8	4.8	0.64	14.9	85.1	0.87	--	0.49
2A. Reduced	87.9	6.3	0.85	39.0	61.1	0.63	0.65	-do-
2C. Reduced	86.1	7.3	1.02	57.1	42.9	0.48	0.49	-do-

* assuming that the ring-condensation index, $\frac{2(R-1)}{C}$ of reduced coal would remain the same as in the original, the aromaticity of the reduced coals has been calculated from the formula: $f_a = (1 - \frac{H}{C}) + 1 - \frac{2(R-1)}{C}$. For the computation of ring-index of the original coals, however, the aromaticity determined by pyrolysis has been assumed to be correct.

Table 3 - Non-aromatic Carbon-Hydrogen Distribution in Typical Vitrains*

(Reproduced in part from B.K.Mazumdar and A.Lahiri^{4,5})

Rank % C d.m.f.	Primary Data				Deductions **												
	+fha = Char C	e (i.r.) C _{CH} +C _{CH₂} %	a (n.m.r.) H _{CH₂} %	Non-arom. hydrogen H _{CH} %	Non-arom. carbon C _{CH₂} %	Non-arom. carbon C _{CH} %	Non-arom. carbon C _{CH₃} %	b = Aromaticity fa	city	Aromaticity fa	city	Aromaticity fa	city	Aromaticity fa	city	Aromaticity fa	city
82.5	0.25	20.6	0.23	0.88	2.12	0.66	1.22	12.7	7.9	4.9	1.89	0.69	0.94	0.93	0.93	0.93	0.93
85.0	0.22	18.7	0.26	0.95	2.04	0.54	1.39	12.2	6.5	5.6	1.93	0.71	0.93	0.93	0.93	0.93	0.93
87.5	0.17	14.9	0.35	1.06	1.80	0.34	1.56	10.8	4.1	6.2	2.10	0.76	0.93	0.93	0.93	0.93	0.93
90.0	0.11	9.9	0.54	1.25	1.38	0.14	1.58	8.3	1.7	6.3	2.30	0.82	0.93	0.93	0.93	0.93	0.93

* Deductions are shown in case of 4 out of 5 samples studied by Dryden⁶⁶. The values of e, a and H₀ refer to his samples.

** Subject to the assumption that all the tertiary CH and secondary CH₂ groups are embodied in the alicyclic structures.

+ Authors' maximum values of alicyclic; see Fig.3 and also footnote in page 3.

Table 4 - Compatibility of the different estimates of aromaticity with those of Alicyclicity.

Rank % C, d.m.f.	Aromaticity, f_a		Preferred Values* of Alicyclicity (authors')		$f_a + f_{ha}$ Van Krevelen et al's ++	
	Statistical approaches (van Krevelen et al) 69	Chemical approaches (authors)†	f_{ha}			Authors'
81.5	0.83	0.67	0.25	1.03	0.92	
85.0	0.85	0.70	0.22	1.07	0.92	
87.0	0.86	0.75	0.17	1.03	0.92	
89.0	0.88	0.80	0.12	1.00	0.92	
90.0	0.90	0.84	0.08	0.98	0.92	

* from Fig.3. These values are considered to be the maximum; see footnote in page 3

† typical values from Fig.2.

++ the sum would still be higher if methyl-carbon is taken into consideration.

Table 5 - Comparative study of the three Methods of Dehydrogenation

Samples	Analysis		% of H removed during dehydrogenation	
	C	H	Sulphur (Vesterberg)	Iodine
<u>Vitrains</u>				
1	79.0	5.2	31	25
2	83.5	5.6	28	27
3	85.7	5.2	19	21
4	89.8	4.8	13	12
<u>Reduced Vitrains</u>				
1	86.1	7.3	43	44

* Authors' assessment. 37

Table 6 - Selectivity of Sulphur (Vesterberg's) in the Dehydrogenation of the Hydroaromatic Structure in Coal 49.

Sample No. & Particulars	Analysis, d.m.f.	C	H	Field of		% of H removed		Extra H removed in case of reduced Samples	Alicyclicity, $\frac{C_{H_{10}}}{C}$	
				Reduced	Vibrain per 100 gm. starting vibrain	By S (Vesterberg)	by S (Vesterberg)		Found	Calculated
1	2	2	3	4	5	6	7	8	9	
2. Original Vibrain	89.8		4.3			12.6		0.08		
2c. Reduced**	86.1		7.3	104.4	2.67	43.4	2.68	0.45		0.45
2d. Reduced**	86.1		5.9	104.3	1.30	52.1	1.23	0.26		0.25

* Compare column 5 with 7. This indicates the amenability of the hydroaromatic structure to complete dehydrogenation.

** Ethylene-diamine free yield and analysis.

+ From the amount of H₂ formed without suspecting any side-reactions

** The "theoretical" alicyclicity of reduced vibrains is based on the alicyclicity of the original vibrain and the extent of H-addition to it.

Table 7 - Average Aromatic Ring Size of Coal as Obtained by Different Approaches

Rank	Aromatic ring size by oxidation technique 27,40										No. of benzene rings per mean structural unit from	
	C	H	O	OH	CO	COOH	C-O-C	H/C exp. atomic	atomic H/C of unsubstituted aromatic	No. of benzene rings per average aromatic nucleus of coal	A-ray Diatomic Susceptibility	Statistical methods (van Krávelen et al 69)
81.5	65.4	2.3	30.0	4.0	6.5	16.0	5.5	0.41	0.63	4		4.4
84.4	65.5	2.5	29.0	2.6	7.9	15.9	2.6	0.41	0.62	4		
87.3	67.6	2.2	28.2	2.2	9.0	14.0	3.0	0.39	0.60	4.5	2-5*	4.7
89.3	72.9	2.6	22.1	1.0	11.3	8.0	1.8	0.41	0.60	4.5		5.0
89.6	70	2.2	25.2	1.5	11.0	11.2	1.5	0.38	0.57	5		5.2
93.2	88.1	2.6	7.4	2.1	2.4	2.1	0.8	0.35	0.39	12-15	12	6.5

* This represents the range of assessment rather than the average size. Measurements have also indicated that the average number of atoms per layer varies from about 14 atoms at 78% C to about 18 atoms at 90% C and about 36 atoms at 94% C. These would excellently correspond to the number of benzene rings per layer estimated from oxidation studies.

Table 8 - A Summary of the Essential Structural Parameters of Coal*

Typical Vitraains		Distribution of carbon		Distribution of hydrogen		Distribution of benzene rings				
C	H	H/C	fa**	fhar**	fal (C-CH ₃) By diff.	*** H ₂ %	**Har H ₂ O	H ₂ Har*** H ₂ O	††No. of benzene rings per mean structural unit.	
81.0	5.4	0.80	0.67	0.25	0.08	5.0	0.23	0.45	0.32	4
82.5	5.3	0.77	0.68	0.24	0.03	4.9	0.25	0.42	0.33	4
85.0	5.4	0.76	0.71	0.22	0.07	5.1	0.29	0.41	0.30	4
87.5	5.3	0.73	0.75	0.17	0.08	5.2	0.33	0.35	0.32	4.5
90.0	4.8	0.64	0.82	0.11	0.07	4.7	0.46	0.20	0.34	5
93.2	3.5	0.45	0.97	nil	0.03	3.5	0.80	nil	0.20	12

* The distribution of C and H in different forms had also been earlier^{33,39,40} presented but the present one is considered to be more accurate.

** maximum aromaticity and alicyclic values from oxidation and dehydrogenation studies respectively.

+ mean of physical and chemical determinations.

†† calculated from methyl carbon

††† obtained by difference; this would be found to be largely consistent with the detailed distribution of hydrogen in CH and CH₂ forms recently deduced⁴⁵ by the authors from i.r. and n.m.r. data (Table 3).

*** % H less 'hydroxyl' hydrogen.

Table 9 - Comparative Analysis of Coals and Permanganate Treated Coals at different Stages of Degradation.

Reproduced from A. Banerjee, B. K. Mazumdar and A. Lahiri ⁶³7

Sl. No.	Analysis of Coal, d.m.f.			Nature of coke button (original coal)	Time of treatment with $KMnO_4$ in hrs. (at room temperature)	%Loss of organic matter	Analysis of Treated Coal d.m.f.			Nature of coke button (treated coal)
	C	H	%				C	H	%	
1.	69.2	4.5	--	--	** 0.5	67.2	69.6	4.8	--	--
2a.	81.8	5.4	29.6	medium hard greyish bead	0.5	19.4	81.0	5.3	--	--
b.	"	"	"	"	1.0	25.9	81.6	5.5	30.4	weak but coherent
c.	"	"	"	"	2.0	36.3	82.1	5.4	30.1	-do-
d.	"	"	"	"	24.0	36.1	81.2	5.5	31.5	-do-
e.	"	"	"	"	** 0.5	27.0	81.3	5.4	--	--
f.	"	"	"	"	** 0.5**	83.1	80.0	5.5	--	--
3.	86.7	5.3	-	Highly swollen porous coke.	1.0	23.7	86.5	5.3	--	Medium hard porous coals
4a.	89.9	4.9	14.9	"	1.5	14.5	89.1	4.7	14.1	Highly swollen porous coke.
b.	"	"	"	"	2.5	14.3	89.3	4.7	14.8	-do-

+ All vitrain samples. ** In contrast to the preceding experiment, in this case, more than 60% of the coal could be converted into soluble products because of 3 successive treatments of 10 minutes duration each, instead of a single treatment.

* different concentration of $KMnO_4$, alkali or acid and varying ratio of $KMnO_4$ to coal were used. This is of no consequence in respect of the analysis of the treated coals.

** dil. H_2SO_4 acid medium and the rest, alkaline.

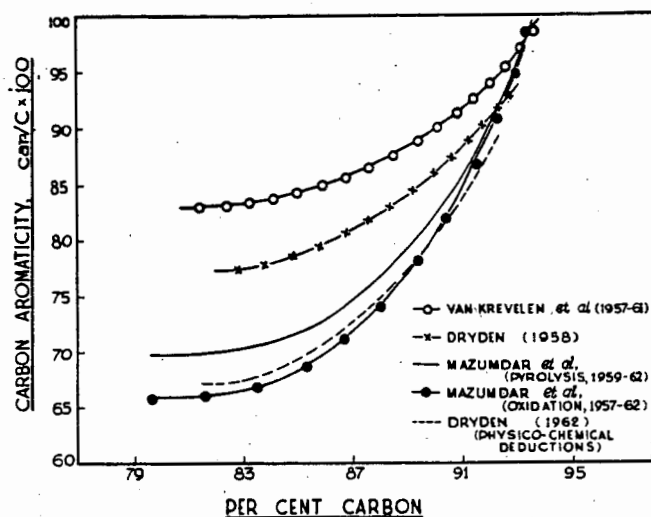


Fig. 1 - Aromaticity of coal by different approaches.

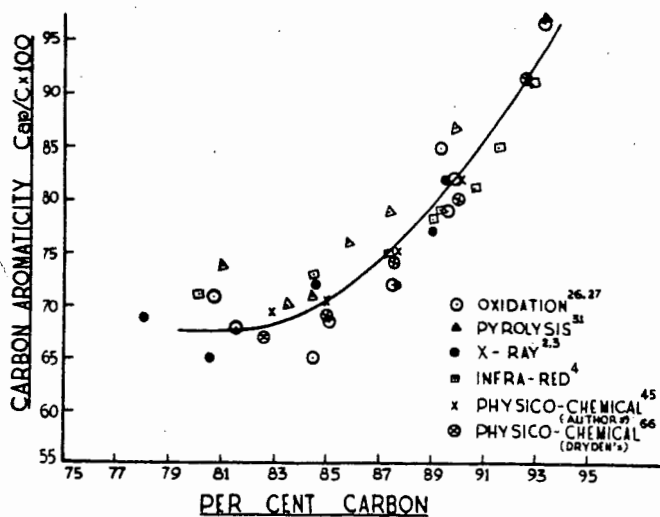


Fig. 2 - Mean aromaticity of coal and its variation with rank as determined by chemical methods and its comparison with values from some of the physical and physico-chemical approaches.

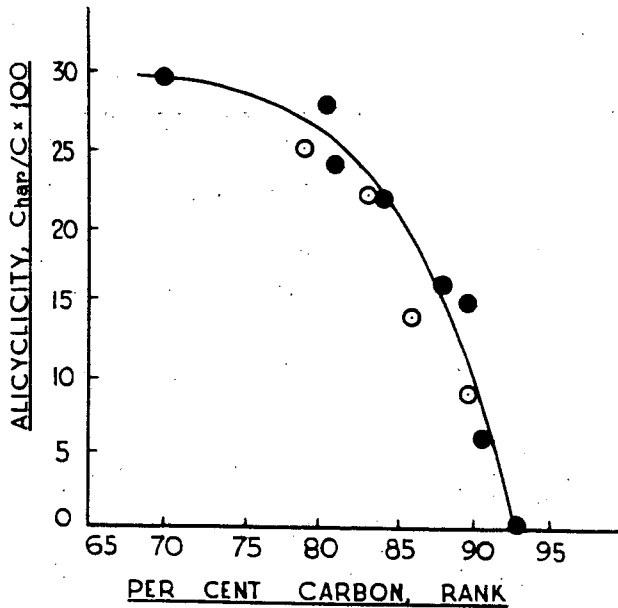


Fig. 3 - Variation of the alicyclicity of coals with rank
 ● - values obtained in 1952 by dehydrogenation with sulphur^{32,33}; ○ some recent determinations.

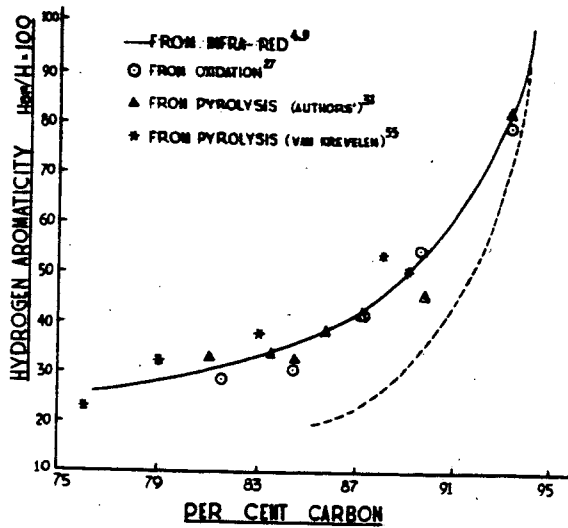


Fig. 4 - Variation of the hydrogen aromaticity with rank : a comparison of the physical and chemical estimates.

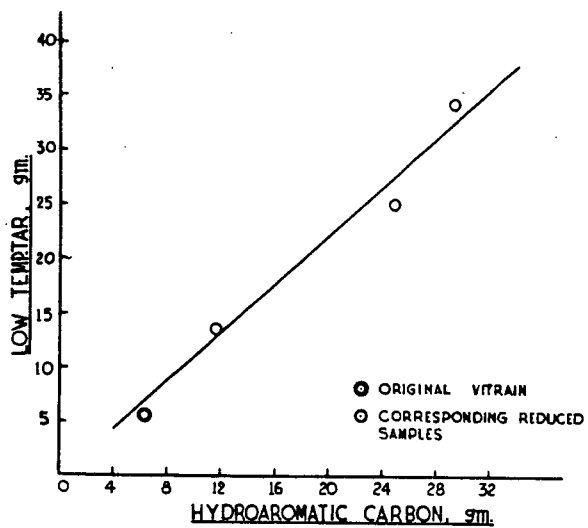


Fig.5 - Role of hydroaromatic structure in the formation of tar.
[reproduced from Ganguly, S., Mazumdar, B.K. and Lahiri, A.⁵⁶]

CATALYTIC DEALKYLATION OF TAR ACIDS

John S. Berber and Leslie R. Little, Jr.

U. S. Department of the Interior, Bureau of Mines,
Morgantown Coal Research Center, Morgantown, W. Va.

Low-temperature carbonization has long been considered as a possible method for the utilization of lignite and other low-grade coals. Various fixed-bed processes were developed and tried prior to the first World War, but most of them met with limited success, and none became commercially significant. In the low-temperature carbonization process, the tar produced contains large quantities of tar acids. Depending on the coal carbonized and the conditions employed, the tar acids content of the tar will vary from around 15 to 50 percent. In the carbonization of Texas lignite, the distillable fraction of the low-temperature tar contains around 25 volume-percent tar acids of which only around 3 to 4 volume-percent are low-boiling phenols. The low-boiling tar acids, which are commercially obtained from coke-oven tar phenols, cresols, and xylenols have well-developed markets and uses and command a good price in the pure state. The market for the higher boiling phenols or tar acids is limited, and when marketed as impure mixtures, they sell at a much lower price than the lower boiling phenols. Owing to the limited market for these high-boiling phenols, large quantities of these coke-oven tars containing tar acids are burned as residual fuel. Using fluidized-bed techniques developed during the last decade in the petroleum industry, workable low-temperature carbonization processes have been developed and offer great potentialities, providing that the market value of the carbonization products can be increased, for example, by converting high-boiling tar acids to low-boiling phenols.

Low-temperature tars have a high degree of alkylation. Methods of removing some or all of the alkyl groups, or decreasing their chain length, consequently are of considerable interest. One method of conversion presently under study by the Bureau of Mines is the catalytic dealkylation at atmospheric pressure in which the alkyl groups are split off from the phenolic ring, yielding lower boiling homologs. Numerous catalysts of the silica-alumina type developed for petroleum cracking are available for study. The ideal catalyst would naturally be one that promoted cleavage of the alkyl group--aromatic nucleus carbon-carbon bond at the same time avoiding rupture of the phenolic carbon-oxygen bond, which would result in a high yield of phenol itself. The Bureau plans to test individual catalysts at three temperature levels to determine the most promising catalyst and the best temperature range, which will then be more comprehensively evaluated to fix optimum operating conditions for maximum phenol yield.

Three types of catalysts were used in Bureau tests performed in the laboratory glass reactor in which low-boiling methanol solubles were dealkylated. A silica-alumina catalyst in pellet form gave yields of light phenols of approximately 30 volume-percent of the feed acids. The same catalyst, crushed to 16-20 mesh,

showed somewhat greater activity and yields. With cobalt-molybdenum catalyst, yields of light phenols were very low, and large amounts of gas and carbon were produced. With a cobalt catalyst, a fair yield of light phenols was obtained even though the total conversion was low.

Experimental

Catalytic Dealkylation Laboratory-Scale Apparatus. The Bureau's laboratory-scale glass dealkylation unit was set up as shown in the schematic diagram (Figure 1.). A picture of the apparatus is shown in Figure 2. A calibrated feed reservoir of 250-ml. capacity was connected to a small bellows-type pump whose stroke could be adjusted to deliver from 15 to 3,000 cc./hr. of liquid feed. The pump discharged through a length of 1/8-inch stainless-steel tubing entering the reactor through a glass feed tube inserted in the top head of the reactor. An earlier feed device was tried, consisting of a 100-cc. hypodermic syringe mounted over the reactor and in contact with a motor-driven rotating threaded rod, which slowly depressed the syringe plunger. During operation, the plunger repeatedly stuck in the syringe barrel resulting in intermittent feeding and breakage hazards. This method was used in Runs 4 and 5, and was then replaced by the pump.

The reactor unit was of all-glass construction, designed as shown in Figures 3 and 4. The body of the reactor was a cylinder approximately 1-1/4-inch O. D. by 1-inch I. D. and 36 inches overall length, fitted at top and bottom with standard taper glass joints. It was fabricated entirely from "Vycor" 96 percent silica glass, affording safe operation up to 900°C. Eight inches from the bottom of the tube, indentations were made in the tube wall to hold a perforated porcelain disk, which served as a catalyst support. The reactor head, made of Pyrex glass, had three taper joints at the top. Through the central taper joint, a Pyrex thermocouple tube was inserted, extending lengthwise through the reactor tube and terminating at the porcelain support. The feed inlet tube fitted into a second joint; the third was not used. There were two small side connections with spherical joints, one for the entering of the carrier gas and the other for a pressure tap connected to a mercury manometer for measuring the pressure drop across the reactor packing. The bottom adapter, also of Pyrex, served to connect the reactor to the product receiver, a 500-cc. Erlenmeyer flask of actinic glass, immersed in an ice bath. Exit gases passed off through a small side tubulure and were metered through a wet-test meter. A tube packed with glass wool was placed in the off-gas line to protect the meter against dust or carbon particles and entrained vapors.

The reactor was mounted vertically within an electrically heated furnace, 31 inches overall length with a heating zone 30 inches long, rated at 2,200 watts and operable to 1,850°F. Temperature adjustment and control were obtained with a variable transformer in the power supply to the furnace. This furnace was installed after Run 22. Before that, two smaller 750-watt furnaces, each 13 inches long, were mounted end-to-end to encompass the reaction zone. With this arrangement, an unheated zone occurred where the two units came together, causing heat losses at that point, consequently, a poor heat transfer. A more uniform heating was obtained using the larger furnace.

Helium was used as the carrier gas to maintain flow throughout the system and to sweep feed and product vapors through the reactor. The gas was supplied from cylinders through appropriate regulators; the flow rate was measured by a

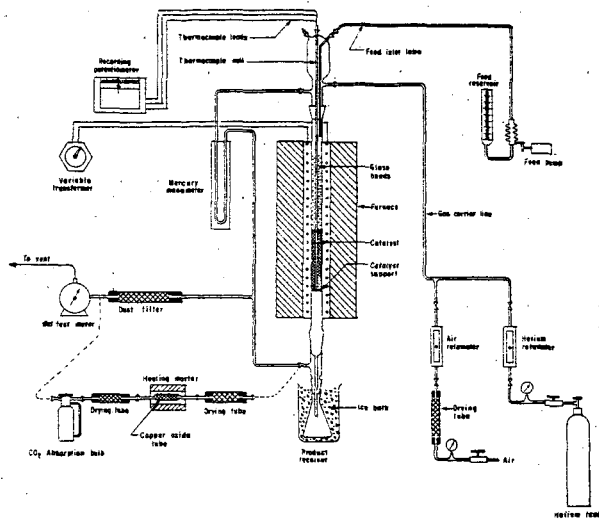


Figure 1. Schematic Diagram of the Laboratory Glass Dealkylation Apparatus.

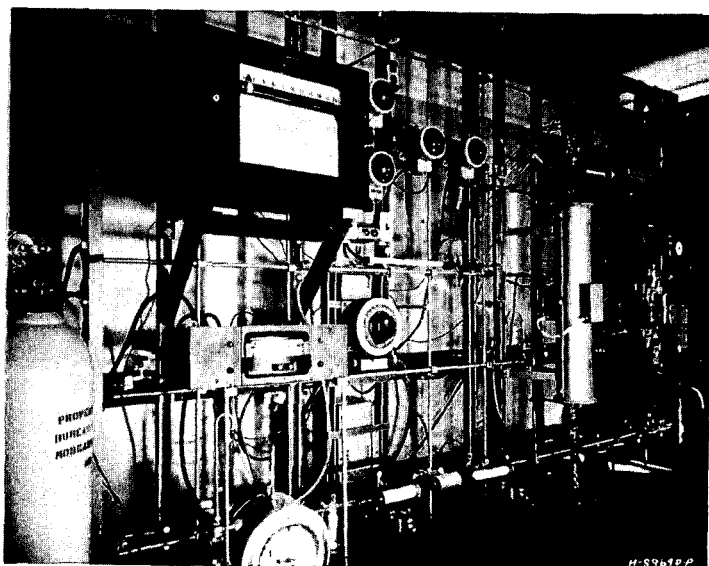


Figure 2. Picture of the Dealkylation Unit.

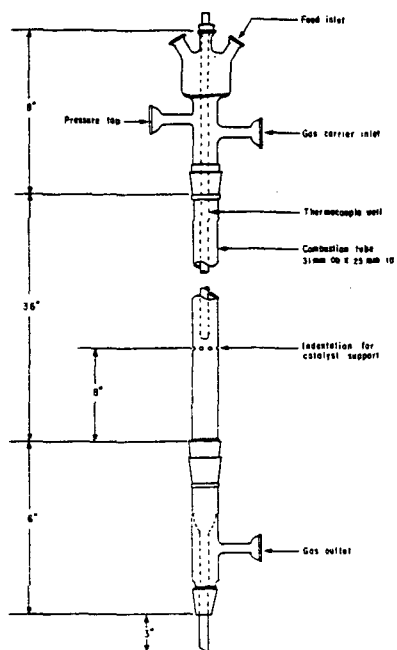


Figure 3. Dealkylation Glass Reactor.

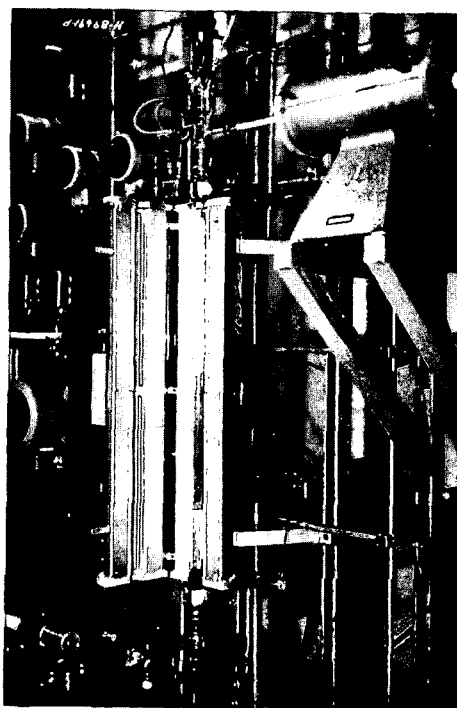


Figure 4. Picture of the Dealkylation Glass Reactor.

rotameter and was adjusted with a small needle valve at the rotameter inlet. Temperatures in the reactor were measured with chromel-alumel thermocouples connected to a Brown "Elektronik" six-point recording potentiometer. The pressure drop across the reactor packing, as noted before, was read on a mercury manometer connected across the inlet and outlet of the reactor.

In preparing for a test, the reactor tube and top head were assembled, and the thermocouple well was inserted. A weighed amount of catalyst was poured into the reactor through one of the openings in the top head. The height of catalyst above the support disk was measured, and the volume was calculated from calibration data previously obtained on the empty tube. Glass beads 4 mm. in diameter were poured on top of the catalyst to a convenient height, forming a preheating zone. The reactor was clamped into position within the furnace, and the necessary connections were made with the rest of the apparatus. Feed material was added to the feed reservoir. The specific gravity of the feed was determined at room temperature by weighing a graduated cylinder containing 100 ml. of feed.

Procedure. The tar acids for the dealkylation study were obtained from samples of low-temperature lignite tar supplied by the Texas Power and Light Company. The samples were products from a solvent extraction pilot plant in which hexane and methanol were used in a double-solvent operation to separate neutral and acidic components. Tar acids were recovered from the methanol extract by first stripping off solvent, then distilling the acids into two fractions designated as high-boiling and low-boiling methanol solubles.

We originally planned to use the total high-boiling methanol solubles for feed. This material was solid at room temperature and was therefore diluted with an equal volume of toluene to render it fluid and permit its pumping into the combustion tube of the glass reactor. With this feed, operating difficulties were caused by deposition of nonvolatile resinous substances, which plugged the reactor. Similar deposits occurred when a low-boiling methanol solubles residue boiling above 225 °C. was used. Tar acids of intermediate boiling range did not cause any plugging. Because of its greater ease of handling, we decided to work with low-boiling methanol solubles. Samples of this stock were fractionated under vacuum on a Podbielniak high-temperature distillation apparatus using a 2:1 reflux ratio. The fraction boiling between 230 °C. and 266 °C. was retained as feed for the dealkylation study. In Runs 4 through 17, the feed was diluted with toluene; beginning with Run 18, the feed acids were used directly with no dilution (Table I).

The feed materials were analyzed for total acids by extraction with 10 percent caustic solution, considering the total caustic-soluble portion as phenols. The first batch of feed distillate showed 97.5 volume-percent tar acids, whereas the second batch analyzed only 82.0 volume-percent. A third feed fraction, not yet used, showed 81.0 volume-percent acids. The variation in the first material was probably owing to insufficient mixing before sampling, and for subsequent tests, the feeds should be fairly uniform.

Catalysts were commercial types furnished by various manufacturers. In most of the tests, a silica-alumina cracking catalyst, Socony-Vacuum TCC type 34 "Durabead," was used. Its composition is about 90 percent silica and 10 percent alumina, with less than 0.1 percent contaminants, which are primarily sodium salts. The catalyst comes in bead form and was sized to -4, +6 mesh before using.

Table 1. Laboratory-Scale Catalytic Dehydration of Tere Acids.

Run number	4	5	6	7	9	10	11	13	14	15	16	17	18	19	20	21	22	23	24	25	26	27	
Catalyst type	a	a	a	a	a	a	a	a	a	a	a	a	a	a	a	a	a	a	a	a	a	a	a
Catalyst weight, g.	87.0	92.6	116.8	116.8	94.8	94.8	94.8	84.4	83.4	83.4	83.4	80.5	80.5	80.5	80.5	83.8	83.8	81.6	152.7	152.7	152.7	174.8	174.8
Catalyst volume, cc.	131	143	165	137	137	137	134	134	134	134	121	121	121	121	121	127	127	128	128	128	128	132	132
Condition of catalyst	New	New	New	Regen.	New	Regen.	New	Regen.	New	Regen.	New	Regen.	New	Regen.	New	Regen.	New	Mixed	New	Regen.	New	Regen.	New
Length of run, hrs.	1.08	1.55	3.00	2.67	1.08	1.58	2.08	2.12	2.09	2.10	1.17	1.55	0.92	1.80	1.63	1.60	1.70	1.50	1.45	1.50	1.50	1.35	1.35
Feed composition	c	f	g	g	g	g	g	g	g	g	h	h	i	i	i	i	i	i	i	i	i	i	j
Total feed, ml.	--	99	199	120	223	216	222	204	228	212	199	171	168	168	168	164	158	168	148	141	136	149	149
Total feed, g.	89	93	186	112	205	204	209	193	215	201	184	160	167	167	166	163	157	167	147	140	135	149	149
LHSV, vol. total feed/ vol. catalyst/hr.	--	0.44	0.40	0.28	1.51	1.00	1.03	0.73	0.80	0.79	0.71	1.21	0.90	1.51	0.77	0.79	0.78	0.77	0.77	0.76	0.71	0.84	0.84
Carrier gas flow rate, SCFH	0.36	0.36	0.36	0.36	0.36	0.36	0.36	0.16	0.36	0.36	0.36	0.36	0.36	0.36	0.36	0.36	0.36	0.36	0.36	0.36	0.36	0.36	0.36
Operating conditions																							
Reactor ΔP, mm. Hg	1-9	0	0	0-5	0-65	0-50	0-98	0-48	0-68	0-18	0-74	0	0	0	0	3	3	2	0	0	0	0	0
Preheat temperature, °F.	--	800	539	489	543	607	844	891	839	843	456	640	518	748	724	781	781	507	569	615	727	643	643
Top catalyst temperature, °F.	--	825	824	842	783	835	712	702	759	711	688	699	675	703	746	703	746	703	788	704	860	782	782
Bottom catalyst temperature, °F.	--	860	868	823	813	860	847	821	825	825	829	829	829	825	828	825	803	734	832	734	906	831	831
Liquid product, ml.	--	86	181	101	201	204	205	189	214	194	180	160	154	164	158	149	138	157	124	122	109	139	139
Liquid product, g.	--	72	79	165	93	186	186	190	174	197	182	166	148	153	161	155	148	136	156	122	120	106	138
Carbon deposited, g.	--	6.83	11.53	9.81	7.03	8.32	5.63	7.90	8.81	7.22	8.75	4.49	6.58	5.69	6.66	7.05	9.04	5.73	19.30	15.40	21.0	14.38	14.38

a Socony-Vacuum "Durabead," silica-alumina, 4-6 mesh.

b Socony-Vacuum "Durabead," silica-alumina, 16-20 mesh.

c Girder T-300, cobalt molybdenum on alumina, 3/16" tablets.

d Girder T-300, cobalt molybdenum on alumina, 1/8" tablets.

e 50 vol. % toluene + 50 vol. % 230-266°C. LBMS-1 (97.5% acetic).

f 50 vol. % toluene + 50 vol. % 230-266°C. LBMS-1 (100% acetic).

g 50 vol. % toluene + 50 vol. % 230-266°C. LBMS-1 (98.0% acetic).

h 50 vol. % toluene + 50 vol. % 230-266°C. LBMS-1 (97.5% acetic).

i 100 vol. % 230-266°C. LBMS (97.5% acetic).

j 100 vol. % 230-266°C. LBMS-2 (82.0% acetic).

In Runs 21, 22, and 23, the catalyst was ground and a -16, +20 mesh portion was used. The two other catalysts used up to now were Girdler G-35B, in 3/16-inch tablets, containing 13-1/2 weight-percent cobalt and molybdenum on an alumina support; and Girdler T-300, in the form of 1/8-inch tablets containing about 60 percent cobalt on kieselguhr. All three catalysts were used as received.

Helium carrier gas was admitted to the system from the supply tank, adjusting the flow rate to 0.36 SCFH. Power was applied to the furnace and the temperature, as measured by the bottom catalyst bed thermocouple, was gradually raised to the desired operating temperature. When the temperature was stabilized at the desired level, the feed pump was turned on to start the run. The liquid feed stream coming into contact with the preheat zone vaporized and passed downward over the packed catalyst. The cracked vapors entered the product receiver, cooled by an ice bath, where the liquid product collected and helium and noncondensable product gases passed off to the gas meter.

The run was continued until sufficient liquid product was collected for analysis. Depending on the charge rate, a run lasted from one-half to 3 hours. Pertinent operating data were recorded on log sheets at 10 to 15 minute intervals. After feed was discontinued at the end of a run, helium flow was maintained, and the reactor was kept at temperature for about an hour to purge the reactor completely of all vaporizable products.

The total liquid product was weighed, its volume was measured at room temperature, and it was then distilled using a glass Vigreux column 1/2-inch in diameter and 10 inches long. An initial fraction, boiling up to 160°C. (Table II) was distilled at atmospheric pressure. A second fraction with a boiling range of 160°-230°C. was distilled at 10 mm. Hg pressure. The tar acids content of this fraction was determined by extraction with sodium hydroxide solution. The amount of tar acids thus determined was considered the total yield of light phenols. Tar acids in the distillation residue were similarly determined. The acids in the caustic extract were recovered by neutralizing the extract with dilute sulfuric acid and were retained for possible future analysis.

During the cracking operation, considerable carbon was deposited on the catalyst. This carbon was removed by burning it off in an air stream, thus regenerating the catalyst. The reactor was brought to 1,000°F. on helium; air was then substituted for helium at a rate sufficient to maintain 1,050° to 1,100°F. during the regeneration. Carbon dioxide produced was absorbed in an absorption bulb packed with "Ascarite." The absorption bulb was preceded by a small tube, was packed with cupric oxide, and was heated to 700°C. by a small mortar, which converted any carbon monoxide to the dioxide. Drying tubes containing "Drierite" placed before and after the cupric oxide tube trapped any water vapor in the gas stream. The total weight of carbon dioxide formed was then taken as a measure of the carbon formed in the run, assuming that the catalyst deposit consisted entirely of carbon.

Discussion and Conclusions

The study on dealkylation of tar acids undertaken at the Bureau's Morgantown Research Center was concerned chiefly with the selection of a most effective catalyst for the production of low-boiling phenols and the examination of different variables in determining the maximum yield. This is a preliminary study. Not all of the

Table II. Fractional Distillation of the Dealkylated Tar Acids

Run number	4	5	6	7	9	10	11	13	14	15	16	17	18	19	20	21	22	23	24	25	26	27	
Yields, wt. % of feed																							
Liquid product	80.7	85.1	88.8	82.5	90.7	91.6	90.8	90.2	91.5	90.4	89.8	92.7	91.8	96.1	93.5	91.0	86.7	93.8	83.3	85.5	78.5	93.1	
Carbon	--	7.4	6.2	8.7	3.4	4.1	2.7	4.1	1.1	3.6	4.7	2.8	3.9	3.4	4.0	4.3	5.7	3.4	13.2	11.0	15.5	9.7	
Gas + loss (by difference)	--	7.5	5.0	8.8	5.9	4.3	6.5	5.7	4.4	6.0	5.5	4.5	4.3	0.5	2.5	4.7	7.6	2.8	3.5	3.5	6.0	-2.8	
Distillation of liquid product																							
IBP - 160°C., vol. %	--	68.7	60.9	64.3	56.8	53.2	58.6	59.0	53.3	59.2	57.2	56.7	7.5	5.5	7.6	9.8	14.4	7.1	9.7	7.4	13.5	6.3	
160 - 230°C., vol. %	--	8.6	6.6	6.8	2.7	2.2	3.4	10.6	17.3	17.5	16.0	20.5	41.5	35.0	36.8	29.5	35.8	12.6	5.2	12.4	2.6	25.4	
Residue > 230°C., vol. %	--	18.3	30.0	24.0	40.3	--	36.0	30.7	24.0	23.3	25.4	22.2	49.6	56.9	54.2	59.8	48.6	79.4	84.2	77.9	81.9	67.2	
Tar acids in 160 - 230°C. fraction, vol. %	--	73.2	78.3	65.2	58.3	66.7	51.1	87.0	90.0	89.5	88.5	80.0	79.2	80.0	84.0	85.6	88.0	82.3	73.3	80.0	--	82.2	
Tar acids in residue, vol. %	--	83.0	--	--	--	--	--	--	--	--	--	--	--	66.6	68.0	70.0	63.0	75.5	78.0	78.0	78.0	80.0	
Total conversion, vol. % feed acids	--	73.6	--	--	--	--	--	--	--	--	--	--	--	68.9	61.4	63.5	60.9	72.6	42.5	43.6	46.1	47.6	39.0
Yield light phenols, vol. % feed acids	--	10.9	9.6	7.6	2.9	2.8	3.3	17.4	29.8	29.3	26.2	31.4	31.0	27.9	29.7	23.6	28.2	9.9	3.3	8.8	<2.6	23.7	

variables (such as temperature, space velocity, catalyst size, catalyst regeneration characteristics, type of feed stock, use of additives to feed such as steam or pyridine, etc.) were examined, and more research work will follow to study and determine the results of these variables.

The following conclusions can be drawn from the actual studies on the dealkylation of tar acids:

1. Tar acid feed stocks containing high-boiling residua are not suitable for dealkylation studies because they form nonvolatile, resinous deposits that plug the reactor. Fractions of intermediate boiling range did not form plugs, and successful tests were carried out using tar acids boiling from 230° to 266°C.

2. Silica-alumina catalyst, typified by Socony-Vacuum TCC-34 "Durabead," is very effective in dealkylation of high-boiling phenols to lower boiling homologs. Yields of around 30 volume-percent of feed acids were obtained operating at around 825°F. and with liquid hourly space velocities of about 0.8.

3. Girdler G-35B, a cobalt-molybdenum catalyst, appears unsatisfactory for dealkylation of tar acids because of low phenol yields and considerable losses of feed to carbon and gas.

4. A high-cobalt catalyst, Girdler T-300, showed possibilities of being highly selective in light phenol production, providing total conversion of feed acids can be increased.

5. The new laboratory-scale glass dealkylation unit (Fig. 1) has been shown to be suitable for carrying out catalyst screening tests and for future evaluation studies on individual catalysts.

Reference to specific commercial brands, materials, or models of equipment in this article is made to facilitate understanding and does not imply endorsement by the Bureau of Mines.

PROCESS CONDITIONS FOR PRODUCING A
SMOKELESS BRIQUETTE FROM HOT CHAR

G. M. HABBERJAM
and
H. R. GREGORY

NATIONAL COAL BOARD, COAL RESEARCH
ESTABLISHMENT, STOKE ORCHARD,
CHELTENHAM, ENGLAND.

PROCESS CONDITIONS FOR PRODUCING A SMOKELESS BRIQUETTE
FROM HOT CHAR

1. INTRODUCTION

In the United Kingdom the implementation of the Clean Air Act of 1956 involves the setting up of an increasing number of smokeless zones throughout the country. In order to maintain sales of solid fuel, appliances to burn the present fuels smokelessly are being developed, and increased supplies of reactive smokeless fuels are being made available. To contribute to these supplies, a process for the production of a smokeless fuel from low rank coal has been developed at the Coal Research Establishment of the National Coal Board. A general account of this development has recently been given in another paper⁽¹⁾, and it is proposed here to review in detail some of the investigations which were carried out to determine the range of application and necessary process conditions.

The choice of low rank coal, volatile content greater than 35%, as a starting point is particularly appropriate in the U.K. as this material in small size gradings is economic to mine and well situated with respect to the markets.

To convert this material into a suitable smokeless fuel requires that it be both upgraded in size and rendered smokeless, without markedly reducing its reactivity. It was known⁽²⁾⁽³⁾ that low rank coal could be made smokeless by a process of partial carbonisation and it was thought likely that considerable reactivity would be retained in the char.

It was decided to attempt to briquette the char in the simplest possible way, i.e. without a binder of any kind. All attempts to briquette cold char using pressure alone have proved unsuccessful, but several attempts to briquette char when hot had shown promise.

Thus in 1931 Hardy⁽⁴⁾, working in Belgium, took out his first patent on the hot briquetting of char and several more were filed, the last in 1937. The first Hardy patents cover a process which was intended to briquette finely divided coals and lignite; the raw coal was heated in a rotary oven to a 'plastic or globulated state', and compacted directly on discharge. The tars generated in the carbonisation process were claimed to act as binder.

Hardy's process was not a commercial success and in a much later assessment by Darmont⁽⁵⁾ this was attributed to difficulties arising in the production of char under controlled conditions; agglomeration was a big problem. Similar difficulties seem to have been encountered by Piersol in his work in Illinois⁽⁶⁾⁽⁷⁾.

Interest in the briquetting of hot char was reawakened by Jappelt in 1952⁽⁸⁾, who gave an extensive, though largely qualitative account of the factors involved in successful char briquetting. His work is of particular interest in that he concentrates on weakly caking coals, uses a rotary oven for preparing the char and advocates the use of an extrusion press for compaction.

In the light of these earlier investigations, the line of investigation adopted was to prepare the char under controlled conditions, and briquette it whilst still at a high temperature. This paper sets out to establish the process conditions for making a strong smokeless fuel from high volatile weakly caking coals by this method.

The strength of any compact produced by the direct briquetting of hot char can be expected to depend upon the following factors:-

1. The nature of the raw material.
2. The carbonisation conditions.
3. The compaction conditions.
4. The after-treatment or cooling of the briquettes.

It is not proposed in this paper to consider all the process variables, even if this were possible, but rather to focus attention on those which have been found to be the most important.

The paper first describes some of the laboratory investigations carried out under 1, 2, and 3 above, and later reviews these in the light of experience on a continuous plant. An account is then given of the necessary quenching conditions obtained from plant investigations. Finally after a brief sketch of the present state of the process a summary of the main findings is given.

2. LABORATORY INVESTIGATIONS

2.1. Description of Apparatus

The laboratory experiments were concerned with determining the conditions for the production of a strong briquette from char. It was not practicable to examine the conditions for the production of a smokeless product on this scale as insufficient product was available for test.

Fine coals (-10 mesh B.S.S.) of N.C.B. Coal Rank Classification Nos. 700, 800 and 900 (high volatile bituminous coals of low caking power) have been used; in coals of this type a reduction of volatile matter content to about 23% is sufficient to produce a completely smokeless char.

Preliminary experiments were conducted by heating a small briquetting mould ($\frac{1}{2}$ inch diameter) to temperatures in the low temperature carbonisation range (375-500°C) and introducing small charges of fine coal. After heating this material for about 5 minutes a plunger was introduced into the mould and the char was briquetted between the jaws of an hydraulic press. Strong compacts could be made in this way but this method of heating was not practical for commercial exploitation and, as the temperature of the material was not uniform, accurate temperature measurement was not practicable.

Experience at this research establishment had shown that low rank coals (CRC.700,

800 and 900) could be carbonised in this range with considerable accuracy of control using a fluid bed carboniser: the agglomeration problems had been overcome. Accordingly, a small laboratory reactor two inches in diameter was constructed which operated on a batch principle. In this reactor a coal charge could be loaded and carbonised at any temperature up to 550°C for any desired time. The char produced could be fed directly into a preheated mould and briquetted at any desired pressure.

The apparatus developed, which is illustrated in Fig. 1, was made up of the 2 inch fluid bed reactor which could be discharged into a 0.6 inch (dia.) heated mould held in the jaws of an hydraulic press. Fluidisation was normally carried out using nitrogen preheated to the chosen temperature of carbonisation and introduced into the base of the bed via the briquetting mould. Other fluidising gases, or mixtures of gases, could readily be substituted for the nitrogen flow. Control of the bed temperature was carried out by external heating and cooling coils wound round the reactor.

In operation both the reactor and the mould were first raised to the carbonisation temperature with hot nitrogen flowing through the system. A coal charge was then loaded into the carboniser and the heaters adjusted until the carbonisation temperature was reached; this took 2 to 3 minutes and thereafter the temperature was closely controlled ($\pm 5^\circ\text{C}$) for the required carbonisation time. At the end of this period the fluidising flow was stopped, and the distributor plate opened to allow char to fall directly into the mould. The char was then briquetted. To prevent any surface oxidation each briquette was allowed to cool in a small closed container.

2.2. Testing Methods for Laboratory Samples

The quality of the briquettes was assessed by a destructive mechanical test. This consisted of a combined shatter and abrasion test in which single briquettes were first subjected to a standard abrasion treatment in a commercial abrader. The $\frac{1}{8}$ inch material from this test was then dropped four times through a height of 6 ft., and the residue of $\frac{1}{4}$ inch material weighed. This was expressed as the percentage of the weight of the initial briquette. The index so formed was regarded as a purely relative measure of briquette quality. In some experiments the density of the briquettes was determined before the destructive test.

2.3. Results of Laboratory Work

2.3.1. Nature of the Raw Material:

Whilst initial tests carried out with a single coal quickly confirmed that strong compacts could be made by heating the coal to temperatures in the range 375°C - 550°C and compacting the char at 6 ton/sq.in., it was necessary at an early stage to know whether the process would be applicable to a wide range of low rank coals.

Samples of small coal, from six different collieries situated in the East and West Midlands divisions of the Board were selected and briquetted using carboniser temperatures between 375°C and 475°C. The coal was ground to -10 mesh B.S.S., and the total residence time in the reactor was 8 minutes and the briquettes were made at a pressure of 6 ton/sq.inch.

The results of shatter and abrasion tests on these briquettes are shown in Fig. 2. Despite the fact that the samples ranged over different coal seams, had widely different ash contents (2 - 16%), and covered a volatile matter content range of 35 - 41% (see Table 1), the difference in briquetting performance between these samples was not significant.

In a later attempt to briquette as wide a range of materials as possible,

special maceral concentrates, prepared from a low rank coal by hand selection, were also examined. These covered a much wider range of materials than would ever be expected to arise from normal commercial preparation of low rank coals. It was found⁽⁹⁾ for example that it was necessary to have inertinite concentrations of 60-70% before an unbriquettable material was obtained.

Size of grind can also be expected to affect the strength of char briquettes. Laboratory experiments have indicated that strength falls with increasing particle size.

To summarise, there is wide tolerance in the type of low rank material selected for the process provided that the material is crushed to a suitable size before briquetting (-10 mesh B.S.S. would appear adequate).

TABLE 1
Laboratory investigations of different coals -
Details of coals used

Coal Sample			Gray-King Coke Type	Ash Content % (dry basis)	Volatile Matter Content % d.a.f.
Division	Colliery	Seam			
East Midlands	Bestwood	High Main	B	7.2	38.1
"	Calverton	High Main	A	11.7	36.8
"	Denby Hall	Mixed	C	16.5	37.8
"	Thoresby	Top Hard	D	10.9	35.6
West Midlands	Birch Coppice	Mixed	B	11.1	41.2
"	Dexter	Mixed	A	1.7	38.0

2.3.2. The Carbonisation Conditions

The results already obtained for different coals (Fig. 2) also show that at a residence time of 8 minutes the best briquettes are produced at a temperature of about 425°C.

The general effect of carbonisation variables on briquette quality may now be considered. Using fluid bed carbonisation the major variables can be considered to be the temperature of operation, the residence time of material in the reactor, and the nature of the fluidising atmosphere. In all these laboratory experiments the residence time was measured from the instant of loading the charge and thus also includes the heating-up period of 2-3 minutes.

These carbonisation variables were examined in two experiments. In each case Calverton coal C.R.C. No. 902 was used.

In the first of these an inert atmosphere (nitrogen) was used, briquettes being made over a range of temperatures from 350°C to 500°C and a range of residence times of 5 min to 80 min. Three replicates of this experiment were made, each replicate being suitably randomised.

The variation in density with temperature and residence time is shown in Fig. 3, and that of mechanical quality as given by the combined shatter and abrasion test in Fig. 4.

It may be seen that both mechanical quality and density are a maximum in the temperature range 400-450°C, and that both decrease with increase in residence time.

In Fig. 4 contours are included to show the residual volatile matter contents (dry ash free) of the briquettes. These indicate that the best briquette quality is achieved about the 30% volatile matter content, but that strong briquettes can be produced down to and below a 25% volatile matter content, at which level very little smoke emission would be expected.

Having established that it was possible to produce briquettes using an inert atmosphere in the carboniser, a second experiment was undertaken to test the effects of using other atmospheres. In all cases the same fluidising flows were maintained, and the atmospheres selected were:-

- (i) Nitrogen as with the previous experiment.
- (ii) Nitrogen/hydrogen mixture (90:10 parts by volume).
- (iii) Steam.
- (iv) Air/nitrogen (50:50 parts by volume).

The latter atmosphere was of particular importance in that in a continuous commercial reactor it was likely that the carbonisation heat would be obtained by heat of reaction, and air would be used as a fluidising gas. In the small reactor used, with the cooling coil working at maximum capacity the air/nitrogen mixture was the richest which could be used: at higher oxygen concentrations control was impossible.

With these atmospheres briquettes were prepared in the temperature range 400° to 500°C using residence times of 8 and 16 minutes. The results are given in Table 2. For all the atmospheres, the temperature range for good briquetting was found to be substantially the same, and the fall in quality with increasing residence time was confirmed. It may be seen, however, that briquette quality was significantly reduced when the air/nitrogen mixture was used for fluidising.

From these investigations it is clear that to produce strong briquettes long residence times in the carboniser must be avoided; briquettes must be made in a limited optimum temperature range, and reactions with oxygen in the fluidising gas must be kept to a minimum.

TABLE 2

Variation of Briquette Strength* with Fluidising
Atmosphere, Carbonisation Temperature and Residence
Time. (Laboratory Results).

Fluidising Atmosphere	Residence Time (min)	Carbonisation Temperature °C				
		400	425	450	475	500
Nitrogen	8	95	94	97	96	92
	16	92	95	94	94	53
Nitrogen/Hydrogen 90:10 parts (vol.)	8	92	97	96	96	95
	16	92	93	94	91	80
Steam	8	86	96	96	94	83
	16	81	92	93	88	38
Air/Nitrogen 50:50 parts (vol.)	8	85	89	91	87	83
	16	76	84	86	72	22

- Figures given are the percentages of $\frac{1}{4}$ " material remaining after test.

2.3.3. The Compaction Conditions

It was mentioned in the introduction that char cannot be briquetted cold, and in the experiments so far described, care has been taken to maintain the briquetting mould at the carboniser temperature. Such a procedure may however be inconvenient on plant, and consequently a short investigation was made of the effect of cooling before briquetting. In this experiment briquettes were made using a single coal (Calverton C.R.C. 902) carbonised at 450°C for 15 minutes. After this period the char could be cooled to any desired temperature by switching over to cold nitrogen as fluidising gas, cutting the bed heaters, and turning on the external cooling. When the desired temperature drop had been achieved the char was then transferred to a mould maintained at the reduced temperature and briquetted (in this case at a pressure of 8 ton/sq.in.).

The results of the strength tests are shown in Fig. 5 where it can be seen that whilst quality falls slowly with temperature down to a temperature of about 250°C, after this point it falls rapidly.

The actual variation of compaction density with pressure is shown in Fig. 6, and it can be seen that at 6 ton/sq. inch the compaction curve is already becoming very steep at the temperatures involved. Pressures of 6-8 ton/sq. inch have proved adequate for all the coals studied both in laboratory and plant experiments.

3. SMALL SCALE PLANT INVESTIGATIONS

3.1. Description of Plant

A description of various experimental plants for the production of briquettes by this process has already been given elsewhere⁽¹⁾, so that it will only be necessary to add a brief description here. The particular plant used for most of these investigations was a small one capable of handling 100 lb coal/hour, Fig. 7. The reactor was 8 in. in diameter and was continuous in operation. Coal was fed into the vessel by screw feeder and char was withdrawn through a conical base to avoid agglomeration difficulties. It was normally run with cold air as the fluidising gas, all the process heat being derived by reaction with the coal.

Briquettes were made on an hydraulic extrusion press which normally produced a cylindrical compact 2 inches in diameter, and $1\frac{1}{2}$ inches long, this size being very suitable for domestic grates. With the limited plant throughput this size of briquette implies a briquetting rate of about 8 briquettes per minute, and thus speed of briquetting was low by commercial standards.

3.2. Testing Methods

As appropriate to this plant quality was assessed by larger scale tests, these consisted of:

- (i) Shatter test - 10 lb. of product was dropped four times through 6 ft. on to a steel plate, and the weight percentages of +1 inch material determined; and,
- (ii) Abrasion test - 5 lb. of product was subjected to 625 revolutions at a standard rate (25 r.p.m.) in a smooth steel trommel, the weight percentages of the resulting $\frac{1}{8}$ inch material being determined.

For brevity in this paper the results of these separate tests have been combined in a single strength index by forming the product of the indices. This single strength index then bears some resemblance to the combined shatter and abrasion test results obtained from the laboratory investigations. Whilst the strength tests were intended for relative assessment of the product it is considered that where the index obtained exceeded 80% the briquettes would transport well, whereas if it was less than 50% they would transport badly.

3.3. Results of Plant Work

In the following review of the effect of process variables the product has in all cases been dry cooled (i.e. allowed to cool in sealed drums). On a full scale plant cooling in sealed drums would not be possible and development of briquette quenching methods is described later in section 3.3.4.

3.3.1. Nature of the Raw Material

Low rank coals from 24 different collieries were examined covering the range of Gray King coke types A to F. Using a temperature of 425°C and a residence time of 20 min, it was found possible, in all cases, to produce strong briquettes (i.e. combined shatter and abrasion index greater than 80%, see Table 3). At this carbonising temperature the smoke emission of the briquettes, as shown by tests in an open grate, was small in all cases.

TABLE 3

Plant investigations of different coals
Details of coals used and the strength of briquettes
Produced at 425°C

Division	Coal Sample		Gray King Coke Type	Ash Content % (dry basis)	Volatile Matter Content % d.s.f.	Strength of bqs. made at 425°C (%)
	Colliery	Seam				
E.Midlands	Babbington	Deep soft	F	2.1	37.2	91
"	Thoresby	Top hard	F	5.2	35.3	93
"	Rufford	Top hard	E	4.9	37.7	93
"	Welbeck	Top hard	E	4.8	35.5	92
"	Babbington	Deep hard	D	3.1	35.9	92
"	Gedling	Top hard	C	6.0	38.8	92
"	Radford	Tuption	C	3.1	37.8	93
"	Shirebrook	Clowne	C	4.0	37.1	92
"	Whitwell	High Hazel	C	4.0	35.6	91
"	Bestwood	High main	B	7.5	37.8	91
"	Bestwood	Main bright	B	1.5	38.5	92
"	Gedling	High Hazel	B	6.5	39.8	93
"	Ollerton	Top hard	B	5.2	37.9	90
"	Warsop	High Hazel	B	9.1	36.3	91
W.Midlands	Coventry	Mixed	C	1.9	39.4	91
"	Haunchwood	Mixed	B	5.6	40.7	90
"	Newdigate	Mixed	B	2.9	39.1	92
"	Arley	Mixed	A	5.0	39.2	91
"	Dexter	Mixed	A	4.2	36.8	89
N.Eastern	Kiveton Park	High Hazel	F	2.7	36.1	87
"	Markham Main	Barnsley	D	3.8	36.8	90
Scottish	Dalkeith	Barrs	C	5.0	41.0	89
"	Dalkeith	5 ft	C	4.8	40.6	90
"	Dalkeith	6 ft	C	3.8	40.0	91
"	Woolmet	Ell	B	3.1	36.8	89

The pressure required to make these compacts was about 6 ton/sq.inch, although for the higher coke types somewhat lower pressures were often adequate.

The plant results therefore show that the hot char briquetting process is applicable to a wide range of low rank coals, and thus confirm and extend the earlier laboratory findings.

3.3.2. The Carbonisation Conditions

The plant investigation of the effect of carbonisation variables on briquetting has been rather more restricted because of plant limitations than that in the laboratory. An investigation using Dexter coal, C.R.C. No. 902, has, however, been made of the variation of briquette quality with temperature (in the range 375°C to 450°C), and residence time (15 min to 45 min). In order to achieve the longer residence times it was necessary to dilute the fluidising air with nitrogen, although on a larger plant a deeper bed could be used.

The results of combined shatter and abrasion tests carried out on briquettes made using a constant pressure of 7 ton/sq. inch for the above range of carboniser variables are given in Fig. 8. As with the laboratory results it may be seen that the strongest briquettes are made in the range 400°C - 450°C, and that quality diminishes with increasing residence time.

As with the laboratory briquettes the volatile matter content for optimum strength is higher than the 23% at which the char is completely smokeless.

3.3.3. The Compaction Conditions

In the laboratory it was shown that any substantial reduction of temperature between carboniser and press produces a weaker briquette.

Tests were carried out on the plant by removing heating and lagging from the short feed line connecting carboniser and press. The briquetting temperature as indicated by thermocouples in the char stream are given in Table 4, together with the shatter and abrasion indices of the briquettes produced.

TABLE 4
Variation of Briquette Strength* with Briquetting
Temperature. (Plant Results)

Carbonisation Temperature	425°C
Briquetting Temperature	Briquette Strength*
425°C	93
400°C	87
350°C	84
285°C	83

• Results quoted are the combined plant shatter (+ 1") and abrasion (+ $\frac{1}{8}$ ") test results.

+ All briquettes were prepared at a pressure of 7 ton/sq. inch.

Over the limited range of temperature drop investigated in this way there was a reduction in quality with increasing temperature drop; this confirmed the laboratory results. It is preferable to permit no fall in char temperature between the reactor and the press: indeed there may be a case for using a rising temperature gradient.

With respect to other briquetting variables it has been found on the plant that density increases with pressure, but that the rate of increase falls at higher pressure, as would be expected. This is true also of briquette strength, but on extrusion presses another effect is important. At high pressures the separation between successive briquettes becomes poor, and in some cases continuous lengths of undivided briquette emerge from the nozzle. For briquette appearance it would thus appear that pressures which are too high can be a positive disadvantage and this seems to be particularly the case with the more highly caking coals. However, wherever this phenomenon has been encountered it has been found possible to make strong briquettes at pressures below those which bring about severe sticking.

3.3.4. Quenching Conditions

In bulk production of char briquettes it is necessary to introduce a cooling stage to prevent spontaneous combustion of the product and it has already been pointed out that, in the assessments so far of process variables, the product has been dry quenched in sealed drums. Cooling in this way takes between 12 hours and 2 days, depending on whether 90 lb or 250 lb drums are used.

Quite early in these investigations wet quenching by immersion in water was considered as an alternative. By this means briquettes can be quenched to a safe temperature (i.e. about 50°C) in 20 min., but such cooling produces internal cracking and gives substantially lower shatter indices than those obtained for a dry cooled product. This is particularly true for briquettes produced at 425°C, and for the more highly caking coals.

Experiments on cooling briquettes in fluid beds of cold sand and in dry ice quickly demonstrated that the rate of cooling rather than the nature of the coolant was responsible for the cracking.

When a briquette emerging from a press at about 400°C is plunged directly into cold water it suffers a large thermal shock. The shock can be reduced by cooling the briquettes more slowly, either in an inert atmosphere or by spraying lightly with water, prior to complete immersion. That such a two-stage cooling procedure reduces internal cracking is illustrated in Fig. 9, where sections of briquette dry cooled in sealed tins for 10 and 20 min. before immersion in water are compared with briquettes which were immediately immersed.

Plant investigations have shown that it is desirable to reduce the average temperature gradually to about 150°C before immersion in water. The first cooling stage can be performed by cooling on a conveyor in a steam atmosphere for 30 min., or by a shorter period, (15 min.) of spray quenching (see Fig. 10), followed by 8 min. immersion in water. These two-stage treatments gave briquettes closely comparable in strength with those cooled in sealed drums. For commercial exploitation, steam cooling, followed by water immersion, is preferred.

3.3.5. Smoke Emission & Fuel Performance

With the greater supply of product from the plants it was possible to carry out open, i.e. stool-bottom, grate tests⁽¹⁰⁾ and coke grate tests⁽¹¹⁾ for radiation and visible smoke. Smoke emission may be measured optically using a photo-electric cell to measure the obscuration of a light beam traversing the flue or the smoke may be collected in an electrostatic precipitator and weighed. The second method is likely to be accepted as a British Standard method but for our purpose the convenience of the optical method outweighed the rather better accuracy of the gravimetric method.

Optical smoke indices are given in Table 5. Values obtained from other "naturally smokeless" coals are included for comparison. The parent coal, in this case Dexter C.R.C. No. 902, gave an index of 93.

It can be seen that smoke emission decreases rapidly with increasing carbonisation temperature and decreasing volatile matter content until the product becomes virtually smokeless at 23% volatile matter content. Further, the range of smoke emission of the "naturally smokeless" fuels given in Table 5, is wide enough to give considerable latitude in process conditions for the production of a strong briquette.

TABLE 5

Smoke Emission Indices for briquettes burned in
stool-bottom and coke grate tests

- a) Smoke index of briquettes made from Dexter char; 30 min. residence time in carboniser.

Carbonisation temperature °C of the briquettes .	375°C	400°C	410°C	425°C	450°C
Volatile matter content d.a.f. of the briquettes	32.3	27.9	26.0	23.4	21.0
Smoke emission index in stool-bottom tests	23	10	4	2	< 1
Smoke emission index in coke grate tests	18	13	5	2	< 1

- b) Sample smoke indices of other coals for comparison

				<u>Index</u>
(i)	<u>Stool-bottom grate</u>			
	International coal	16.5% V.M. d.m.m.f. (3" x 2")		35
	Deep Navigation coal	14.0% V.M. d.m.m.f. (3" x 2")		7
	Penrikyber coal	12.7% V.M. d.m.m.f. (3" x 2")		3
	Commercial Low Temperature Coke	(+ $\frac{3}{4}$ ")		3
(ii)	<u>Coke Grate</u>			
	International coal	16.5% V.M. d.m.m.f. (2 $\frac{1}{4}$ " x 1 $\frac{1}{4}$ ")		33
	Deep Navigation coal	14.0% V.M. d.m.m.f. (2 $\frac{1}{4}$ " x 1 $\frac{1}{4}$ ")		8
	Penrikyber coal	12.7% V.M. d.m.m.f. (2 $\frac{1}{4}$ " x 1 $\frac{1}{4}$ ")		4
	Commercial Low Temperature Coke	(+ $\frac{3}{4}$ ")		2

The critical air blast test¹² showed the fuel to be "reactive" in that the required air blast was less than the minimum flow used in this test (0.008 cu. ft. air/min). The general performance of the briquettes in stool-bottom grate tests is illustrated in Table 6; it can be seen that, apart from smoke, the performance of the briquetted fuel equals that of the parent coal.

TABLE 6

Performance of Dexter coal and Dexter char briquettes
in stool-bottom grate tests*

Fuel Tested	Dexter 2 $\frac{1}{4}$ " x 1 $\frac{1}{4}$ " coal	Dexter Char Briquettes (425°C)
Time to reach 6,000 B.t.u./h after ignition (min)	28	29
Peak radiation after ignition B.t.u./h	10,410	8,060
" " " 1st refuel "	10,530	9,940
" " " 2nd " "	9,140	9,990
" " " 3rd " "	8,550	9,130
Gross radiation (2000-2000 B.t.u./h) B.t.u.	67,380	69,070
Average radiation per hour "	6,670	6,470
" " " pound "	2,900	3,020
of fuel burned		

* In the stool-bottom test a fire is lit using 9 lb. of coal and recharged three times using 5 lb. of coal per refuel.

4. DISCUSSION

So far we have reviewed some of the main process variables involved in briquetting hot char in an extrusion press as revealed by laboratory and small pilot plant investigation. We have shown that a strong briquette can be made and that there is a fair range of conditions under which the briquette is also smokeless, but we have not considered some of the variables which are of great importance to the commercial success of the process.

First is the ability of the carbonising and briquetting systems to operate continuously over reasonable periods without shutdown. The carbonising system is particularly prone to troubles associated with agglomeration in the bed and the extrusion press is susceptible to high rates of die wear. In order to get some measure of these likely difficulties a 500 hr. run on an 18 in. dia. carboniser/2" dia. extrusion press rig was attempted. Only minor difficulties were encountered in the carboniser and die wear was found to be much less troublesome than had been expected.

For commercial use it is necessary to operate the extrusion press at much higher speeds than is possible on small pilot plant where the limit was about 40 strokes per minute. The limit was set primarily by the capacity of the carboniser but was also influenced by the transient shock waves which are characteristic of hydraulic presses operating at high speed. Recent experience on a variable speed mechanical press, Fig. 11, has shown that good briquettes can be made at speeds of 80 strokes per minute, and that higher speeds may well be possible. Attempts have also been made to briquette the char on roll presses, these have been successful but demand very close control of carboniser conditions.

Briquette shape is important commercially and some of the variants possible on an extrusion press are illustrated in Fig. 12. In order to obtain optimum fuel performance on an open fire, briquette weight should not exceed 100 grms.

Tonnage quantities of briquettes have been made for market and transport trials, and Fig. 13 gives some idea of the appearance of a wagonload of dry quenched briquetted after a transport test.

The fuel has been shown to be an acceptable premium grade smokeless fuel for the domestic market. It is smokeless at volatile contents between 23 and 26% and is made without unpleasant and expensive binder. Preparations for commercial development are already in an advanced stage. It remains to exploit the virtues of this process in the manufacture of closed stove and metallurgical fuel, and to extend the range of coals which can be processed in this way.

ACKNOWLEDGMENTS

The work described was carried out in the research laboratories of the National Coal Board at Stoke Orchard, Cheltenham, England; it is published by kind permission of Dr. W. Idris Jones, Director General of Research. The authors acknowledge the helpful discussion and careful experimentation of many colleagues.

The views expressed are those of the authors and not necessarily those of the Board.

REFERENCES

1. W. Idris Jones and J. Owen, Smokeless fuel from low rank coals carbonised in a fluid bed. Paper to Inst. of Fuel. To be published 1962.
2. R.J. Piersol, State of Illinois Geol. Survey, Rep. of Investigations No. 37, (1935).
3. D.H. Gregory and W.N. Adams, Int. J. Air Pollut., 1, 263, (1959).
4. H.A. Hardy, Brit. Pat. No.'s 356, 236 (1931), 357,330 (1931), 445, 207/8 (1936), 460 394 (1937).
5. G. Darmon, Fuel, 31, 75 (1952).
6. R.J. Piersol, State of Illinois Geol. Survey, Rep. of Investigations No. 31, (1933).
7. R.J. Piersol, State of Illinois Geol. Survey, Bull. 72. (1948).
8. A. Jappelt, Erdöl u. Kohle, 6, 613 (1953).
9. S. Bennett, K. Elsworth, G.M. Habberjam and M.F. Woods. The effect of maceral composition on the binderless briquetting of hot char. (to be published).
10. National Coal Board Analysts Handbook, Section XV, (1956).
11. British Standard 3142, (1959).
12. British Standard 1264, (1945).

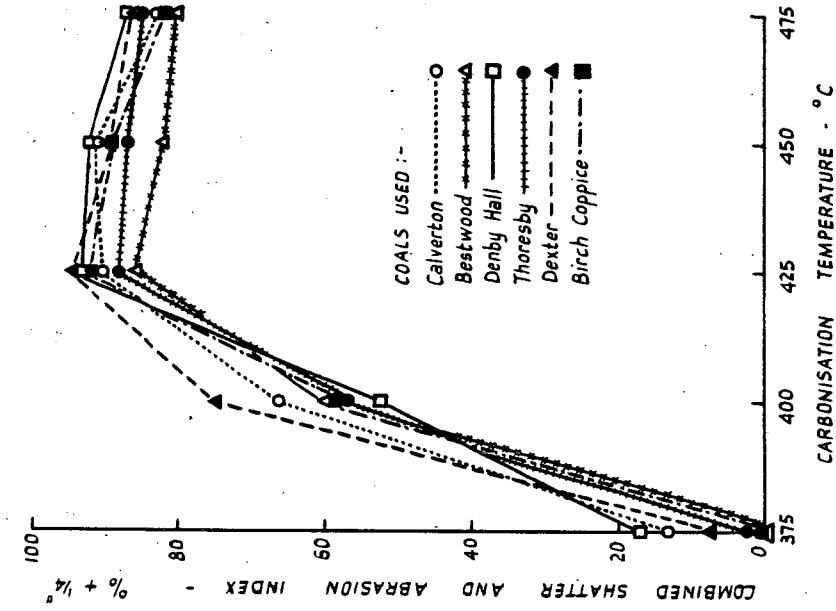


FIG. 2. BRIQUETTING PERFORMANCE OF SIX LOW RANK COALS.

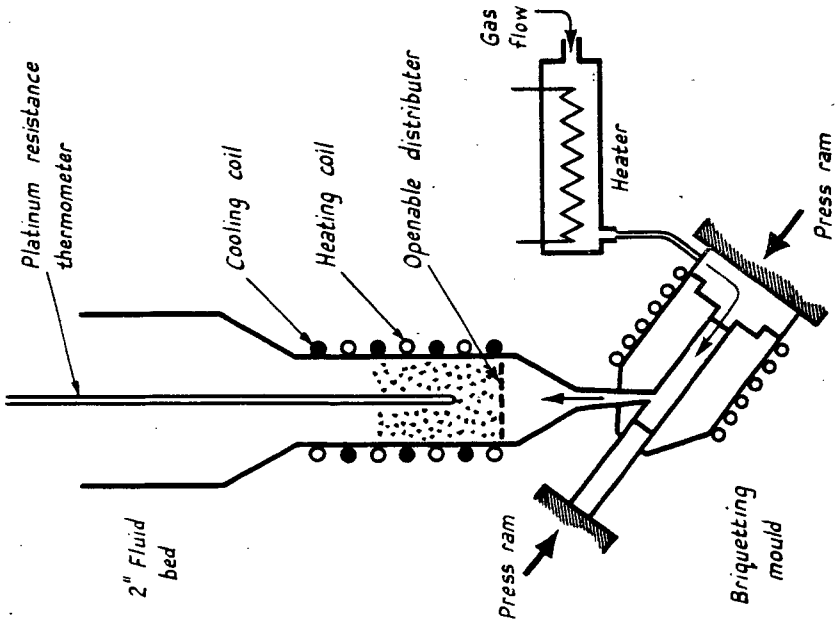


FIG. 1. LABORATORY BRIQUETTING APPARATUS

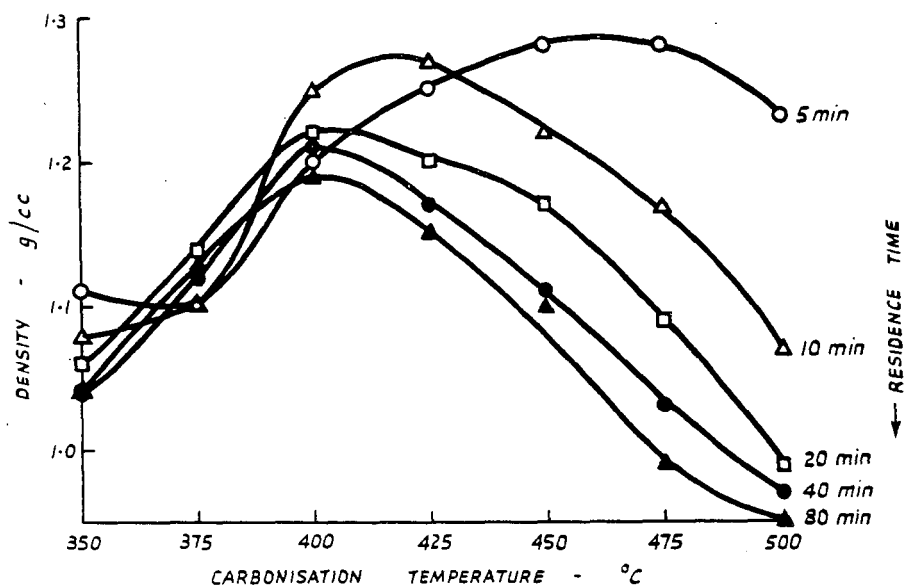


FIG. 3. VARIATION OF DENSITY WITH TEMPERATURE AND TIME.

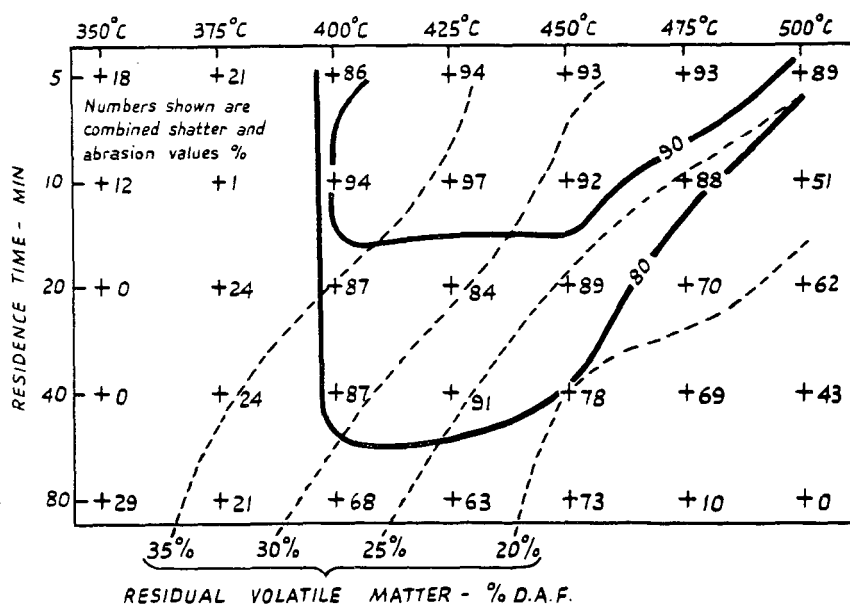


FIG. 4. VARIATION OF STRENGTH WITH TEMPERATURE AND RESIDENCE TIME. (LABORATORY RESULTS)

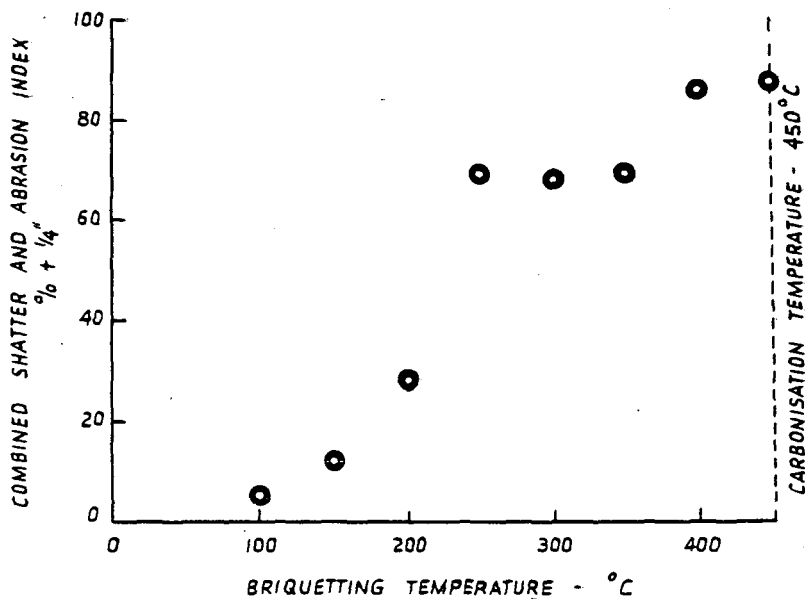


FIG. 5 EFFECT OF BRIQUETTING TEMPERATURE ON STRENGTH.

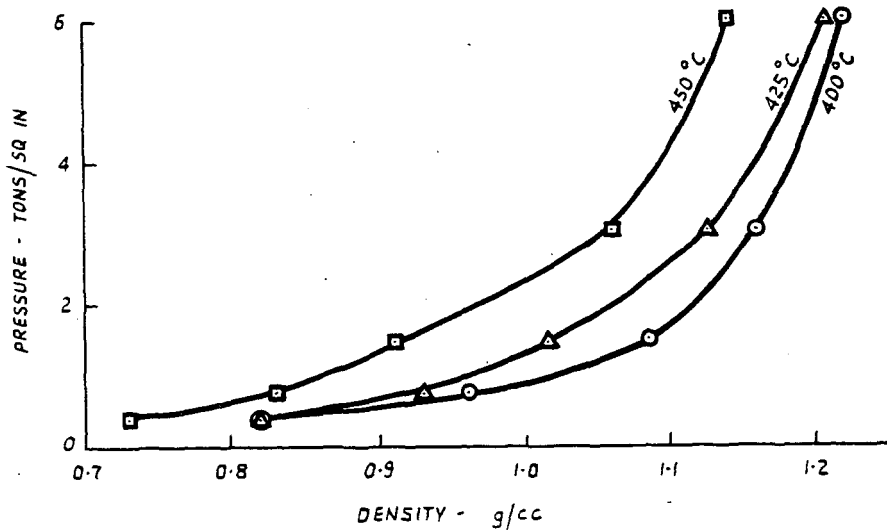


FIG. 6 VARIATION OF COMPACTION WITH PRESSURE.

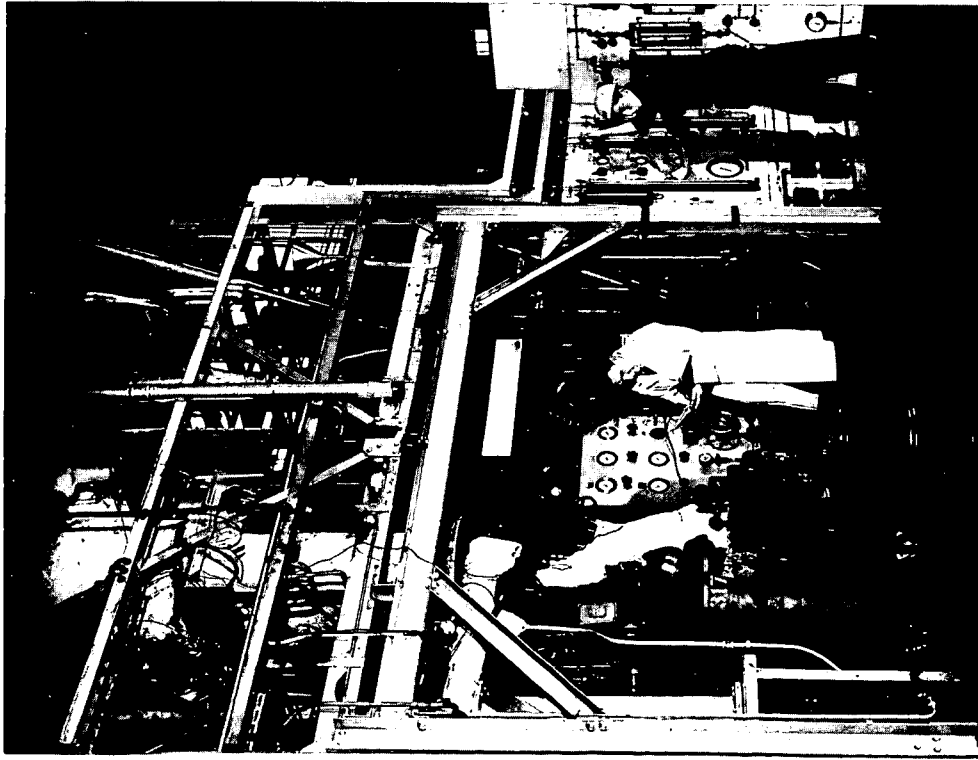


FIG. 7. 100 lb/h PLANT

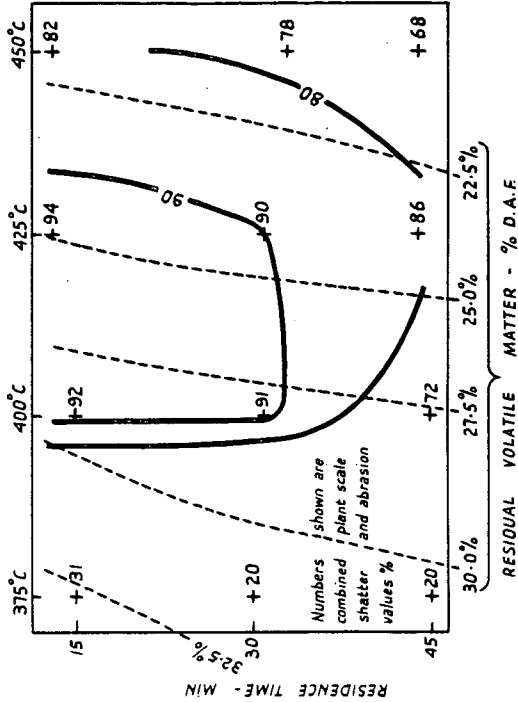
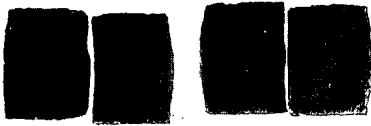


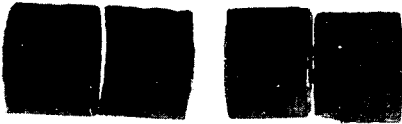
FIG. 8. VARIATION OF STRENGTH WITH TEMPERATURE AND RESIDENCE TIME. (PLANT RESULTS)



Briquettes dry quenched



*Briquettes wet quenched after
20 min. dry quenching*



*Briquettes wet quenched after
10 min. dry quenching*



Briquettes wet quenched

FIG. 9. SECTIONS OF BRIQUETTES AFTER QUENCHING



FIG. 10. TWO-STAGE QUENCHING FACILITIES ON A
SMALL PILOT PLANT

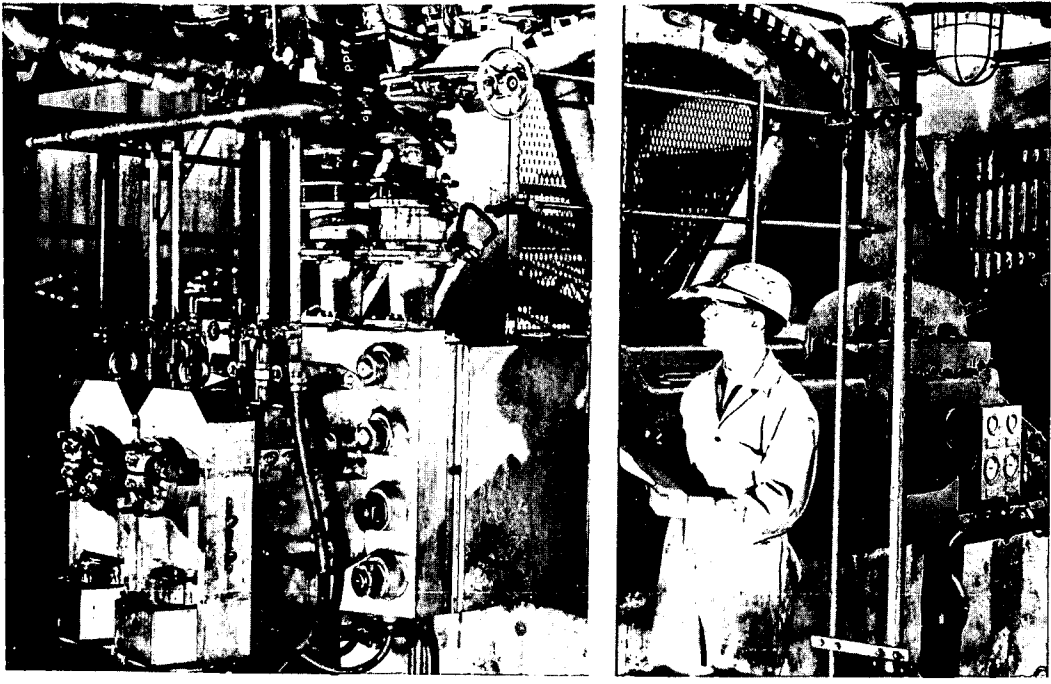


FIG. 11. MECHANICAL EXTRUSION PRESS

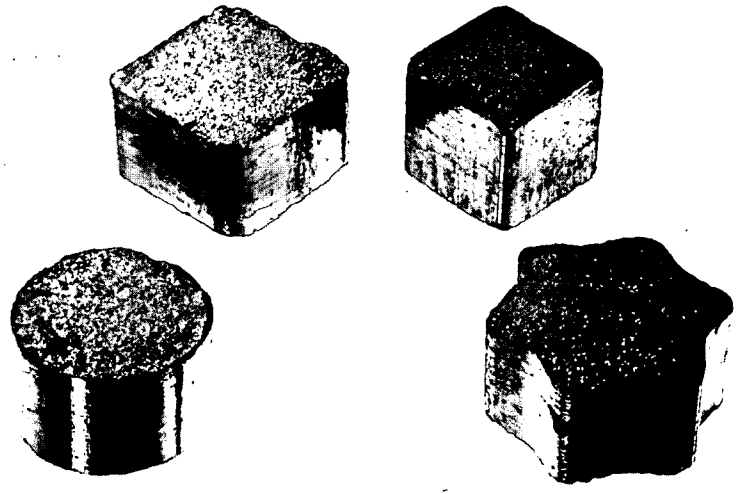


FIG. 12. EXTRUSION BRIQUETTES OF VARIOUS CROSS - SECTION

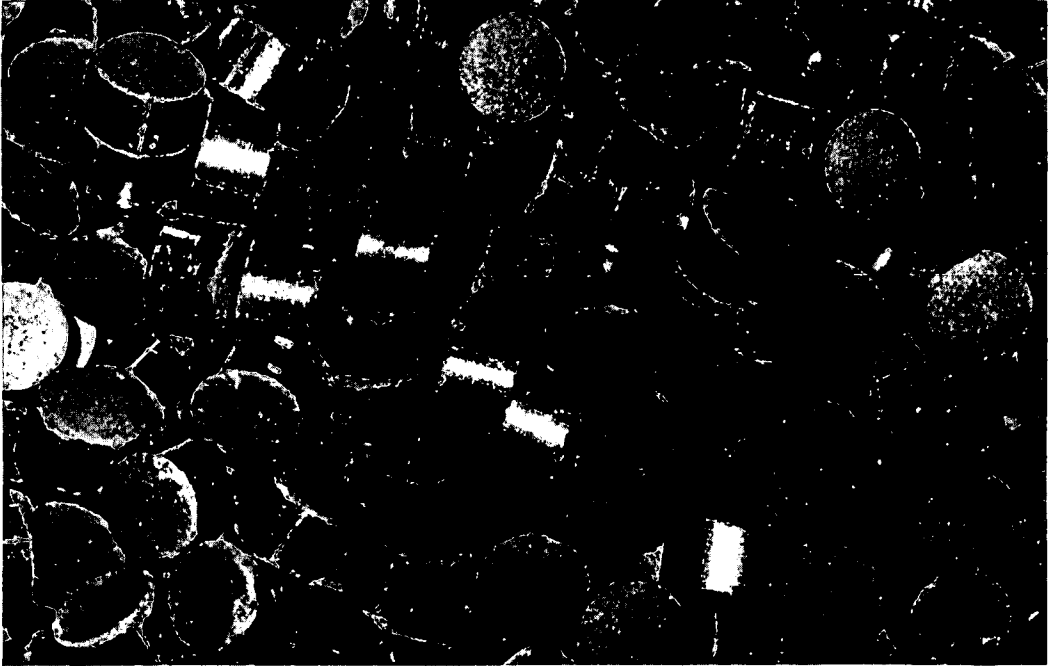


FIG. 13. BRIQUETTE APPEARANCE AFTER 200 MILES
RAIL TRANSPORT

THE SLOW OXIDATION OF METHANE. I. A KINETIC STUDY

Hsien-Cheng Yao

Scientific Laboratory, Ford Motor Company, Dearborn, Michigan

Introduction

A number of rate expressions have been proposed for the oxidation of methane based upon measurements of the changes which occur in the total pressure of the reacting gas mixture. Bone and Allum (1) found that the rates of reaction were affected by the initial composition of the mixture. The highest rate under a given set of conditions was obtained when the ratio of the initial pressure of methane to that of oxygen was 2 to 1. This result was confirmed recently by Egerton and his co-workers (2). Norrish and Foord (3) proposed the rate equation:

$$\text{rate}_{\max} = \frac{k(\text{CH}_4)_0^2(\text{O}_2)_0 P_0 d}{S} \quad (\text{I})$$

where $(\text{CH}_4)_0$, $(\text{O}_2)_0$, and P_0 are initial pressures of methane, oxygen, and total pressures of methane, oxygen, and total pressure respectively, d is the diameter of the reaction vessel, and S is the surface activity per unit area. Later, Hoare and Walsh (4) suggested the rate expression

$$\text{Max rate} \propto (\text{CH}_4)_0^m (\text{O}_2)_0^x (P_0)^t e^{-E/RT} \quad (\text{II})$$

where m , x , and t are reaction orders which vary with the reaction vessel used. The m values ranged from 1.6 to 2.4, the x value from 1.2 to 1.7, and the t values from 0.5 to 0.9.

Recently Egerton and his colleagues (2) and Karmilova *et al* (5) have followed not only the changes in the total pressures but also the changes in the concentrations of reactants, intermediates, and products in each experiment. This was done by repeatedly preparing identical systems and then quenching them at various time intervals; these quenched systems were then analyzed for each component. On the basis of such experiments, Karmilova proposed the expression

$$\frac{d(\text{CH}_4)_{\max}}{dt} = k(\text{CH}_4)_0^\alpha (\text{O}_2)_0^\beta P_0^\gamma \quad (\text{III})$$

where $\frac{d(\text{CH}_4)_{\max}}{dt}$ represents the rate values ("constant rates") obtained from the

slopes of the straight line portion of the rate curves (zero order plots). The values of α , β , and γ were given as 1.62, 0.96, and ≈ 0.1 respectively. The sum of these is approximately 2.7 which agrees well with the value ($n = 2.6$) obtained by Egerton *et al* (2) but which differs from that of Norrish and Foord (3) ($n = 4.0$).

The most recent equation has been proposed by Enkolopyan (6), Semenov (7), Karmilova (8) and their co-workers on the basis of a theoretical treatment of the mechanism of the oxidation:

$$\frac{d(\text{CH}_4)_{\text{max}}}{dt} = \frac{2k_2 k_3}{k_8} \left(\frac{k_2 k_3}{k_2' k_3'} \right)^{\frac{1}{2}} (\text{CH}_4)^2 (\text{O}_2) \quad (\text{IV})$$

In this equation, the k 's are rate constants of a series of free radical reactions and (CH_4) and (O_2) are instantaneous partial pressures of methane and oxygen.

Although these authors (8) believed that equation IV is in good agreement with equation III, these equations are not identical. The maximum rate in the former (III) expression is dependent upon the initial partial pressures of methane and oxygen and that in the latter (IV) upon the instantaneous partial pressures of the reactants. Moreover, equation IV does not agree with many of their experimental results. For example, equation IV demands that the rate be second order with respect to methane and first order with respect to oxygen. Yet, the experimental results show that in some cases the rate of methane and oxygen consumption and of carbon monoxide formation is constant up to 50% completion of the reaction (5).

The foregoing resume makes it clear that additional evidence is still needed before the extent of the validity of the previously proposed rate equations and reaction mechanisms for the oxidation of methane can be established. Such evidence is difficult to obtain from the experimental techniques customarily used. Measurements of the changes in total pressure are inadequate for the determination of the reaction order with respect to methane and to oxygen or of the activation energy. Also, while the quenching technique can provide such evidence, it is laborious, time-consuming, and requires a vast number of separate experiments to examine in detail all the parameters in the reaction.

In addition to the experimental limitations of the earlier work, the role of carbon monoxide - the most stable intermediate in the oxidation of methane - has not yet been clarified. Yet, evidence has shown (5) that the oxidation of methane and of carbon monoxide occur simultaneously in the later stages of the reaction. Thus, the rate equation cannot be complete without including an expression for the oxidation of carbon monoxide.

In the present work, the oxidation of methane has been re-examined in detail. The partial pressures of methane, oxygen, and carbon monoxide have been followed by periodic withdrawal and analysis of small samples of the reacting gas mixture by means of gas chromatography. This technique permits a rapid, convenient, and accurate analysis for the separate components throughout each oxidation experiment.

Using this new technique, data have been obtained from which the reaction order with respect to methane and to oxygen can be examined and from which the apparent energies of activation can be calculated. A study has also been made of the methane-initiated oxidation of carbon monoxide.

Experimental

I. Reactants

Research grade methane, 99.54% pure (Phillips Petroleum Co.) was used without further purification. Oxygen, 99.5% pure (Liquid Carbonic, Division of General Dynamics) and carbon monoxide, c.p. grade (Matheson Co.) were dried through a column of 5A molecular sieve material (Fisher Scientific Co.) before use.

II. Apparatus

The apparatus consists of a gas introduction system, reaction vessel, gas sampling system, and a gas chromatograph connected as shown in Figure 1. The gas

chromatograph (Perkin-Elmer Corp. Model 154D) is equipped with a thermistor detector and a 2-meter column packed with molecular sieve material ("Column I").

III. Measurements of Partial Pressures

To measure the partial pressures of each of the gases during the oxidations, it was necessary to establish the relation between the chromatographic peak height and the quantity of each individual gas. For this purpose, gases were introduced through inlets 3 to the sampling capillary 9 located between stopcocks C and D. This capillary, 1 mm I.D. and 70 mm long, contained about 0.08 ml of gas. The pressure of the gas was measured on manometer 2. C and D are 3-way stopcocks with 1 mm. bore and Teflon plugs, while E is a 2-way glass stopcock with 2 mm. bore. By manipulating stopcocks C and D and also E, the gas trapped in the sampling capillary was pushed by the carrier gas, helium, into the gas chromatograph and a corresponding peak appeared on the recorder chart. The peak heights were plotted as a function of the pressures of the gases as shown in Figure 2. Thus for a given condition, $P = aH$ where P is the gas pressure, H is the peak height, and a is the proportionality constant. The value of a varies with the pre-set conditions, such as column temperature, flow rate of carrier gas, and volume of sampling capillary. In addition, repeated use of the chromatographic column may also change a . In the work reported here, the value of a for each individual gas was re-ascertained before each oxidation experiment.

IV. Oxidation Experiments

For the oxidation experiments, the separate gases were admitted through inlets 3 to the individual gas burets 5. The desired amounts (approx.) of the components of the reaction mixture were then pumped from the gas burets into the reaction vessel 7 using pump 6. The cylindrical reaction vessel was constructed of borosilicate glass (30 mm. I.D. with a volume of 100 ml.) and contained a thermocouple well along its longitudinal axis. In some experiments as indicated below, the vessel was used without further treatment and in others, it was first treated with hydrofluoric acid; for this treatment, the vessel was shaken with 20-25% hydrofluoric acid in water, then washed exhaustively with distilled water, and dried at 400°C at less than 1 mm. of Hg.

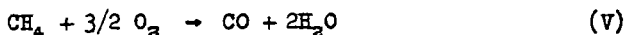
During the course of the oxidation experiments, the reaction vessel was maintained at the desired operating temperatures $\pm 1^\circ\text{C}$ by the thermocouple, temperature controller (Wheelco), variable transformer and furnace 8.

To determine the composition of the gases in the vessel at the start and during the experiments, a large fraction (ca. 55%) of the gas mixture was withdrawn from the reaction vessel and passed through the sampling capillary by lowering the mercury level in the modified 125 ml Toepler pump 11. Raising the level returned the gas through the capillary to the vessel. Two cycles were needed before each sampling in order to obtain reproducible analyses; each cycle required only about 15 seconds. The small sample of gas (0.08 ml.) was then pushed into the gas chromatograph with helium as described above. In such manipulations, some helium was inevitably introduced into the reaction vessel during sampling but it appeared to have no effect upon any of the reactions studied.

Results and Discussion

In many of the experiments reported earlier, carbon monoxide accumulated in much larger amounts than any other reaction intermediates, such as formaldehyde or hydroperoxide. In addition, Karmilova et al (9) were able to show by tracer techniques that the carbon dioxide formed in the oxidation of methane was produced almost

exclusively from the oxidation of carbon monoxide. Thus, although the less stable intermediates may contribute to the mechanism, the kinetics of the overall oxidation can be examined in terms of the stepwise reactions represented by equation V and VI.



I. The Oxidation of Methane to Carbon Monoxide (eq. V)

A. The reaction order with respect to methane and oxygen. To minimize the effect of carbon monoxide on the reaction kinetics, the ratio of the initial pressures of methane, $P_{\text{CH}_4}^0$, to that of oxygen, $P_{\text{O}_2}^0$, was increased in some experiments. When the ratio is about 3 or higher, the reaction is zero order with respect to oxygen and to methane; the results of typical experiments with both untreated and HF-treated vessels are shown in Figure 3. With such high ratios, the rates of consumption of methane and oxygen and the rates of accumulation of carbon monoxide are constant up to 90% completion of the reaction. These rates can be expressed as:

$$-\frac{dP_{\text{O}_2}}{dt} = k_1 \quad (\text{VII})$$

$$-\frac{dP_{\text{CH}_4}}{dt} = \frac{dP_{\text{CO}}}{dt} = 2/3 k_1 \quad (\text{VIII})$$

where k_1 is the zero order rate constant.

When the ratio of $P_{\text{CH}_4}^0$ to $P_{\text{O}_2}^0$ is reduced to unity or less, the rates are constant only up to about 30 to 70% completion. In these experiments, sufficient carbon monoxide accumulates so that it is oxidized competitively with methane. The rate equations (VII and VIII) can no longer be applied for the whole reaction but only for the initial stage where the rates are constant (Figure 4).

These constant rates have been observed by all previous investigators but have been generally identified by them only as "maximum rates" (equations I, II, and III). They were interpreted differently by previous investigators. Semenov (7, 10) has suggested that the oxidation of methane is a free radical chain degenerating process in which the formation of formaldehyde is the slow step of the reaction and the steady state of formaldehyde results in a constant rate. This interpretation has been accepted by many previous investigators. Recently, however, Karmilova *et al* (11) found that the rate remains constant even when the concentration of formaldehyde undergoes a marked decrease and, therefore, the postulation of the steady state concentration of formaldehyde as a controlling feature of the reaction is untenable. To explain these constant rates, they proposed that the oxidation of methane undergoes additional catalysis by one of the reaction products formed after formaldehyde. The observed constant rate may then result from a superposition of the rates of two autocatalytic processes, the increase in the rate of one due to oxidation of methane being compensated by the decrease in the rate of the other. They suggested several possible additional catalysts, such as hydrogen peroxide, hydroxy radical, etc. No evidence was given to support this view.

B. The effect of initial pressures of methane and oxygen. The results for the effect of $P_{\text{CH}_4}^0$ and $P_{\text{O}_2}^0$ on the value of k_1 are shown in Tables 1 and 2. In general,

k_1 increases with increasing either $P_{\text{CH}_4}^0$ or $P_{\text{O}_2}^0$, or both. $P_{\text{CH}_4}^0$ has more effect upon k_1 than does $P_{\text{O}_2}^0$. An empirical equation is proposed to account for the dependency of k_1 on the initial pressures:

$$k_1 = k_1' \frac{P_{\text{CH}_4}^{0a} P_{\text{O}_2}^0}{P_{\text{CH}_4}^0 + P_{\text{O}_2}^0} \quad (\text{IX})$$

where k_1' is a pressure independent rate constant. The values of k_1' are listed in Column 5 of Table 1 and Column 6 of Table 2. The validity of equation IX is indicated

by the linear relationship in the plot of k_1 vs $\frac{P_{\text{CH}_4}^{0a} P_{\text{O}_2}^0}{P_{\text{CH}_4}^0 + P_{\text{O}_2}^0}$ for the reactions at

different temperatures in an HF-treated vessel as shown in Fig. 5. For the reaction

in an untreated vessel, k_1 at 399°C increases linearly with $\frac{P_{\text{CH}_4}^{0a} P_{\text{O}_2}^0}{P_{\text{CH}_4}^0 + P_{\text{O}_2}^0}$ until it

appears to reach a limiting value of about 0.17 mm, min⁻¹ (Figure 6).

The increase in the maximum rates ("constant rates") as the initial partial pressures increase - observed in this as well as in earlier work (equations I, II and III) - is not accounted for by equation IV which is based on a free radical chain reaction mechanism.

The apparent energy of activation for the oxidation of methane calculated from k_1' values at four different temperatures (Figure 7) is 36.2 kcal/mole. This value differs from the values [43 (5, 6), 60.8 (12), and 61.5 (13)] obtained by earlier workers from the maximum rates.

C. The induction period. For the reactions below 455°C, an induction period has been observed which ranges from 1 min. to 350 min. as shown in Tables 1 and 2. The initial pressures of methane and oxygen affected this induction period but the exact relationship remains to be established. In general, the reactions in the untreated vessel had longer induction periods than those in the HF-treated vessel. It was noted that the induction period was extremely long when an untreated vessel was used for the first time. Also, the induction period is longer for reactions at lower temperatures than those at high temperatures. At 482°C and above with an HF-treated vessel, the induction period is negligible.

II. Methane-Initiated Oxidation of Carbon Monoxide (Equation VI)

In the course of the oxidation of methane when the ratio of the partial pressure of carbon monoxide to methane becomes appreciable, then the rate of disappearance of methane no longer follows the zero order equation (eq. V). Additional attention must therefore be devoted to the oxidation of carbon monoxide and to the role it plays in the oxidation of methane.

The oxidation of carbon monoxide itself requires temperatures of about 1000°C (14); however, in the presence of water vapor, this temperature may be lowered to about 400°C (15). There is no doubt that methane can also initiate the oxidation of carbon monoxide (15). A detailed study of this reaction is presented below.

A. Reaction in the presence of water. Since water can also initiate the oxidation of carbon monoxide, a comparison was made between the effect of methane and that of water. As shown in Fig. 8, when the mixture of carbon monoxide, oxygen and water vapor was heated at 427°C in an HF-treated vessel, the oxidation was slow. It became fast after methane was introduced.

B. Reaction order with respect to carbon monoxide and oxygen. In these experiments, dried carbon monoxide and oxygen were introduced into the HF-treated vessel at various temperatures ranging from 427° to 516°C. The reactions were extremely slow. However, the rate of reaction increased rapidly when a small amount of methane was introduced. The results of one such experiment are shown in Fig. 9. In all the present results, the methane-initiated oxidation of carbon monoxide is a second order reaction, first order with respect to carbon monoxide and to oxygen. The rate can be expressed as:

$$-\frac{dCO}{dt} = k_2 P_{O_2} P_{CO} \quad (X)$$

where k_2 is the second order rate constant. The temperature dependence of k_2 (Fig. 7 and Table 3) leads to an apparent activation energy of 60.7 kcal/mole.

As shown in Fig. 9, the linear relationship of the second order plot was maintained despite the decrease in pressure of methane from 13 mm to almost zero during the course of the reaction. This was observed in every experiment on the methane-initiated oxidation of carbon monoxide. k_2 does not depend, therefore, upon the instantaneous pressure of methane. Instead, there appears to be some relationship (Table 4) between k_2 and the initial pressure of methane - analogous to that exhibited by k_1 - although no satisfactory correlation has yet been obtained.

In another type of experiment (Fig. 10), additional carbon monoxide was added to a reacting mixture of methane and oxygen (and carbon monoxide produced) when the methane had decreased to 3.2 mm. A linear relationship was again obtained for the

second order plot of $\log \frac{2P'_{O_2} - P_x}{P_{CO}}$ versus time t . In this expression, P'_{O_2} is the

pressure of oxygen at the time when carbon monoxide was introduced, P_x is the pressure of carbon dioxide produced after that time, and P_{CO} is the instantaneous pressure of carbon monoxide. In this experiment k_1 , 8.9 mm, min⁻¹, was determined from the initial rate of consumption of oxygen and k_2 , 8.2 x 10⁻⁵ mm⁻¹, mm⁻¹, was obtained from the slope of the second order plot. This value of k_2 agrees well with those of Table 3 and once again appears to be related to the initial pressure of methane. If it depended upon the instantaneous pressure of methane when the carbon monoxide was added, viz. 3.2 mm, k_2 should be below 2.6 x 10⁻⁵ mm⁻¹, mm⁻¹ (Table 4).

III. Nature of the Oxidative Process

In the present work, during each sampling procedure, about 55% of the gas mixture was withdrawn from the reaction vessel to the Toepler pump at room temperature for about 15 seconds and then returned to the vessel. In the second cycle, this was repeated so that more than 80% of the reaction mixture may have been quenched during

each sampling. Even in the experiments which had relatively long induction periods, the sampling procedure had no discernible effects upon the rate curves. Therefore, it appears that the oxidation of methane must be a heterogeneous reaction inasmuch as quenching would affect the kinetics of a homogeneous reaction. Also, the apparent energy of activation for the oxidation of methane is 36.2 kcal/mole whereas that of carbon monoxide is much higher, i.e., 60.7 kcal/mole. It is difficult on the assumption of a homogeneous reaction to reconcile this wide disparity in energies of activation with the observations that both gases oxidize competitively during the reaction. Likewise, the rate of oxidation of methane depends upon the initial pressures of methane and oxygen rather than upon the instantaneous pressures as would be expected for a homogeneous reaction.

Some consideration of the possible nature of the heterogeneous process is warranted. On the basis of the present results, it appears that methane and oxygen react initially to form certain active sites or intermediate complexes on the surface of the reaction vessel. These active sites in turn can catalyze the oxidation of both methane and carbon monoxide which are zero order and second order reactions, respectively. The activity of these sites per unit area depends upon the initial concentrations and remains constant throughout the reaction. As the oxidation proceeds, carbon monoxide is produced in the reaction. This product in turn competes with the methane for the same active sites. A similar suggestion has been made by Von Meersche (16). As the concentration of the carbon monoxide becomes significant with respect to that of methane, then the consumption of methane deviates from the zero order rate. If the methane and carbon monoxide did not compete for the active sites but instead competed for the remaining oxygen, then the zero order rate for the consumption of methane should remain constant throughout the reaction. However, this has not been observed.

The detailed mechanism of this reaction and the nature of the active sites remain to be studied.

Summary

1. A stepwise oxidation of methane to carbon monoxide and then to carbon dioxide is demonstrated. The oxidation of methane to carbon monoxide is a zero order reaction with respect to both methane and oxygen. The zero order rate constant is dependent upon the initial pressures of both methane and oxygen. The correlation of this constant with initial pressures is indicated by an empirical equation. The apparent energy of activation for this reaction was calculated to be 36.2 kcal/mole.

2. The reaction in an untreated vessel has a longer induction period and slower rate than that in an HF-treated vessel.

3. The oxidation of carbon monoxide is initiated by methane or its oxidation product and is a second order reaction, first order with respect to oxygen and to carbon monoxide. The second order rate constant appears to vary with the initial pressure of methane. The apparent energy of activation for this reaction is 60.7 kcal/mole.

4. The oxidation of methane appears to be a heterogeneous process. It is suggested that during the induction period, methane and oxygen react to form active sites or intermediate complexes on the surface of the reaction vessel. Methane and its oxidation product, carbon monoxide, then compete for these sites rather than for oxygen.

Acknowledgment

The author is indebted to Dr. C. H. Ruof for his encouragement and guidance in the course of this work.

References

- (1) W. A. Bone and R. E. Allum, Proc. Roy. Soc. A134, 578 (1932).
- (2) A. C. Egerton, G. J. Minkoff and K. C. Solooja, Proc. Roy. Soc., A235, 158 (1956).
- (3) G. W. Norrish and S. G. Foord, Proc. Roy. Soc., A157, 503 (1936).
- (4) D. E. Hoare and A. D. Walsh, Fifth Symposium on Combustion, Reinhold Publishing Corporation, New York, 1955, PP 467-484.
- (5) L. V. Karmilova, N. S. Enikolopyan and A. B. Nalbandyan, Zhur. fiz. Khim, 31, 851 (1957); *ibid* 34, 550 (1960).
- (6) N. S. Enikolopyan, Seventh Symposium on Combustion, Butterworths Scientific Publications, London 1959, P. 157.
- (7) N. N. Semenov, Some Problems of Chemical Kinetics and Reactivity, Pergamon Press, New York, 1959, Vol. 2, PP 103-117.
- (8) L. V. Karmilova, N. S. Enikolopyan, A. B. Nalbandyan and N. N. Semenov, Zhur. fiz. Khim 34, 1176 (1960).
- (9) L. V. Karmilova, N. S. Enikolopyan and A. B. Nalbandyan, Zhur. fiz. Khim, 35, 1458 (1961)
- (10) N. N. Semenov, Chemical Kinetics and Chain Reactions, Oxford 1935
- (11) L. V. Karmilova, N. S. Enikolopyan, A. B. Nalbandyan Zhur. fiz. Khim, 35, 1435 (1961)
- (12) A. C. Egerton, G. J. Minkoff and K. C. Salooja, Combustion and Flame, 1, 25 (1957).
- (13) R. Fort and C. N. Hinshelwood, Proc. Roy. Soc. A129, 284 (1930).
- (14) J. H. Burgoyne and H. Hirsch, Proc. Roy. Soc. A227, 73 (1954).
- (15) D. E. Hoare and A. D. Walsh, Trans Faraday Soc. 50, 37 (1954).
- (16) M. Von Meersche, Ann. Min. Belg., 48, 643 (1949).

Table 1 - Oxidation of Methane in an HF-Treated Vessel at Various Temperatures

Expt. No.	T°C	P _{O₂} , mm	P _{CH₄} , mm	k ₁ , mm, min. ⁻¹	k ₁ ' x 10 ⁵ , mm ⁻¹ , min. ⁻¹	Induction Period, min.
32	399	127	317	1.5	5.22	40
33	"	83.4	364	1.44	5.83	35
34	"	380	330	3.02	5.18	16
35	"	378	148	0.89	5.65	20
36	427	399	151	2.82	17.1	14
37	"	151	344	6.5	18.0	5
38	"	154	126	1.7	19.5	10
39	"	154	346	5.64	15.3	4
40	"	372	364	11.7	17.5	5
41	454	347	161	8.0	45.2	3
42	"	185	355	18.2	42.2	1
43	"	115	106	2.55	43.4	3
44	"	204	187	8.9	48.9	3
45	"	265	234	16.6	57.1	3
46	"	312	306	23.2	49.1	4
47	"	308	371	33.0	52.9	4
24	482	383	306	47.5	86.4	< 1
25	"	209	298	32.0	87.4	"
26	"	122	308	23.1	86.2	"
27	"	278	267	37.5	101	"
28	"	196	272	32.5	105	"
29	"	186	107	6.5	89.4	"
30	"	112	342	28.3	98.1	"
31	"	111	346	24.3	83.6	"

Table 2 - Oxidation of Methane in an Untreated Vessel at 399°C

Expt. No.	P _{O₂} , mm	P _{CH₄} , mm	k ₁ , mm, min. ⁻¹	k ₁ ' mm ⁻¹ , min. ⁻¹	Induction Period, min.
2*	79	408	0.13	4.8 x 10 ⁻⁶	350
3	96.4	306	0.17	7.0 x 10 ⁻⁶	55
4	226	288	0.17	4.7 x 10 ⁻⁶	50
5	151	265	0.16	6.3 x 10 ⁻⁶	48
6	83.6	273	0.15	8.6 x 10 ⁻⁶	56
7	39	372	0.15	11.4 x 10 ⁻⁶	40
8	74	311	0.16	8.6 x 10 ⁻⁶	50
9	243	111	0.042	5.0 x 10 ⁻⁶	150
10	220	71.4	0.043	11.2 x 10 ⁻⁶	60
11	236	156	0.17	12.0 x 10 ⁻⁶	40
12	280	94	0.06	9.0 x 10 ⁻⁶	40
13	287	95.5	0.033	8.6 x 10 ⁻⁶	50
14	179	75	0.05	12.7 x 10 ⁻⁶	120
15	246	120	0.06	6.2 x 10 ⁻⁶	150

*E2 was in a new vessel used for the first time.

Table 3 - Dependency of k_2 on Temperature

Expt. No.	$P_{CH_4}^0$, mm	$T^{\circ}C$	k_2, mm^{-1}, min^{-1}
E104	13.0	516	1.70×10^{-4}
E98	12.5	516	1.20×10^{-4}
E103	13.5	504	7.36×10^{-5}
E99	14.0	482	2.27×10^{-5}
E102	13.4	482	3.125×10^{-5}
E101	11.0	454	5.5×10^{-6}

Table 4 - Dependency of k_2 on $P_{CH_4}^0$ (482°C)

Expt. No.	$P_{CH_4}^0$	k_2
118	3.7 mm	$2.6 \times 10^{-5} mm^{-1}, min^{-1}$
116	8.1	4.8×10^{-5}
117	14.9	5.0×10^{-5}
115	19.7	6.7×10^{-5}

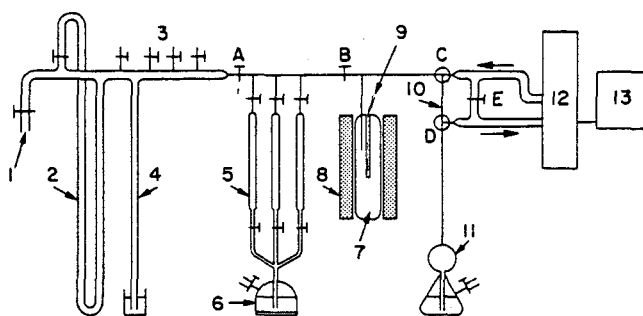


Fig. 1. - Reaction system. 1. Vacuum inlet; 2. Manometer; 3. Gas inlet; 4. Pressure relief device; Gas burets; 6. Mercury pump; 7. Reaction vessel (100 ml.); 8. Furnace; 9. Thermocouple; 10. Sampling capillary; 11. Toepler pump (125 ml.); 12. Gas chromatograph; 13. Recorder.

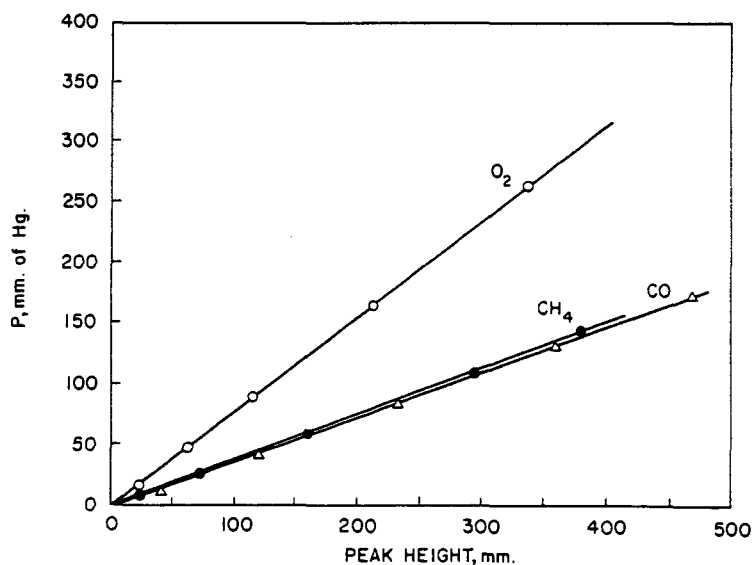


Fig. 2. - Calibration of peak heights against pressures.

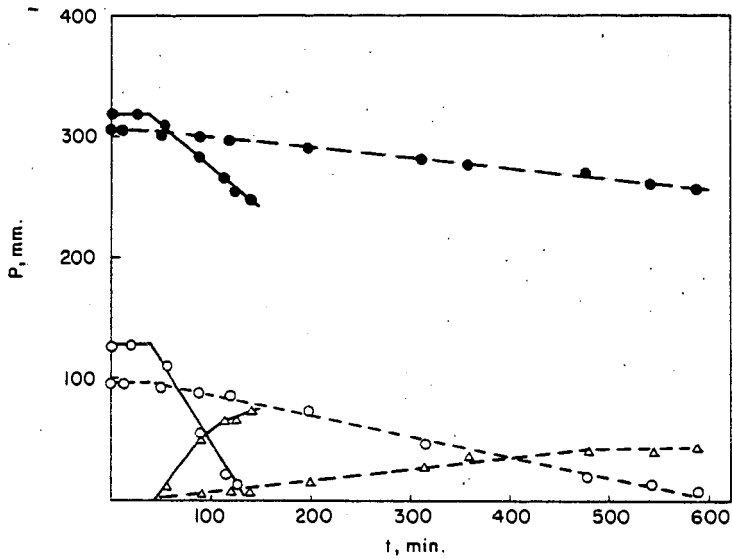


Fig. 3. - Rate curves for the oxidations of methane at 399°C. O, O₂; ●, CH₄; Δ, CO. Broken lines, untreated vessel (E3); solid lines, HF-treated vessel (E32).

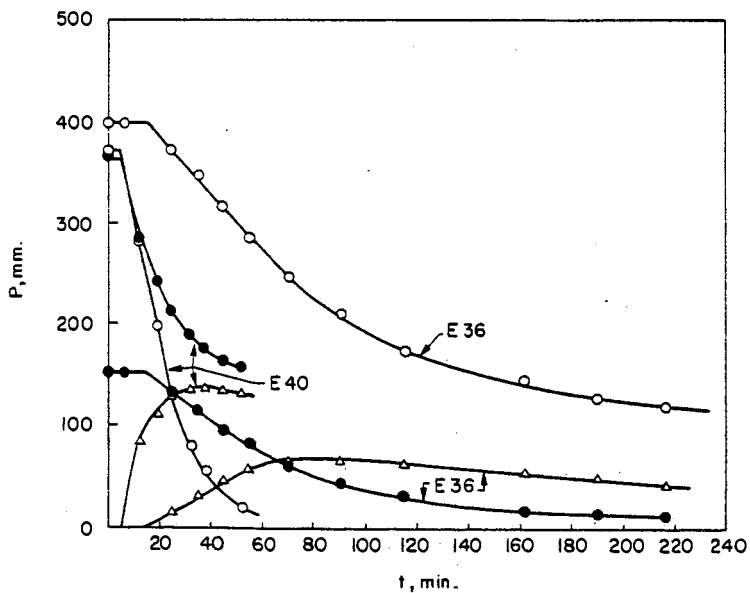


Fig. 4. - Rate curves for the oxidations of methane in HF-treated vessel at 427°C. Experiment 36, $P_{\text{CH}_4}^0/P_{\text{O}_2}^0 = 0.38$; Experiment 40, $P_{\text{CH}_4}^0/P_{\text{O}_2}^0 = 0.98$. O, O₂; ●, CH₄; Δ, CO.

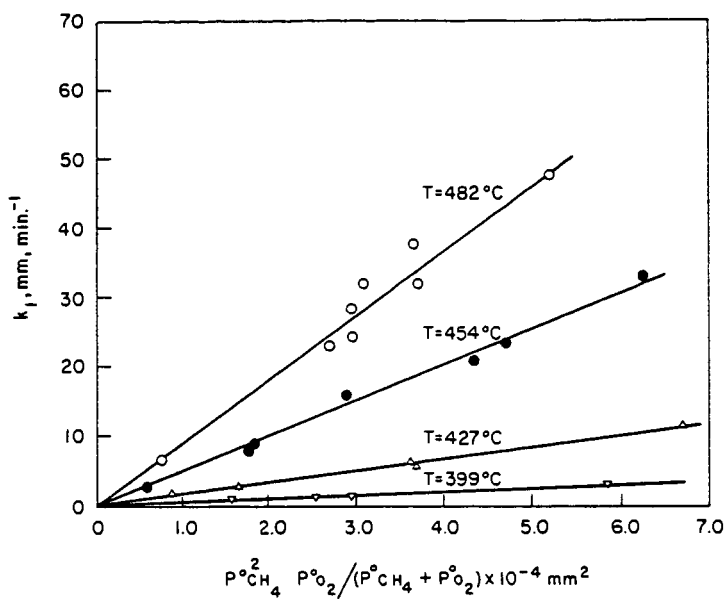


Fig. 5. - Dependence of k_1 on initial pressures of methane and oxygen (oxidations in HF-treated vessel).

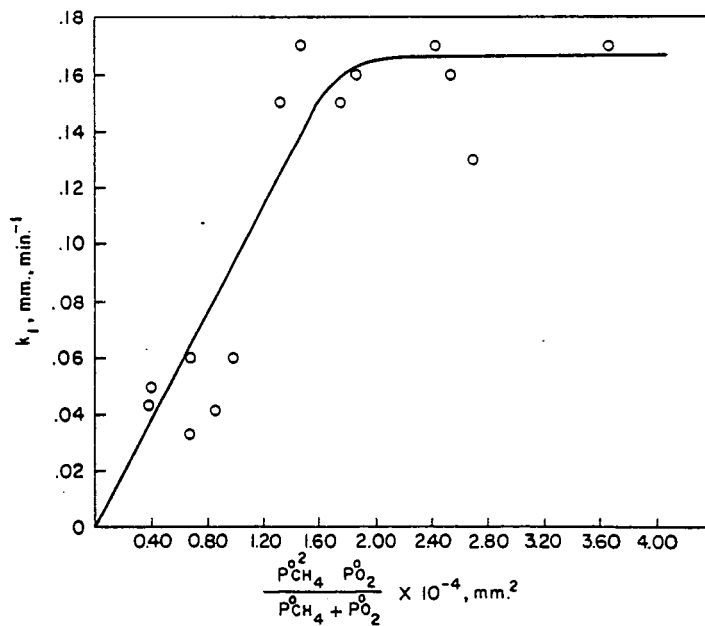


Fig. 6. - Dependence of k_1 on initial pressures (oxidations in untreated vessel at 399°C).

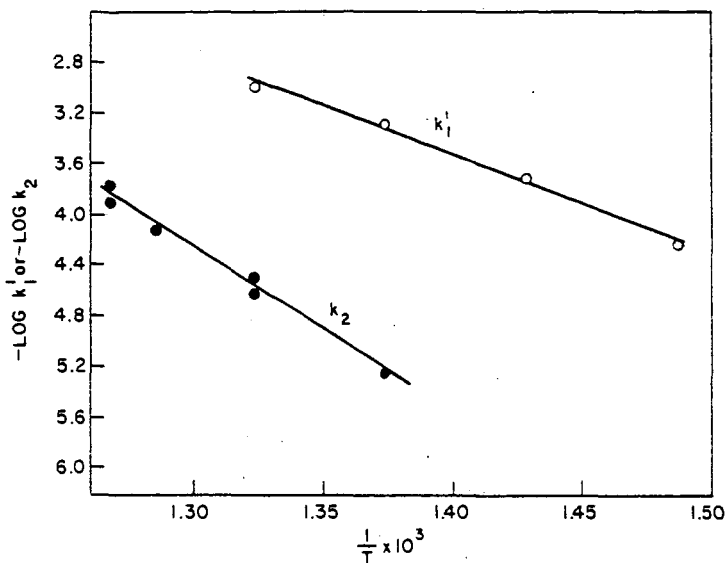


Fig. 7. - Arrhenius plot for the determination of the apparent activation energy.

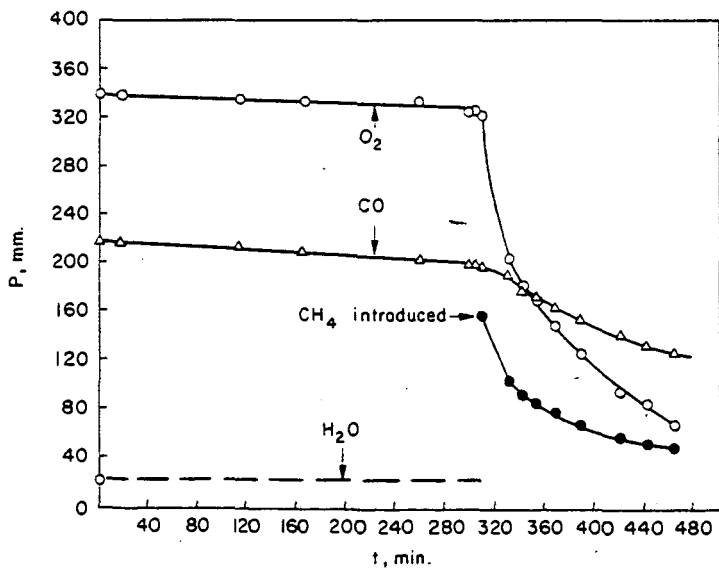


Fig. 8. - Oxidation of carbon monoxide in the presence of water (22 mm. of Hg) and methane at 427° C (E60).

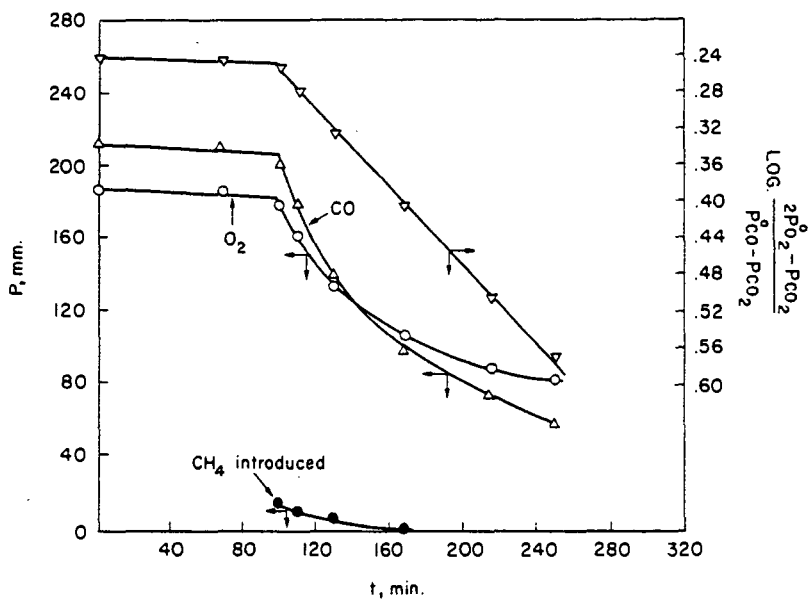


Fig. 9. - Rate curves for the methane-initiated oxidation of carbon monoxide at 504°C.

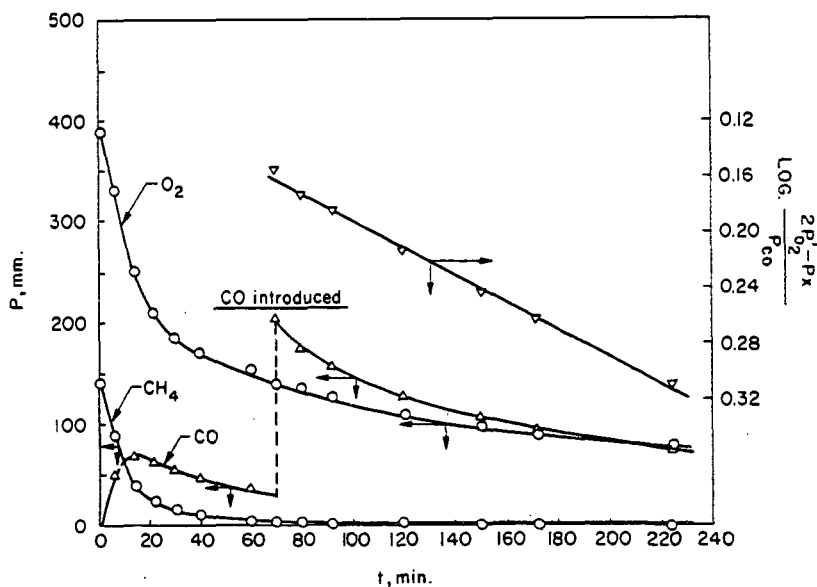


Fig. 10. - Determination of k_1 and k_2 in the oxidation of methane.

New Developments in Catalysts for Producing a High-B.t.u.
Gas via the Hot Gas Recycle Process

A.J. Forney, J.H. Field, D. Bienstock, and R.J. Demski

Pittsburgh Coal Research Center
U. S. Bureau of Mines
Pittsburgh, Pa.

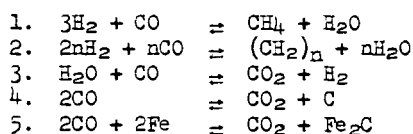
INTRODUCTION

A high-B.t.u. gas can be produced from coal by gasifying the coal to make H_2+CO , and then reacting these gases, after purification, over a catalyst to make a gas consisting essentially of methane. (A satisfactory high-B.t.u. gas would have a minimum calorific value of 900 B.t.u. per cubic foot and a maximum carbon monoxide content of 0.1 percent.) A methanation process under development in the Federal Bureau of Mines at Bruceton, Pa., at the present time is the hot-gas-recycle process.

In the hot-gas-recycle system the exothermic heat of reaction (about 280 B.t.u. per cubic foot of methane produced) is absorbed by the sensible heating of large volumes of recycle gas circulating through the reactor in direct contact with the catalyst. Because of the large volumes of gas and the high cost of compression, it is necessary to have a low pressure drop through the catalyst bed. The development by the Bureau of an active, durable catalyst made of steel lathe turnings that pack with a high void volume and offer little resistance to flow made the hot gas recycle feasible.

This paper describes methanation in two stages using a steel lathe turning catalyst in the first reactor and nickel catalyst in the second to complete the conversion of synthesis gas. By this method the amount of nickel catalyst needed is considerably less than that usually required in methanation processes. Previous results have been reported for use of granular Raney nickel as catalyst in the second reactor.¹ In this paper pilot plant results are shown comparing operation of the second reactor with granular catalysts and with nickel catalysts in the form of plates either of solid Raney nickel or nickel sprayed on steel or aluminum. These latter materials offer a negligible flow resistance and permit efficient use of a small amount of expensive nickel catalyst.

Table 1 shows the principal reactions occurring in the synthesis. Equations 1 and 2 are the synthesis reactions for the formation of hydrocarbons. Equation 3 is the water gas shift reaction. Equation 4 is an undesirable carbon deposition reaction, and 5 the carbide reaction. All these reactions are exothermic at synthesis temperature of 300° C.

TABLE 1. Reactions occurring in hot-gas-recycle process

EXPERIMENTAL PROCEDURE AND RESULTS

A flowsheet of the hot gas recycle process is shown in figure 1. Two reactors are used in series, the first, using steel lathe turnings, converts 70-90 percent of the synthesis gas, and the second, using nickel, converts essentially the remainder. The total feed gas passes down through the first reactor, then through a cyclone trap and is divided. Part flows to the second reactor; the remainder is recompressed to 425 p.s.i.g. and recycled to the reactor, 90 to 95 percent as hot recycle and the balance as cold recycle. As water is condensed and removed from the cold recycle, the amount of cold recycle is used to control the water vapor content of the total recycle gas. The synthesis gas then combines with the recycle gas and flows to the main reactor.

The tail gas flows to the second reactor which is operated at a lower recycle rate. In the absence of a hot-gas compressor, it was necessary to cool the whole recycle stream. The product stream is depressurized, metered, and analyzed.

Table 2 shows the results of typical tests operating with $3\text{H}_2+1\text{CO}$ feed gas using one or two reactors. The first column shows results achieved using only one reactor which contained steel turnings as catalyst. The turnings had been oxidized with steam and reduced with hydrogen to produce an active catalytic surface. The calorific value of the product gas was 720 B.t.u. per cubic foot. The carbon monoxide content was 2.1 percent. The methane content was 31.9 percent with significant quantities of ethane and propane. The feed-gas conversion was 83.4 percent. The second column of the table shows results obtained with both reactors operated in series. The second reactor contained Raney nickel of 4-20 mesh size. The heating value of the product gas increased to 936 B.t.u. per cubic foot, and the carbon monoxide content decreased to 0.1 percent. The methane content was 93.5 percent. In addition to methanating the carbon monoxide, most of the carbon dioxide reacted and the heavier hydrocarbons cracked and were hydrogenated to methane.

Because the Raney nickel catalyst used in the second reactor was in the form of granules, the pressure drop across the second reactor was higher than desired for hot-gas-recycle operation. Raney nickel is too brittle to be machined to lathe turnings, the physical form used for the catalyst in the first reactor. To overcome this difficulty, two types of nickel catalyst plates were devised. Plates were sawed from an ingot of Raney nickel and assembled in a parallel array to fit into the 3-inch diameter reactor as shown in figure 2. Plates were 5-3/4 inches high and 1/8 inch thick. A second type consisted of assemblies made of steel or aluminum plates sprayed with Raney nickel powder or nickel oxide powder using a oxy-hydrogen or oxy-acetylene torch. The powder of 100-300 mesh size was sprayed on 1/16-inch plates to a thickness of 0.040-0.060 inch on each side and edge. An average of 350 grams of Raney nickel or 250 grams of nickel oxide was on the surface of each assembly.

TABLE 2. Synthesis results using one or two reactors, ^{a/} steel turnings in first reactor, granular Raney nickel in second

Reactors	1	2
Space velocity to first reactor, vol. of gas/vol. of catalyst/hour	850	850
Space velocity to second reactor	---	10,000
Exit gas analysis (vol.-percent-dry basis)		
H ₂	48.6	2.8
CO	2.1	0.1
N ₂	0.5	.8
CO ₂	6.3	1.4
C ₁	31.9	93.5
C ₂ =	0	0
C ₂	5.4	0.9
C ₃ =	0.2	.1
C ₃	2.9	.3
C ₄ +	1.6	.1
Heating value, B.t.u./cu. ft.	720	986
H ₂ +CO conversion, percent	83.4	99.3
Avg. temperature, °C. 1st reactor	320	319
Avg. temperature, °C. 2nd reactor	---	321

a/ 3H₂+1CO feed to the first reactor.

The plate assemblies sprayed with Raney nickel were activated by digesting with a 3-percent NaOH solution to remove 20 percent of the aluminum. Those sprayed with nickel oxide were activated by reducing with hydrogen. The nickel oxide was a sinter material of the composition shown in table 3.

TABLE 3. Analysis of Raney nickel and nickel oxide^{a/}

Material	Raney nickel	Nickel oxide
Nickel	42-40	74.2
Aluminum	58-60	
Cobalt		1.04
Iron		1.94
Copper		0.73
Sulfur		.13

a/ Weight percent.

With the steel turnings being used as a catalyst in the first reactor, consecutive tests were made using solid Raney nickel plates, stainless steel plates sprayed with Raney nickel, and aluminum plates sprayed with nickel oxide sinter in the second reactor. At comparable conditions the pressure drop was reduced about 90 percent, from 17 inches with granular Raney nickel; to less than 2 inches of water per foot of catalyst height, with plates.

Table 4 shows other results of these tests. Except for the carbon monoxide content, a satisfactory high-B.t.u. gas was produced. No significant difference in catalyst activity or product composition was observed with these three catalysts in the second reactor. Since the nickel oxide sinter is as satisfactory as the Raney nickel as a catalyst for the second reactor, it would be preferred as it costs only one-third as much per weight of nickel.

TABLE 4. Results of tests using plate assemblies in second reactor^{a/}

Catalyst	First reactor	Second reactor		
	steel turnings	Solid Raney plates	Raney nickel sprayed plates	Nickel oxide sprayed plates
Space velocity, vol./vol./hr.	700	6000	5800	5700
Avg. reactor temp., °C.	321	332	334	329
H ₂ +CO conversion, percent	73.8	97.3	98.0	97.5
Exit gas analysis, (vol.-percent-dry basis)				
H ₂	56.7	9.0	7.5	9.0
CO	4.0	1.8	0.8	0.8
N ₂	1.1	0.7	.8	.9
CO ₂	8.7	2.4	2.1	2.6
CH ₄	23.6	84.5	87.2	85.1
C ₂ =	0	0	0	0
C ₂	3.5	1.0	1.0	1.1
C ₃ =	0.1	0.1	0.3	0
C ₃ -	1.7	.4	.3	.4
C ₄ =	0	0	0	0
C ₄ +	.6	.1	0	.1
Heating value, B.t.u./cu.ft.	566	925	943	927

a/ 3H₂+1CO feed to the first reactor.

An advantage of the flame-spraying technique is evident with the nickel oxide. Nickel oxide granules disintegrated to powder on reduction with hydrogen at 400° C. Although the material was active catalytically, it had no mechanical strength. However, the nickel oxide sprayed on plates adhered firmly to the base metal after reduction. Thermal spraying may be applicable to other catalysts which are catalytically active but structurally weak.

Because the plates operated satisfactorily in the second reactor, a few tests were made using them in the first reactor. Table 5 shows the results of these tests. The solid plates of Raney nickel made a product gas with a heating value of 941 B.t.u. per cubic foot. The use of plates sprayed with Raney nickel resulted in gas with a heating value of 877 B.t.u. per cubic foot and the plates sprayed with nickel oxide, 856. In all cases the carbon monoxide content exceeded 0.1 percent. The plates sprayed with Raney nickel were operated at an average temperature of 255° C. When the temperature was raised to over 300° C. they became inactive.

TABLE 5. Results of tests using plate assemblies in first reactor^{a/}

Catalyst	Solid Raney nickel plates	Raney nickel on stainless steel plates	NiO on aluminum or stainless steel plates
Space velocity, vol./vol./hr.	1250	1500	3000
Avg. reactor temperature, °C.	347	255	393
H ₂ +CO conversion, percent	99.0	93.1	95.4
Exit gas analysis (vol.-percent-dry basis)			
H ₂	4.2	22.6	14.5
CO	0.3	4.3	1.7
N ₂	1.3	0.4	1.2
CO ₂	2.7	0.2	3.3
CH ₄	91.4	63.5	79.3
C ₂ =	0	0	0
C ₂	0.1	4.5	0
C ₃ =	0	0.1	0
C ₃	0	1.7	0
C ₄ =	0	0.1	0
C ₄ +	0	0.7	0
Heating value, B.t.u./cu.ft.	941	877	856

a/ 3H₂+1CO feed gas.

DISCUSSION

At an hourly space velocity of 6,000 and 330° C., sprayed nickel and solid Raney nickel plates produced a gas with the desired calorific value when used in the second stage of the hot gas recycle pilot plant. However, at this space velocity carbon monoxide values of 0.8 to 1.8 percent were too high. When used as a catalyst in the first reactor, at an hourly space velocity of 1,250 and 347° C., the solid Raney nickel plates produced a product gas of 941 B.t.u. per cubic foot and a carbon monoxide content of 0.3 percent, whereas the sprayed sections in the first reactor produced a gas that was unsatisfactory in both respects, calorific value and carbon monoxide content.

This difference in results between the solid Raney nickel plate assemblies and the plates sprayed with Raney nickel may be due to several factors: 1) The coating may have been too thin and the digestion procedure did not activate sufficient nickel; 2) the coating did not adhere to some of the plates, indicating either faulty sand blasting or spraying technique.

These nickel sections have advantages over steel lathe turnings. Higher conversions and higher heating value gas can be achieved in the first reactor; they can be operated at temperatures as high as 450° C. without significant carbon deposition; they are less susceptible to oxidation by steam, which means that the water vapor content of the recycle gas can be greater (less cold recycle gas). The pressure drop is less than with steel turnings, and because a greater temperature differential can be tolerated, a lower recycle flow is required. This decreases the cost of recompressing the recycle gas considerably. Other factors to be determined are the relative lives of the nickel and steel catalysts and their selective sensitivities to sulfur poisoning.

Other materials such as magnetite ore, fused iron oxide, and cobalt oxide have been sprayed on steel sections and tested in bench-scale units, but none were as active as the materials discussed.

CONCLUSIONS

While a good high-B.t.u. gas has been produced in one reactor using sprayed plates in the hot gas recycle process, it is not completely satisfactory according to the specifications. More tests are necessary to determine the optimum operating conditions to make a gas to meet this standard.

This technique of flame spraying catalysts on inert forms may have applications to other processes than hydrocarbon synthesis. Many metals and metal oxides can be sprayed. It is possible by proper technique to remove the base metal from the sprayed material and have a shape composed entirely of the catalyst.

REFERENCES

1. Bienstock, D., J. H. Field, A. J. Forney, and R. J. Demski, Pilot Plant Development of the Hot-Gas-Recycle Process for the Synthesis of High-B.t.u. Gas. BuMines Rept. of Investigations 5841, 1961, 27 pp.

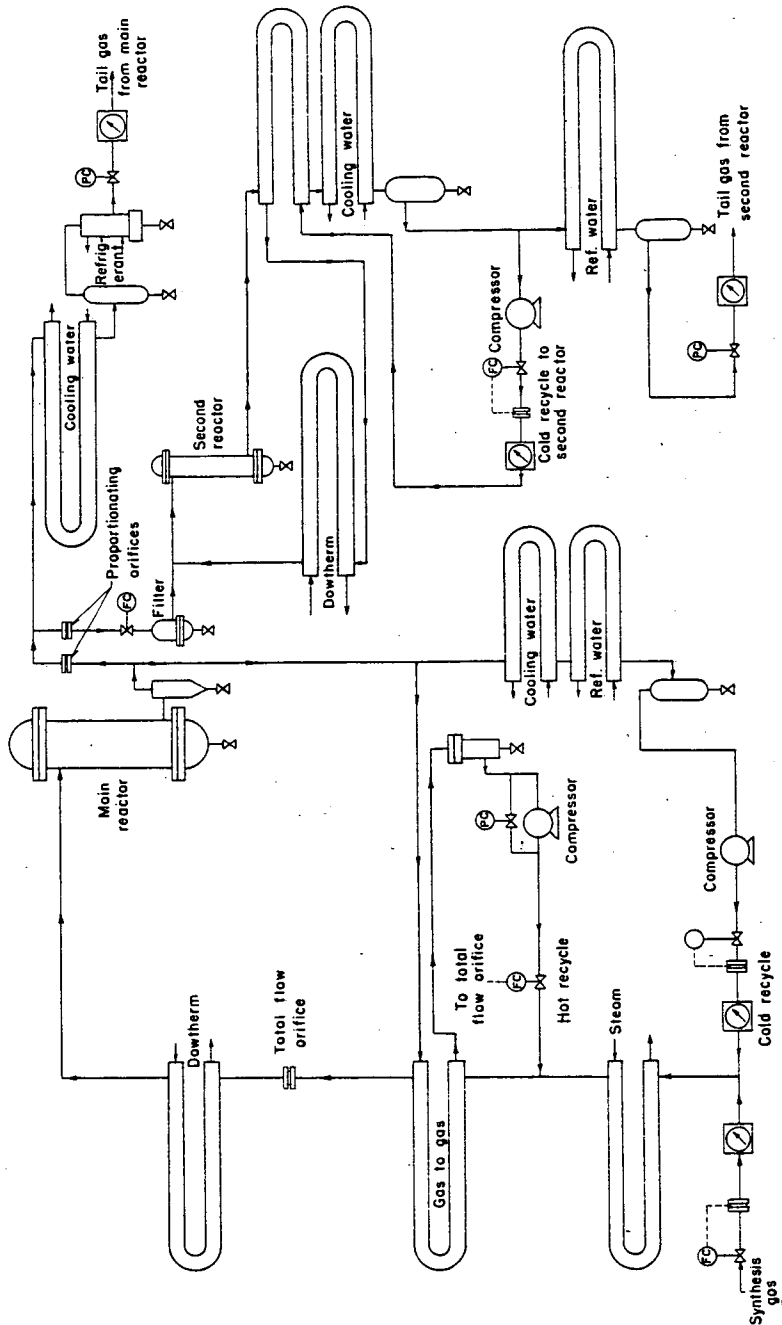


Figure 1. Flowsheet of hot gas recycle process for high-B.t.u. gas production.

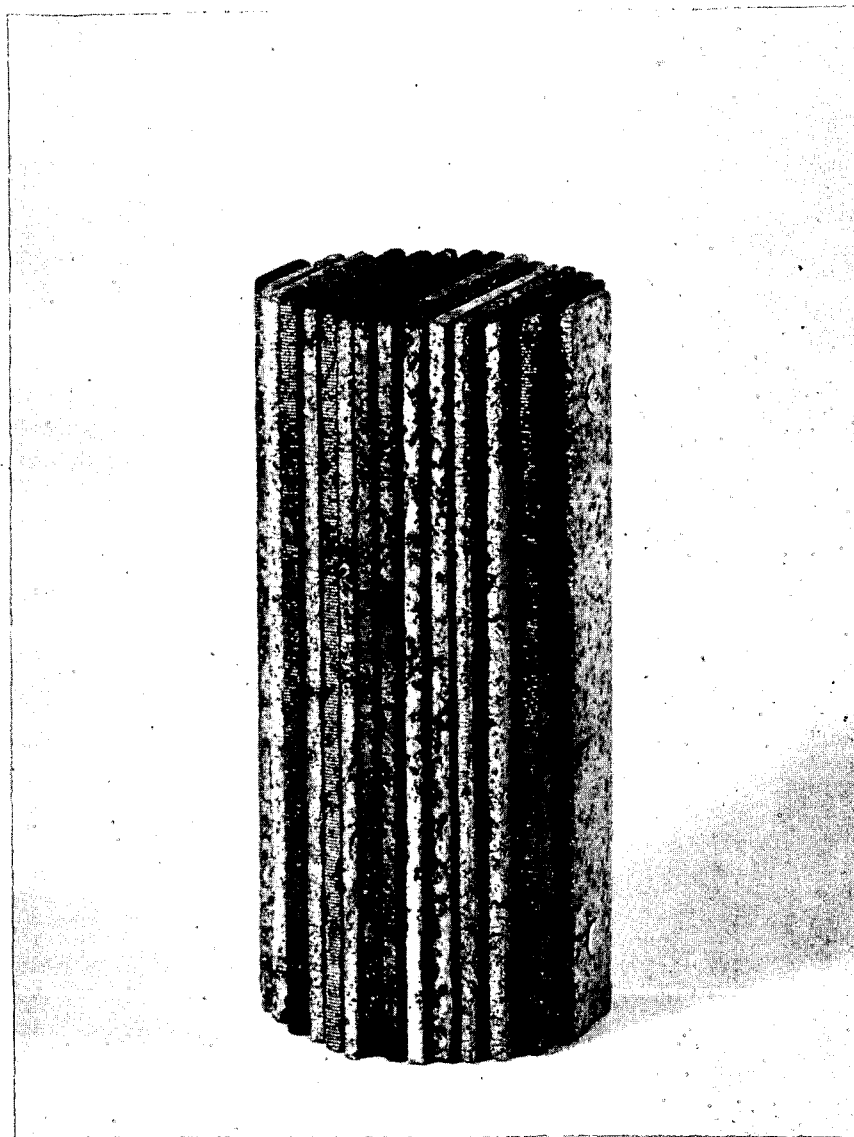


Figure 2. Parallel plate assembly of Raney nickel catalyst.

COMPARATIVE REACTIVITIES OF PETROLEUM COKES

C F Gray and W. J. Metrailler

Esso Research Laboratories
Humble Oil & Refining Company · Baton Rouge Refinery
Baton Rouge, Louisiana

INTRODUCTION

Petroleum coke is produced by coking of high boiling petroleum fractions (residua) to obtain more valuable lighter hydrocarbon products and coke. The two more prominent commercial processes for carrying out the coking operation are Fluid Coking and Delayed Coking.

Fluid Coking is a continuous process. It is carried out in equipment similar to that used extensively for Fluid Catalytic Cracking (1,2). A two vessel system is used in which the small product coke particles are heated by partial combustion in a burner vessel and these particles are circulated to the coking vessel to supply the heat needed. Finely dispersed residuum feed is injected into the coking vessel which operates at 900-975°F. The coke formed by cracking is deposited on the surface of the small coke particles which are then returned to the burner. The burner is, of course, operated at a higher temperature than the reactor. This results in some devolatilization of the coke. These volatiles along with part of the product coke (if necessary) are burned to supply heat.

In the Delayed Coking process, residuum is preheated in a furnace and is then introduced into a soaking drum. This large drum provides sufficient holding time to crack the residuum with the light hydrocarbons passing overhead. The drum eventually fills with coke which is then mechanically removed. Delayed Coking is thus a cyclic process. Coking temperatures in the drum may vary between 800 and 850°F.

In both processes the coke product represents a bottoms fraction and its chemical quality is dependent on the quality of the residuum feed. Non-volatile metals and ash constituents in the feed are deposited essentially 100% in the coke. Sulfur compounds, which are usually concentrated in the heavier petroleum fractions, are further concentrated in the coke to the extent that petroleum coke product normally contains 1.2 to 2.0 times the sulfur concentration of the residuum feed.

The volatiles content and physical properties of petroleum coke produced by Fluid Coking are quite different from the coke produced in Delayed Coking. Fluid coke is exposed to a higher temperature than is delayed coke, about 1100-1150°F. vs. 800-850°F. As a result green (i.e., uncalcined) fluid coke contains about 7 wt.% volatiles (measured at 1742°F.) vs. 10-15 wt.% volatiles in green delayed coke. Also, in Fluid Coking a layer of coke is deposited during each pass and the product has a characteristic onion ring structure, whereas delayed coke product is amorphous in nature. The differences between the two cokes are illustrated by photomicrographs in Figure 1, which

shows cross sections of particles of the two cokes.

Petroleum cokes vary in their resistance to oxidation. This is an important property of coke in many end uses. Good quality cokes, i.e., those having low metals and sulfur contents, generally are calcined and then find their way into carbon electrodes where resistance to oxidation is desirable. Low quality cokes generally are used green as a fuel and rapid oxidation is desirable.

In the work described in this paper, the reactivity of the various cokes was measured by placing the coke in a flowing stream of CO_2 at 1742°F . and recording the weight loss continuously. This technique permits close control of test conditions and does not require removal of large quantities of heat. Other investigators have studied the reaction of CO_2 with carbon. In a recent paper (3), Givry and Scalliet reported on an investigation relating anode reactivity with CO_2 to performance in an electrolytic reduction cell.

EXPERIMENTAL

MATERIALS

Samples of green fluid coke from several commercial fluid coking units were calcined in a muffle furnace to a temperature of 2400°F . The delayed cokes and the coal tar coke were from commercial production. These cokes had been calcined for use in carbon electrodes prior to receipt. Normally, a calcining temperature of about 2400°F . is used in this commercial operation.

A commercially available coal tar binder was used in the preparation of all of the molded carbon specimens. This material was obtained from the Barrett Division of Allied Chemical Company.

PHYSICAL AND CHEMICAL INSPECTIONS OF MATERIALS

Pertinent inspections of the calcined cokes used in this study are given in Table I. All tests and inspections were obtained by using techniques which are common in the carbon industry. The coal tar binder had a 215°F . softening point, a coking value of 67.5 and C/H ratio of 1.6.

REACTIVITY TEST

The reactivity of the cokes with carbon dioxide ($\text{CO}_2 + \text{C} \rightarrow 2\text{CO}$) was measured in the reactivity apparatus shown in Figure 2. The sample of carbon was dried overnight at 275°F . and then was placed in the quartz tube. After heating to 1742°F . in an atmosphere of purified nitrogen, a flow of purified CO_2 was started over the sample. The CO_2 rate was about 12 liters per hour. This gave a velocity of 2.2 cm./sec. in the annulus between the sample and the quartz tube. A continuous weight recording device measured the loss of weight of the sample due to reaction with CO_2 . The inlet and exit gas rates and exit gas composition were obtained. The CO concentration in the off-gases ranged from about 3 to 30 percent varying with the reactivity of the sample.

Test data were obtained on granular coke samples and on samples of coke which had been molded into cylindrical test specimens, bound together with coal tar binder. When the reactivity of a granular coke sample was to be measured, a 16 gram sample of 14-35 mesh coke was supported in a platinum mesh basket. Reactivities of the molded carbon specimens were determined by suspending the sample on a platinum wire which passed through a small hole in the specimen. Upon completion of the test on molded specimens, the carbon body was cooled and weighed and then brushed with a stiff bristle brush. Loosely held carbon particles which could be brushed from the sample were reported as "dust." The amount of "dust" measured in this manner is related to the amount of carbon which will be lost from the carbon body as it is consumed.

PREPARATION OF THE CARBON SPECIMENS

The molded carbon specimens used in this study were prepared by mixing the coke and pitch binder in a steam jacketed sigma blade mixer. Mixing was continued for 30 minutes at 300°F. The mixture was molded to form a 3 inch diameter by 5 inch long carbon body which was then baked slowly to about 1900°F. in a muffle furnace. Reactivity test specimens about 3/4 inch in diameter by 2 inches long were cored from the baked carbon body. Three levels of binder content were used in the work reported herein and both fine grained and coarse grained carbon aggregates were employed. The fine grained aggregate consisted of about 75 wt.% 35-200 mesh coke and 25 wt.% coke ground to pass a 100 mesh screen. The coarse grained aggregate was made up of 50 wt.% 4-48 mesh coke and 50 wt.% coke ground to pass a 100 mesh screen.

RESULTS AND DISCUSSION

Comparison of Granular Coke Reactivity

Results of the study of cokes in granular form (14-35 mesh) show that fluid cokes react with CO₂ at a much lower rate than do delayed cokes. (Table I) The coal tar coke which was prepared in a manner similar to delayed coke had the highest reactivity. These data confirm results obtained by Walker et al (4) in a more detailed study of cokes. It is well known that oxidation of carbon occurs more rapidly along crystal edges than along the basal planes. Deposition of carbon in relatively thin layers on the spherical fluid coke particles results in the onion skin structure of fluid coke (5) which is shown in Figure 1. The carbon in this thin onion skin layer is probably oriented such that basal planes of the carbon structure are exposed to a greater extent than are the crystal edges. Thus, one would expect that the reactivity of fluid coke would be low. It is also possible that the higher temperature at which carbon is deposited in fluid coking results in the lower reactivity of this material compared to delayed coke.

The reactivity of petroleum coke increases with its total ash content (Figure 3). The coke was also analyzed for V, Ni, Fe, Na, Ti, Cu, Al, Cr, and Si. Among these metallic contaminants, the concentration of iron appears to correlate best with coke reactivity. It is evident that, for a given ash content, the reactivity of fluid coke is lower than that of delayed coke.

Reactivities of Baked Carbon Specimens

The reactivities of baked carbon specimens prepared from the various granular cokes are given in Table II. It is seen in Figure 4 that the rate of consumption of the carbon specimen is directly related to the reactivity of the granular cokes. This means that the bodies prepared with fluid cokes have lower consumption rates than those prepared from delayed cokes. The carbon bodies prepared with 28 wt.% binder show a higher reactivity than those prepared with 16-18 wt.% binder. This is not surprising in that the binder coke from coal tar has a higher reactivity than any of the petroleum cokes. Also, the binder coke is not baked (calcined) to as high a temperature as were the petroleum cokes and this would be expected to result in its having a higher reactivity.

The particle size distribution of the carbon aggregate does not appear to have a major influence on consumption rate of the carbon bodies. Only two comparisons of this factor were made in this study, one with delayed coke and one with fluid coke. Neither coke showed much difference in consumption rate between fine and coarse grained carbon bodies.

Most carbon bodies are consumed in commercial use either as part of the process operation or as a result of exposure to oxidizing atmospheres. When the carbon is consumed there is a tendency to form loose particles of carbon or "dust." The generally accepted explanation for "dusting" is that the binder carbon is consumed faster than the carbon aggregate. The unconsumed portion of the carbon aggregate then becomes loose and can be brushed from the main body of carbon. The amount of loose carbon formed during our experiments is shown in Table II. It is immediately obvious that the quantity of "dust" formed was much lower for the carbon bodies prepared with fluid cokes than for those prepared from delayed cokes. This is true for both fine grained and coarse grained carbon aggregates. However, the fluid coke specimens were not as reactive and less total carbon was consumed in the standard four hour test. Additional data will have to be obtained at equivalent total consumption to establish how the amount of "dusting" obtained with fluid coke aggregate compares with delayed coke at a given consumption level.

Data have been obtained which show (Figure 5) that the use of low reactivity fluid coke to supply the carbon fines reduces the formation of "dust." High reactivity delayed coke was used to supply the coarse carbon aggregate in these samples, which were made up of 50 wt.% coarse coke and 50 wt.% fine coke as described previously. For comparison, samples were prepared using delayed coke having the same particle size distribution. Both reactivity and dust formation (at the same carbon consumption) were lower for the carbon specimens containing the low reactivity fine fluid coke. One possible explanation is that the low reactivity coke fines act as a diffusion barrier and reduce the rate of consumption of the bonding carbon. Thus the overall reactivity of the carbon surface is more in balance and less dust is formed.

CONCLUSIONS

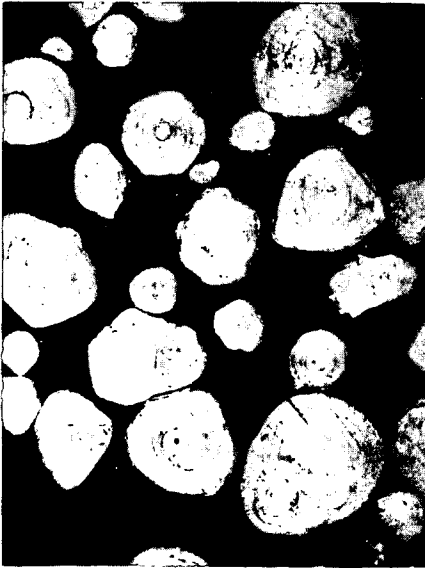
Data on nine commercially available cokes show that the process used to prepare the coke is a major factor influencing its reactivity. Ash content,

particularly iron content, is of secondary importance. Fluid coke has a lower reactivity than delayed coke at the same impurity level. The lower reactivity measured on granular cokes is carried over into carbon bodies prepared from these cokes. Binder content also influences reactivity of the carbon body. There is also an indication that less carbon dust (loose carbon) is formed when low reactivity coke is used to supply the fine coke aggregate.

LITERATURE REFERENCES

1. Voorhies, A., Jr. "Fluid Coking of Residua", Proceedings of the Fourth World Petroleum Congress, Section III F, Reprint 1. Rome: Carlo Colombo Publishers, 1955.
2. Voorhies, A., Jr. and Martin, H. Z. Oil Gas J. 52, No. 28, 204-7 (1953).
3. Givry, J. P. and Scalliet, R., Paper presented at the AIME Annual Meeting, February 18-22, 1962, New York, New York.
4. Walker, P. L., Jr., Rusinko, F., Jr., Rakazawski, J. F., and Liggett, L. M. "Proceedings of 1957 Conference on Carbon", 643-58. New York: Pergamon Press, 1957.
5. Dunlop, D. D., Griffin, L. I., Jr. and Moser, J. F., Jr. Chemical Engineering Progress 54, No. 8, 39-43 (1958).

FIGURE 1
COMPARISON OF UNCALCINED COKES



ABOUT 63X



DELAYED



FLUID

ABOUT 425X

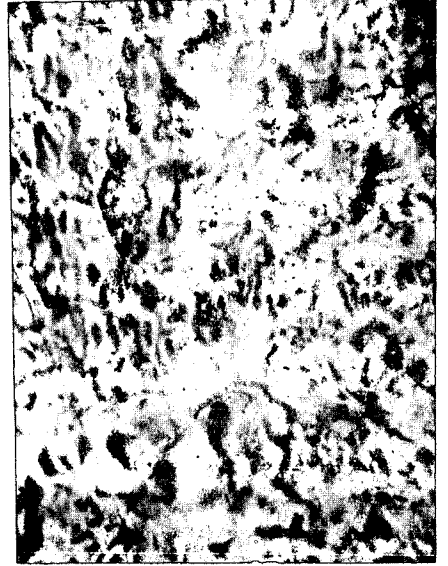


FIGURE 2
REACTIVITY MEASURING APPARATUS

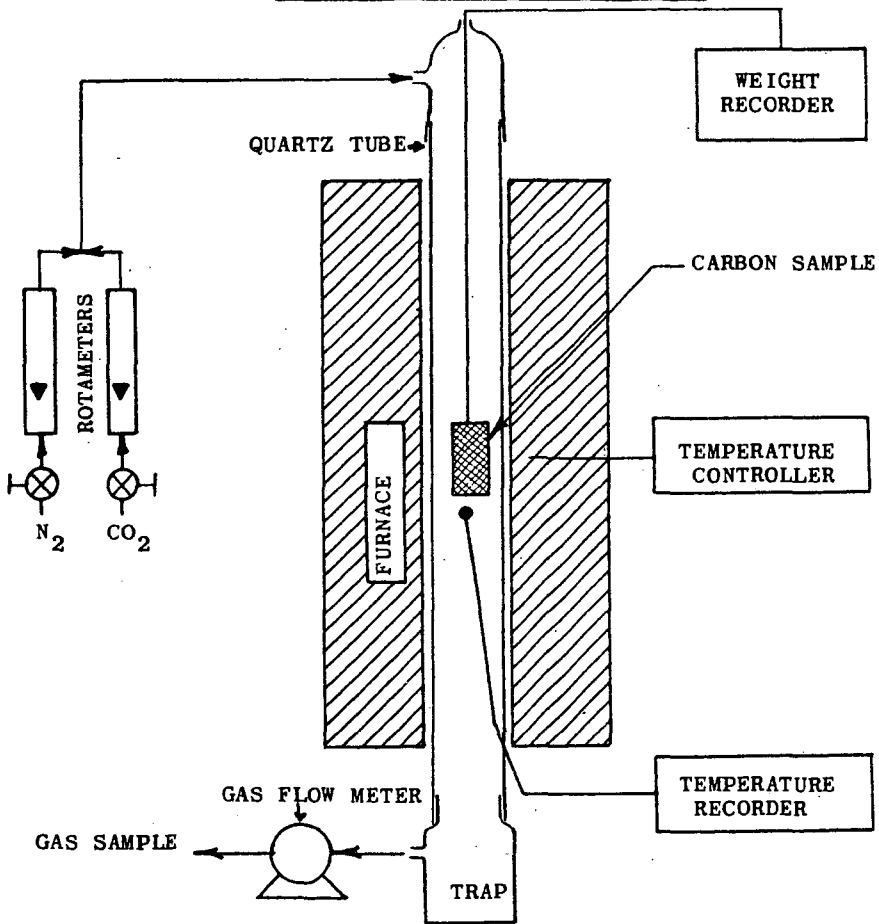


FIGURE 3
CARBON REACTIVITY IS AFFECTED BY ASH CONTENT

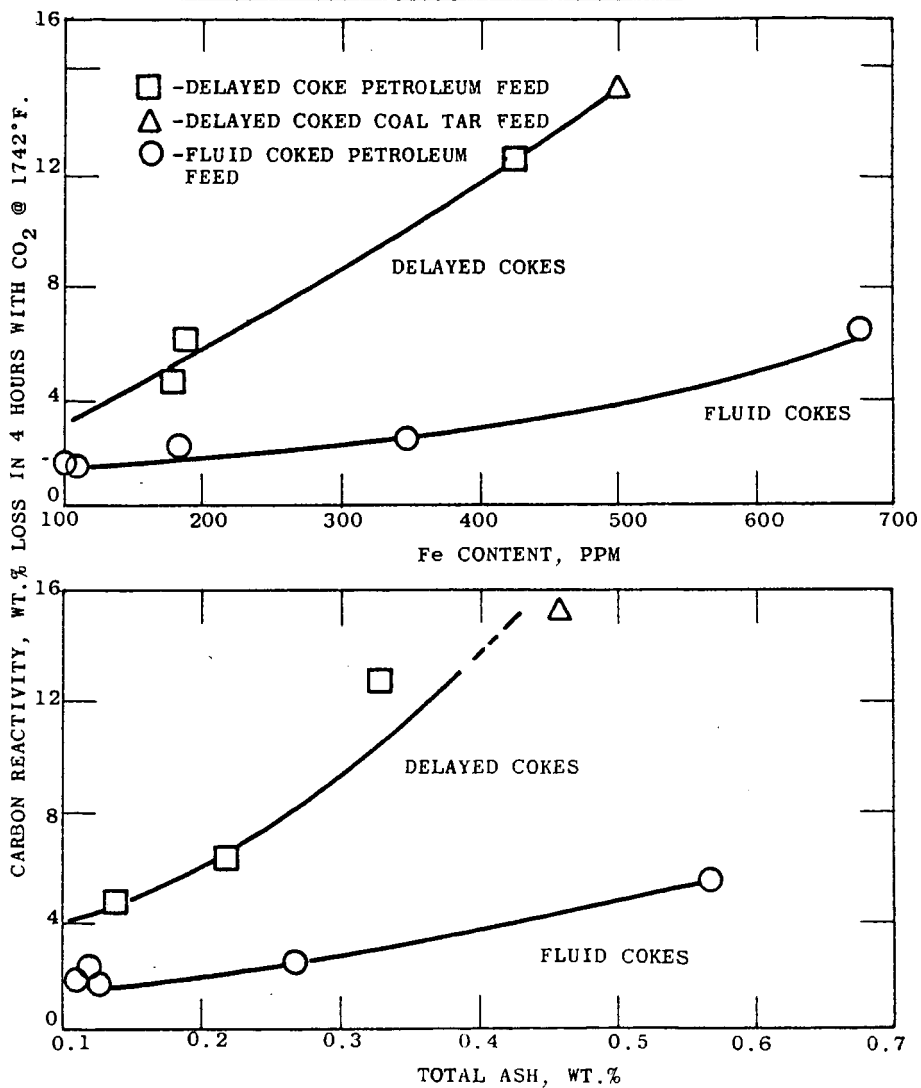


FIGURE 4
COMPARISON OF REACTIVITIES OF CARBON BODIES AND GRANULAR COKES

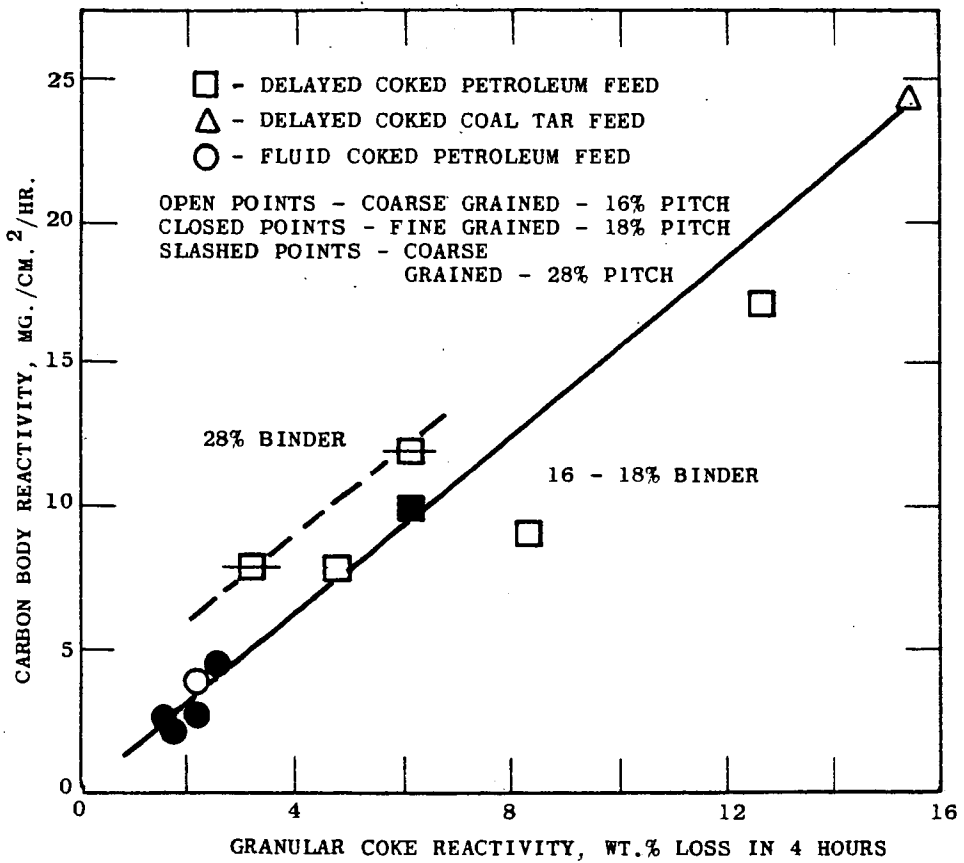


FIGURE 5

CARBON DUST FORMATION VS. CARBON CONSUMPTION IN COARSE GRAINED SPECIMENS

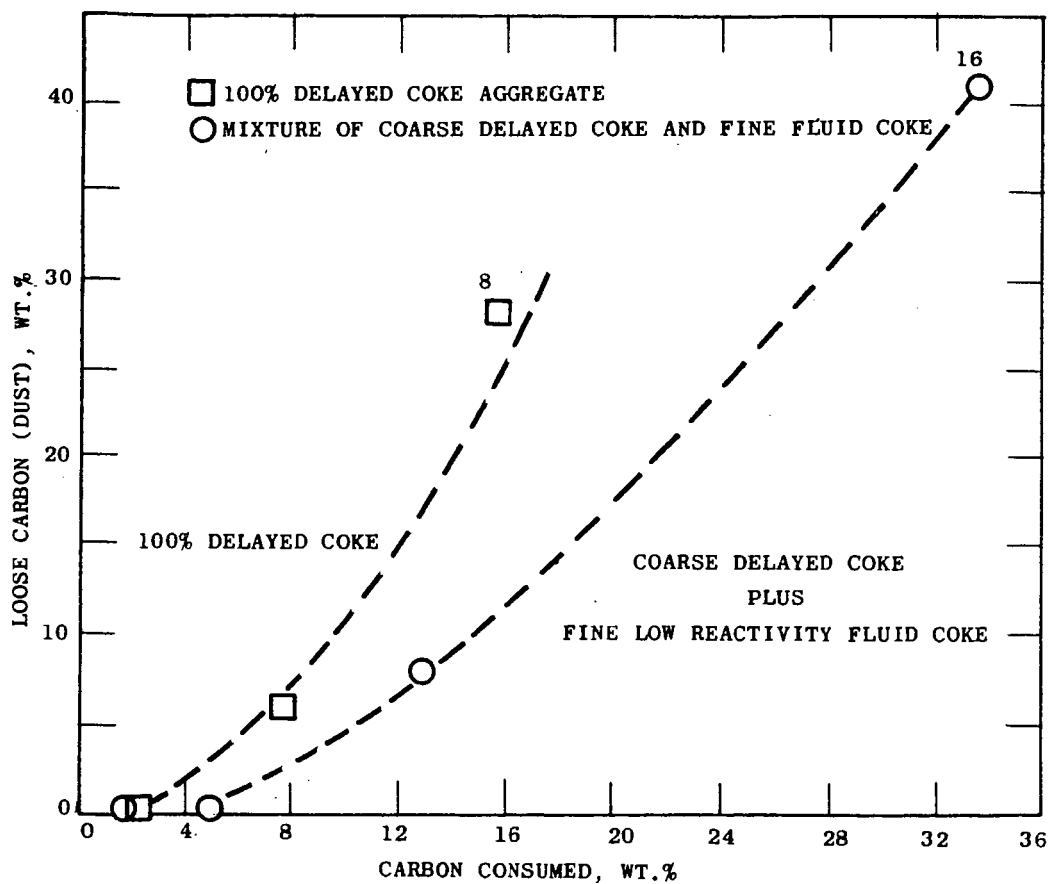
NOTE: NUMBERS INDICATE HOURS OF EXPOSURE TO CO₂ @ 1742°F.

TABLE I

DATA ON GRANULAR COKES

ALL COKES WERE CALCINED AT ABOUT 2400° F.

Sample No.	Coking Process Used	Feed Source	Impurities in Coke		Granular Coke Reactivity* Loss, Wt. % in 4 Hrs.
			Total Ash, Wt. %	Fe, Wt. %	
DP-1	Delayed	Petroleum	0.14	180	4.7
DP-2	Delayed	Petroleum	0.22	190	6.2
DP-3	Delayed	Petroleum	0.31	430	12.7
FP-1	Fluid	Petroleum	0.12	185	2.2
FP-2	Fluid	Petroleum	0.11	100	1.7
FP-3	Fluid	Petroleum	0.13	110	1.6
FP-4	Fluid	Petroleum	0.27	350	2.5
FP-5	Fluid	Petroleum	0.57	670	6.5
DCT	Delayed	Coal Tar	0.46	500	15.4

* Measured by exposing 14-35 mesh coke to CO₂ @ 1742° F. - 750C

/hc
3/22/62

TABLE II
 REACTIVITY OF MOLDED CARBON SPECIMENS

Coke Aggregate	% Binder	Reactivity Test Time, Hrs.	Carbon Loss		Loose Carbon, Wt. %
			mg./cm. ² /hr.	Wt. %	
<u>Coarse Grained</u>					
DP-1	16	4.0	7.9	5.5	3.2
DP-2	16	4.0	9.7	6.7	9.2
DP-3	16	4.0	17.0	11.5	7.8
DCT	16	4.0	24.5	15.4	11.4
FP-1	16	4.0	4.3	3.0	0.3
<u>Fine Grain</u>					
DP-1	18	4.0	7.9	5.3	3.4
FP-1	18	4.0	2.9	1.9	0.2
FP-2	18	4.0	2.2	1.5	0.3
FP-3	18	4.0	2.5	1.6	0.2
FP-4	18	4.0	4.7	3.0	0.3
<u>Coarse Grained</u>					
DP-1	28	1.5	9.9	2.4	0.3
DP-1	28	4.0	→11.9	7.5	5.9
DP-1	28	8.0	12.3	15.5	27.7
DP-1	28	16.0	12.1	31.9	**
DP-1 + FP-1*	28	1.5	7.0	1.8	0.1
DP-1 + FP-1*	28	4.0	→7.8	5.2	0.5
DP-1 + FP-1*	28	8.0	9.5	12.7	7.1
DP-1 + FP-1*	28	16.0	12.4	33.8	40.9

* Sample FP-1 used to supply the fine coke portion.

** Unconsumed carbon disintegrated.

/hc

3/22/62

Reactivities of Low Rank Coals

Neal Rice and Edward Prostel

Natural Resources Research Institute
 University of Wyoming
 Laramie, Wyoming

During the past years, various investigations were undertaken at the University of Wyoming on the utilization of low rank coal. In several of these, the reactivity of the coal products was important and therefore was given consideration. In connection with the development work on reducing carbon, the reaction of the carbon to CO_2 was tested and in connection with the use of processed coal for barbecue briquets, the reactivity to air was investigated. Results of this work are reported here as they appear of general significance.

Carbon Dioxide Reactivity

In order to show results from as wide a rank of coals as possible, three Wyoming coals were chosen, ranking from high volatile C Bituminous to subbituminous C. These coals were carbonized in a closed retort to 950°C . The heating rate was 5°C per minute. Table I shows the proximate and ultimate analyses, also the heating values of the chars. Listed are also the coals from which the chars are derived and two commercial cokes, one Western coke furnished by the Colorado Fuel and Iron Corporation and one Eastern coke furnished by Pittsburgh Coke and Chemical Company.

TABLE I
 ANALYSES OF COKES, CHARS AND COALS
 (Moisture Free, in Percent)

NAME AND RANK			VM	FC	Ash	H_2	C	O_2	N_2	S	Btu/lb.
Cokes	Pitt. Foundry	Hvab	0.4	93.9	5.7	0.2	91.2	1.4	1.0	0.4	13140
	C F and I	Hvab	3.5	83.6	13.1	1.1	83.5	0.8	1.0	0.5	12250
950° Chars											
	DOClark	Hvab	1.1	93.4	5.5	0.7	91.0	1.4	0.9	0.5	13580
	Elkol	Subb	2.5	93.2	4.3	1.0	90.7	2.2	1.4	0.4	13510
	Wyodak	Subc	2.1	82.2	14.7	1.1	80.6	1.3	0.9	0.4	12400
Coals	DOClark	Hvcb	39.3	57.0	3.7	5.8	72.2	15.4	1.6	1.3	13220
	Elkol	Subb	43.0	54.5	2.5	5.0	72.4	17.8	1.5	0.8	12580
	Wyodak	Subc	42.3	47.7	10.0	4.5	65.6	17.8	1.1	1.0	11340

The reactivity of the char to carbon dioxide was measured by conducting CO_2 over the char and measuring the proportion of CO to CO_2 in the effluent. As it is known that the surface area often is closely related to the reactivity, the densities, in methanol as well as in mercury, were also measured. From the densities, the porosities were calculated. Results are shown in Table II.

The chars from a lower rank coal have a higher reactivity than the chars from a higher rank coal and all are higher than the reactivities of the cokes. In Figure I, this relationship is shown graphically. The lower the rank of the coal, the higher the reactivity of the carbon residue.

TABLE II
 Reactivity, Density and Porosity
 of
 Chars and Cokes
 Moisture Free

Rank	Rank	Reactivity		Density	Porosity
		CO ₂	McOH	Hg	
Hvab	Foundry Coke	13.3	2.031	1.736	0.145
Hvab	C F & I Coke	71.8	1.869	1.617	0.135
Hvcb	DOClark Char	119.1	1.820	1.415	0.223
Subb	Elkol Char	137.5	1.840	1.382	0.249
Subc	Wyodak Char	146.0	1.810	1.100	0.392

It appears that this tendency is related to the porosity of the material. The higher porosity of the low rank chars facilitates the access of the oxidizing gas to the carbon surfaces. It is widely believed that diffusion is a limiting factor in reaction rates when gas reacts with a porous solid. It would perhaps be more to the point to say that the reactivity is governed by the concentrations of CO₂ and CO at the surfaces regardless how these concentrations were achieved. It would appear logical to assume that the rough low rank surfaces are more open to attack by the CO₂ than the glossy surfaces of the coke. The surface area of the lowest rank char under study, Wyodak, is about 27 m² per g whereas those of the two cokes are 2 and 3 m² per g respectively.^{1.)} Diffusion deeply into the piece of coke or char may take place but reaction is retarded by mounting concentrations of the product gas, CO, within the particle. The concentrations of the two gases are affected by the rate at which the one is supplied and the other is removed, and by the relative concentrations which prevail.

Milliken^{3.)} has suggested that the micelles of the lower rank coals may be composed at least partially of di-phenyl linkages and that these linkages are oriented about sixty degrees from planar. This results in steric hindrance which prevents formation of large blocks of oriented and planar molecules, thus leaving a greater random porosity. It also should be considered that the lower rank coals yield much water and carbon dioxide while being carbonized in the lower temperature ranges. There are thus many carbon-to-OH and carbon-to-oxygen linkages broken and probably left in a condition which encourages reaction of the peripheral carbon molecules with the oxidizing gas. The higher rank coke, never having been freed of such an amount of water and oxygen, has fewer sites open for attack and thus a lower reactivity.

In order to examine the possibility that the analysis of the coal substance would throw some light on these differences in reactivity, the ultimate analyses of the moisture and ash free chars and cokes are shown in Table III. As will be seen carbon and hydrogen content is similar down the columns. Oxygen, determined by difference, is not significant. As has been pointed out by Peters^{2.)}, it would appear that the chemical analysis gives no explanation for the differences in reactivity.

The two commercial cokes shown in Figure I were made under conventional coking conditions which involve comparatively slow temperature rise and longer periods at maximum temperature. The longer period at coking temperature, this so-called soaking period, also affects the CO₂-reactivity of the coke. Extended periods at high temperature reduce the CO₂-reactivity. Thus the two points, 1 and 2, would have been higher, closer to the level of the chars, if the cokes had been made at the same conditions as the chars.

TABLE III
 Ultimate Analyses of Chars and Cokes
 (Moisture and Ash Free)

Rank	Name	H ₂	C	O ₂	N ₂	S
Hvab	Foundry Coke	0.6	96.8	1.2	1.0	0.4
Hvab	C F & I Coke	1.0	96.3	1.3	0.9	0.5
Hvcb	DOClark Char	0.7	96.4	1.5	0.8	0.6
Subb	Elkol Char	1.0	95.0	2.2	1.4	0.6
Subc	Wyodak Char	1.2	95.8	1.1	1.0	0.5

To examine the effect of heat soak on reactivity, a char from DOClark coal was heat soaked for various periods, and then subjected to the reactivity test. The results are shown in Figure II. Heat soaking for 3 hours reduced the reactivity by about 15% and soaking for 48 hours by 35%. It is known that any char and any coke shrinks with continued heat soaking. This, of course, results in higher densities and lower porosities, and it must be expected that such changes result in closure or partial closure of openings and a reduction of the reaction surface. Thus, reactivity to CO₂ and doubtless to other gases is decreased with extended heating cycles. However, the nature of the surface of the char made from subbituminous coal is so open that no amount of heat soaking will lower its reactivity to that of a metallurgical coke.^{4.)}

The higher reactivity of the chars made from lower rank coals must be ascribed to their surface structure, and such chars must find applications where high reactivity is an advantage.

Reactivity Measured by Ignitability of Smokeless Briquets

Several investigations were made on the suitability of processed coal for barbecue briquets. Such briquets should be easy to ignite and should develop a reasonable amount of heat. Further, they should burn with a minimum of odor or smoke. The amount of heat, intensity of smoke and odor are outside the scope of this discussion. Remains the ignitability. This is determined to a large extent by the shape and size of the briquet, and especially by the degree of compaction which affects the apparent specific gravity. If, however, these and other factors of processing are kept uniform, the ignitability can serve as measure of the reactivity of the carbon substance.

In the ignition test, 5 briquets of uniform pillow shape are placed on a brick, four in a square, one-fourth inch apart, and one on top. The brick is placed off the floor. Room temperature is kept uniform and noticeable draft is avoided. 30 ml of lighter fluid is poured over the briquets uniformly and the briquets are ignited. The percentage of surface burning is estimated at close intervals for each briquet, and the average recorded. The time elapsed when 80% of the surface is burning is termed "Ignition time". It is not too difficult to train an operator within a few days so that the estimating can be done with reasonably close reproducibility.

Figure III shows the ignitability relative to the volatile content. The coal used was air-dry North Dakota lignite with 9.6% of moisture, 36.0% of volatile matter and 10.2% of ash. The coal was carbonized to various volatile contents, and the char briquetted with cereal binder. As will be seen from the curve, the optimum ignition time was achieved with 15 to 18% of volatile matter. At this stage, the volatile matter of the coal has been reduced by about 80%. All carbon dioxide has been evolved, and there is apparently an optimum compounded of the amount of volatile matter retained by the char and the quality of this volatile matter.^{1.)} It had been known for a long time that in the stated volatile range, the coal is best suited for

effective combustion at ordinary furnace temperatures. It may be surprising, however, that under the stated extreme conditions where the low ambient temperature slows the combustion, the same volatile content indicated the highest reactivity.

A great number of various lignites were carbonized, the char briquetted, and the briquets subjected to the ignition test. Processing conditions were uniform. There were again considerable variations in ignition time. Some were traced to variations in ash content, some to aggregate size. Yet there remained distinct differences. These were traced finally to the structure of the coal. In every instance, the lower ignition time was achieved with char from a coal with laminated structure, at least in part of the coal. Figure IV shows samples of the laminated and of the more compact structure. The former is black and has a shiny, velvety appearance, the latter is dull and often brownish. The one apparently originates from either leafy or bark matter, and the other from solid wood.

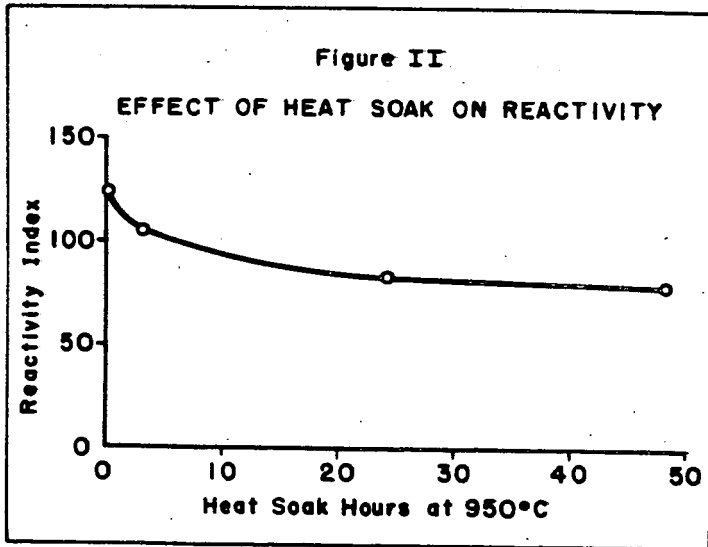
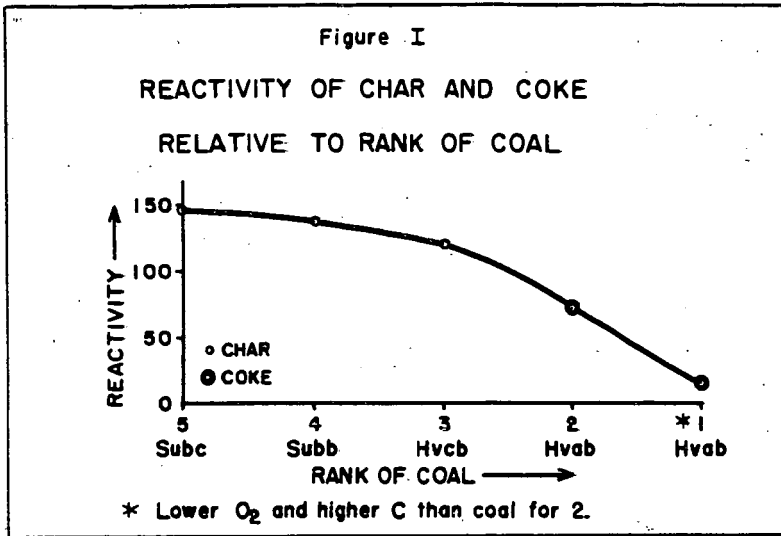
In another investigation, briquets were tested which were produced from char derived from subbituminous C coal. The volatile matter was kept uniform, also the ash content. To vary the amount of reaction surface, the size of the aggregate was varied. Changes in ignitability obtained with changes in aggregate size are shown in Figure V. The aggregate sizes shown are nominal. All aggregates were graded, and uniform grading was used in each case. It will be seen that the tests were confined between U.S. No. 20 and 70 screen sizes. Sizes beyond these limits had to be ruled out for reasons of operating procedures. Within the stated limits, the ignitability increased with decreasing aggregate size.

All the reported results point to the importance of sufficient reaction surface. However, there are, apparently, other factors involved. Many briquets of commercial production were tested which showed an ignition time of 40 minutes. Good smokeless briquets usually showed an ignition time of less than 30 minutes. Very good briquets showed 20, 19, or even 18 minutes ignition time. But this seemed to be the minimum. Any possible introduction of promoters or oxidizing agents is ruled out here and only the reactivity of the coal substance and the oxygen of the air is considered. It appeared that further reduction in aggregate size or further reduction in ash content did not lower the ignition time further.

The oxidation of the char is of course a heterogeneous process^{5.)}, and rather complicated. To accomplish it, however, there must be not only sufficient reaction surface but also sufficient open space for the air to enter and for the products of combustion to leave. For this reason the amount of specific surface beyond a certain optimum cannot be utilized.

References

- 1.) Inouye, K., Rice, Neal and Prostel, Edward, "Properties of Chars Produced from Low Rank Coals of the Rocky Mountain Region", FUEL, London, Volume XLI, pp. 81, January 1962.
- 2.) Werner Peters Dr. rer. nat.; "Comparison of Reactivity Tests on Coke", GLUECKAUF, Volume 96, 16, pp. 997-1006, July 30, 1960.
- 3.) Milliken, Spencer R. - Doctor's Thesis, College of Mineral Industries, Pennsylvania State University, June, 1954.
- 4.) Mueller, W. J., and Jandl, E. A., "Rapid Method for Determining the Reactivity of Coke With CO₂", BRENNSTOFF CHEMIE, Volume 19, No. 2, pp. 45-48, 1938.
- 5.) H. Sommers and W. Peters, "The Kinetics of the Oxidation of Coal at Moderate Temperatures", CHEMIE-INGENIEUR - TECHNIK, pp. 441-453, 1954.



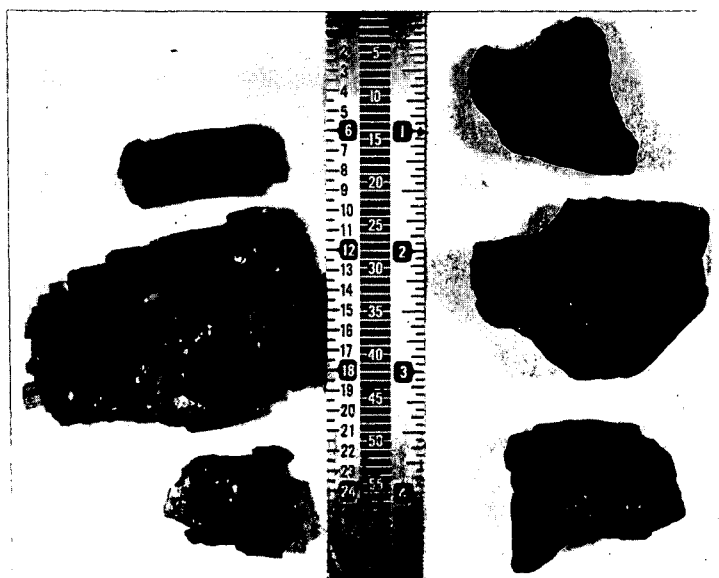
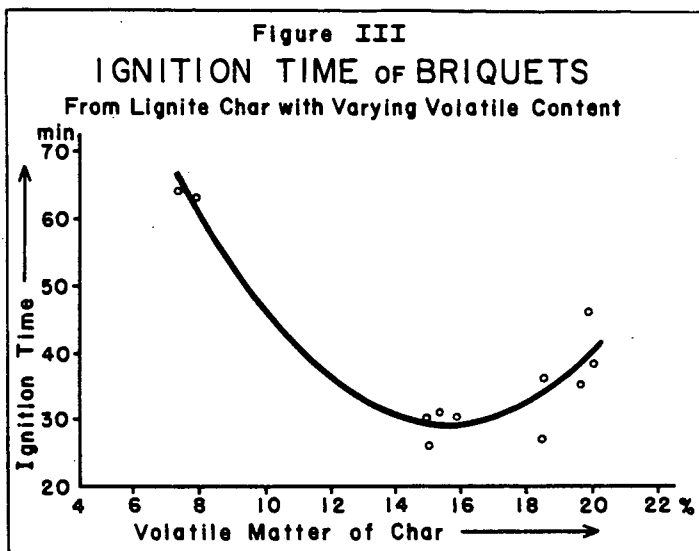
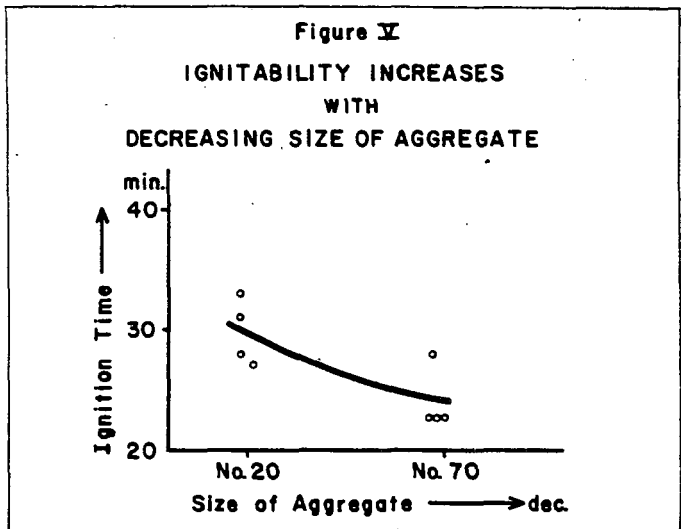


FIGURE IV



ROLE OF FUEL REACTIVITY IN SINTERING

U. N. Bhrany
E. A. Pelczarski

United States Steel Corporation
Applied Research Laboratory
Monroeville, Pennsylvania

Introduction

The sintering process is used to agglomerate the smaller sizes of iron ores that are too small to be fed directly into the blast furnace. In this process, a heterogeneous mixture of iron ore, fuel, and usually flux is deposited as a bed about 8 to 15 inches deep on an endless, moving sinter strand. The strand moves over a series of windboxes that by means of suction draw a downdraft of air through the bed. As the bed moves into position over the first windbox, the fuel in the top of the bed is ignited by gas burners. After ignition, the air flow through the bed sustains the oxidation reaction and at the same time causes the combustion zone to propagate downward to the bottom of the bed. In this manner, only a comparatively small region (combustion zone) of the bed is being heated to sintering temperatures at any one time. Much of the heat released in the combustion zone is then transferred by forced convection, radiation, and conduction to preheat the portion of the bed lying beneath the advancing combustion zone. Thus, because of good heat recovery, the process requires only a small amount of fuel (about 3 to 5% carbon).

The fuel is randomly distributed throughout the bed and may be considered as discrete particles embedded within a massive matrix of inert material. Furthermore, because of the low concentration of fuel in the bed, the fuel particles are well dispersed and can be visualized as distinct entities oxidizing essentially independently of each other when enough air is available for their combustion.

The combustion process can be considered¹⁾ to occur in two regions, as follows: (1) the region where true chemical reaction controls the oxidation rate, and (2) the region in which the mass transfer of oxygen from the bulk gas stream to the carbon surface is controlling. At temperatures below about 1500 F, the reaction rate is independent of air velocity, whereas above this temperature the rate of combustion is directly influenced by velocity and is limited by the mass transfer rate of oxygen. Kuchta, Kant, and Damon²⁾ have shown that in the second region the reaction rate is proportional to the 0.47 power of the air velocity. Furthermore, at very high air velocities the rate approaches that given by the Arrhenius equation for an activation energy of about 30 k cal/g mole. Meyer³⁾ reported similar activation energies and he as well as Mei Chio Chen, et.al.,⁴⁾ showed that the oxidation of carbon is first order with respect to the partial pressure of oxygen.

Wicke⁵⁾ suggests that for the combustion of carbon the activation energy is about 58 k cal/g mole and that lower values than this are probably due to diffusional effects in the porous interior of the carbon. He further states that differences in reactivity are due solely to variations in internal surface area and that depending upon the type of carbon being oxidized, the specific surface may increase by as much as 1400 percent as carbon is gasified. Smith and Polley⁶⁾ report similar results for the oxidation of fine thermal carbon at 600 C. They concluded that because the increase in surface area is not accompanied by a decrease in particle diameter, the particle must develop internal porosity. These results are in accord with Wicke's and tend to confirm his observation that a reaction also occurs on the internal carbon structure. The bulk of the work reported in the literature for oxidation rates of carbon has dealt with low-ash-content materials. However, Grendon and Wright⁷⁾ have studied the combustion of cokes and coals as well as low-ash carbons

through ash barriers. They advance the possibility that the permeability of the residual ash layer surrounding partially burnt commercial fuels influences the burning rate.

Schluter and Bitsianes⁸⁾ have used the combustion model proposed by Tu et al.¹⁾ in an attempt to predict the width of the fuel combustion zone present in sintering processes. In general, the measured widths were two to three times larger than those predicted. In a prepared discussion of their paper, they have stated that since the rate of combustion of fuel in the sintering process is diffusion controlled, the reactivity of the fuel should have little effect on the processes inherent in sintering. However, no experimental data are presented in substantiation. Furthermore, their model is limited to a case where the fuel is assumed to be a dense sphere of shrinking radius that burns only on its surface and hence cannot allow for the effect of porosity and ash that would affect the diffusional resistances.

Dixon and Voice⁹⁾ state that the sintering process demands a relatively unreactive fuel. Too high a reactivity lowers the thermal efficiency of the process and necessitates a higher fuel content in the sinter bed. For example, with fuel reactivities varying from critical air blast (C.A.B.) values of 0.092 to 0.035 ft³/min, no appreciable effect on the thermal efficiency of the sintering process was noted. However, with a highly reactive wood charcoal (C.A.B. = 0.003 ft³/min), there was a considerable drop in thermal efficiency.

The present paper gives the results of a study completed with eight different fuels for characterizing the fuels with respect to their performance in the sintering process, in which a unique combustion situation exists. The oxidation kinetics of cokes containing different amounts of ash are also included. From these studies, a reactivity index is developed for classifying fuels with regard to their behavior in the sintering operation.

Materials and Experimental Work

The materials used in this work were commercially available cokes, coals, and charcoal. The chemical composition and the physical properties are given in Table I.

A Stanton Thermobalance, (a) two rotameters, and associated hardware for transporting a synthetic air mixture to the reaction chamber were used in this work. Figure 1 is a schematic drawing of the experimental assembly.

The Thermobalance is an integral unit housing a continuously recording temperature controller, a height-adjustable muffle furnace, and an automatic continuously weighing and recording analytical balance. Mounted on one pan of the balance is a silica rod for supporting a fuel sample in the muffle furnace. The furnace may be raised or lowered by means of pulleys to provide access to the sample holder. Furnace temperatures are indicated and controlled by means of a thermocouple located near the furnace wall (see Figure 1). Two other thermocouples situated directly above and below the carbon sample measure the incoming and exit gas temperatures. For all runs, except for the temperature study, the muffle furnace was set at a control point of 1250 plus or minus 4 F.

A typical run was made as follows: the furnace was set at the desired temperature and allowed to come to equilibrium with a synthetic air mixture flowing through the furnace at a flow rate of 11 liters per minute. The coke sample (0.5000 gram each) obtained by riffing a large batch of coke (-20 +28 Tyler mesh) was dried at 130 C for two hours prior to weighing. The sample was then placed in an inconel wire basket having inside dimensions of 0.6 by 0.6 by 0.5 inch. The bed depth of the coke sample in the basket was 0.12 inch. After the basket containing the coke was placed on the silica support rod of the Thermobalance, the muffle furnace was lowered in place; the loss of weight with time was recorded continuously.

(a) Made in England and distributed by Burrell Scientific Company.

Theory

In the manner proposed by Tu et.al.,¹⁾ it can be shown that the combustion rate of carbon is given by

$$N_c = \frac{P_g}{R_d + R_c} \quad (1)$$

where P_g is the partial pressure of oxygen in the bulk gas stream (atm)
 R_d is the diffusional resistance to mass transfer (hr)(atm)/lb mole
 R_c is the chemical resistance (hr)(atm)/(lb mole)
 N_c equals the rate of carbon consumption (lb moles/hr)

Now if reaction conditions are chosen such that chemical reaction controls the rate of carbon consumption, that is, $R_c \gg R_d$, equation (1) reduces to

$$N_c = \frac{P_g}{R_c} = ak p_g \quad (2)$$

where a = area available for reaction
 k = the specific reaction rate constant as given by the Arrhenius equation

In the case of a packed bed of particles having appreciable depth, p_g varies with the depth of the bed. Hence, under isothermal conditions, it becomes necessary to integrate equation (2) between the limits of the inlet and outlet gas compositions to obtain the average value of the rates existing in every part of the bed. Generally it is difficult to maintain isothermal conditions, because the oxidation of carbon is highly exothermic and the reaction temperature tends to rise. However, by use of a differential reactor, rising temperatures are easily treated because rate data may be obtained at each incremental temperature change. Under these circumstances, equation (2) becomes

$$N_c = \alpha a \quad (3)$$

where α is a constant

Equation (3) describes the oxidation of carbon in a chemical-reaction-controlled regime. However, the sintering process occurs at high temperatures of about 2700 F. In this region, the oxidation rate of carbon is controlled by the mass transport of oxygen from the bulk gas phase to the carbon surface; that is, diffusional resistance is much larger than the resistance due to chemical reaction. Hence the carbon combustion can be approximated by modifying equation (1) to

$$N_c = \frac{P_g}{R_d} = k_g a p_g = \frac{DPa}{RTz P_{bm}} p_g \quad (4)$$

where D = diffusion coefficient (ft²/hr)
 R = gas constant (ft³)(atm)/(lb mole)(°R)
 P = total pressure (atm)
 k_g = mass transfer coefficient (lb moles)/(hr)(ft²)(atm)
 z = effective film thickness (ft)
 T = temperature (°R)
 P_{bm} = log mean pressure of inert gas in the film

Equation (4) implies that in a diffusion-controlled regime, the oxidation rate is independent of the carbon being burned and depends only on the transport of oxygen. Within limits, this is true; but with cokes or carbons of widely different porosities and varying ash contents, the effective film thickness (z) and the area available for reaction (a) may be vastly different at identical air flow rates. Second, with fuels having a high ash content, it is known that an ash structure can surround the unburnt carbon⁷⁾ and may impede combustion through its effect on the diffusion

coefficient. Thus the properties of the fuel can influence the combustion rate of carbon in the sintering-temperature (diffusion-controlled) region.

Results and Discussion

The Effect of Temperature on the Oxidation Rate of Coke

Most of the kinetics work was performed with coke C because it had been found to be an excellent fuel for sintering. In the study of the effect of temperature on the oxidation rate, the correlating temperatures were the exit gas temperatures leaving the bottom of the differential reactor. In general, these temperatures are about 150 F higher than the furnace temperature. But optical-pyrometer measurements of the top of the packed bed of particles at temperatures above 1400 F gave temperatures about 25 to 50 degrees higher than the exit gas temperatures. Visual observation of the bed showed a considerable nonuniformity in burning; discrete particles of coke could be seen burning more brilliantly than others in various parts of the bed. Consequently, exit gas temperatures were assumed to be representative of the bed temperature.

The results of the oxidation tests at various temperatures are presented in Figure 2. In these tests, the exit gas temperature increases and reaches a maximum and thereafter decreases with time to a constant level. For proper evaluation of the reaction rate, the weight-loss data must be corrected for volatile matter. This was done by heating the coke to various temperatures in N_2 and obtaining devolatilization rate curves. The volatile matter loss is then subtracted from the gross weight loss to obtain the weight loss due to oxidation.

With these data, an Arrhenius plot was made of the reaction rate expressed in pound moles of carbon consumed per hour per square foot of total surface area. The results are presented in Figure 3. Also included in this plot are the data given by Wicke²⁾ for electrode carbon. Only at temperatures below about 1400 F do the experimental data lie along the curve given by Wicke. This corresponds to an activation energy of 58 k cal/g mole, which indicates that the oxidation of carbon is controlled by chemical reaction. As the temperature is increased above 1400 F, the effect of diffusion becomes increasingly significant and the data deviate considerably from the straight-line Arrhenius relationship.

From the kinetic data of curve 2, Figure 2, the total surface area of coke C was calculated with the use of a known specific reaction rate constant for electrode carbon. The calculated surface area based on points taken over the entire curve was $3.0 \text{ m}^2/\text{gram}$ (standard deviation 0.39). Experimental nitrogen adsorption (BET) surface-area measurements showed that the surface area of coke C was essentially constant at $3.4 \text{ m}^2/\text{gram}$ at various degrees of oxidation. A similar calculation for charcoal H (Figure 4) at 30 percent weight loss gave a total surface area of $4.8 \text{ m}^2/\text{gram}$, whereas the BET method gave a value of $5.2 \text{ m}^2/\text{gram}$ for a fresh sample. These values indicate that the combustion of different fuels is primarily dependent on the surface area of the material. It should be mentioned that these calculations are based only on the fixed carbon available in the coke sample, whereas the BET method makes no distinction between ash and carbon contributions to the total area. Consequently, for high-ash materials it is expected that the adsorption technique will yield surface areas considerably different from those calculated from the oxidation curves.

These two fuel samples cover the extreme oxidation rates encountered in this report; that is, coke C burns at the slowest rate and charcoal H at the most rapid. As the oxidation rates for both fuels correlate rather well with their BET surface areas, it appears that the gross oxidation phenomenon in a chemical-reaction-controlled regime where excess oxygen is always available is directly related to the total surface area of the solids. However, a more fundamental study would probably reveal that

additional carbon properties such as anisotropy and lattice defects influence the true kinetics of oxidation. In addition, the impurities also have an effect on the oxidation rate.

The Air Oxidation of Various Sinter Fuels

To determine their relative ease of oxidation, eight different fuels were oxidized in air at a furnace temperature of 1250 F. (The compositions of the fuels are given in Table I.) The results of this study are presented in Figure 4.

Each fuel was tested in duplicate runs to check on data reproducibility. Figure 4 indicates that the fuels can be ranked in order of increasing reactivity, that is, ease of oxidation, as follows: C, E, G, F, D, A, and H. Coke B behaves somewhat anomalously in that it has the fastest initial burning rate, but quickly slows down. We believe that because of its high ash content (Table I), the ash can decrease the carbon surface available for reaction and also increase the diffusional path across which the mass transfer of O_2 occurs. Consequently, as more and more carbon is consumed, the ash becomes increasingly significant in preventing the exposure of carbon surface to the oxidizing gas, and the rate of oxidation diminishes.

Several tests were also completed to obtain oxidation data at a furnace temperature of 1600 F. The results of this work are presented in Figure 5. A comparison of Figures 4 and 5 shows that in general the oxidation curves for both low- and high-temperature tests are ranked in the same manner; that is, coke C is still represented as the slowest burning coke regardless of the temperature of oxidation, and similarly for the other cokes. A slight anomaly does exist: the low-temperature work indicates that charcoal D and coke A should behave similarly, whereas the high-temperature data suggest a higher reactivity for the activated charcoal. It is believed, however, that this difference is due to the experimental technique and may be explained as follows. The size of the sample and the cross-sectional area of the reactor basket used in both cases were the same. Consequently, the height of the sample in the basket for coke A as compared with the height for charcoal D varies with the ratio of the apparent specific gravities. Thus the sample height for coke A is 1.48 times that for charcoal D. This has two adverse effects on the oxidation rate: (1) the pressure drop across the basket increases causing more air to flow around the basket rather than through it, and (2) the partial pressure of CO_2 increases in the bed. These two factors tend to depress the reaction rate. At low temperatures, this result is not evidenced because the reaction rate is slow and the air flow is large enough to offset any effects due to changes in partial pressure of oxygen.

A short study was made to determine the variation of the coke particle size with increasing degree of oxidation. These data, for coke C initially minus 20 plus 28 mesh, are presented in Table II. The particle size is relatively independent of the percent oxidation. Even after 87 percent weight loss, the oxidized sample still contained 71.5 percent of the original screen size. This is in agreement with the results reported by others.^{5,6} A sample oxidized at a furnace temperature of 1600 F exhibited considerable fusion of the particles as reflected by the creation of 21.2 percent of a plus 20-mesh fraction. As the initial particle size was all minus 20 plus 28 mesh, the data suggest that at higher temperatures, the oxidation rate of high-ash fuels may be affected by partial fusion or sintering of the ash. In particular, if the ash becomes sufficiently fluid to occlude the surface of the carbon, a corresponding decrease in rate should occur.

The Reactivity Index as a Measure of Fuel Performance in Sintering

In the sintering process, only the fixed carbon is considered to be useful for generating the required heat flux. Voice and Dixon⁹) in summarizing the available literature on the subject report that any heat generated by the combustion of volatiles lowers the thermal efficiency of the sintering process.

As no one property of the fuel, such as ignition temperature, fixed carbon content, or ash content, can adequately describe its behavior during the combustion process, a reactivity index based on 50 percent weight loss of fuel has been defined. For this purpose, we choose to set the air oxidation test conditions just outside of the region in which chemical reaction alone controls the oxidation rate, where the differences in the reactivities of fuels could be easily distinguished. For our equipment, this corresponds to an air flow rate of 11 liters per minute and a furnace temperature setting of 1250 F.

A measure of the reactivity of fuels under these conditions is the area under the percent weight loss versus time curve (Figure 4). In this manner, fuels having a fixed carbon content of as low as 50 percent may be included in this index. The area under the curve is then normalized to place all measurements on a per gram of fixed carbon basis. Thus the reactivity index ϕ is defined as

$$\phi = \frac{\int_0^{t_{50}} \frac{m(t) dt}{m_0/f}}{10^{-4} F} = 10^{-4} F \int_0^{t_{50}} w(t) dt \quad (5)$$

where t_{50} = time for 50 percent weight loss
 $m(t)$ = weight loss in grams as a function of time
 m_0 = initial sample weight (grams)
 f = weight fraction of fixed carbon in sample
 $w(t)$ = percent weight loss of sample as a function of time
 F = percent weight fraction of fixed carbon in sample

The reactivity index ϕ is correlated with sinter production rate as shown in Table III. Sufficient samples were not available for sinter pot tests to be run on all the fuels studied. However, the data establish the general trend. Fuels having a reactivity index greater than 1.65 appear to yield a sinter production rate of about 4.2 tons per day per square foot. These fuels are acceptable for the sintering process. Below an index of 1.65, the production rate decreases. The performance of those fuels having a reactivity index between about 1.35 and 1.65 can be improved by blending with a better-quality fuel. Fuels having an index of less than 1.35 are unsatisfactory for use as sinter fuel.

Fuel Reactivity and the Mechanism of Sintering

We have observed that the oxidation of the more reactive fuels results in a higher carbon monoxide concentration in the waste gas. This is due to incomplete combustion of the fuel and/or the gasification of carbon. In either case, the thermal efficiency of the sintering process is lowered and a higher fuel content in the sinter bed is often required to accomplish the desired result. Highly reactive fuels also tend to minimize thermal efficiency because of their susceptibility to rapid weight loss at relatively low temperatures. The decrease in thermal efficiency may be visualized by considering the temperature profile that exists in a sinter bed.

In general, there are three regions of major interest: the sinter-mix preheat zone, the combustion zone, and the sinter cooling zone.¹⁰⁾ In a downdraft sintering process, these zones leave the bottom of the packed bed in the given order. Consider now only the preheat and combustion zones. As sinter feed mixture passes under the ignition burner, the fuel in the top part of the bed is ignited to initiate the formation of the combustion zone. At the same time, the downdraft of air drawn through the bed is rapidly transferring heat from the combustion zone to the immediately preceding preheat zone. At this particular time, the unreacted fuel in the preheat zone is exposed to temperatures varying between the ambient bed temperatures and those of the approaching flame front. If the fuel is highly reactive, then a significant portion of the carbon may be lost through oxidation with air in the preheat zone. This results in smaller amounts of carbon being available for combustion in the combustion zone, and thus reduces the heat flux for sintering. Furthermore, the

reactive fuel burns quickly and generates an intense heat in a narrow combustion zone. Consequently, the normal heat-transfer process from gas to solid cannot keep up with the rapidly moving combustion zone, and the result is the formation of a weak sinter.

If a less reactive fuel is used, premature oxidation of the carbon in the preheat zone is minimized, and more complete burning occurs. This causes a relative increase in the width of the combustion zone that (1) permits the heat-transfer processes occurring in the bed to operate in phase with the combustion process, and (2) prevents localized melting because more uniform temperatures are obtained in the combustion zone. It is known that excessive fusion tends to cause the sinter bed to slag over and thus to depress production rates, whereas too little fusion results in weak sinter. Consequently, a good sinter fuel will permit operation between these two extremes.

On the basis of the reactivity index, as well as the oxidation data of Figure 4, the results tend to indicate that the slower burning fuels are most desirable for sintering purposes. This is consistent with our present understanding of the sintering process. In general, the reactivity index appears to yield useful information on the expected production rate that may be obtained with a given fuel. It ranks sinter fuels on a relative scale with respect to their performance in the sintering process. The test is particularly useful for the evaluation of small samples.

Conclusions

Evidence is presented that tends to show that in a chemical-reaction-controlled regime, the oxidation kinetics of carbonaceous fuels depend upon the total (BET) surface area of the fuel particles. This is in agreement with the observations of Wicke.⁵⁾

A reactivity test based on the oxidation characteristics of various sinter fuels has been developed. This index correlates with the production rates of iron-ore sinters. In general, the best sinter production rates are obtained when the sinter fuels are slow burning; that is, when they are relatively unreactive.

References

1. Tu, C. M., Davies, H., and Hottel, H. C., IEC, 26, 749, 1934.
2. Kuchta, J. M., Kant, A., and Damon, G. H. IEC, 44, 1559, 1952.
3. Meyer, Z., Physik. Chem., BL7, 385, 1932.
4. Mei Chio Chen, Christensen, C. J., and Eyring, H., J. Phys. Chem., 59, 1146, 1955.
5. Wicke, E., 5th Symposium on Combustion, Pittsburgh, 245, 52, 1954 (Published 1955).
6. Smith, W. R., and Polley, M. H., J. Phys. Chem., 60, 689, 1956.
7. Grendon, H. T., and Wright, C. C., "Transactions of the Eleventh Annual Anthracite Conference of Lehigh University," May 7-8, 1953, Bethlehem, Pa.
8. Schluter, R., and Bitsianes, G., in "Agglomeration," edited by Knepper, W. A., Interscience Publishers, New York, 1962, p. 585.
9. Dixon, K. G., and Voice, E. W., Journal of the Institute of Fuels, 251, p.529, 1961.
10. Ban, T. E., et.al. in "Agglomeration" edited by Knepper, W. A., Interscience Publishers, New York, 1962, p. 511.

TABLE I
The Chemical Composition of Various Sinter Fuels

Fuel	A (coke)	B (coke)	C (coke)	D (charcoal)	E (coal)	F (coke)	G (coke)	H (charcoal)
Sulfur*	0.65	0.78	1.22	0.10	0.57	0.93	3.61	0.11
Fixed Carbon	86.08	60.61	85.40	86.69	74.16	87.75	86.80	86.83
Volatile Matter	6.29	12.87	4.30	5.83	7.80	4.21	12.65	8.16
Ash	4.94	25.51	10.01	4.08	16.26	7.28	0.51	4.55
Total Carbon	86.92	66.32	87.90	88.67	76.47	88.43	90.70	87.80
Moisture	2.69	1.01	0.29	3.40	1.78	0.76	0.04	0.46
True Specific Gravity	1.65	1.69	1.89	1.77	1.70	1.81	-----	-----
Apparent Specific Gravity	1.05	1.60	1.70	1.55	1.64	1.46	1.33	1.291

*Compositions in weight percent.

TABLE II

The Effect of Air Oxidation on the Particle Size
of Coke C

Percent Oxidized*	0	10	21	40***	67.5	87****
Screen Analysis of**						
Oxidized Fuels (Cumulative %)						
Tyler Mesh						
+20	0	5.1	2.4	-	5.7	21.2
-20 +28	100	96.0	93.1	85.4	77.5	71.5
+35	-	98.6	96.5	91.5	96.0	89.1
+48	-	98.8	96.9	93.2	97.9	92.5
+65	-	98.9	97.3	96.1	99.1	95.4
+100	-	99.0	98.0	97.7	99.6	96.8

* Samples oxidized at a furnace temperature of 1250 F at an air flow rate of 11 liters per minute.

** Screen analysis obtained by hand screening of samples for two minutes.

*** Ro-tapped for 15 minutes.

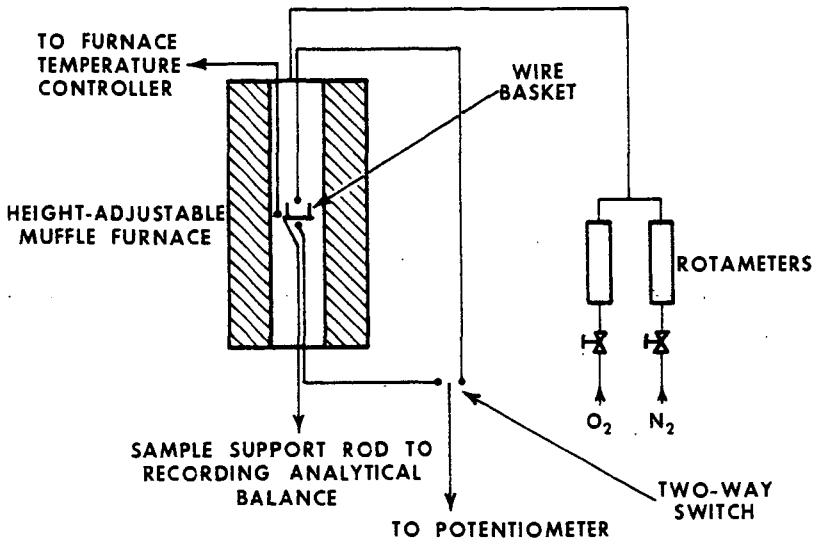
**** Furnace temperature 1600 F.

TABLE III

The Correlation of Sinter Production Rate With the
Reactivity Index of Sinter Fuels

Fuel	Reactivity Index (\emptyset)	Sinter Production Rate Tons/day/ft ²
C (coke)	2.50	4.2
E (coal)	1.84	4.2
F (coke)	1.70	---*
G (coke)	1.68	4.2
D (charcoal)	1.43	---*
A (coke)	1.40	3.8
H (charcoal)	1.25	---*
B (coke)	1.24	3.4

*Insufficient sample to run sinter pot test.



SCHMATIC DRAWING OF EXPERIMENTAL EQUIPMENT

FIGURE 1

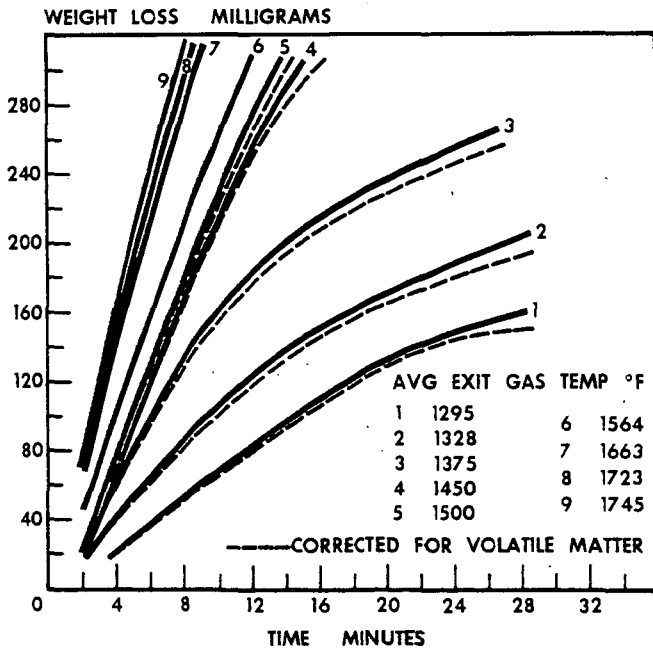


FIGURE 2

AIR OXIDATION OF COKE C AT VARIOUS TEMPERATURES

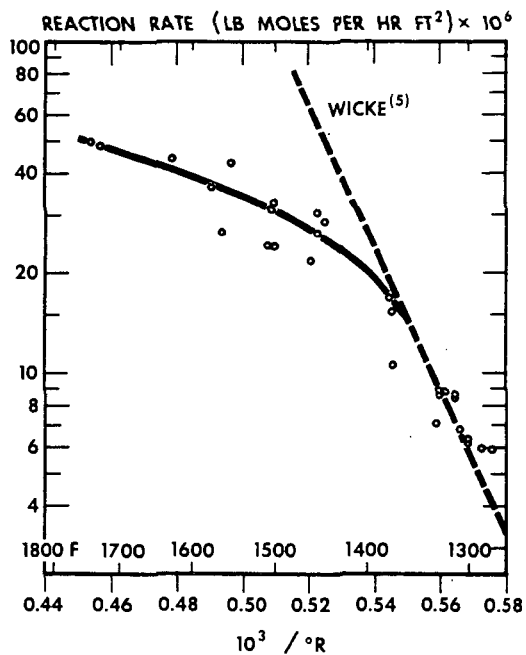


FIGURE 3

EFFECT OF TEMPERATURE ON THE SPECIFIC REACTION RATE OF COKE C

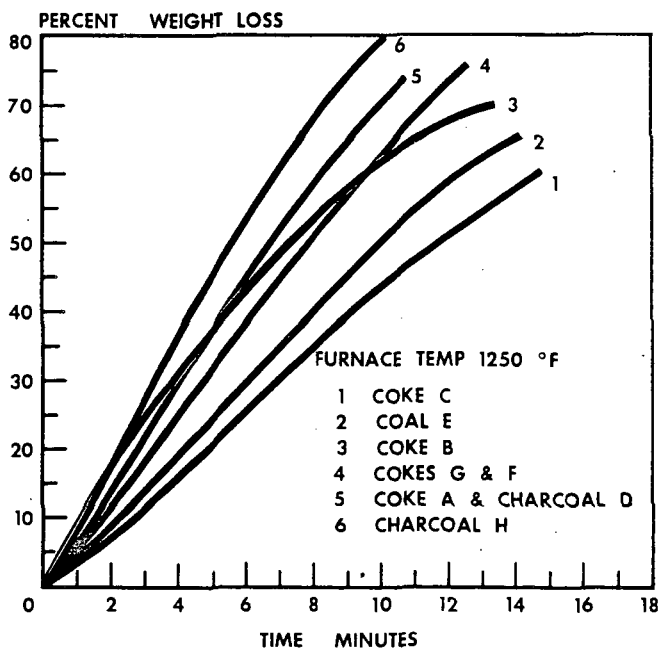


FIGURE 4

AIR OXIDATION OF VARIOUS FUELS

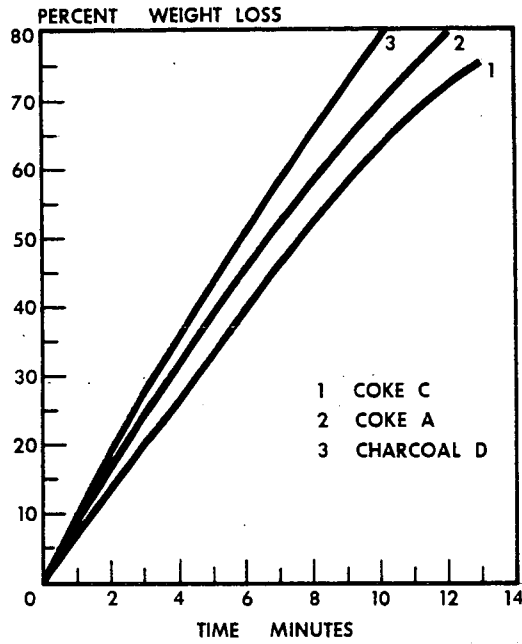


FIGURE 5

AIR OXIDATION OF VARIOUS FUELS AT 1600 F

BLAST FURNACE TESTS WITH COKES OF DIFFERING REACTIVITY

By A. A. Triska

Great Lakes Carbon Corporation, Chicago 1, Illinois

Pig iron is produced in blast furnaces by heating and reducing iron ore with furnace coke and products of combustion. Combustion and gasification of the coke near the bottom of the furnace provide the required temperatures and reducing atmosphere. This paper deals with coke savings observed on commercial blast furnaces when petroleum coke was added to the coal blend before carbonizing in by-product ovens. An analysis of the furnace operating results indicate that changes in coke structure which affect reactivity were responsible for reduction in coke rate.

HISTORY

Blakley and Cobb (1) in England, and Broche and Nadelman (2) in Germany, are typical of many investigators who have speculated for many years on desirable coke characteristics for blast furnace use. They concluded that a coke arriving at the tuyeres in larger proportions was desirable. To attain this, the gasification of coke carbon further up the shaft must be reduced. This gasification is called "solution loss" which involves the reaction of coke carbon with carbon dioxide originating from indirect reduction of iron oxides and calcination of carbonates.

Our experience with special foundry coke indicates that a furnace coke less reactive to gasification in the upper and cooler portion of the furnace can be produced. A coke of this type contains less internal pore surface and thicker cell walls. When used in cupolas, a coke reduction is experienced, in addition to use of more air per pound of coke charged, higher combustion temperatures, and higher concentration of carbon dioxide in the off-gas. The increased carbon dioxide concentration indicates that the reaction of coke carbon with carbon dioxide can be depressed in cupolas. Thus, if the same can be accomplished in a blast furnace, the "solution loss" would be reduced.

The practical advantage experienced by the use of special foundry coke in cupolas led to the idea that blast furnace coke could similarly be improved. Hence, plant scale blast furnace tests were planned.

PRELIMINARY PLANT TESTS AT OBERSCHELD, GERMANY

A one month test, with a low internal surface dense foundry coke, was made in a small blast furnace producing foundry pig iron at Hessische Berg-Und Huttenwerke, Oberscheld, Germany. In this test various proportions of normal furnace coke were replaced with dense H-C Coke, a special foundry coke. This coke was produced by Verkaufs Vereinigung Fur Teererzeugnisse who operate under a license agreement with Great Lakes Carbon Corporation.

Table I summarizes the results of a 166-hour test on the Oberscheld blast furnace in which 33.4 percent H-C Coke was substituted for normal coke. The data show the average practice for normal coke and for a mixture of 2/3 normal coke and 1/3 of H-C Coke.

The replacement of 33.4 percent normal coke by H-C Coke was accompanied by an increase in silicon and a reduction of sulphur in the hot metal, reflecting increased hearth temperatures. As a result, the operator chose the following changes in practice while producing iron of comparable sulfur content :

- 1) Coke rate reduction of 44 pounds per ton of hot metal
- 2) Blast temperature reduction of 144°F
- 3) Increase in hard to reduce ore of 174 pounds per ton of hot metal
- 4) Reduction of scrap iron of 192 pounds per ton of hot metal
- 5) Reduction in stone rate of 138 pounds per ton of hot metal with equal slag volume at a basicity reduction from 1.40 to 0.95.

TABLE NO. I

H-C COKE PERFORMANCE VS NORMAL COKE
OBERSCHELD BLAST FURNACE TEST II
 (Working Volume - 7230 Cu. Ft.)

<u>TEST CONDITIONS</u>	<u>NORMAL COKE</u> (28 Days)	<u>H-C COKE MIX</u> (166 Hours)
<u>FURNACE COKE</u>		
Normal Coke, %	100 Days	66.6
H-C Coke, %	-	33.4
<u>COKE ANALYSIS</u>		
Ash, %	8.7	7.2
Sulfur, %	0.92	0.97
<u>FURNACE CHARGE</u>		
Pounds Coke/THM (As charged)	1860	1816
Pounds Stone/THM	384	246
Ore, % Fe	40.2	41.7
Pounds Scrap Iron/THM	426	234
Pounds Hard To Reduce Ore/THM	224	398
Pounds Oxygen in Ore/THM	618	732
<u>PRODUCTION</u>		
Tons Hot Metal Per Day	167.0	173.6
Hot Metal, % Silicon	3.22	2.93
% Sulfur	0.016	0.021
Slag Volume, Pounds/THM	1338	1342
Slag Basicity, Base/Silica and Alumina	1.40	0.95
Off Gas, % Carbon Dioxide	8.2	9.1
% Carbon Monoxide	32.3	31.5
% Hydrogen	2.4	2.0
% Nitrogen	57.1	57.4
<u>OPERATING CONDITIONS</u>		
Blast Temperature, °F	1526	1382
Blast Pressure, PSIG	9.38	9.41
Wind Delivered, CFM	10430	10400

It was difficult to evaluate the results given in Table I in respect to coke savings by the use of H-C Coke as the burden used during the test period differed considerably from the one normally used. During the test period on H-C Coke 398 pounds of so called hard to reduce ore were used per ton of hot metal compared with 224 pounds during the base period. With normal practice it was reported an excess of 250 pounds or hard to reduce ore results in cold iron at Oberscheld. The significance of an increase of 174 pounds of ore per ton of hot metal cannot be fully appreciated unless it is pointed out that extremely dense Kiruna D, Swedish Magnetite, was charged in 4-6 inch lumps. Such ores would tend to contribute to carbon dioxide at low levels in the blast furnace and result in more solution loss. A reduction in the scrap per ton of hot metal from 426 pounds in the base period to 234 pounds in the test period is also significant because an additional amount of iron had to be reduced from ore.

In order to obtain a better understanding of coke saving, the practice values obtained were evaluated with the use of the Flint Coke Rate Formula (3) (4) which corrects for burden and iron analysis variations. The results thus calculated are shown on Graph No. I. The significance of this Graph was that a calculated coke saving occurred and increased linearly with H-C Coke replacement of normal furnace coke. Of special importance was the excellent correlation of the results with variation of percentages of H-C Coke used from which it was concluded that the data obtained are reliable. This conclusion ultimately led to the development of a special furnace coke.

TABLE NO. II

RESULTS OF H-C COKE REACTIVITY
OBERSCHELD TEST II

<u>OPERATING VARIABLES</u>	<u>CHANGE IN PRACTICE VALUE</u>
Coke Reduction, pounds/THM	87 (a)
Blast Temp. Reduction °F	144
Stone Reduction, Pounds/THM	138
Slag Basicity Reduction, Base/Silica and Alumina	0.45
CO ₂ , Increase in Off-Gas, %	0.9

(a) Corrected for burden variation with Flint Coke Rate Formula.

Table No. II. shows that the preliminary Oberscheld blast furnace tests with special foundry coke resulted in reduced coke rate, reduced stone usage and increased carbon dioxide content in the off-gas. Of special interest is the fact that normal desulfurization was obtained despite the reduction of 0.45 slag basicity from 1.40 to 0.95 at equivalent slag volume and slag sulfur content. (1.3). These findings were anticipated from our cupola experience with dense foundry coke.

DEVELOPMENT OF P-C COKE

Before making further blast furnace tests a special low cost furnace coke was developed simulating the useful reactivity characteristics displayed by 33.4 percent H-C Coke mixtures with normal furnace coke. This coke, called P-C Coke, was manufactured in normal by-product ovens and was produced from coal blends containing appropriately sized petroleum coke. A three (3) month and a one (1) month plant scale blast furnace test were made with this coke at two (2) large steel plants in the States.

COOPERATIVE COLORADO FUEL AND IRON CORPORATION TESTS

The initial use of P-C Coke in a blast furnace was made at the Pueblo Plant of The Colorado Fuel and Iron Corporation. This coke was produced from their normal high volatile coals and the replacement of low volatile coals with minus 1/8 inch petroleum coke furnished by Great Lakes Carbon Corporation. Petroleum coke is the residue obtained from coking residual petroleum oil.

TABLE NO. III

P-C COKE PERFORMANCE VS REGULAR COKE
CF&I THREE MONTH PLANT TEST

(Hearth Dia., 20 Ft., 3 In., Working Vol., 26015 Cu. Ft.)

<u>TEST CONDITIONS</u>	<u>REGULAR COKE</u>	<u>P-C COKE</u>	
	<u>BASE PERIOD</u> (158 Days)	<u>AVERAGE</u> (85 Days)	<u>AVERAGE</u> ^(a) (23 Days)
<u>COKE ANALYSIS</u>			
Ash, %	11.6	11.8(b)	11.8(b)
Sulfur, %	0.57	0.63	0.61
<u>FURNACE CHARGE</u>			
Pounds Coke/THM (As charged)	1514	1414	1350
Pounds Stone/THM	605	547	509
Theoretical Pig Yield, %	53.3	52.8	53.6
<u>PRODUCTION</u>			
Tons Hot Metal Per Day	651	655	709
Hot Metal, % Silicon	1.13	1.10	1.08
Hot Metal, % Sulfur	0.044	0.045	0.047
<u>OPERATING CONDITIONS</u>			
Blast Temperatures, °F	1075	981	1000
Blast Pressure, PSIG	19.9	21.5	21.4
Wind Delivered, CFM	35560	34410	35320

Note (a) Snowfall 0.1" water compared to normal of 0.03".

Note (b) Problems in Washery caused coal ash increase. Petroleum coke contains 0.3 percent Ash.

Table III summarizes the results of a three (3) month blast furnace P-C Coke test in comparison with normal practice. The data shown in Table III represent the average values obtained. It is to be noted that the information was gathered from operating records. The values appearing in the last column under the heading "Average" (23-day) represent a 23 day, consecutive period included in the 85 day test run. A review of Table III indicated the following :

1. Hearth Temperature Increase - Visual inspection of the tuyeres, at the time, when P-C Coke first reached the hearth, showed an increase in temperature. An increase in the percent of silicon and a reduction in sulfur in the hot metal produced also reflected an increase in hearth temperature. This increase in hearth temperature permitted, and in fact required, changes in practice to produce hot metal of the usual analysis.

Average changes in practice for the 85 day period on P-C Coke follows :

1. Coke rate reduced 100 pounds.
2. Stone rate reduced by 58 pounds.
3. Blast temperature reduced by 94° F.

Inasmuch as the carbon content of the coke remained essentially constant a reduction of this order of magnitude in the coke rate indicates that more heat was obtained from each pound of P-C Coke charged. This follows because the heat required per ton of iron did not change significantly as the chemical and physical character of the burden remained fairly constant.

2. Solution Loss - A reduction in solution loss is indicated by the use of more air (1.8 cubic feet) per pound of P-C Coke charged, despite a reduction of 2620 cubic feet of wind per ton hot metal. This shows that a larger percentage of the coke reaches the tuyeres and less of it was gasified above the tuyeres. The reduction in gasification above the tuyeres is attributed to the lower reactivity of the P-C Coke towards carbon dioxide. The twofold effect of decreasing solution loss and bringing more carbon to the tuyeres is larger than one might at first anticipate.

For simplicity it will be assumed that solution loss of carbon is decreased by 48 pounds or 4 pound mols per ton hot metal.

HEAT EFFECTS OF REDUCING SOLUTION LOSS

Heat Loss due to Solution Loss	$4C + 4 CO_2$	$= 8 CO$	296,780 BTU
Heat Gain due to Combustion	$4C + 2O_2$	$= 4 CO$	<u>190,200 BTU</u>
Additional Heat Available			486,980 BTU

Thus from the above tabulation it can be seen that a reduction in solution loss of 50 pounds increases the available heat by about 500,000 BTU per ton of hot metal.

3. Blast Temperature - Because the furnace was a little tighter the operators chose to operate with a 94°F lower blast temperature on P-C Coke. By improving the physical character of the burden (such as pellets, etc.,) so as to reduce blast pressure, a still further improvement in coke rate would have been possible by keeping the blast temperature closer to normal levels. As an alternate some 3 to 4 grains of moisture could have been added to the blast to obtain a faster rate of driving and more tonnage. The effect of blast humidity is manifest in the 23 day period when the average rainfall (snow) was above normal. Hot metal tonnage and coke rates were more favorable during this period as shown in Table III.
4. Blast Pressure - The slight tightening of the furnace with P-C Coke resulting in a blast pressure increase of 1.6 pounds was, in the main, ascribed to a reduction of the volume of the raceway. The reasoning for this was that the conditions appeared similar to those experienced by others with increased blast temperature (5) or oxygen enrichment (6). Credence to this hypothesis was further given by the practice in the 23 day period resulting in normal wind rates and 9 percent capacity increase with a 164 pound coke reduction. The increased coke rate reduction shows the potentials that exist with improved practice such as increased humidity in blast and better gas solid contact.

Further, foundry experience with dense coke leads to the theory that the maximum carbon dioxide concentration in the combustion zone with P-C Coke is higher and located closer to the tuyeres than with normal coke. A condition of this type would explain the tightening of the furnace and loosening with steam.

OPERATING VARIABLES CHANGED BY USE OF P-C COKE

Table IV summarizes the change in practice values attributed, in the main, to improved useful coke reactivity. To some extent the reduction in coke rate was also contributed to by the increase of 11.0 to 14.2 percent in the iron concentration in the charge caused by a reduced coke and lime volume in the 85 and 23 day periods respectively. The increase in air requirement per pound of coke charged and reduction in air required per ton of hot metal is in agreement with our dense foundry coke experience in cupolas and is significant.

Manes and Mackay (7) with thermal and equilibrium data, constructed a simplified model of a blast furnace to derive a quantitative estimate of coke rate. They show a coke saving results from an increase in air per pound of coke charged with concomitant reduction in air per ton hot metal. This is the same finding as found in the CF&I test.

TABLE IV.RESULT OF P-C COKE REACTIVITY
CF&I THREE MONTH PLANT TEST

<u>OPERATING VARIABLES</u>	<u>CHANGE IN</u>	
	<u>PRACTICE VALUE</u>	
	<u>AVERAGE</u>	<u>AVERAGE</u>
	<u>(85 Days)</u>	<u>(23 Days)</u>
More-Air/Pound Coke Chg., Cu. Ft.	1.8	1.5
Less Air/THM, Cu. Ft.	2620	6450
Less Coke/THM, Pounds	100	164
Less Blast Temp. °F	94	75
Less Stone/THM, Pounds	58	96
Increase in Daily Metal Production, %	0.6	8.9

P-C COKE STRUCTURE

Before reviewing the reducing and temperature conditions in a blast furnace as related to fundamentals of coke gasifications, the significant structural characteristics of P-C Coke are discussed. Of special importance are those P-C Coke characteristics which affect its rate of gasification at various temperatures experienced in a blast furnace.

The physical coke characteristics relating to gasification are significantly affected by inclusion of petroleum coke in the coal blend when producing P-C furnace coke. These become readily apparent when viewed under a microscope.

The effect of replacement of low volatile coal with petroleum coke in a given blast furnace coal blend is shown in Figures 1 and 2 at 10X magnification. In Figure 1 the normal blast furnace coke produced with low volatile coals is shown. The black portions are the pores filled with a black resin while the light portions are the cell walls. The specimen before photographing requires a high degree of polish. In this operation, great care was exercised so that some of the fragile extremely thin cell walls are not in part destroyed. Normal furnace coke in Figure 1 at 10X magnification gives the appearance of discontinuity of some of the fine white cell walls. When this is viewed under a microscope at 40X magnification the continuity of the cell walls can be observed. It is, however, to be noted that in Figure 4 at 40X magnification the discontinuity of the fine cell walls is again noted. The reason for this is the lack of photographic sensitivity with the bright lighting required. This type of lighting is required for accentuating the petroleum coke highlights and was used for all photographs. When keeping this in mind it is noted that the normal furnace coke shows a larger number of relatively small pores with considerable thin cell walls as compared to P-C Coke shown in Figure 2. Further comparing the 10X magnification of normal and P-C Coke it is noted that P-C Coke has larger pores.

In Figure 2, attention is called to the amorphous-appearing white highlights in the cell walls. These highlights are petroleum coke particles which are firmly bonded into carbonized coal matrix. Close inspection as shown by 40X magnification of P-C Coke in Figure 3 also reveals that larger particles of petroleum coke are tightly bonded into the matrix and that fine petroleum coke particles are included in the cell walls thus contributing to their thickness. For comparison purposes Figure 4 shows a 40X magnification of normal furnace coke. This again shows in comparison to Figure 3 that the cell walls in P-C Coke are massive and thick. In order to observe the effect of low volatile coal in the normal furnace blend, a coke was produced in a commercial oven without the use of low volatile coal in the high volatile coal blend. The coke thus produced is shown in Figure 5 at 40X magnification. An inspection shows that even thinner cell walls resulted with the removal of low volatile coal from the normal furnace coke blend. Therefore, the thicker cell walls in P-C Coke are not attributed to the removal of low volatile coal from the blend, but rather to its replacement with petroleum coke. To accomplish this the petroleum coke must have altered the coalescence of the plastic coal in such a manner as to produce thicker cell walls in the P-C Coke.

That petroleum coke contributes to the coalescence of cell walls at first may seem surprising as it does not become plastic in the same manner as bituminous coking coals on heating. In order to assist in clarification of this property, petroleum coke was macroscopically inspected before and after carbonization. Figure 6 shows a 10X magnification of petroleum coke before carbonization. The black portions are the pores filled with a black resin and the light portion represents the cell walls. Of interest are the black lines traversing the cell walls. These lines are thermal shrinkage cracks and on carbonization result in structural weakness in the P-C Coke produced. In order to eliminate this weakness, petroleum coke must be precrushed to about 90 percent or more minus 1/8 inch in size, before inclusion in the coal blend. An impact type mill has been found quite satisfactory for this purpose.

On carbonization of petroleum coke the thermal shrinkage cracks are accentuated as illustrated in Figure 7. These fissures, of course, can be substantially eliminated by precrushing. The amorphous appearing cell walls are bordered by a darker appearing homogeneous mass. This is the carbonization product of the heavier volatile content of the petroleum coke as it was expelled thermally from the internal portion of the petroleum coke. At one point of the thermal treatment during carbonization this material was plastic. This plastic portion of petroleum coke is not visible in P-C Coke. It was therefore concluded that it is diffused with the plastic material from the coal contributing to both bonding and coalescence of the cell walls.

However, as the plastic mass is limited, petroleum coke does not exhibit the bonding characteristics on heating typical of bituminous coking coals. This may explain why a more thorough blending with petroleum coke is desirable for higher tumbler values. From the macroscopic analysis it was concluded that the major structural differences between P-C Coke and normal furnace coke are :

1. Carbon Concentration - There is a higher concentration of carbon or a more continuous outside carbon surface of P-C Coke due to thicker cell walls caused by coalescence and inclusion of fine petroleum particles in the cell walls. (This is also confirmed by a 12.5 percent increase in apparent specific gravity of P-C Coke as compared to normal furnace coke.)
2. Internal Surface - There is a substantial reduction of internal surface area due to reduction of the number of fine pores.
3. Larger Pores - There are larger pores in P-C Coke due to coalescence of the plastic material from coals.

These enumerated P-C Coke characteristics enhanced the coke performance in the blast furnace test runs.

Before discussing the gasification characteristics of P-C Coke in relation to blast furnace conditions it may be well to enter into a brief review of the fundamental coke gasification concepts.

FUNDAMENTALS OF COKE GASIFICATION

Coke gasification has been studied extensively by a larger number of investigators over the years and reported in the literature. The accepted theory states gasification is a surface phenomenon which is greatly accelerated by temperature and retarded by surface films. The surface film which is the boundary between coke and oxidizing gases varies in thickness depending on the rate of coke gasification and disengagement of these gases. This is a dynamic balance and increased gas velocities passing over the coke reduce the film thickness. Diffusion through the surface film to the coke at high temperatures follows the mass law in that increase in available reactants results in increased rate of coke gasification in a given volume and thus higher temperatures result. This has been amply demonstrated in blast furnaces with oxygen enrichment of the blast. This same phenomenon occurs with a variation of apparent specific gravity of coke. Increased specific gravity results in more available carbon per unit surface under the film, as the carbon is more densely packed. In the past it has been demonstrated in the blast furnaces that higher temperatures and better driving rates were obtained when relatively light charcoal was replaced by heavier beehive coke and then again, when beehive coke was replaced by heavier high temperature by-product coke.

The work reported by Tu, et al., (13) sheds further light on the film diffusion theory of carbon combustion. Graph No. III summarizes some of the pertinent results showing variation of combustion rate with temperature, gas velocity oxygen concentration. He also shows that the rate of combustion varies linearly with percent oxygen up to 25 percent. At high temperatures where diffusion through the surface film is controlling, the rate of reaction varies as the 0.4 to 0.7 power of the mass velocity. In addition in this range, the rate of combustion varies approximately as the 0.6 to 1.1 power of the arithmetic mean temperature in degrees Kelvin. The work of Dubinsky (14) shows carbon gasification with carbon dioxide increases enormously in the temperature range of 1200 to 1400°C. In this range, temperature has relatively little effect on the rate of combustion for a given carbon in air.

Investigators have shown that coke gasification can be considered to occur in three steps, depending on temperature (8), (9), (15), (16). Graph No. IV, according to Wicke, illustrates this concept.

STEP I - At low temperatures, Step I occurs. In this range the rate of conversion of carbon dioxide to carbon monoxide is determined by total available surface carbon and the activation energy of coke. The total available (carbon) surface, includes both the external surface and internal pore surface which, for furnace coke, is in the range of two (2) square meters per gram.

From Graph IV it is noted that the rate of reaction increases rapidly with temperature in Step I.

STEP II - With increasing temperatures, the rate of increase of the reaction slows and a transition stage "a" is entered. Subsequently, Step II is reached in which the rate of reaction is so rapid that carbon dioxide, as it approaches the coke and its pores through the gas film, is in part converted and therefore the amount of carbon dioxide concentration reaching the internal pore surfaces of the coke is reduced.

This area, for convenience, can be referred to as pore diffusion zone. As a result less total effective surface becomes available for reaction and the rate of increase of the reaction is reduced to one half of that in Step I. The temperature range in which it occurs, by definition, is Step II.

STEP III - At further increasing temperatures, the rate of increase of the reaction slows and a transition stage "b" is entered. Subsequently, Step III is reached in which the rate of reaction is so high that no carbon dioxide is available for internal pore diffusion. In this area gas diffusion through the film is controlling. The diffusion coefficient is only slightly affected by temperature increases and therefore the rate of reaction increase is slowed down.

BLAST FURNACE CONDITIONS AFFECTING COKE GASIFICATION

An analysis was made of the fundamentals concerning blast furnace conditions and coke gasification to permit an explanation of the significant coke savings obtained with P-C Coke. A literature search revealed a considerable fund of information which must be carefully sifted to permit rationalization applicable to conditions existing in a blast furnace.

Of considerable interest on coke gasification is the work reported by B. Heynert and J. Williams (8), N. Peters and H. Echterhoff (9) and others (10), (11), (12). One of the main difficulties is to assess the relation of temperature in the blast furnace with gas composition. An approximation of this is possible with the sampling procedure used by Schurmann et al (10).

Graph II -A, based on work by Schurmann, shows the relation of temperature, with percent carbon monoxide, carbon dioxide, and total percent of carbon gases in a commercial blast furnace. The concentrations of carbon monoxide and dioxide, are strongly affected by temperature and the Boudouard reaction. From this Graph, it readily can be seen, that a desirable coke is one that will depress the reduction of carbon dioxide, to carbon monoxide. It is to be noted, that in the temperature

region where reactions of this type predominate, carbon dioxide is available from carbonate and iron oxide reduction in addition to that from carbon monoxide oxidation accompanied by carbon deposition. Therefore, a coke saving results with a coke which promotes increased concentration of carbon dioxide in the off gas, as it is more effectively used in oxygen removal.

The relation of temperature at various blast furnace elevations above the tuyeres, with percent carbon monoxide, carbon dioxide and the total percent of carbon gases, as reported by Heynert and co-workers, is shown in Graph II. Analyzing this curve from the point of view of carbon gases, four distinct zones are apparent.

ZONE I - The combustion zone in front of the tuyeres is considered as Zone I. In this zone for practical purposes no iron oxides are present and temperatures are at 3000°F and somewhat higher. Under these conditions the overall reaction of coke carbon with hot blast is :

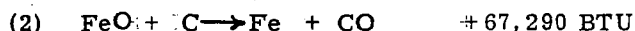


This reaction provides heat and reducing gases for iron ore reduction. High temperatures are developed which play an important role in hearth reactions. High temperatures result in hot metal with high silicon and low sulfur content due to the slag reactions. High temperatures, other conditions being equal, are the result of more carbon reaching the tuyeres and therefore the coke rate can be reduced to obtain comparable quality iron. If, however, the higher temperatures are also contributed to by the combustion characteristics of the coke then additional coke savings are possible by a stone saving to obtain comparable iron.

ZONE II - The area immediately above the combustion zone is characterized by the absence of carbon dioxide. This is due to the existing high temperatures at which carbon dioxide is unstable and, in the presence of carbon, decomposes to carbon monoxide. This area is the pure "direct reduction zone" in which the overall reaction of iron oxide is :



This reaction is pictured as going through the following mechanism :



Since reaction (2) consumes a considerable amount of heat the temperature drops rapidly in this area and as carbon monoxide is formed its concentration increases rapidly.

ZONE III - This area above the "direct reduction zone" is characterized by the appearance of stable carbon dioxide as temperatures have dropped sufficiently and a reduction of carbon monoxide occurs. The termination of this zone is the temperature range in which the Boudouard reaction reverses. To assist in showing

this the total carbon oxides are plotted on Graph II. Zone III can be referred to as "indirect reduction" zone. It is, of course, recognized that even though the direct reduction has been depressed some of it still proceeds. Besides this reaction a number of others occur with the end products consisting principally of Wustite, sponge iron, carbon monoxide and carbon dioxide.

The bulk of these reactions requires less heat than "direct reduction" and therefore the temperature drop in this zone is less until a point is reached where a strong endothermic reaction occurs. This area is where the main portion of the carbonates decompose and possibly other endothermic reactions occur. As there is an excess of carbon monoxide from Zone II for conversion of iron oxides to carbon dioxide, it is obvious that an unreactive coke, minimizing the reduction of carbon dioxide in Zone III, results in a coke rate reduction.

ZONE IV- Zone IV is characterized by the falling off of the total carbon oxide concentration and a rapid drop in ambient temperature. The total carbon oxide volume is reduced due to carbon deposition from the reaction of two volumes of carbon monoxide to one volume of carbon dioxide. The iron ore reduction reactions, similarly as in Zone III, proceed in this area with the modification that the end products favor carbon dioxide formation over carbon monoxide formation. The higher concentrations of carbon dioxide favor the oxidation of free metallics. Again in this zone it is obvious that a coke favoring the stabilization of carbon dioxide will result in a coke saving.

Inspecting the temperature profile on Graph II, it is noted that the carbon dioxide concentration is higher than predicted by the Boudouard equilibrium. This phenomenon is due to the fact that the temperature profile measures the ambient temperature while the Boudouard reaction is controlled by the reacting carbon surface temperature. This surface temperature is lower than the ambient temperature as strong endothermic reactions occur on its surface.

From the foregoing thermal and chemical considerations it was shown that a reduction in coke rate will occur in a blast furnace with a coke resulting in:

1. Increased temperature when gasified at the tuyeres.
2. Increased percent of coke gasifying at the tuyeres.
3. Reduced reaction rate with carbon dioxide to form carbon monoxide.

That an increase in the percent of coke gasified at the tuyeres results in coke saving was also demonstrated by M. Manes and J. S. Mackay (7). By means of a simplified mathematical model of a blast furnace, they showed that a coke rate reduction occurs with an increase in air per pound of coke charged with a concomitant reduction of air per unit of ore. They further deduced that "secondary reduction" (ore reduction below 1000°C) increased under these conditions.

DESIRABLE COKE CHARACTERISTICS

Considering the conditions affecting coke gasification in a blast furnace and the coke gasification fundamentals presented, it is apparent that a coke having the following characteristics will result in a coke rate reduction in a blast furnace:

1. Reduced Internal Surface

A coke with reduced internal surface will produce less carbon monoxide in the cooler upper portions of the stack and therefore a coke saving results. Further, a larger proportion will remain for gasification at the tuyeres and thus more heat is released in the hearth.

2. Increased Pore Diameter

A coke with increased pore diameters results in increased gasification with iron oxide in the pore diffusion range. This zone is significantly extended in a blast furnace from about 1000°C to as high as 1700°C due to the existing high gas velocities reducing surface film thickness. Therefore, a coke with large pores presents more available surface and gasifies more rapidly at temperatures existing in the direct reduction zone. The furnace level to which the direct reduction zone extends depends on temperature. As direct reduction consumes large amounts of heat, the acceleration of this reaction has a cooling effect and therefore the direct reduction zone stops at a lower level in the furnace.

3. Increased Carbon Concentration

A coke with higher concentration of carbon on its surface furnishes more reactants per unit area. Hence, at the tuyeres, the combustion temperature is increased as the reaction takes place in a smaller volume due to the mass action law. Consequently in the combustion zone, at equal total heat release, higher temperatures occur. Further it would appear that the carbon dioxide concentration becomes higher and also occurs at a point, closer to the tuyere nose. It may also be speculated that the higher temperatures occurring at the higher carbon dioxide concentration at localized areas in the combustion zone of the blast furnace contributes to the reduction of limestone usage (more acid slag) for proper metal quality control.

SUMMARY AND CONCLUSIONS

P-C Coke and H-C Coke, when used in blast furnaces, resulted in significant changes in operating results. These are summarized in Table V.

TABLE V.
EFFECT OF SPECIAL COKES VS NORMAL COKE IN BLAST FURNACES.

<u>OPERATING VARIABLES</u>	<u>P-C COKE</u>	<u>H-C COKE</u>
	<u>(85 Days)</u>	<u>(166 Hrs.)</u>
Burden Compared to Regular Practice	Normal	Variable
Coke Saving/THM, Pounds	100	87(a)
More Air/Pound Coke Charged, Cu. Ft.	1.8	-
Less Air/THM, Cu. Ft.	2820	6120
Less Blast Temp. Required °F	94	144
Stone Saving/THM, Pounds	58	138

(a) Corrected for burden variation.

Inspection of the changes in operating results obtained with P-C Coke and H-C Coke clearly indicates that use of these special cokes effect a substantial coke saving as a result of reactivity characteristics differing from normal by-product furnace coke. In the case of P-C Coke, and by the indications obtained with H-C Coke, it was noted :

1. More air was required at the tuyeres per pound of coke charged, showing that a smaller proportion of coke is gasified in the stack and a larger proportion at the tuyeres.
2. Less air was required per ton of hot metal produced showing that the coke carbon was more effectively used with the oxygen from the ore.
3. Higher temperatures were experienced in the combustion zone as verified by a reduction in stone usage while producing comparable quality iron despite a reduction of both coke rate and blast temperature.

In view of the results obtained and the fundamental concepts presented, it was concluded that the reduced coke rate obtained with P-C Coke was caused by improved useful coke reactivity. This improvement was attributed to the following coke characteristics :

1. Less internal surface,
2. Larger pores,
3. Thicker cell walls.

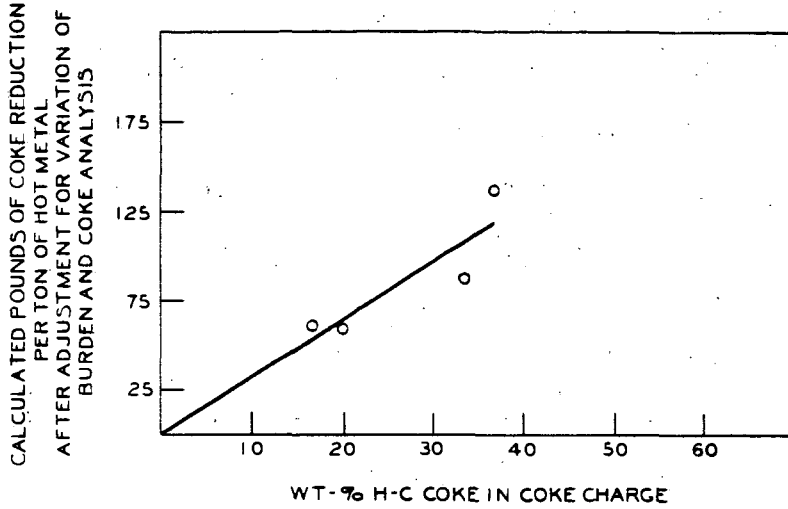
ACKNOWLEDGEMENT

This work could not have been accomplished without the active interest and efforts of J. D. Price, retired Coke Plant Superintendent, J. W. Carlson, Blast Furnace Superintendent, J. R. Purdy, Coke Plant Superintendent, and their staffs, all of The Colorado Fuel and Iron Corporation, and H. Loos, Works Manager, Hessische Berg U Huttenwerke AG, Oberscheld plant and his staff. Grateful thanks are extended to both these companies for permission to use data developed at their plants and to Professor T. L. Joseph for his many timely suggestions.

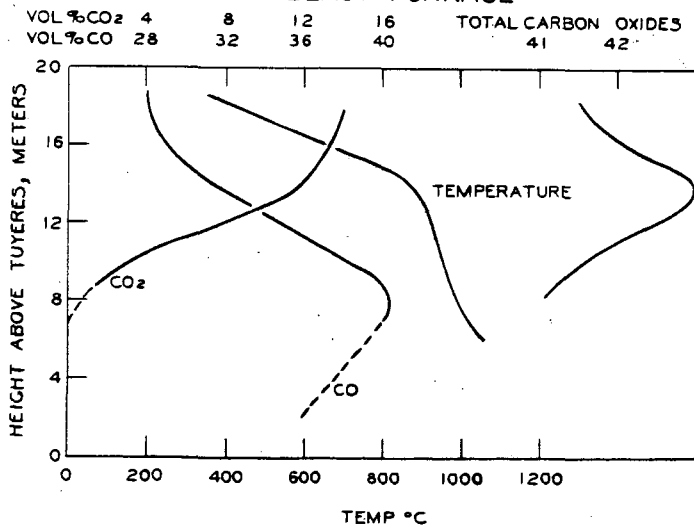
LITERATURE CITED

- (1) T. H. Blakley, J. W. Cobb, Inst. Gas Res. Fellowship Rept. 1931-1934 Com. No. 104
- (2) Broche and Nadelman Stahl U. Eisen, 53 (1953)
- (3) R. V. Flint, Blast Furnace & Coke Oven Proc. AIME (1952)
- (4) R. V. Flint, Blast Furnace & Steel Plt., 47-76, Jan. 1962
- (5) T. L. Joseph, Blast Furnace & Steel Plt., March & April 1961
- (6) M. A. Shapirovalov, Stahl, H-5, 535-538, May 1958
- (7) M. Manes and J. S. Mackay, Jr. of Metals, April 1962, 308-314
- (8) G. Heynert and J. Williams, Stahl U. Eisen, 79, 1545-1554, (1958)
- (9) W. Peters, H. Echterhoff, Blast Furnace & Coke Oven Proc. AIME (1961)
- (10) E. Schurman, W. Zischkale, P. Ischebeck and G. Heynert, Stahl U Eisen 80, 845-861, (1960)
- (11) G. Heynert, W. Zischkale and E. Schurman, Stahl U Eisen, 80, 931-990, (1960)
- (12) G. Hedden, Lecture "Second European Simp. on Chem. Engr." Amsterdam (1960)
- (13) C. M. Tu, H. Davis, and H. C. Hottell; Ind. Engr. Chem., 26, 749-759 (1934)
- (14) M. S. Dubinsky, Thesis, Mass. Inst. Tech. (1932)
- (15) E. Wicke, K. Hedden, and M. Rossberg, Brenst. Warme Kraft 8, (1956)
- (16) G. Hedden, Chem. Ind-Techn., 30, 125-132, (1958)
- (17) B. Osann, Stahl U Eisen, 36 (1916) 477-434 and 530-536.

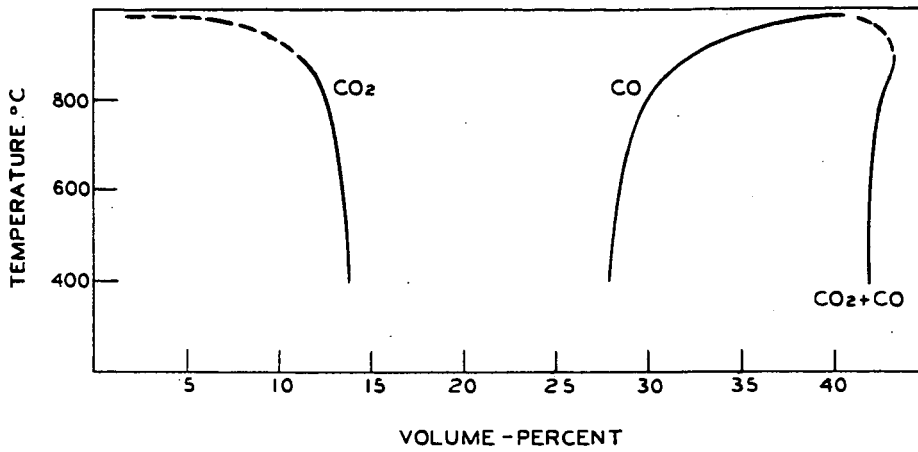
GRAPH I
 COKE SAVING VS WT-% OF H-C COKE IN CHARGE



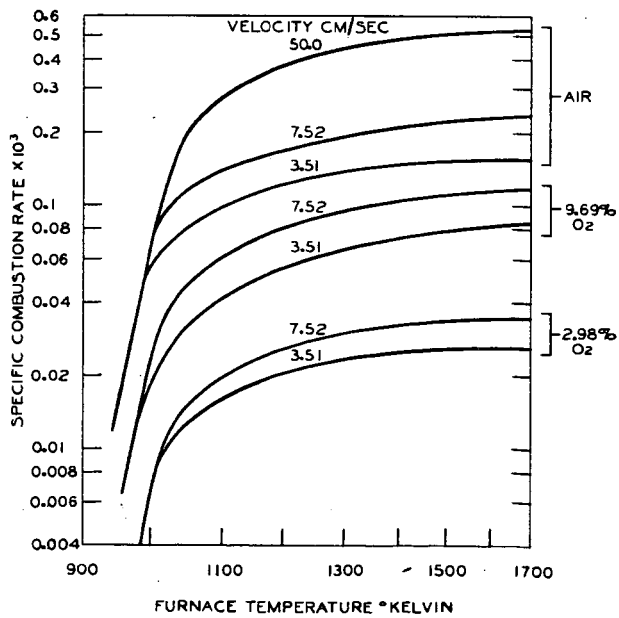
GRAPH II
 PROFILE OF TEMPERATURE AND OXIDES OF CARBON IN BLAST FURNACE



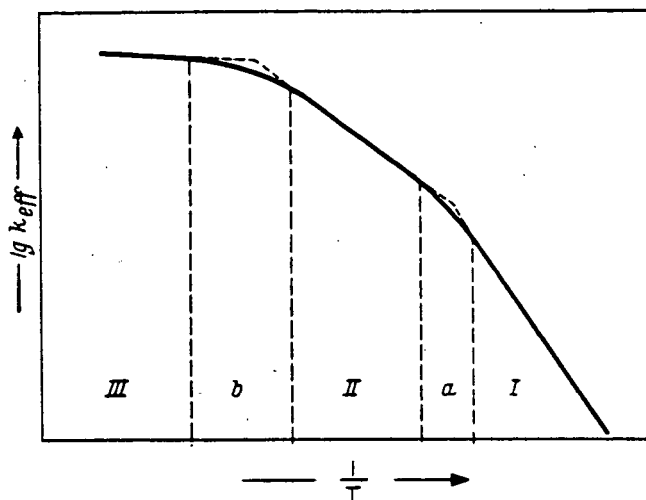
GRAPH II
OXIDES OF CARBON AT VARIOUS TEMPERATURES



GRAPH III
RATE OF COKE COMBUSTION WITH GAS VELOCITY
AND OXYGEN CONCENTRATION



GRAPH IV
RATE OF GASIFICATION



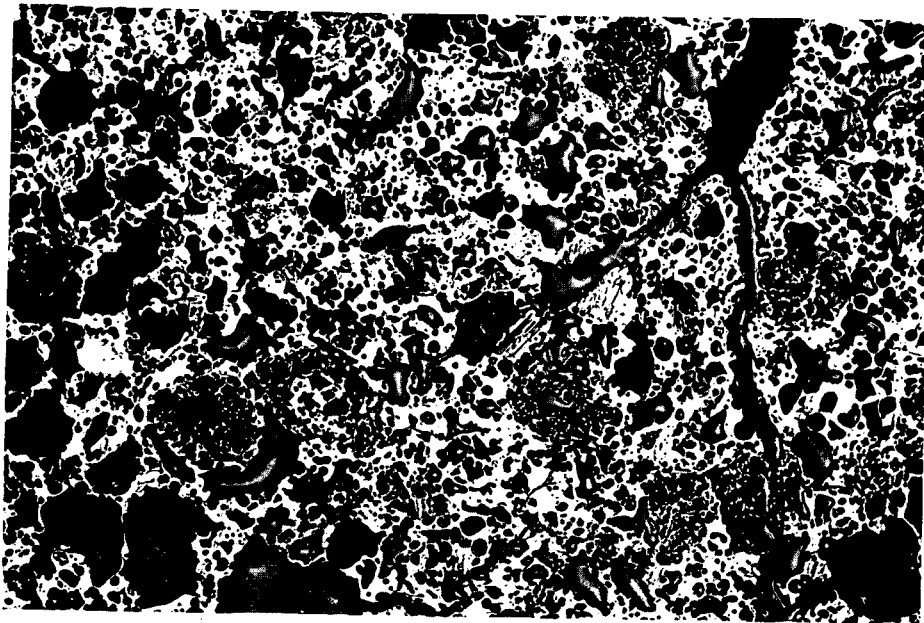


Fig. 1 CF&I NORMAL COKE, 10X

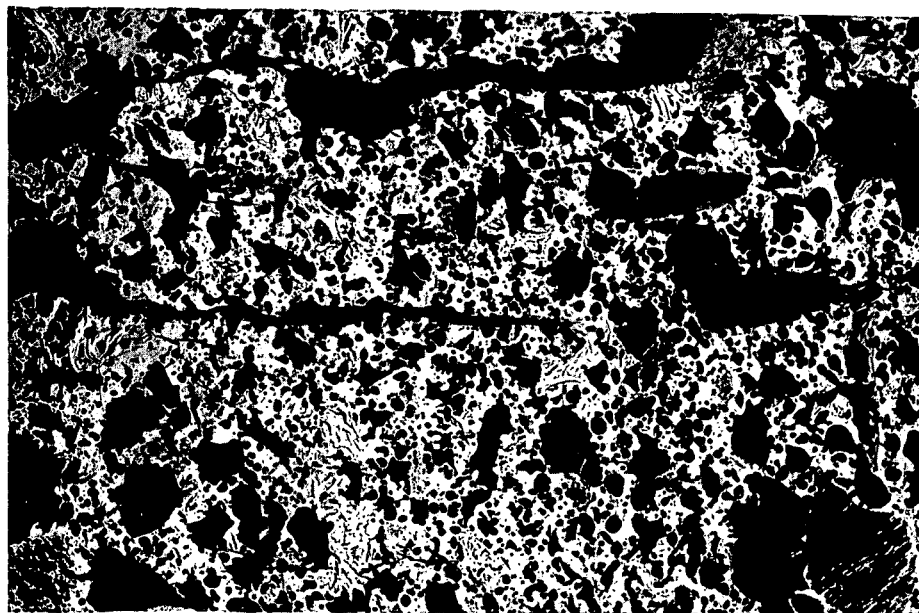


Fig. 2 CF&I P-C FURNACE COKE, 10X

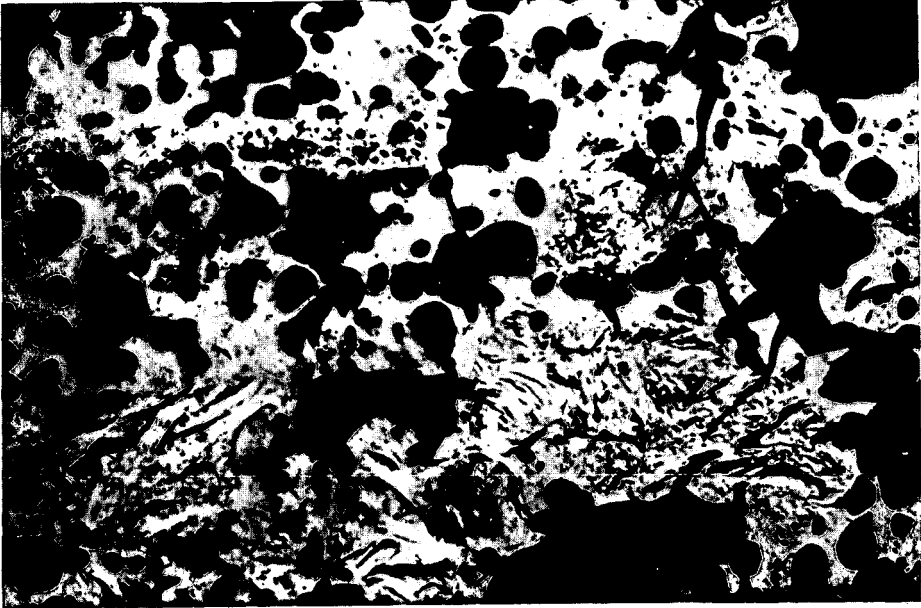


Fig. 3. CF&I P-C FURNACE COKE, 40X

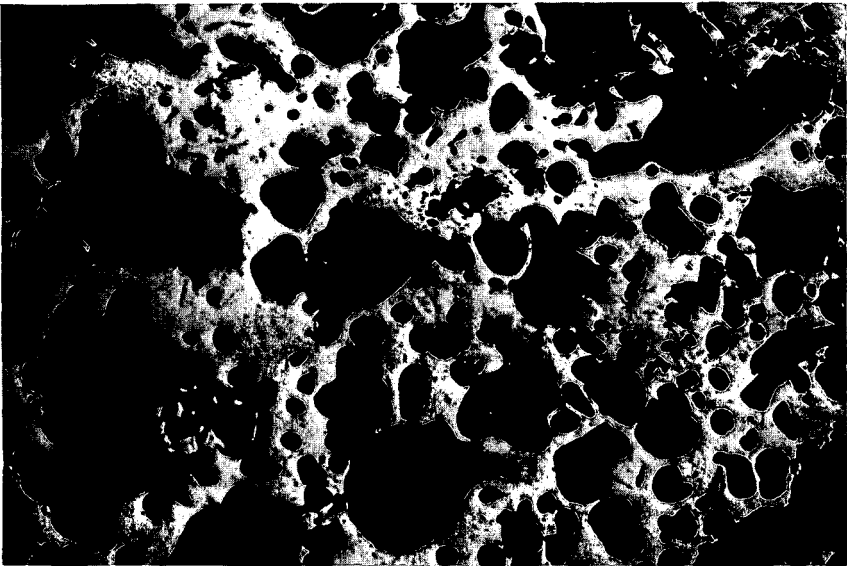


Fig. 4. CF&I NORMAL COKE, 40X

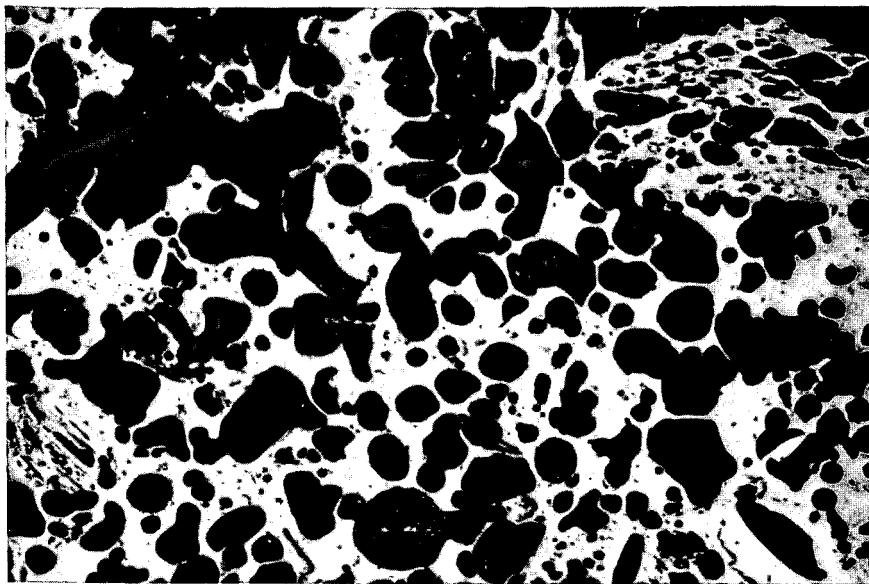


Fig. 5 COKE FROM 100% H. V. COAL, 40X

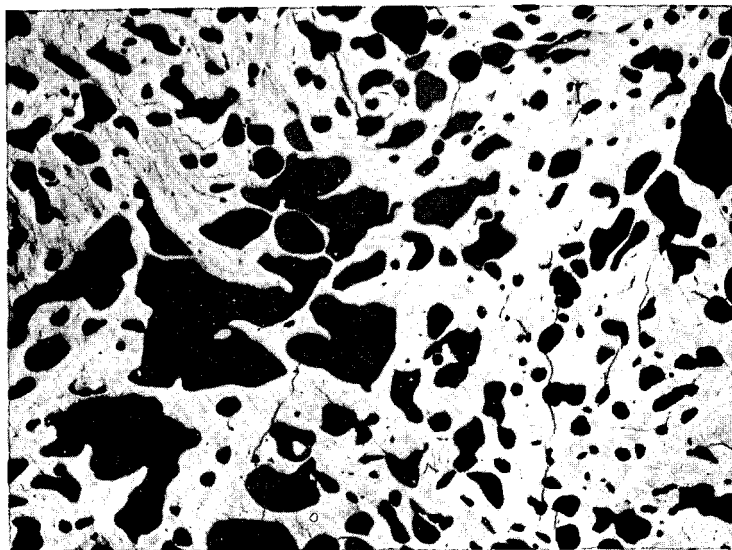


Fig. 6 RAW PETROLEUM COKE, 10X

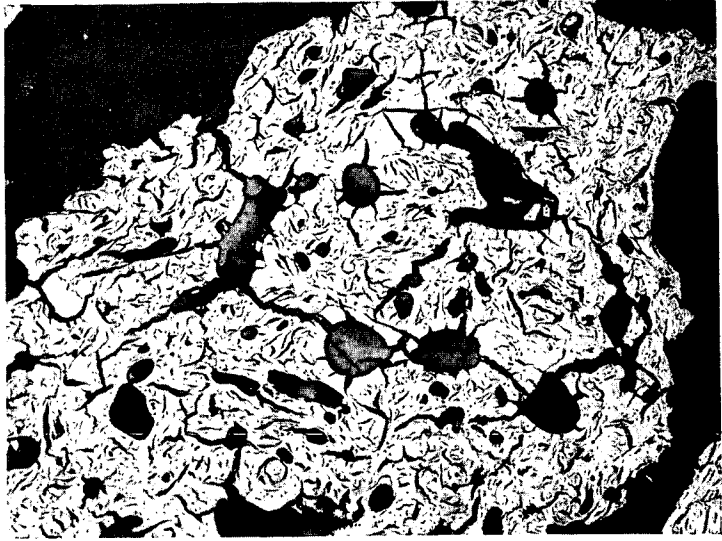


Fig. 7. CARBONIZED PETROLEUM COKE, 10X

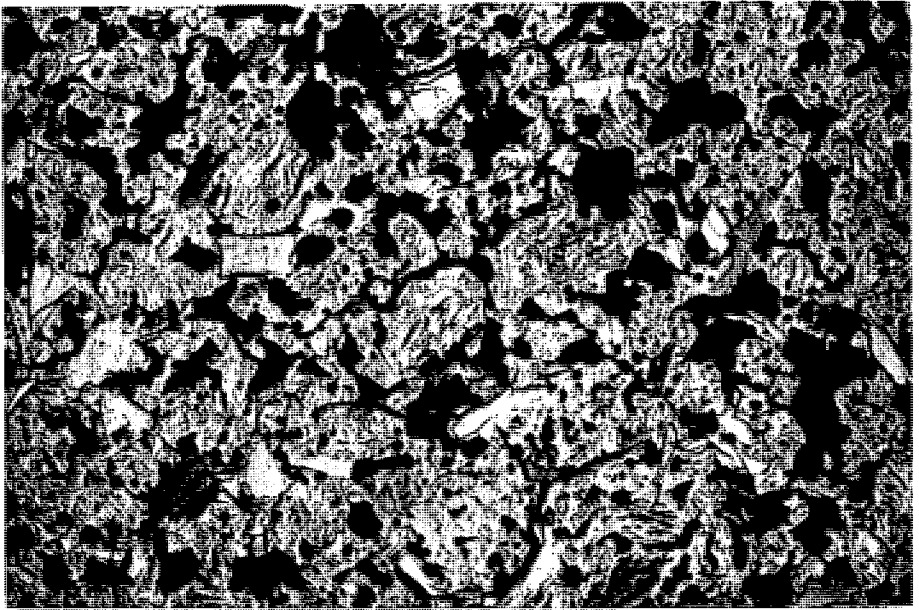


Fig. 8 DENSE FOUNDRY COKE, 10X

REACTIVITY OF COALS IN HIGH-PRESSURE GASIFICATION WITH HYDROGEN AND STEAM

Harlan L. Feldkirchner and Henry R. Linden

Institute of Gas Technology
Chicago 16, Illinois

One of the major obstacles to the design of a reactor for direct conversion of coal to high heating value gas by destructive hydrogenation at high pressure (hydrogasification) has been the lack of information on the rate and course of the reactions during the initial period of rapid conversion of the more reactive coal constituents. Kinetic studies have generally been made with highly devolatilized chars and carbons to avoid the problem of changes in feed composition during heatup. Where the rates of formation of low molecular weight hydrocarbons from reactive coals and low-temperature chars have been measured, experimental conditions did not permit both rapid heatup and short product gas residence times to minimize side and secondary reactions.

The primary variables affecting the rate of hydrogasification are coal reactivity, temperature, pressure and feed gas composition. The coal reactivity, in turn, varies with the initial coal properties, the extent of conversion, the length of time at reaction conditions and the severity of the reaction conditions. In previous studies, significant diffusional resistances have not been encountered (15,16), although they might become important at higher temperatures, or with more reactive feedstocks.

PREVIOUS WORK

In work at the Institute, the major objective has been the determination of the conditions for the direct production of a high heating value gas in a practical continuous reactor system. The feasibility of this approach had been indicated in batch reactor tests (4), and has recently been confirmed in a countercurrent moving-bed continuous reactor. Earlier results obtained with low-temperature bituminous coal char in a fluid-bed reactor at 1400° to 1500°F. and 500 to 2000 p.s.i.g. (10) did not fully attain the desired objective of 30 to 50% char conversion to a gas of 900 B.t.u. per SCF, (standard cubic foot at 60°F., 30 inches of mercury and saturated with water vapor). To obtain high conversions of hydrogen and coal to a high-methane content gas, long coal and hydrogen residence times and low hydrogen to coal feed ratios were used. These conditions make it difficult to interpret the rate data, since the effects of equilibrium hindrance cannot be accurately defined because of lack of thermodynamic activity data for coal and char at levels of conversion.

The U. S. Bureau of Mines (7-9) employed a reactor tube, 5/16 inch in inside diameter, which was heated by passing an electric current through it. Pressures up to 6000 p.s.i.g. and a nominal operating temperature of 800°C. (1472°F.) were investigated. During the 2-minute heatup period, and afterward, hydrogen was passed through the tube at a sufficiently high rate that gas residence times were only a few seconds. Substantial yields of liquids were obtained during the relatively long heatup period, so that the rates of gasification observed at 800°C. were for the less reactive, residual material. The liquids yields decreased with decreases in hydrogen rate as a result of the increase in residence time. For example, an increase in gas residence time from 6 to 30 seconds resulted in a decrease in liquid hydrocarbons from 26 to 4.5 weight % (moisture-, ash-free basis), of a high-volatile bituminous coal.

In contrast, negligible quantities of liquid hydrocarbons were formed in the fluid-bed tests at the Institute (10). In these tests, low-temperature bituminous coal char or lignite (-60, +325 sieve size, U. S. Standard) were fed cocurrently with hydrogen to the hot fluidized bed, resulting in rapid heatup. However, product gas residence times were on the order of one minute, so the absence of liquid products could have been the result of secondary vapor-phase reactions.

In the work described herein, tests were conducted in which both coal heatup and product gas residence time were of the order of a few seconds. No measurable amounts of liquid products were formed and methane was the major gaseous hydrocarbon produced, with only trace quantities of higher paraffins, olefins and aromatics being formed. Some carbon oxides and nitrogen were also evolved during the initial phases of the reaction.

APPARATUS

A flow diagram of the reaction system is shown in Fig. 1. The -16, +20 sieve size (U. S. Standard) coal charges were fed in single batches (usually 5 or 10 grams) from a hopper mounted on top of the reactor. At zero time, a full-opening, air-operated ball valve, connecting the reactor and feed hopper, was opened and the coal charge was dropped into the reactor. A synton vibrator was mounted on the hopper to aid in solids feeding. A pressure-equalization line connecting the top of the hopper and the reactor inlet kept both vessels at the same pressure.

Feed gases were preheated to the desired operating temperature within the reactor. Exit gases passed through a water-cooled coil, a liquids knockout pot, a high-pressure filter and a pressure-reducing back-pressure regulator, before sampling, metering and monitoring.

Gas inlet flow rates were controlled manually and were measured by an orifice meter. Steam was generated at the desired operating pressure in an electrically-heated stainless steel coil by feeding water from a weigh tank with a metering pump.

The reactor barrel was constructed of N-155 super alloy and was designed for operation at a maximum pressure of 1500 p.s.i.g. at a maximum temperature of 1700°F. A complete description of the reactor has been given elsewhere (11), along with design details concerning the use of externally-heated reactors at high temperatures and pressures. The reactor was 2 inches in inside diameter, 4 inches in outside diameter and 60 inches in inside length. An Inconel X thermowell, 3/8 inch in outside diameter, was mounted in the center of the bottom closure and extended 58 inches into the reactor. A removable, stainless steel insert, 1-5/8 inches in inside diameter and containing a 1/2-inch outside diameter thermowell sleeve, was installed in the reactor to contain the coal charge and provide for complete recovery of the coal charge after each test. The bottom of the insert was filled with sufficient alundum pellets to position the coal charge in the center of the third heating zone from the top.

Reactor temperatures were maintained by four individually-controlled electrical resistance heating elements, each 12 inches long. Reactor pressures were controlled at the desired values by means of a back-pressure regulator and were continuously recorded along with orifice pressures.

The double-ended reactor contained an Autoclave Engineers self-sealing (modified Bridgman) closure at each end. The closures were rated for 1400°F. operation at 1500 p.s.i.g. This high-temperature service was facilitated by use of either 16-25-6 or Inconel alloy seal rings. A boundary lubricant of molybdenum disulfide, applied in aerosol form to produce a thin boundary layer coating, was used on all closure threads and on the seal rings.

PROCEDURE

Feed gas mixtures, which were prepared by mixing during compression, were stored at pressures up to 3000 p.s.i.g. Commercially available grades of electrolytic hydrogen (99.8% pure), nitrogen (99.6% pure), helium (99.99% pure) and technical grade methane (95.0% pure) were used. All feed gases, except steam, contained approximately 2 mole % helium tracer for exit gas flow rate measurement.

The feed gas orifice was calibrated before each run with a wet test meter and the exit gases were also metered with this meter as a check on the helium tracer method for exit gas flow rate measurement. In tests with pure steam feed, helium sweep gas was used to purge, from the exit gas system, the small volumes of permanent gases formed. The exit gas specific gravity was monitored continuously with a recording gravitometer as an aid in selecting times for exit gas sampling. A sampling manifold was installed in the exit gas line, upstream of the metering and monitoring system to allow rapid sampling at small time intervals. Gas analyses were performed by mass spectrometer. The combined nitrogen and carbon monoxide

content of the exit gas, determined by mass spectrometer, less nitrogen introduced in the feed gas, was assumed to be carbon monoxide, except in selected tests where carbon monoxide was determined by infrared spectrophotometer.

The four coals investigated were a medium volatility anthracite, a North Dakota lignite, a Pittsburgh Seam bituminous coal and a low-temperature bituminous coal char. The char was prepared from bituminous coal from the Montour No. 10 Mine by a fluidized-bed pretreatment process of the Consolidation Coal Co. Analyses of these feeds are shown in Table 1.

Most runs were conducted for a total time of 15 minutes or less. The reactor was first heated up to the desired operating temperature. Then gas flow, at the desired rate, was started through the reactor. The heat input to the reactor was then adjusted so that all temperatures within the reactor remained constant. When the system was stabilized completely, the run was initiated by opening the valve between the feed hopper and reactor.

At typical conditions of 1500 p.s.i.g., 1700°F. and a hydrogen flow rate of 100 SCF per hour, the first hydrogasification products appeared in the exit gas at the sampling manifold in approximately 10 seconds. During the initial period of high conversion rate, samples were taken at time intervals as short as 5 seconds to delineate the exact course of the reaction. Temperatures at the center of the coal charge, at a point 6 inches above the charge and at the bottom of the insert were recorded continuously by means of a high-speed temperature recorder which recorded each temperature at approximately 3-second intervals.

When the reaction rate had reached a value too small to be measured accurately at the high gas rates employed (usually after about 600 seconds), the run was stopped. The electric heaters were turned off and the reactant gases were purged from the reactor with nitrogen. The reactor was kept filled with nitrogen until the temperature had reached a low enough value to allow retrieval of the coal residue.

RESULTS

Exploratory Tests

Before the test program was initiated, several exploratory tests were conducted at the base conditions of 1000 or 1500 p.s.i.g. and 1700°F., with a hydrogen flow rate of 100 SCF per hour. It was necessary to select sample weights which gave small temperature changes and low concentrations of methane in the exit gas, without impairing analytical accuracy.

Table 1.-COAL ANALYSES

Coal Type Source	Bituminous Coal Char Low Temperature Consolidation Coal Co. (Montour No. 10 Mine)	Anthracite Medium Volatility Anthracite Experiment Station, U. S. Bureau of Mines
Particle Size, U.S. Standard Sieve	-16, +20 -40, +50	-16, +20
Ultimate Analysis, wt % (dry basis)		
Carbon	78.3	83.3
Hydrogen	3.46	2.47
Nitrogen and Oxygen (by difference)	10.03	2.90
Sulfur	1.01	0.88
Ash	7.20	10.45
Total	<u>100.00</u>	<u>100.00</u>
Proximate Analysis, wt %		
Moisture	1.7	0.7
Volatile Matter	17.3	5.7
Fixed Carbon	73.9	83.2
Ash	7.1	10.4
Total	<u>100.0</u>	<u>100.0</u>
Coal Type Source	Bituminous Coal Pittsburgh Seam Consolidation Coal Co. (Montour No. 4 Mine)	Lignite North Dakota Truax-Traer Co. (Velva Mine)
Particle Size, U.S. Standard Sieve	-16, +20	-16, +20
Ultimate Analysis, wt % (dry basis)		
Carbon	75.9	65.4
Hydrogen	5.01	4.49
Nitrogen and Oxygen (by difference)	8.99	23.21
Sulfur	1.54	0.45
Ash	8.56	6.45
Total	<u>100.00</u>	<u>100.00</u>
Proximate Analysis, wt %		
Moisture	1.1	6.8
Volatile Matter	33.5	41.2
Fixed Carbon	56.9	46.0
Ash	8.5	6.0
Total	<u>100.0</u>	<u>100.0</u>

With 50- and 20-gram samples of low-temperature bituminous coal char (-8, +16 sieve size) the maximum exit gas methane content was too high and the temperature changes during the run were too great to allow the assumption of differential reaction conditions. In tests with 10- and 5-gram samples of -16, +20 sieve size low-temperature bituminous coal char, the exit gas methane contents approached the desired levels, and reaction rates (expressed as pounds carbon converted to gaseous hydrocarbons per pound of carbon remaining in bed per hour) were similar.

With low-temperature bituminous coal char at nominal run temperatures of 1700°F., two periods of high rate were observed (Fig. 2). The second period of high rate, occurring after approximately 30% carbon gasification, was a result of increases in the temperature of the char sample due to the inability to dissipate the high heat of reaction to the surroundings. This was substantiated by conducting a further test with a 3-gram sample weight. Here only a slight increase in rate was obtained at carbon conversions above 30%. In tests with unpretreated coals, and with bituminous coal char at 1300°F. and 1500°F., no second period of high rate was observed.

It was also necessary to select a coal particle size for the remainder of the test program. An effect of particle size on the rate of reaction could indicate the presence of significant diffusional resistances. Tests were conducted with 10-gram samples of -16, +20 and -40, +50 sieve size material (Fig. 3). These test results indicate negligible effects of particle size on the reaction rate. The displacement of the rate curve for the -40, +50 sieve size material was probably due to the slower feeding rate of the more finely divided material, or to an initial holdup in the coal feed hopper. Based on duplicate tests to check reproducibility, it was believed that these small differences were within the limits of experimental and analytical accuracy.

From the results of these exploratory tests, the following base conditions were selected for the remainder of the tests, unless otherwise noted:

Temperature:	1700°F.
Pressure:	1500 p.s.i.g.
Sample weight:	5 and 10 grams
Coal particle size:	-16, +20 sieve size
Feed gas flow rate:	100 SCF per hour

Typical results for the four feeds used in this study are given in Table 2.

Effects of Variables

The effect of temperature and extent of conversion on the rate of reaction of low-temperature bituminous coal char and hydrogen was measured in a series of tests conducted at 1500 p.s.i.g. and at 1300°F., 1500°F. and 1700°F. (Fig. 4). During the initial phases, the reaction rate was not significantly affected by temperature in the range studied. Only after approximately 20% carbon gasification did the effects of temperature become apparent. The rate constants for the residual char would be expected to follow the pseudo-first-order relationship:

$$r = kp$$

where r = rate of reaction in pounds of carbon as methane equivalent per hour per pound of carbon in bed.
Methane equivalent includes carbon in all gaseous hydrocarbons produced.

k = rate constant.

p = hydrogen partial pressure in atmospheres.

This expression has been shown by Blackwood (2) to be applicable in the temperature range of 650° to 870°C. (1202° to 1598°F.) for the reaction of coconut char with excess hydrogen at pressures up to 40 atmospheres. Birch (1) has also applied it successfully to correlate data on the hydrogenation of the residual (aromatic) carbon portion of Australian brown coal with excess hydrogen in a fluid-bed reactor for the temperature range from 750° to 950°C. (1382° to 1742°F.). Zielke and Gorin (15) showed that, in the temperature range of 1500° to 1700°F. and at 1 to 30 atmospheres, with devolatilized Disco bituminous coal char the apparent reaction order is 2 at low pressures and approaches 1 at high pressures.

In Table 3, pseudo-first-order hydrogasification rate constants for these chars are compared with the values for low-temperature bituminous coal char after 25 to 30% carbon conversion (Fig. 4). Agreement is quite good, except for the acid-extracted, high-temperature coconut char. The rates for this specially-prepared low-reactivity material are up to one order of magnitude lower, as would be expected.

All of the above results were obtained in differential-bed reactors of various types, except for the data for Australian brown coal, which were obtained in an integral fluid-bed reactor. However, methane concentrations in the product gases were low enough to minimize equilibrium hindrance effects. The data for coconut char are based on the carbon initially present in the bed, but this is not significant in view of the low conversions.

Table 3.-COMPARISON OF RATE CONSTANTS OF VARIOUS INVESTIGATORS

<u>Investigator</u>	Blackwood (1,2)	Birch (1)	Zielke and Gorin (15)	This Study
<u>Coal</u>	High-Temperature Coconut Char	Brown Coal	Disco Bit. Coal Char	Low-Temp. Bit. Coal Char
<u>Conversion</u>	Less than 10% Char Conversion	More than 40% Carbon Conversion	0-30% Carbon Gasification	25-30% Carbon Gasification
<u>Temperature, °F.</u>	k, rate constant*			
1300	1×10^{-4}	6×10^{-4}	--	2×10^{-3}
1500	9×10^{-4}	4×10^{-3}	$6-2 \times 10^{-3}$	4×10^{-3}
1700	6×10^{-3}	2×10^{-2}	1×10^{-2}	3×10^{-2}

* For Birch, Zielke and Gorin and this study, k has units of lb. of C as CH₄ equiv./lb. C in bed-hr.-atm. H₂ part. press. For Blackwood, units are lb. of C as CH₄ equiv./lb. C fed-hr.-atm. H₂ part. press.

Fig. 5 further demonstrates the similarity in hydrogasification rate constants of the residual portion of coals and chars with greatly different initial properties. The rate constants during the high-rate period are roughly proportional to the volatile matter content of the feed, but at high conversion levels they approach one another. It can be seen that the results obtained with 5-gram samples of lignite and anthracite could not be closely duplicated with 10-gram samples, whereas with bituminous coal good agreement was obtained. The apparent rate constants with the larger samples were much higher for lignite and considerably lower for anthracite. This is not believed to be primarily due to lack of reproducibility.

The combined effect of changes in total and in hydrogen partial pressure at 1500° and 1700°F. is shown in Figs. 6 and 7. The separate effect, at 1700°F., of a decrease in hydrogen partial pressure from 1500 to 1000 p.s.i. by the addition of nitrogen, is shown in Fig. 8. These results apparently reflect that, during the initial high-rate period, both pyrolysis and hydrogenolysis occur. Increases in hydrogen partial pressure would increase the rate of hydrogenolysis compared to pyrolysis. Thus, an increase in total pressure tended to broaden the range of the initial high-rate period. An increase in hydrogen partial pressure at constant total pressure both broadened the rate curve, and increased its peak, during the initial high-rate period.

The true effect of hydrogen partial pressure during the highly exothermic residual char hydrogenolysis period was obscured at 1700°F. by the large temperature increases, depending on sample weight. However, it can still be observed qualitatively that increases in total pressure as well as in hydrogen partial pressure gave the expected increases in rate.

With devolatilized Disco bituminous coal char, Zielke and Gorin showed that the effect of methane partial pressure on hydrogasification rate is simple equilibrium hindrance (15). However, the results obtained with a partial pressure of 500 p.s.i. of nitrogen and with a partial pressure of 500 p.s.i. of methane were not significantly different during the initial high-rate period (Fig. 8). This indicates no substantial equilibrium hindrance effect during this period, in spite of the large reduction in driving force for the reaction $C + 2H_2 \rightarrow CH_4$, if a carbon activity of 1 is assumed. On that basis, the equilibrium methane partial pressure at 1700°F. and 1500 p.s.i. is only about 700 p.s.i. The absence of a hindrance effect at low conversions is further evidence of the much higher initial carbon activity. The effect of 500 p.s.i. methane partial pressure in the feed gas during the low-rate period could not be determined because the product gas methane concentration measurement was not accurate enough to obtain meaningful data.

Course of Coal-Hydrogen Reactions

The description by Birch and others (1) of the sequence of coal-hydrogen reactions, at sufficiently high temperatures, pressures and residence times to give methane as the major product, is in agreement with observed experimental results of this study. In somewhat modified form, this sequence is:

1. A high-rate period comprising pyrolysis of the more reactive structural units such as aliphatic hydrocarbon side chains and oxygenated functional groups, and hydrogenation and hydrogenolysis of the intermediate pyrolysis products.
2. A low-rate period of direct attack of hydrogen on the residual aromatic carbon structure.

Evidence for the two steps during the high-rate period can be found in the increase in organic liquid products formation with decreases in product gas residence time observed by Hiteshue and others (7) at relatively low reaction temperatures encountered during heatup. Absence of substantial organic liquid product yields would correspond to the completion of the vapor-phase hydrogenolysis reactions, which would then be the chemical rate-controlling step in methane formation during the initial high-rate period. Since, in this study, there was no major effect on the high-rate period from temperature changes in the 1300° to 1700°F. range at a pressure of 1500 p.s.i.g., a physical process may have been controlling under these conditions of extremely rapid hydrogenolysis.

Although no measurable liquid hydrocarbon formation occurred, even at 1300°F., as a result of rapid heatup of the coal charge, the presence of small amounts of C₂- to C₄-aliphatic hydrocarbons during the high-rate period indicates the initial formation of higher molecular weight intermediates which have been converted to methane by hydrogenolysis (12-14). In this case, ethane would have to be present in quantities exceeding the methane-ethane-hydrogen equilibrium values. In tests with bituminous coal char, ethane concentrations actually did exceed equilibrium values at the peak of the high-rate period (Fig. 9). The formation of small amounts of benzene during the high-rate period is further evidence of the similarity with hydrocarbon hydrogenolysis.

A better picture of the sequence of coal-hydrogen reactions under coal hydrogasification conditions can be obtained from the changes in hydrogen distribution with conversion of various feeds. The upper set of plots in Fig. 10 shows the ratio of total hydrogen in the exit gas to the total hydrogen in the feed gas for a series of tests conducted at 1700°F. and 1500 p.s.i.g.. The lower set of curves in Fig. 10 shows the changes in gaseous feed hydrogen consumption with conversion, for the same series of tests.

It can be seen that the initial high rate period is characterized by donation of hydrogen from the coals and char, as well as by large consumption of feed hydrogen, indicating the occurrence of both pyrolysis and hydrogenolysis reactions. The maximum feed hydrogen consumption tends to occur at higher carbon gasifications than the maximum hydrogen evolution, in accordance with the sequential nature of the pyrolysis and hydrogenolysis reactions. The rate of feed hydrogen consumption is an excellent indication of feed reactivity, except that with the low-temperature bituminous coal char, a second period of high consumption occurs as a result of uncontrollable temperature increases.

Lignite, because of its high oxygen content, donated relatively little hydrogen and consumed a disproportionately large amount of gaseous feed hydrogen. This is due to the large amount of water formation which can be readily measured in flow reactors, but could not be determined experimentally in the present work. It should be noted that, at the high hydrogen partial pressures used in this study, the only other major path for oxygen rejection is as carbon monoxide, since carbon dioxide formation is practically suppressed.

Steam-Hydrogen Coal Gasification

Much kinetic information on the reaction of steam-hydrogen mixtures and char exists for temperatures of 1500° to 1700°F. at hydrogen partial pressures below 30 atmospheres (3,5,6,16). The addition of steam was found to substantially increase the rate of methane formation at these low hydrogen partial pressures. Extrapolation to hydrogen partial pressures sufficiently high to give rates of methane formation which are of practical interest, indicates that the effect of steam becomes less significant. In the present study, the rates of the steam-char and hydrogen-char reactions with an equimolar steam-hydrogen mixture were measured at 1700°F. and 1500 p.s.i.g. The rates of these two reactions (measured by the rates of evolution of gaseous carbon oxides and gaseous hydrocarbons) are shown in Fig. 11 as functions of total carbon gasification. The results of the two tests conducted with 5- and 10-gram sample weights are in good agreement, and the second high-rate period, characteristic of the char-hydrogen tests at 1700°F., is absent. This is probably due to smaller temperature changes, with both exothermic hydrogenation reactions and endothermic steam-carbon reactions occurring simultaneously.

Unlike much of the earlier work at relatively low hydrogen partial pressure, the char-hydrogen reaction proceeded much more rapidly than the char-steam reaction, especially at the higher conversions. However, from comparison with Figs. 7 and 8, the rate of char conversion to gaseous hydrocarbons was below the level expected for a feed gas hydrogen partial pressure of 750 p.s.i. Thus, the relatively high rates of

carbon oxide formation at low conversion levels may have been largely due to steam reforming, catalyzed by the reactor walls, of a portion of the gaseous hydrocarbons produced. However, even if the total gasification rate is considered in a comparison with char-hydrogen results, there is no indication of the acceleration of methane formation by steam addition which has been observed at lower hydrogen partial pressures.

The rate of the steam-char reaction with an equimolar steam-helium mixture at 1700°F. and 1500 p.s.i.g., shown in Fig. 12, was much higher than in the previous test with a steam-hydrogen feed at equal steam partial pressure. This is the result of the well-established inhibition of the steam-carbon reactions by hydrogen (6). Substantial quantities of gaseous hydrocarbons were also formed initially, probably largely by pyrolysis rather than by reaction of char with hydrogen formed in steam decomposition, or direct reaction of steam and char. This is supported by the fact that more hydrogen was produced than could be accounted for by carbon oxide-forming reactions.

CONCLUSIONS

Gasification of various coals with hydrogen and added steam at high temperatures and pressures, under conditions of very rapid coal heatup and product gas residence time of only a few seconds, has confirmed the generally accepted model derived from data without as detailed a definition of the critical initial stages of conversion. During this initial period, gasification rates are very rapid and the course of the methane-forming reactions is similar to that in hydrogenolysis of hydrocarbons. However, the reactivity of the pyrolysis intermediates formed during the high-rate period appears to be much greater than that of typical petroleum hydrocarbons since no measureable liquid products were obtained at temperatures as low as 1300°F., and methane was the predominant product. Materials as different as lignite, bituminous coal, anthracite and low-temperature bituminous coal behaved similarly, except that initial conversion rates increased roughly in proportion to their volatile matter content, and hydrogen consumption and carbon oxide formation was affected by oxygen content. However, the conversion rates of the relatively unreactive residues were approximately the same. At the high hydrogen partial pressures employed in this study, steam addition did not accelerate methane formation as observed in previous studies at relatively low hydrogen partial pressures. The inhibiting effect of hydrogen, on reactions with steam which form carbon oxides, was observed for the initial high-rate period, as well as during the conversion of the residual char.

ACKNOWLEDGMENT

This work was conducted under the sponsorship of the Research Department of the Consolidated Natural Gas System (now Con-Gas Service Corporation) under the guidance of F. E. Vandaveer and H. E. Benson. Thanks are due to E. B. Shultz, Jr., who designed most of the apparatus and helped develop the experimental procedure. A. E. Richter and R. F. Johnson assisted in data collection and D. M. Mason and J. E. Neuzil supervised the analytical work.

REFERENCES CITED

1. Birch, T. J., Hall, K. R., Urie, R. W., J. Inst. Fuel 33, 422-35 (1960).
2. Blackwood, J. D., Australian J. Chem. 12, 14-28 (1959).
3. Blackwood, J. D., McGrory, F., Australian J. Chem. 11, 16-33 (1958).
4. Channabasappa, K. C., Linden, H. R., Ind. Eng. Chem. 48, 900-5 (1956).
5. Goring, G. E., Curran, G. P., Tarbox, R. P., Gorin, E., Ind. Eng. Chem. 44, 1051-65 (1952).
6. Goring, G. E., Curran, G. P., Zielke, C. W., Gorin, E., Ind. Eng. Chem. 45, 2586-91 (1953).
7. Hiteshue, R. W., Anderson, R. B., Friedman, S., Ind. Eng. Chem. 52, 577-9 (1960).
8. Hiteshue, R. W., Anderson, R. B., Schlesinger, M. D., Ind. Eng. Chem. 49, 2008-10 (1957).
9. Hiteshue, R. W., Lewis, P. S., Friedman, S., Paper CEP-60-9, Operating Section, American Gas Association, 1960.
10. Pyrcioch, E. J., Linden, H. R., Ind. Eng. Chem. 52, 590-4 (1960).
11. Shultz, E. B., Jr., Feldkirchner, H. L., Pyrcioch, E. J., Chem. Eng. Progr. Symposium Ser. 57, No. 34, 73-80 (1961).
12. Shultz, E. B., Jr., Linden, H. R., Ind. Eng. Chem. 49, 2011-16 (1957).
13. Shultz, E. B., Jr., Linden, H. R., I and EC Process Design and Development 1, 111-6 (1962).
14. Shultz, E. B., Jr., Mechaes, N., Linden, H. R., Ind. Eng. Chem. 52, 580-3 (1960).
15. Zielke, C. W., Gorin, E., Ind. Eng. Chem. 47, 820-5 (1955).
16. Zielke, C. W., Gorin, E., Ind. Eng. Chem. 49, 396-403 (1957).

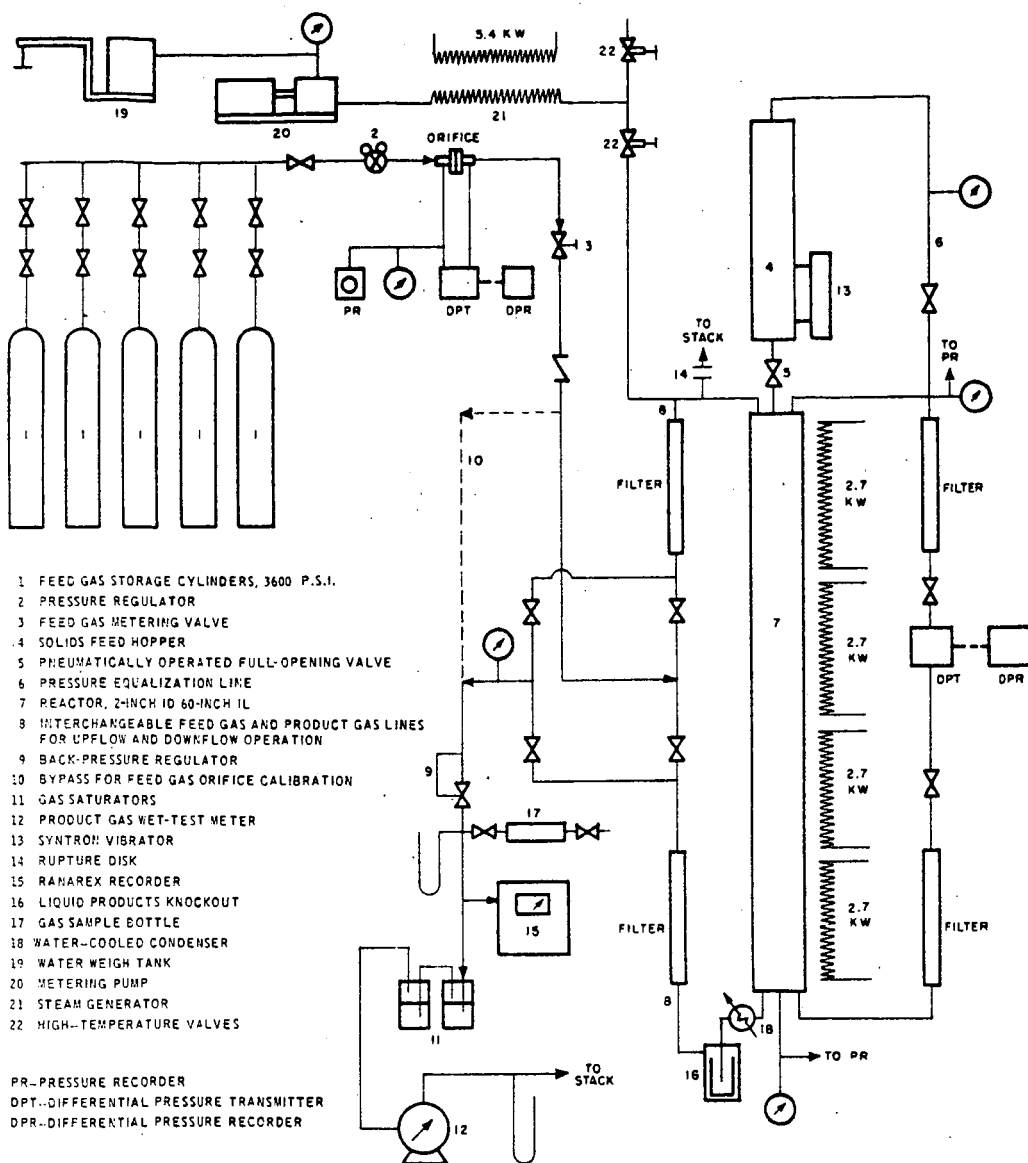


Fig. 1. Semiflow reactor system for study of rates of hydrogasification of solid fossil fuels at temperatures to 1700° F. and pressures to 3000 p.s.i.g.

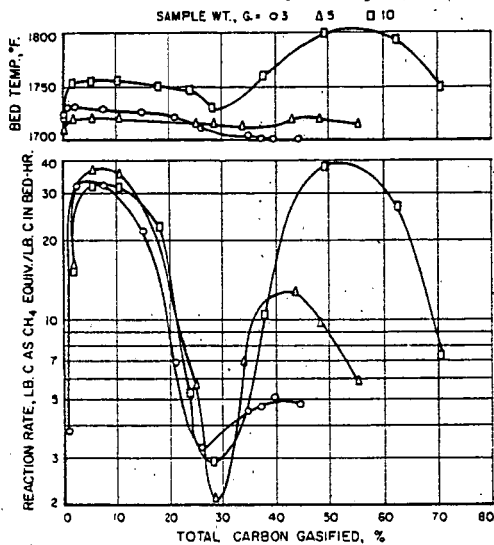


Fig. 2.-Apparent effect of sample weight on rate of char hydrogasification at 1700° F. and 1500 p.s.i.g.

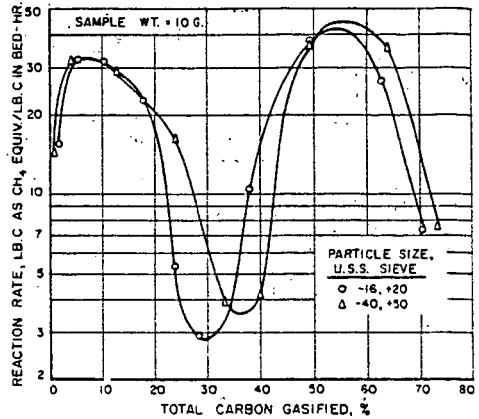
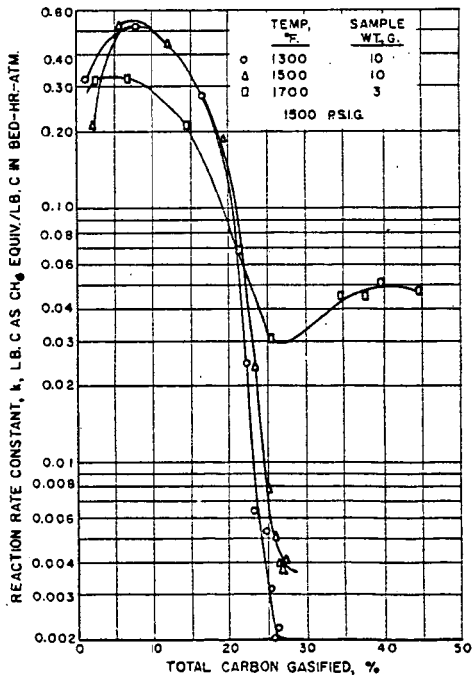


Fig. 3.-Effect of char particle size on rate of hydrogasification at 1700° F. and 1500 p.s.i.g.

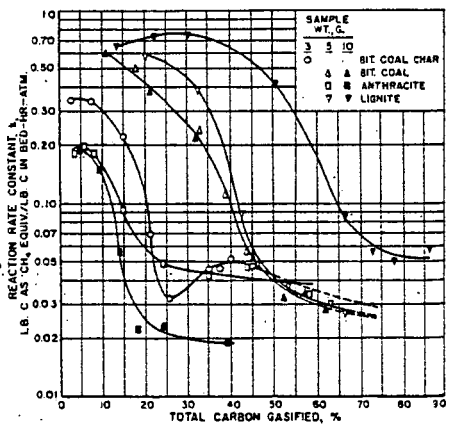


Fig. 5.-Reaction rate constants for various feeds at 1700° F. and 1500 p.s.i.g.

Fig. 4.-Effect of temperature and conversion on reaction rate constant for bituminous coal char

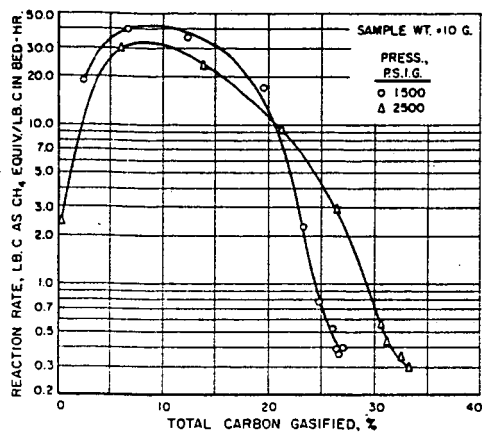


Fig. 6.-Effect of pressure on rate of char hydrogasification at 1500° F.

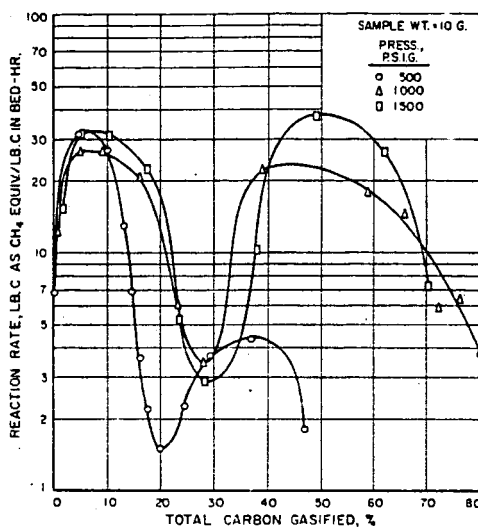


Fig. 7.-Effect of pressure on rate of char hydrogasification at 1700° F.

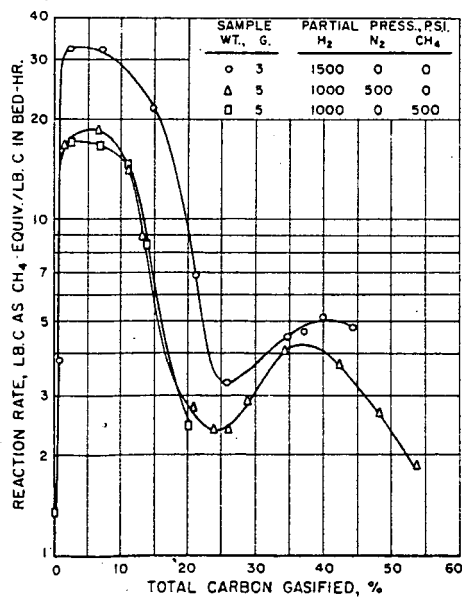


Fig. 8.-Effect of hydrogen and methane partial pressure on rate of char hydrogasification at 1700° F. and a total pressure of 1500 p.s.i.g.

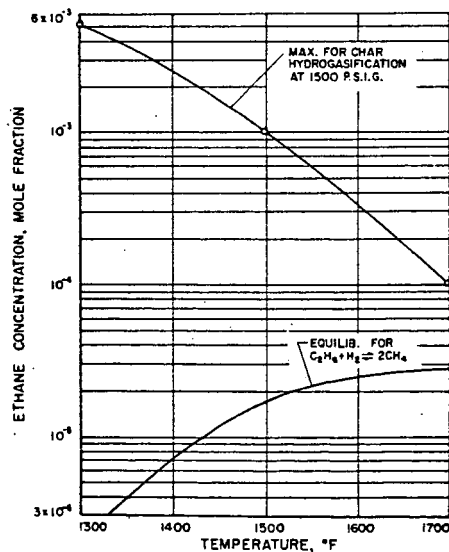


Fig. 9.-Approach of ethane concentrations to equilibrium values as a function of temperature

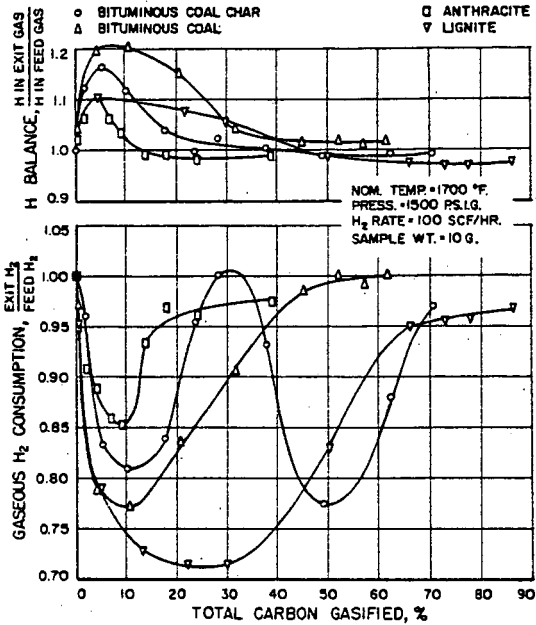


Fig. 10.-Gaseous hydrogen balances as a function of conversion of various feeds.

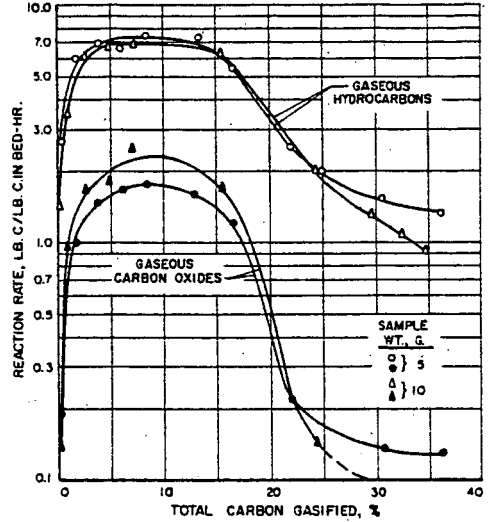


Fig. 11.-Effect of conversion on rate of gasification of coal char at 1700 °F. and 1500 p.s.i.g. with an equimolal steam-hydrogen mixture

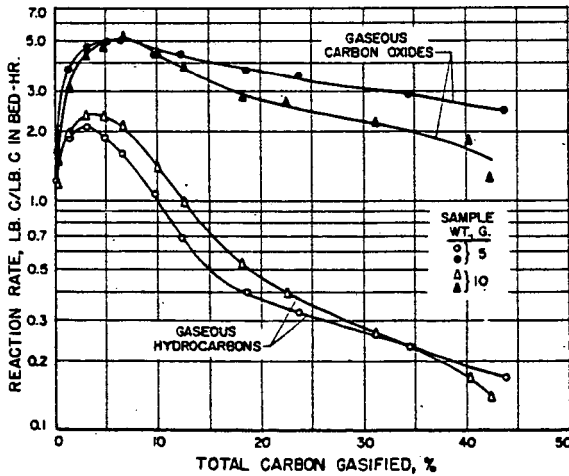


Fig. 12.-Effect of conversion on rate of gasification of coal char at 1700 °F. and 1500 p.s.i.g. with an equimolal steam-helium mixture.

THE REACTIVITIES OF SUSPENSIONS OF COALS
IN STEAM AT 900 - 950° C. (1,700° F.)

John J. S. Sebastian and Robert L. Day

Morgantown Coal Research Center, Bureau of Mines,
U. S. Department of the Interior, Morgantown, W. Va.

Investigators generally agree that the reaction of steam with various types of carbon and cokes, which has been widely investigated at the Morgantown Coal Research Center of the Bureau of Mines (5) and elsewhere, (3) (7) (8) (9) (10) (14) (15) (16) (18) is related to the reaction of steam with coal. Despite this relationship, knowledge of the kinetics of the steam-carbon reaction does not disclose nor reveal the kinetic behavior of coals of various rank and type in coal gasifiers. The conclusions drawn from studies of the reactivities of various types of carbon furnish little or no information on process rates, which can be used in the design of improved types of commercial coal gasification equipment.

Several investigators (2) (11) (12) (13) studied the kinetics of the reactions of coals, generally with air, oxygen or carbon dioxide, but restricted their research to relatively low temperatures, specific types of coals, fixed beds of coarse particles, etc. Others tried to fit theoretical rate equations to data from large-scale gasifiers, modifying their constants accordingly. Attempts to extrapolate these results to other types of coals suspended or entrained in steam at considerably higher temperatures and pressures (4) have never proved satisfactory and, in many cases, have failed. It is doubtful that a generally applicable rate equation can be established for substances as complex structurally and as widely different in composition as coals of various rank, type or grade. Generalization for all types of coals, cokes or chars, or the use of questionable assumptions to extend the applicability of a rate equation to all gasification conditions does not seem justified.

A "falling particle" technique has been developed by Dotson and Holden (5) of the Bureau of Mines at Morgantown, W. Va., for the determination of the reaction rates of carbons with steam. The method originally devised for finely divided carbons was recently modified by the authors and developed for the rapid determination of the reactivities of coals. The essential feature of the method is that it closely simulates the conditions existing when powdered coals entrained in steam are gasified in large-scale gasifiers.

The purpose of the work here described was to determine the "relative reactivities" of various types of coals when their particles react with steam at 1,700° F. Specifically, the object was to separate the overlapping effects of thermal decomposition and actual steam-carbon reaction when steam interacts with coals at high temperatures.

"Reactivity" of solid fuels is generally defined (7) as the velocity or time-rate of the reaction between a solid fuel and an oxidizing gas, usually O_2 , CO_2 , or H_2O , under a given set of experimental conditions, including temperature, pressure (4), particle size, size consist, and bulk density. "Relative reactivity" is defined here as the relative rapidity of reaction between a fuel and an oxidizing gas (steam in our case) in a given apparatus under the same set of experimental conditions. It is an experimentally obtained index figure, useful in comparison with other fuels. Pertaining to an average (measured) residence time, the term "relative reactivity"

signifies no more than what the name implies: reactivities of various fuels related to each other. It should not be confused with "kinetic reaction rate."

The term "kinetic reaction rate" is a more fundamental characteristic of a given fuel reacting with a given gas; it is independent of the gasifier design, and is usually more significant from a process engineering standpoint. However, its determination is more time consuming. The kinetic reaction rate usually expresses, in form of a rate equation, the functional relation between reaction rate and reactant concentration at any given temperature and pressure. For maximum usefulness from a design standpoint, full knowledge of the kinetic rate includes the effects of all variables on the reaction rate, particularly temperature and pressure (4) (17), and the physical state of the reactants, such as particle size, size consist, and bulk density. The effects of mass transfer rate and flow pattern, insofar as they affect the overall reaction rate, should also be known.

Although work is being planned on the determination of the kinetic rates of the reaction of steam with coals at higher temperatures and pressures, this paper is restricted to the study of the more rapidly determined relative reactivities of coals (-60 + 65 mesh) interacting with steam at 1,700° F. and atmospheric pressure. The reactivities are expressed in terms of (1) "fuel conversion," given as weight-loss in grams per gram of dry, mineral matter - free coal; or (2) "carbon conversion," shown as grams of carbon gasified per gram of carbon in the coal. In either case, the conversion of the coal to gas is due both to thermal decomposition and reaction with steam.

Apparatus and Experimental Technique

The reactor developed and used to determine the relative reactivities of coals by the falling particle technique is shown schematically in Figure 1. The 3-inch inside diameter 9-foot long alloy steel reactor tube is electrically heated by 9 (pairs) prefabricated semicircular embedded-coil-type heating elements 11.5 inches high and 5 inches outside diameter, each controlled by a variable transformer. Elements at the top and bottom serve to balance the heat losses; the other 7 elements control the temperature in the 85-inch long isothermal zone. Longitudinal temperature profiles or traverses are determined from time to time, and the heat input is adjusted to maintain isothermal conditions.

Doubly distilled water passing through a rotameter is vaporized in a small electrically heated tube, and the steam thus formed is preheated to 800 - 1,000° F. before injection into the reactor. The steam flow-rate is adjusted for the desired steam-to-coal ratio, generally 3 pounds of steam per pound of dry mineral matter - free fuel, and the vibratory feeder is started. The uniformly sized (-60 + 65 mesh per inch) coal particles in the feed bowl move upward along a spiral track until each particle is swept by nitrogen, flowing at a rate of about 1.2 std. cu. ft. per hour, through a hole into the feed-tube and thence into the reactor. The coal feed-rate, generally 50 g. per hour in the reactivity tests described, is controlled by adjusting the voltage input to the vibrating mechanism.

The coal particles, blanketed by nitrogen, fall through a 7-inch long 5/16-inch inside diameter feed-tube, the latter surrounded by a 5/16-inch wide annulus (not shown in Figure 1) through which the steam is passed downward at about 1,000° F. The coal particles thus preheated in the feed-tube are entrained in the steam and enter the top of the reactor-tube through a 1-inch inside diameter circular opening at its center. The entering particles together with steam and nitrogen spread somewhat, but direct contact with the wall is prevented as they are carried downward in laminar flow (conventional Reynolds number about 20) blanketed with gases. Accelerated by gravity, they continue to fall through the steam, nitrogen, and generated gases, virtually at free-falling velocity. Calculated for a reactor temperature of 1,700° F. (900 - 950° C.) and for a low-volatile bituminous coal fed at 50 grams per hour, with

a steam-to-coal ratio of 3:1, the linear velocity of the steam-nitrogen mixture in the upper part of the reactor was 0.19 ft. per sec. As the measured average terminal velocity of the coal particles was 1.33 ft. per sec., the difference is their free-falling velocity: 1.14 ft. per sec.

Since the coal particles travel 6 times faster than the entraining steam-nitrogen mixture, it is clear that the fuel particles fall in the reactor tube almost freely through the gases. The flow, therefore, is not so much of the entrainment type, but is rather an unsteady or partial suspension, and the term "falling particle technique" properly describes it. (An isotope tracer method used to determine the residence time of the fuel particles, and thus their terminal velocity, will be described in another paper to be published by the authors.) Laminar flow inside the reactor prevents direct contact between the particles and the heated reactor tube. Nevertheless, because of the small heat capacity of the fuel particles, and the effective transfer of heat --- partly by radiation from the reactor walls and partly by convection and conduction through the steam medium --- the falling particles are rapidly heated to the isothermal reactor temperature of 1,700° F.

The concentration of fuel particles in the upper part of the reactor, under the conditions stated, is estimated to be about 50 mg per dm³ of reactor volume containing a gas mixture of 85 percent steam and 15 percent nitrogen. On an average, approximately 8 1/2 particles of -60 + 65 mesh coal are in partial entrainment (suspension) at any given time in each cm³ of steam-nitrogen mixture flowing at a rate of 265 cc. per sec. (33.9 cu. ft. per hour) in the upper part of the reactor at 1,700° F. The average distance between the suspended particles, if they are assumed to be spherical and have an average diameter of about 0.21 mm., is approximately 6 mm. The latter value thus estimated is analogous to the term "mean free path," although used here in a different sense.

As shown in Figure 1, the residue and product gas recovery system is at the bottom of the reactor tube. The solid residual is collected in a receiver bottle, and is cooled, weighed and analyzed. Most of the excess steam and some fine soot collects in the condensate receiver; the rest of the soot is removed from the gas by means of a wash bottle. Traces of tar vapors in the product gas are caught on filter papers in a Buchner funnel, and the gas is metered, sampled, and vented.

A photograph of the apparatus is shown in Figure 2. Next to the control board in the foreground, the insulated reactor tube is seen with the product recovery train below it. The fuel-feeding and steam-generating systems are located on the upper platform partly visible at the top of the picture.

As the reactivity of powdered or granular fuel is affected by the size of the particles, it was necessary to investigate possible degradation of particles as they fall through the reactor-tube. Do the solid fuel particles abrade each other and, if so, is this size reduction balanced, in case of bituminous coals, by swelling of the particles when they pass through the plastic stage, usually between 700° F. and 1,000° F.? To answer these questions, the apparent (or bulk) specific volumes of two different coals and a char were determined, before and after a single passage through the reactor under the usual conditions at 1,700° F. Specific volumes were determined by filling a 10-cc. graduated cylinder with the particles, uniformly tapping, and then weighing the contents. The results are shown in Figures 3 and 4 with the apparent (bulk) specific volume in each case given below the photomicrograph of the sample. The specific volume data shown on these pictures are helpful in this evaluation since any increase in the apparent (bulk) specific volume or, conversely, decrease in bulk density may be due to (1) formation of fines (degradation), and/or (2) swelling of each particle with corresponding increase in porosity.

In addition to the microscopic examinations, the extent of degradation in fall was determined by drop-testing samples (-60 + 65 mesh per inch size) through the reactor-tube, in still air, at room temperature. A Wyoming high-volatile bituminous-C

coal (Serial No. 16) and a char, made by low-temperature carbonization from a Colorado bituminous-A coal, (Serial No. 7), were so tested for size degradation. In each case the procedure was identical: 100 grams of the sample was dropped 123 inches at a rate of 72 grams per hour (1.2 g. per min.), and the product was screened through a 65-mesh per inch standard screen, uniformly shaking and tapping it in each case. The results were negative. In both cases the size degradation was small, although the char was somewhat more resistant to breakage than the coal. The breakage index, which is the percent retained on the 65-mesh screen before the drop-test minus that retained after the drop-test, was 1.7 percent for the coal and 0.2 percent for the char. The time of fall during the drop-tests, determined visually, was 4.4 seconds for the coal and 3.5 seconds for the char.

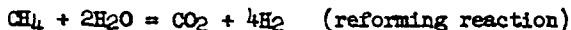
These results confirm what is evident from Figures 3 and 4: any size degradation from attrition of the particles by themselves and by the reactor wall is negligible and is well within the expected experimental error. Even this slight size reduction is more than balanced in the case of bituminous coals by the swelling of the particles as they pass through the plastic stage. There is plenty of evidence of swelling and formation of hollow spheres, as shown by the photomicrographs in Figures 3 and 4, as well as by the considerable increase in bulk specific volumes.

Experimental Fundamentals

Tests to determine the relative reactivities of coals were carried out under as nearly identical conditions as possible, thus maintaining at all times the major operating variables as constant as practicable. The most essential variables affecting the reactivities of powdered coals are: (1) type and size of test-reactor; (2) type, chemical composition and microstructure (porosity) of the coal; (3) particle size of the coal, its size consist and density; (4) coal throughput; (5) steam input rate (or steam-to-coal weight-ratio); (6) residence (or contact) time; (7) temperature; and (8) pressure. In developing a rapid practical method for testing coals for reactivity, the objective was to establish the correct magnitude for these variables in order to obtain measurable, but not excessive, fuel and carbon conversions.

An important variable in need of study was the required steam-to-coal ratio. The results of this study are illustrated in Figures 5 and 6. Figure 5 shows the effect of steam concentration (in terms of steam-to-carbon weight-ratios) on the components of the gases evolved. The yields of gases are seen to increase with increasing steam-to-carbon ratios, but most of the increase in the total gas yield was due to the rising trend in hydrogen evolution. This interesting fact points to a possible interaction of steam with hydrocarbon groups and other radicals attached to the coal molecule, and it appears that the interaction increases with the steam concentration. Although the diagram in Figure 5 refers to a low-volatile bituminous coal, yield curves showing identical trends were obtained with high-volatile bituminous coals.

The interaction of steam appears to facilitate thermal decomposition at a lower temperature, causing the detachment of alkyl groups and other radicals from carbon atoms in the coal matrix. This may result in the formation of "defect sites," probably with an electron lost or removed from the carbon atom from which a radical (possibly in ionic state) was detached. The existence of such defect sites owing to electron absences (or "positive holes") has been recognized by Gray (6) and his co-workers. The methane, ethane, other paraffin hydrocarbons, carbon monoxide, etc., thus entering the gas phase may react with additional steam to form CO_2 and H_2 . For example:



and



This is a plausible explanation of the hydrogen evolution (Figure 5) accompanying the interaction of steam with the coal molecule. There is plenty of evidence that steam thus interacts with coal both in carbonization and gasification, i.e., whenever thermal decomposition of coal takes place in the presence of steam (14). The defect carbon sites, often called "reaction sites" or "active sites," thus formed are vulnerable to attack by steam:



The importance of steam-to-carbon ratio thus established, experiments were made to determine its effect on the reactivity, measured as fuel or carbon conversion. Figure 6 shows that for both high and low volatile coals the reactivity rises asymptotically up to a ratio of about 3:1. Above this ratio, additional steam does not significantly increase the carbon conversion, i.e., a maximum has been reached. A ratio of 3:1 was thus chosen, as too much excess steam would increase the flow-rate, thereby decreasing the contact time below the limit of effective conversion needed for most of the reactivity tests.

Similarly, accurately measurable conversion was the criterion used in determining or choosing the optimum values of other essential variables. Thus, all of the tests were made with coals closely sized to pass a 60-mesh per inch U. S. standard sieve but retained on a 65-mesh sieve. The coal-feed rate was fixed at about 50 grams per hour and kept as constant as possible throughout each test. The temperature was kept uniform throughout the 83-inch long isothermal zone between 1,650 and 1,750° F., the maximum variation being $\pm 25^\circ$ F. The average residence time of the coal particles in the isothermal zone ranged from 5.2 seconds for subbituminous and low or high-volatile bituminous coals to 6.6 seconds for anthracites. (The determination of these values by an isotope-tracer method will be discussed by the authors in a future paper.)

The optimum values for the variables, thus determined, were kept as constant as possible so that the results of the reactivity tests depended only on the type, composition, and microstructure of the coal tested.

Materials Tested

Descriptions of the types of fuels tested for their reactivities are given in Table 1. The coals are presented in the order of increasing rank, ranging from lignites to anthracites. Also included in Table 1 are several types of chars derived by low-temperature carbonization from the specific types of coals shown in the table. Although the reactivities of these chars were determined in the same apparatus by the same technique described above for coals, the objective of the work with chars was sufficiently different to merit separate discussion in a future paper.

Proximate and ultimate analyses of the fuels tested are shown in Table 2 on a dry, "mineral matter - free" basis. Included in this table are in each case the percent mineral matter, calculated in conformity with ASTM standards (1) and the C/H ratio. Use of the "mineral matter - free basis" resulted in a much better alignment of data along the curves shown in various diagrams representing the functional relation between reactivity and various coal constituents or ratios.

Results and Discussion

Usually two, but in some cases up to five, reactivity tests were made on each of the 12 types of coals listed in Tables 1 and 2. The test results for each batch of coal were averaged and plotted on the following diagrams.

All of the reactivity test data (including data on several chars produced by low-temperature carbonization at the Bureau of Mines Denver Coal Research Center from

some of the coals investigated) are shown in Figure 7. This diagram illustrates the relative reactivities, in terms of fuel conversion, of coals of various rank (geological age) and their corresponding chars (connected with broken lines and arrows), as a function of steam concentration. Expressed on dry, mineral matter - free basis, coals of the same rank fall approximately along straight lines, each line indicating a given reactivity level. Most of the lines tend to be horizontal or slightly upward sloping and are usually parallel. The deviations in slopes, however, may not be significant owing to experimental errors in analyses or sampling. Actually, they should slope slightly upward, as in Figure 6, although for the shorter range of steam-to-coal weight-ratios, 2.2 to 3.5 shown in Figure 7, the upward trend is not as noticeable.

In general, it may be concluded that the reactivities of coals are inversely proportional to their rank or geological age. From this it follows that the reactivity is a function of the chemical composition and microstructure (porosity, density, etc.) of the coal as these, in turn, depended on the type of vegetation and geologic factors that existed when the coal beds were formed in various prehistoric ages. Since coals of various rank characteristically differ in volatile matter --- the ASTM (1) classifies them into ranks largely on the basis of volatile matter (on mineral matter - free basis) and calorific value --- it is evident that the reactivity must be related to the volatile matter as determined by the standard ASTM test. However, volatile matter and gas yield measured in reactivity tests are related terms, although by no means are they identical. The volatile matter test is intended to duplicate, to some extent, coke oven conditions in small-scale carbonization in a crucible at 950° C. (1,740° F.); the reactivity test is a combination of carbonization and gasification in steam medium at about 1,700° F. The gas yield, therefore, does not include the water formed as a result of carbonization, but it does include the product gases resulting from the steam-carbon reaction (CO , CO_2 , and H_2) to the extent that this reaction takes place at 1,700° F. When fuel conversion is plotted versus volatile matter (Figure 8) and against gas yield (Figure 9), similar S-curves result, but the latter curve is much steeper. The significance of this difference is subject to further interpretation with additional experimental evidence on hand.

Thus, as has been claimed by several investigators (13), the reactivities of coals of various rank and type are functions of the volatile matter as determined by the standard ASTM test. Yet, the functional relation is not linear, as claimed in the past with considerable deviations admitted, but a mild-sweep S-curve, as shown in Figure 8.

While volatile matter has served for some time as an approximate, although auxiliary, index of rank, the results of this investigation show that the total carbon content and C/H ratio are more sensitive indicators of the ranks of coals. In plotting the reactivity against the carbon in coals, it was found that both the fuel and carbon conversions are cubic parabolic functions of the total carbon content. When plotted on mineral matter - free basis, not a straight line but a well-defined S-curve is obtained (see Figure 10). The reactivity decreases with increasing carbon content, very rapidly in case of younger coals, much more slowly with h.v. bituminous coals, and rapidly again in case of l.v. bituminous coals and anthracites.

On the other hand, the reactivities of coals, expressed in terms of either fuel or carbon conversion, are nearly perfect hyperbolic functions of the carbon-to-hydrogen weight-ratio (C/H), as shown in Figure 11. This appears to be significant both from the standpoint of fuel classification and process engineering, i.e., selection of coals for effective gasification. The C/H ratio appears to be an excellent indicator of rank, and may also be an indicator of the quality of synthesis gas, or that of high-B.t.u. gas or liquid fuel that can be produced by gasification and subsequent synthesis. In spite of this, it is not suggested that either the volatile matter, or total carbon content, or C/H ratio could be used as the sole index of rank.

An entirely different method of plotting the reactivity data is presented in Figures 12 and 13. The purpose of these diagrams was to determine the extent of the

reactivity, in terms of fuel conversion, caused by (1) thermal decomposition (devolatilization) and (2) the actual steam-carbon reaction. The effects of these two factors overlap in the reactivity tests described. We can say with considerable certainty that each particle of coal thermally decomposes with the evolution of volatile matter as its temperature rises to 1,700° F. The steam thereupon reacts with carbon atoms deprived of hydrocarbon, hydroxyl, carboxyl, and other side chains, i.e., it reacts with the so-called "fixed carbon." As the volatile matter evolved in thermal decomposition consists of much volatile carbon (in the form of CH₄, CO₂, CO, etc.), the fixed carbon remaining is always numerically less than the total carbon in the coal. Thus, if we deduct the percent of volatile matter (i.e., grams of coal converted to gas per 100 gram sample), as determined by the ASTM test at 1,740° F. (950° C.), from the fuel conversion (in terms of grams of coal converted to gas per 100 gram sample) at about 1,700° F., the difference will be the percent fixed carbon that reacted with steam to form CO, CO₂, and H₂. The two temperatures, 1,740° F. and 1,700° F. are sufficiently close to permit the approximation.

An interesting observation can be made and conclusion drawn by examining closer the diagram in Figure 12 on the reactivity of fixed carbon in relation to the total carbon content of coals of various rank. It shows that the actual steam-carbon reaction generally decreases with increasing order of rank from lignites to anthracites. However, a similar plot of conversion by the steam-carbon reaction alone versus the fixed carbon content (Figure 13) shows more clearly than the previous diagram that the rapidly descending curve tends to become asymptotic beyond 65 percent fixed carbon on dry mineral matter - free basis. In other words, steam at 1,700° F. reacts with carbon in younger coals with surprising ease, but less and less easily with carbon in older coals of increasing rank, while the carbon in coals from h.v. bituminous rank to anthracites is nearly equally reactive.

The conclusion drawn is significant, yet understandable in light of the explanation given above under Experimental Fundamentals. Lignites and other young coals have many more alkyl side chains and several other radicals attached to the benzenoid coal matrix than older bituminous coals, and still less in anthracites. When these radicals crack off the carbon atoms as a result of the interaction of steam, the "defect" sites remaining are vulnerable to attack by H₂O molecules, which explains the decreasingly lower reactivities of coals from lignites to anthracites.

Acknowledgments

The authors wish to acknowledge the helpful suggestions of the following Bureau of Mines personnel: Harry Perry, Dr. H. H. Lowry, and Dr. L. L. Hirst.

Table 1

DESCRIPTION OF TYPES OF FUELS TESTED FOR THEIR REACTIVITIES

Serial No. ^{1/}	Rank of coal *Type of char	Name of bed	Mine	Locality
		Description of carbonization conditions		
1	Young Lignite			Sandow, Texas
2*	Char made from Texas lignite (Serial No. 1)	Carbonized at 930° F. with an air-to-coal ratio of 3.73 std.cu.ft/lb. maf coal.		
10	Older lignite	Healy	Reynolds	Lake de Smet Area, Buffalo, Johnson County, Wyoming
12*	Char made from Lake de Smet lignite (Serial No. 10)	Carbonized at 930° F. with an air-to-coal ratio of 4.01 std.cu.ft/lb. maf coal.		
3	Subbituminous-B coal	Adaville No. 1	Elkol Kemmerer Coal Co.	Hams Fork Region, Frontier, Wyo.
16	High-volatile coal bituminous-C	No. 7 Seam	D. O. Clark	Superior, Wyoming
11	High-volatile coal bituminous-C	Rock Springs No. 3	Sweetwater No. 2	Green River Area, Wyoming
4	High-volatile coal bituminous-A	Pittsburgh	Pittfair	Shinnston, W. Va.
5	High-volatile coal bituminous-A	Sewickley	Bunker	Monongalia County, West Virginia
6	High-volatile coal bituminous-A	East Allen	East Allen	Garfield County, Colorado
7*	Char made from Colo. bituminous-A coal (Serial No. 6)	Carbonized at 1,200° F. with an air-to-coal ratio of 13.9 std.cu.ft/lb. maf coal.		
13*	Char made from Colo. bituminous-A coal (Serial No. 6)	Carbonized at 1,200° F. with an air-to-coal ratio of 6.9 std.cu.ft/lb. maf coal.		
15	Medium-volatile bituminous coal	Sewell	Wyoming	Wyoming, West Virginia
8	Low-volatile coal semibituminous	Pocahontas No. 4	Island Creek Coal Co.	McDowell County, West Virginia
9	Anthracite		Penn. & Reading Coal and Iron Co.	Locust Summit, Pennsylvania
14	Anthracite		Underkoffers	Iykens, Dauphin County, Penna.

^{1/} The serial numbers shown identify the type of fuel tested in subsequent tabulations and diagrams. All coals are shown in the order of increasing rank. An asterisk next to the serial number signifies char. See the corresponding heading above for coals and chars, respectively.

Table 2

ANALYSES OF FUELS TESTED

Serial No. 1/	Type of fuel	Mineral matter in fuel, percent	Components, percent mineral matter-free basis				C/H Ratio			
			V.M.	F.C.	C	H				
1	Young Texas lignite	15.7	48.8	51.2	72.9	5.5	18.6	1.4	1.6	13.3
2*	Char made at 930° F.; air-to-coal ratio: 3.72/	20.8	32.5	67.5	77.0	5.8	16.2	1.7	1.3	20.3
10	Older Wyoming lignite	20.0	46.4	53.6	71.7	4.8	22.1	1.0	.4	14.9
12*	Char made at 930° F.; air-to-coal ratio: 4.02/	26.8	29.9	70.1	78.1	3.4	16.2	1.2	1.1	23.0
3A	Wyo. subbituminous-B coal, Adaville No. 1 bed	3.4	42.2	57.8	74.2	5.0	18.8	1.3	.7	14.8
B		3.1	42.5	57.5	73.2	5.2	19.9	1.2	.5	14.1
16	Wyo. high vol. bituminous-C coal, No. 7 bed	3.8	40.4	59.6	78.3	5.3	14.2	1.3	.9	14.7
11	Wyo. high vol. bituminous-C coal, Rock Springs, No. 3 bed	12.1	32.2	67.8	82.8	5.5	9.1	1.8	.8	15.1
4	W. Va. high v. bituminous-A coal, Pittsburgh bed	11.3	38.2	61.8	81.7	5.9	7.2	1.6	3.6	13.9
5	W. Va. high v. bituminous-A coal, Sewickley bed	15.6	39.9	60.1	82.3	5.9	8.0	1.6	2.2	14.0
6	Colo. high v. bituminous-A coal, East Allen bed	24.0	37.3	62.7	83.7	6.2	7.9	1.7	.5	13.5
7*	Char made at 1,200° F.; air-to-coal ratio: 13.92/	49.2	5.1	94.9	82.5	2.7	12.3	1.2	.6	30.6
13*	Char made at 1,200° F.; air-to-coal ratio: 6.92/	31.3	5.7	94.3	92.2	2.0	3.2	1.7	.9	46.1
15	W. Va. medium vol. bituminous coal, Sewell bed	2.8	20.7	79.3	89.5	4.7	3.5	1.6	.7	18.9
8A	W. Va. low vol. semibituminous coal, Pocahontas	5.2	14.0	86.0	91.0	4.4	2.8	1.3	.5	20.7
B	No. 4 bed	5.5	13.8	86.2	91.2	4.4	2.6	1.3	.5	20.7
9A	Pennsylvania anthracite from Locust Summit, Pa.	14.2	5.8	94.2	91.9	2.8	3.7	1.0	.6	32.8
B		15.5	4.8	95.2	91.8	3.2	3.3	1.1	.6	28.7
14	Pennsylvania anthracite from Lykens, Pa.	13.3	5.7	94.3	92.2	3.4	2.3	1.2	.9	27.1

1/ Designations A and B represent the analyses of different batches of the same coal. An asterisk next to the serial number signifies char.

2/ Air-to-coal ratios are based on std. cu. ft. air injected per lb. of coal carbonized.

Literature Cited

- (1) ASTM Standard Methods D 388-38.
- (2) Batchelder, H. R., Busche, R. M., Armstrong, W. P., Ind. Eng. Chem. 45, 1856 (1953).
- (3) Binford, J. S., Jr., Eyring, H., J. Phys. Chem. 60, 486 (1956).
- (4) Blackwood, J. D., McGroory, F., Australian J. Chem. 11, 16 (1958).
- (5) Dotson, J. A., Holden, J. H., Koehler, W. A., Ind. Eng. Chem. 49, 148 (1957).
- (6) Gray, T. J., Detwiler, D. P., et al., "The Defect Solid State," Interscience Publishers, New York, 1957.
- (7) Guerin, H., "Le Probleme de la Reactivite des Combustibles Solid," Dunod, Paris, 1945.
- (8) May, W. G., Mueller, R. H., Sweetser, S. B., Ind. Eng. Chem. 50, 1289 (1958).
- (9) Peters, W., Laak, G. W., Brennstoff-Chem. 42, 84, 323 (1961).
- (10) Pilcher, J. M., Walker, P. L., Jr., Wright, C. C., Ind. Eng. Chem. 47, 1742 (1955).
- (11) Schroeder, H., Brennstoff-Chem., 35, 14 (1954).
- (12) Sebastian, J. J. S., Meyers, M. A., Ind. Eng. Chem. 29, 1118 (1937).
- (13) Sebastian, J. J. S., The Reactivities of Bituminous Coals, presented before the Gas and Fuel Chemistry Division, A. C. S., Atlantic City, N. J., Sept. 1941 (unpublished).
- (14) Sebastian, J. J. S., U. S. Pat. 2,955,988 (Oct. 11, 1960).
- (15) Van Krevelen, D. W., and Schuyer, J., "Coal Science," p. 321-335, Elsevier, New York, 1961.
- (16) Walker, P. L., Jr., Rusinko, F., Jr., Austin, L. G., Gas Reactions of Carbon, Ch. in "Advances in Catalysis," Vol. 11, 384 pp., Academic Press, New York, 1959.
- (17) Warner, B. R., J. Am. Chem. Soc. 65, 1447 (1943); 66, 1306 (1944).
- (18) Zielke, C. W., Gorin, E., Ind. Eng. Chem., 49, 396 (1957).

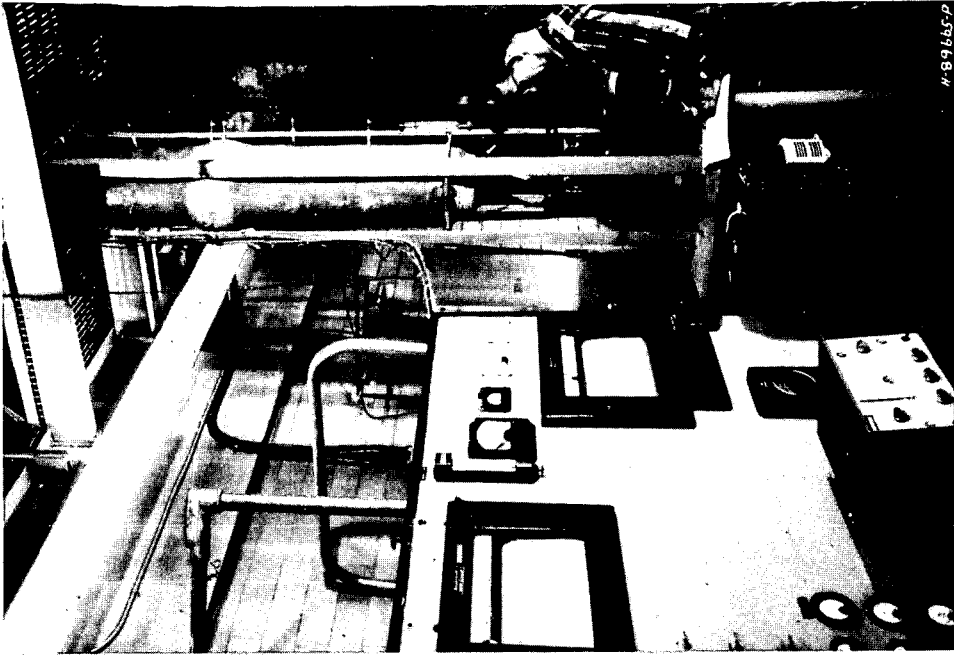


Figure 2. Photograph of Apparatus used for Study of the Kinetics of Reactions of Coals and Chars with Steam.

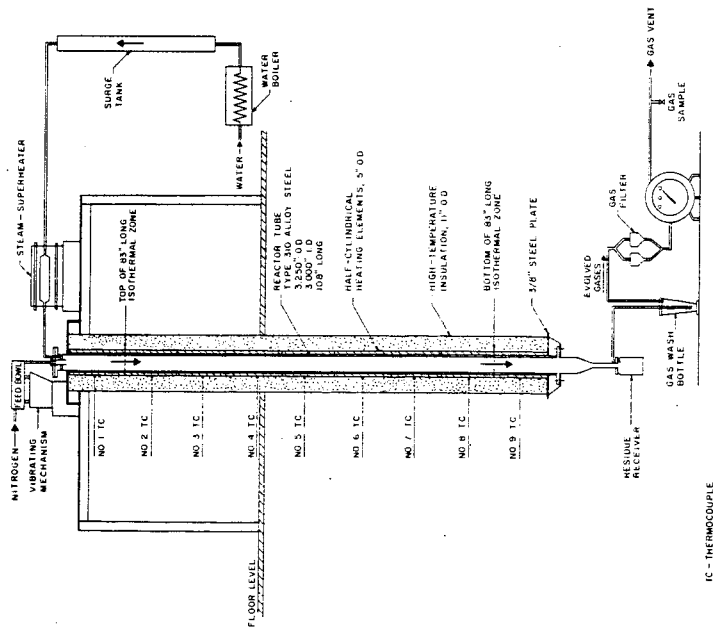
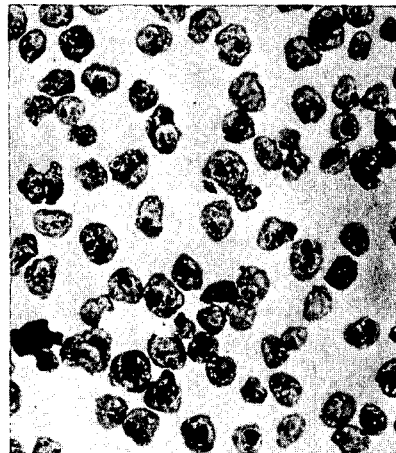
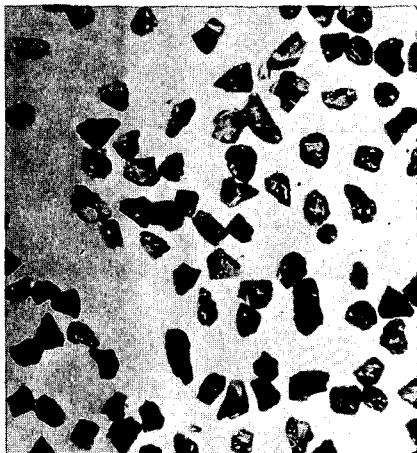


Figure 1. Isothermal Reactor for the Study of the Kinetics of Steam-Coal Reaction at High Temperatures



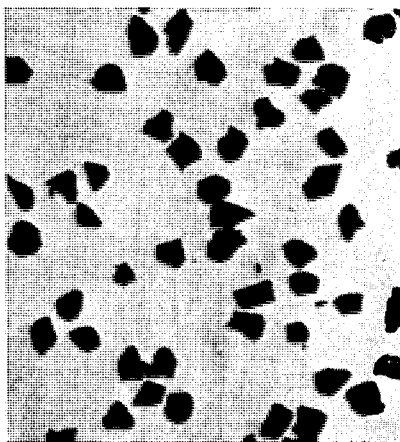
No. 11 - Wyoming H.V. Bituminous-C coal.
Size: -60 + 65 mesh/in; sp vol:
1.39 cm³/g

No. 11-R - Single pass residue obtained
from testing No. 11 coal.
Sp vol: 4.13 cm³/g



SCALE: MILLIMETER
1.0 mm = 1,000 microns

Figure 3. Photomicrographs of a Bituminous-C Coal and its Residue from Reactivity Test made at 1,700° F in Steam Medium (approximate enlargement 17X).



No. 6 - Colorado H.V. Bituminous-A coal.
Size: -60 + 65 mesh/in; sp vol:
1.32 cm³/g

No. 6-R - Single pass residue obtained
from testing No. 6 coal.
Sp vol: 2.99 cm³/g



SCALE: MILLIMETER
1.0 mm = 1,000 microns

Figure 4. Photomicrographs of a Bituminous-A Coal and its Residue from Reactivity Test made at 1,700° F in Steam Medium (approximate enlargement 17X).

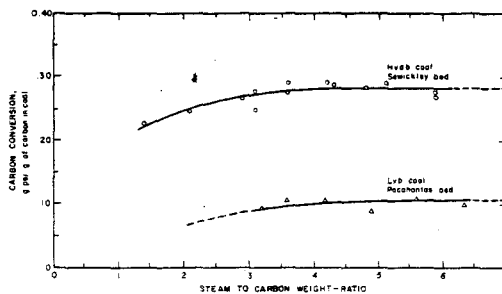
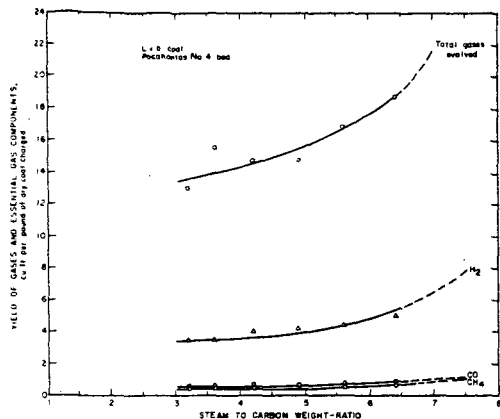


Figure 5. Effect of Steam Concentration on Gas Yield, 1700° F

Figure 6. Effect of Steam Concentration on Carbon Conversion, 1700° F

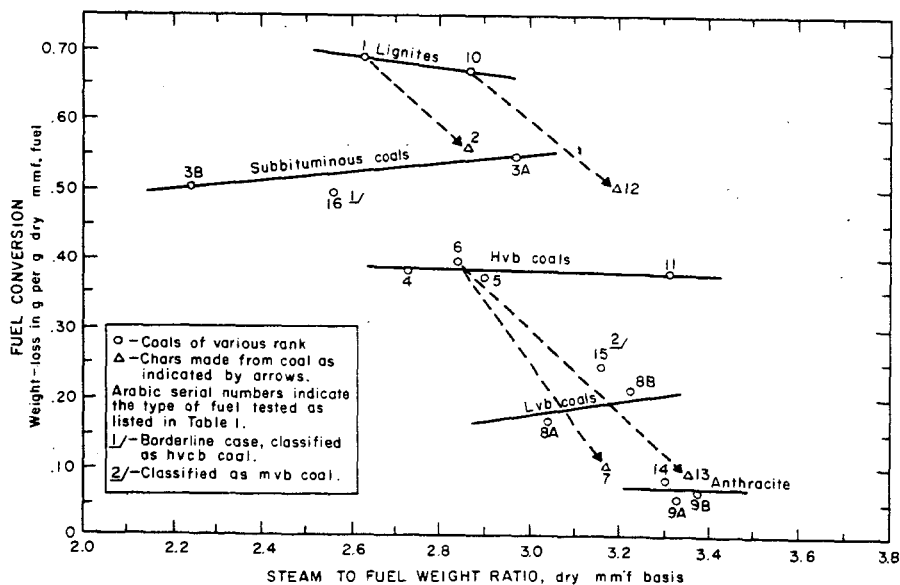


Figure 7. Comparative Reactivities of Coals and Chars

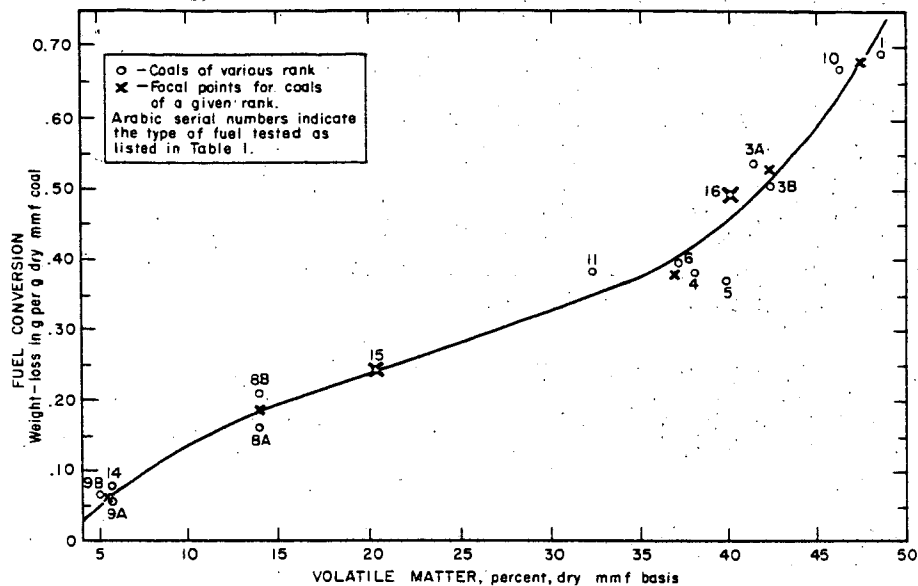


Figure 8. Fuel Conversion as a Function of Volatile Matter
— Steam Reacting with Coals at 1700° F

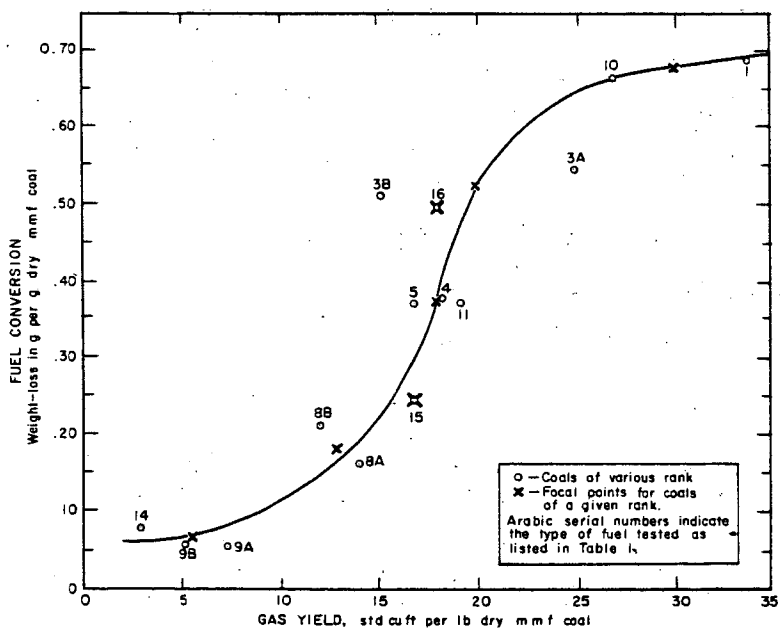


Figure 9. Relation Between Fuel Conversion and Gas Yield
— Steam Reacting with Coals at 1700° F

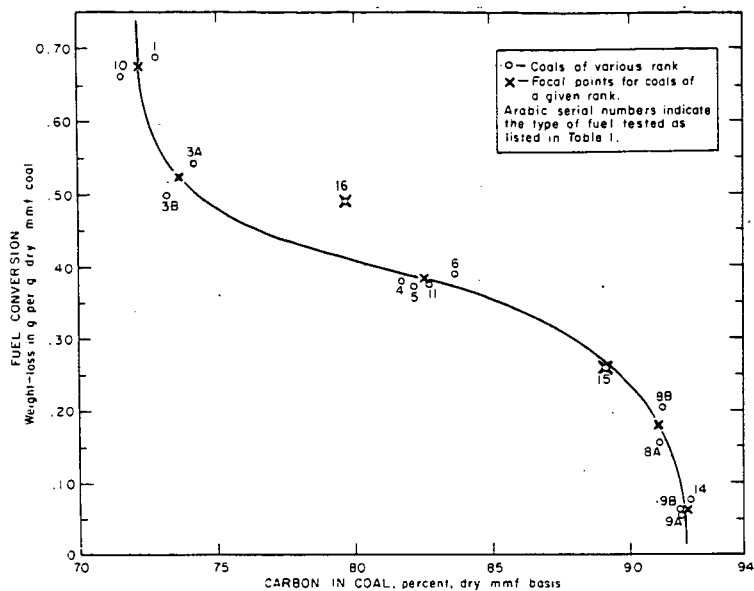


Figure 10. Fuel Conversion as a Function of Carbon Content
— Steam Reacting with Coals at 1700° F

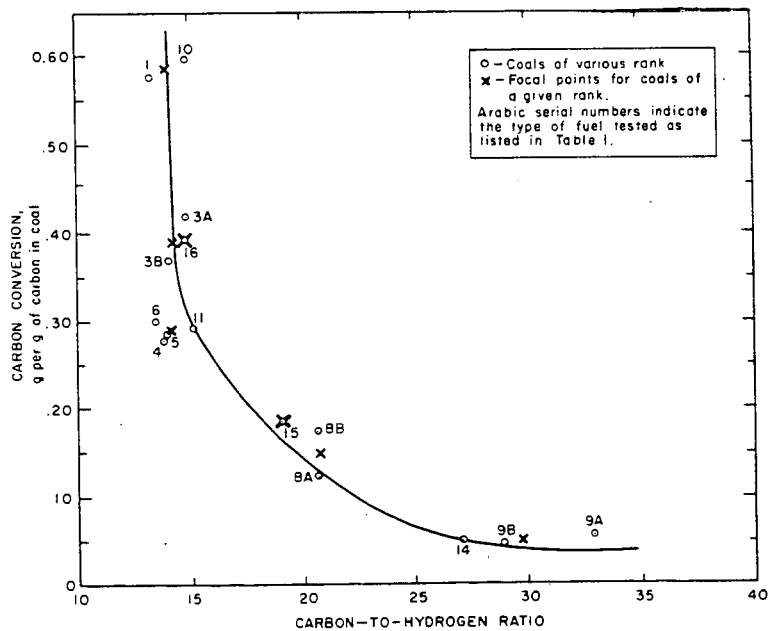


Figure 11. Carbon Conversion as a Function of Carbon-to-Hydrogen Ratio
— Steam Reacting with Coals at 1700° F

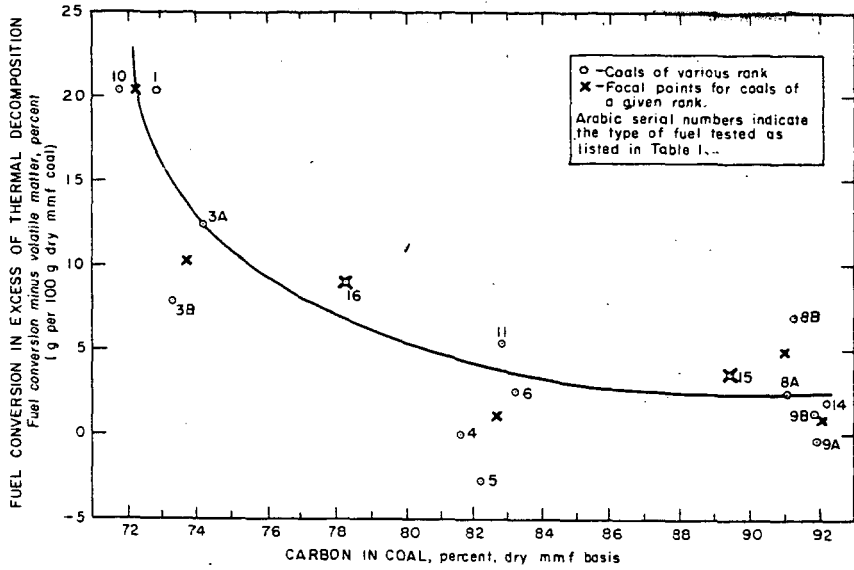


Figure 12. Relation Between Total Carbon in Coal and the Reactivity of Fixed Carbon — Steam Reacting with Coals at 1700° F

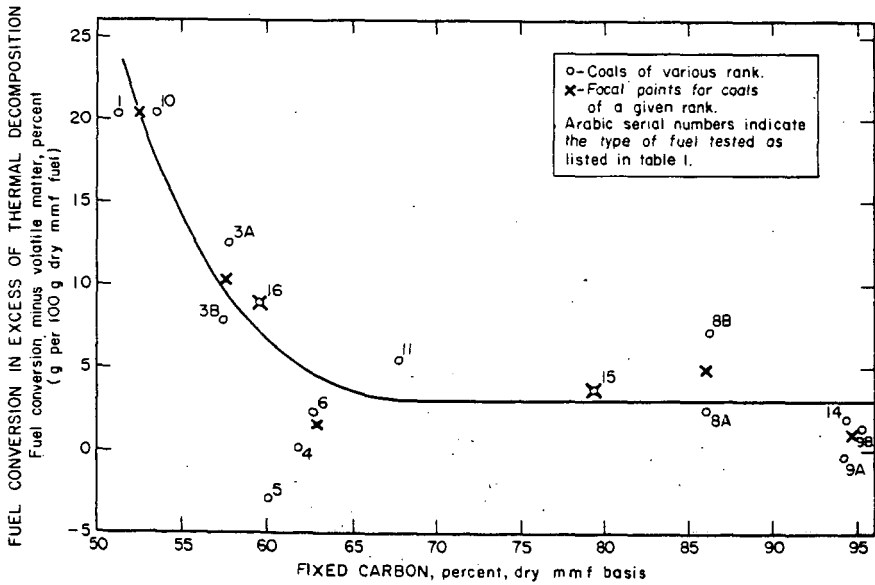


Figure 13. Relation Between Fixed Carbon in the Coal and the Reactivity of Fixed Carbon — Steam Reacting with Coals at 1700° F

Kinetics of Coal Combustion: The Influence of Oxygen Concentration
on the Burning-Out Times of Single Particles

Geoffrey Beeston and Robert H. Essenhigh

Department of Fuel Technology and Chemical Engineering
University of Sheffield, England

1. INTRODUCTION

Single particles of coal burn in two stages. The first is a volatile combustion stage; and the second, with which this paper is primarily concerned, is burn-out of the solid carbon residue left after generation and combustion of the volatiles. Kinetically, this second, burn-out stage is a heterogeneous process in which oxygen reacts directly, at-and-with the solid surface. It has, therefore, been studied extensively, but as it were by proxy using relatively pure carbon in place of the coal; and the validity of extrapolating such results directly to coal residues has generally been then taken very much for granted. Direct work on coal has, of course, been done in the past but the results (1-3) have generally been too few, and the conditions too imprecise, for kinetic studies. Further experiments have, therefore, been carried out on single particles of coal under more precisely specified conditions, to check proposed kinetic equations. The first results obtained, described elsewhere (4,5), were concerned with the variation of burning time as a function of particle diameter and coal rank, with other parameters such as oxygen concentration, temperature, and ambient velocity, kept constant. The success of those first experiments then encouraged extension of the work to investigate the influence of other parameters, and the next one chosen for investigation, was the oxygen concentration; this is of particular interest as it also has direct bearing on the assumed but disputed (6) order of reaction at the solid surface. The object of this present paper is, therefore, to report the results of these further experiments on the influence of oxygen concentration on the burn-out times of the coal particle residues, together with a comparison between the experimental and predicted behaviour.

2. THEORY

As the general theory has been covered extensively in previous reviews and papers (4, 5, 7-9) only the salient points will be quoted in summary here.

The theory is based on the original analysis by Nusselt (10) in which he assumed that the rate controlling process in the reaction was the rate of diffusion of oxygen from the mainstream to the solid particle surface, through a boundary diffusion layer. Reaction at the solid surface was assumed to be instantaneous, or effectively so, and it was also assumed to be first order with respect to the oxygen partial pressure adjacent to the solid surface. With these limiting conditions, Nusselt's prediction was that the total burning time (t_b) of a solid carbon sphere would be proportional to the square of the initial particle diameter (d_0):

thus

$$t_b = K_D d_o^2 \quad (1)$$

where K_D is a predictable burning constant that is a function of temperature and oxygen partial pressure.

This equation was tested in the previous experiments; in the first instance (4) just as it stands using only a few coals, but subsequently (5) the number and rank range of coals was increased to determine the influence of coal rank. To do this, burning times (of both volatiles and residues) of particles in the size range 4000 to 300 microns were measured as a function of diameter. The particles were burned in air, between two small heating coils of resistance wire, under relatively quiescent ambient conditions, at an effectively constant temperature of about 1000°C. In all, 10 coals were ultimately tested, ranging in volatile percentage from 5 to 40, and all were found to obey the eqn. (1). The value of the burning constant K_D had, of course, to be adjusted to allow for the effects of volatile loss and swelling, but the experimental values of the burning constant, K , were found (5) to be in good agreement with the following predicted relationship between K and K_D

$$K = [(C_f/100)/f] \cdot K_D \quad (2)$$

where C_f is the fixed carbon percentage; and f is a swelling factor whose values were found by measurement to be: unity for coals of V.M. less than 5%; and 1.5 for coals of V.M. greater than 10%. The basis of this prediction was the assumption that the coals first lost volatiles at constant diameter, and then swelled by the linear factor f . This then provided a correction factor to the solid density σ that appears in the theoretical relation for K_D

$$K_D = \sigma/3\rho_o D_o (T/T_o)^{0.75} \cdot \ln(1 - p_o) \quad (3a)$$

$$= k/\ln(1 - p_o) \quad (3b)$$

$$\approx k/p_o \quad (\text{for small } p_o) \quad (3c)$$

where ρ_o is the s.t.p. density of air; D_o is the s.t.p. diffusion coefficient of oxygen through nitrogen; T is the absolute temperature; and p_o is the ambient fractional oxygen concentration (of value 0.21 for air).

This set of equations therefore provided us with relations between burning time, or burning constant, and the two additional variables: oxygen concentration and temperature, to be checked by comparison with measurement in further experiments. Our choice of variable for the experiments reported here was the first: that of oxygen concentration, for the reasons outlined in the Introduction. In doing this, we only used a single coal since, as the quantitative influence of rank is given by eqn. (2), we assumed that validation on a single coal chosen at random should be satisfactory. The experiments were then carried out by measuring burning time as a function of oxygen partial pressure, using five different sizes of particle taken from the single coal, as described in the section following.

3. EXPERIMENTAL

To burn the particles in variable but controllable oxygen atmospheres, a small combustion unit was used inside a large perspex (plexiglass) box so that the ambient atmosphere could be controlled at will. The combustion unit was, in principle, that used in the previous experiments (4, 5), in which the coal particles were cemented to silica fibres and held by these, cantilever-fashion, mid-way between two horizontal heating elements of electrical resistance wire.

The coal used was Winter (ex-Grimethorpe); a medium bituminous coal, No. 7 of the set prepared and used previously (5), of analysis: Ultimate - 84.0%C, 5.5%H, 8.3%O, 1.8%N, 0.4%S (d.m.f. by Fereday and Flint (11) equation); Proximate - 36.0% V.M., 2.6% H₂O, 1.7% ash, 0.77% CO₂.

The perspex box used to house the combustion unit had dimensions: 1.5 by 1.5 ft. in plan section, by 3 ft. high, (6.75 cu. ft.). The oxygen atmosphere inside could be adjusted as required over the range 3% to 70% O₂. To make up the required atmosphere, oxygen or nitrogen was metered in as required, and the analysis then checked by Orsat. The reason for making the box so large was that the oxygen depletion during combustion of a particle would not then be significant, and the atmosphere could, therefore, be taken as being effectively infinite, with the 'main stream' or ambient oxygen concentration constant during the reaction thus meeting the specified boundary conditions required by the theoretical analysis. In fact, the box was large enough for a number of particles to be burned without having to open and recharge the box for each particle, and without significant change in the box's atmosphere. To take advantage of this, a rail carrying 18 carriages was mounted in the box, and to each carriage could be attached one silica thread with its coal particle cemented on ready for burning. After burning, the oxygen concentration was checked by Orsat analysis.

The particles on the carriages were moved into position between the coils, as and when required, by means of a control rod extending outside the box. The heating coils were larger than those used previously. In place of the 2-cm diameter flat spirals, wound from 18-gauge Nichrome resistance wire, the new heaters were square elements, of face area about 5 x 5 cm., made of Nichrome strip. This strip was about 1/2 cm. wide, and was wound with 1/2 cm. spacing on a 1/2 cm. thick former; the gaps between the set of strips on one side of the former were, of course, substantially covered by the return strips on the other side so that the whole face area was radiant. The two heating units were then mounted horizontally with their faces about 1.5 cm. apart. The heating was electrical, as before, controlled by a variable transformer unit; with this, element temperatures of up to 1060°C, as measured by an optical pyrometer, could be reached.

Burning times were measured with a stop watch in place of the photocell and pen recorder units used previously. The photocell was abandoned because of light shielding and other difficulties experienced with the larger heating elements. This meant that very short volatile burning times could not be measured - those larger ones that were, were measured with a second stop watch. However, the volatile measurements that were made were found to exhibit such considerable variability in the different oxygen atmospheres that their value was greatly reduced. Most measurements were therefore restricted to the residue burning times alone, using the stop watch which was found to be perfectly satisfactory for these.

With this apparatus, the residue burning times were measured at different levels of oxygen concentration as the principal variable, for each of the following particle sizes: 1870; 1300; 928; 649; and 388 microns. The particles were derived from the single coal, and burned in effectively infinite atmosphere, at an approximately constant temperature of 1000°C.

4. RESULTS

4.1 Qualitative Behaviour - The general behaviour of the particles was as observed before (4, 5): the particles burned in two stages, with the volatiles (when they burned at all) igniting first and burning with the characteristic luminous, flickering flame; and this was then followed in the burn-out stage by the much steadier glow of residue combustion. The particles did not ignite immediately; they required time to heat up to ignition, and this ignition time increased with decrease of oxygen concentration. This may indicate that preliminary, but significant oxidation may be occurring, with significant heat generation, before the volatiles ignited in flaming combustion. This requires closer investigation.

As in the previous experiments, the volatiles of the smaller particles often failed to ignite because of their small quantity and this failure increased, as was to be expected, as the oxygen was reduced. Where the volatiles did ignite in reduced oxygen, the usual fractional lag in time between finish of the volatile flame and start of the residue combustion was occasionally increased to a long delay ranging from two to thirty seconds. At the low oxygen concentrations, below 6%, the burning times also started to become very scattered, and at 3%, the particles failed to ignite at all.

At the other end of the scale, at high oxygen concentrations, the particles showed increasing tendency to decrepitate or explode. This happened whether the coils were already up to temperature before the particle was inserted (as was the case in general in these experiments), or whether the particle was already in position (as in the previous experiments) before switching on the heating current. If decrepitation is due to too rapid generation of volatiles before the coal becomes sufficiently plastic, this suggests that the volatiles generation must be influenced, contrary to previous expectation, by the ambient oxygen concentration. This would seem to imply that the oxygen causes some significant and rapid change in the constitution of the potential volatile material before generation, though how it should do this is by no means clear; this also requires further detailed study. In contrast, the general residue behaviour is far better understood, and more predictable, as described in the sections following.

4.2 Influence of Oxygen Concentration - By combining eqns. (1) and (3b) we have for burn-out of the residues:

$$t_b = [(C_f/100)/f] \cdot kd_o^2 / \ln(1 - p_o) \quad (4)$$

To test this equation, the experimental data obtained have, therefore, been presented in two graphs, Figs. 1 and 2. Fig. 1 is a plot of: $\log_{10} t_b$ against $\log_{10} [\ln(1 - p_o)]$, to show that the slopes of the lines obtained are, within

reason, close to 45° , or -1 . Fig. 2 is the alternative plot of t_b against the reciprocal of $\ln(1 - p_o)$, to show that the plots obtained are again acceptably linear and passing through the origin. Within the limits of accuracy of the measurements, these plots are, therefore, considered to substantiate eqn. (4).

- 4.3 Influence of Particle Size - From eqn. (4) it is clear that the slopes of the lines in Fig. 2 (written as m) are related to particle size by

$$m = [(C_f/100)/f]k.d_o^2 \quad (5)$$

This equation has in turn been tested by plotting $(m)^{1/2}$ against d_o , as shown in Fig. 3. Here again the plot is reasonably linear, and also passes through the origin. Again within the limits of accuracy of this plot, it is considered to substantiate eqn. (5).

- 4.4 Comparison with Prediction - Now, the slope of Fig. 3 (written as M) is an experimental quantity whose value is predicted from the appropriate terms in eqns. (3a) and (5), thus:

$$M^2 = [(C_f/100)/f] \sigma/3\rho_o D_o (T/T_o)^{0.75} \quad (6)$$

For the Winter coal, C_f is 60.7; f is 1.5; and σ is 1.25. For air, ρ_o is 1.3×10^{-3} g/cc; D_o for oxygen diffusing through nitrogen at temperature T_o (273°K) is 0.181 sq.cm/sec. The particle temperature is taken as 1000°C (1273°K), as in the previous experiments. With these values, the calculated value of M^2 is 225; we therefore have for $M_{(calc.)}$ a value of 15, which is precisely the experimental value obtained from the slope of Fig. 3. This exact agreement is clearly fortuitous; but within an error of 5%, which is the estimate of the overall error in both experimental and calculated values, it is clear that agreement is still satisfactory. Since this agreement was obtained by using the rank-influence equation (2), this also supports the assumption made that validation of the tested equations using a single coal, but chosen at random, would probably be satisfactory.

- 4.5 Burning Constant - This is the constant K_D or K of eqn. (1). It is calculated almost universally from measurements made in air, so tabulated values (as in Reviews 7, 8) are given for $p_o = 0.21$. From eqns. (1), (2), (3), and (6), it is clear that

$$K = M^2/\ln(1 - p_o) \quad (7)$$

Hence with a value for: M^2 of 225; and for $\ln(1 - p_o)$ of 0.235 when p_o is 0.21; this gives a value for $K_{(calc.)}$ of 957 sec/sq.cm. This is lower than (though close to) the value obtained in the previous experiments (5) for this same coal (previous value: - 1095 sec/sq.cm) but this may be accounted for in part by the difference between the logarithmic term $[\ln(1 - p_o)]$ and the first term of its expansion $[p_o]$ since the former has been used in this paper, but the latter was used in the previous paper (5); the theoretical alternatives are compared in the two eqns. (3b) and (3c). Use of the first term expansion as in eqn. (3c) is very common, and is generally accepted as being valid for

air or vitiated air. Just how widely the two terms differ at enriched concentrations, is shown by Fig. 4 in which the logarithmic term is plotted against p_o . In vitiated air the two are clearly reasonably comparable, but even in air itself the difference amounts to nearly 12% (0.235 compared with 0.21). Use of the \ln term in place of p_o in the previous experiments would therefore, reduce the value of 1095 to 978. The further difference between this and the new value of 957 is well within 5% but can in any case be attributed to uncertainty in the precise temperature in the two cases. Agreement, however, is regarded as acceptable.

The significance of the logarithmic term also showed up in the graphs of Figs. 1, 2, and 3. To check their sensitivity to the first expansion term in place of the full expression, similar plots were prepared (not reproduced) with p_o in place of $\ln(1 - p_o)$. The plots were found to vary significantly as follows: in equivalent Fig. 1, the plots showed slight but detectable curvature in spite of the fairly considerable scatter; in equivalent Fig. 2, convincingly straight lines could be run through the points, but the plots then showed marked intercepts on the oxygen-function axis, and the displacements from the origin were found to be statistically significant; finally, in equivalent Fig. 3, a straight line could again be run through the points, but again only with a statistically significant intercept. This agreement with the logarithmic term thus provides by far the best substantiation of the original Nusselt analysis in terms of the diffusion-film theory of reaction-rate control. What is yet undetermined, however, are the limits of applicability of the Nusselt equation and analysis; this is considered briefly in the next section.

5. DISCUSSION

- 5.1 Reaction Order - As stated in the Introduction, one of the principal reasons for carrying out the work described was to provide a more direct check on the assumed order of reaction at the solid surface. Now, because of the adjacent diffusion layer, that under these quiescent conditions is rate-controlling, it is only possible to check the surface order of reaction indirectly. To do this we assume some appropriate value for the surface order of reaction and then deduce what net, overall, or 'global' order of reaction should then follow. First of all, in choosing an order for the surface reaction, we have (7) two extreme limiting values: (1) zero, when the temperature is low enough for the surface chemisorption sites to be fully saturated at all times; and (2) unity, when the temperature is high enough for the sequence of chemisorption, followed by desorption, to be effectively instantaneous. At intermediate temperatures the reaction approximates to a fractional order. If internal or pore reaction also takes place, the lower limiting order is then raised from zero to 1/2.

Superimposed on this pattern is the oxygen supply by boundary layer diffusion. Now, in the first place, if the temperature is high enough for first order reaction to prevail then we get the burning time equation that combines both the diffusional and adsorption resistance (9),

$$t_b = K_c d_o + K_D d_o^2 \quad (8)$$

where K_c is the high-temperature chemical burning constant; and K_D is the

diffusional burning constant. This clearly has limits, respectively, of a linear equation, or a square law equation, according to whether diffusion is unimportant or dominant.

At the other extreme of low temperatures, when the reaction order is zero, the burning time equation is linear only (9)

$$t_b = K'_c d_o \quad (9)$$

where K'_c is the low-temperature chemical burning constant.

At intermediate temperatures the burning time is proportional to some intermediate power of the diameter, d_o^n , where n lies between 1 and 2. It is, therefore, obvious that determination of the power index n in any burning time experiments will give a clear guide to the relative importance of the three factors considered: (i) rate of diffusion; (ii) rate of chemisorption; and (iii) rate of oxide-film decomposition. In particular, a value of 2 for n is quite unambiguous in implying that the rate of boundary layer diffusion dominates the reaction control: and the significant corollary of this is that the surface rate-of-adsorption reaction must be first order.

In concluding that the reaction in our experiments was in the high temperature region, and diffusion controlled, we have altogether three confirmatory points provided by the experimental results. (1) The first is the 'square-law' agreement illustrated by the square-root plot of Fig. 3; if the additional chemical term in eqn. 8 — $K_c d_o$ — was also important, the line would be curved with a tendency to an intercept on the t axis. Other checks such as plotting (t_b/d_o) against d_o confirmed that K_c was negligible under the conditions of experiment. (2) We also have the agreement between t_b and the oxygen function $\ln(1 - p_o)$. Since K_c is inversely proportional to p_o (9), then if this was important the plot of t_b against $1/p_o$ would not have been so poor in comparison with the plot of Fig. 2 against $1/\ln(1 - p_o)$, as discussed in sec. 4.5. (3) There is finally the excellent agreement between the experimental and calculated values of the burning constant (written as K instead of K_D after correction for coal rank and swelling by eqn. 2) as described in sec. 4.5.

Since the reaction is evidently diffusion controlled, it follows that the surface reaction must be first order.

- 5.2 Boundary Layer Thickness - A secondary point of interest that also emerges from this is a reflexion on the question of boundary layer thickness. In calculating heat and mass transfer to spheres it is almost universal to use Nusselt's concept of the effective or 'fictitious' boundary layer thickness. If the oxygen concentration at the solid surface of the particle of radius, a , is zero, its value at any other radius, r , from the center of the particle is given approximately by

$$p/p_o = 1 - a/r \quad (10)$$

Since p rises to the main-stream value p_o only when r becomes infinite, the

real, physical boundary layer must clearly be of infinite thickness if it is defined as the distance required for p to reach the main-stream value. If, however, (following Nusselt (10)) the real behaviour indicated by eqn. (10) is replaced by an equivalent behaviour such that p is assumed to rise linearly to p_0 and then to remain constant with r , the main stream value is then reached at the Nusselt fictitious film thickness at $r = 2a$, or one radius out from the surface of the particle. It should be realised, however, that at $r = 2a$, $p = p_0/2$ (from eqn. 10); in other words, the actual, physical rise in p is only half the fictitious value. This can be represented in another way by relating the fictitious film thickness to a definable real, or physical film thickness. This can be defined with physical realism as the distance within which p rises to, say, 99% of the main stream value (this is a standard solution to continuum problems in which some relevant parameter reaches its limiting value only at infinity). We then have that, writing the boundary layer thickness as δ ,

$$\delta_{(\text{physical})} = 100a = 100\delta_{(\text{fictitious})}$$

The significance of this becomes immediately apparent when considering the behaviour of dust flames since the interparticle distance at a stoichiometric concentration is generally of the order only of 30 particle diameters. This means that in real, physical terms, as opposed to fictitious film-thickness terms, most of the oxygen is already well inside the boundary layer of one particle or another in the flame. It is clear, therefore, that direct extrapolation of the results in this paper to particles in dust flames should be made with caution.

Now, in addition to the points made above, a further complication that emerges is the additional inadequacy of the fictitious film concept, even for purposes of calculation, over the range of oxygen concentrations used in our experiments. Because our range was high, and the oxygen function $\ln(1 - p_0)$ could not be approximated by p_0 (as shown in Fig. 4), it means that eqn. (10) — which is also based on the same approximation of p_0 for $\ln(1 - p_0)$ — is also inadequate to describe the behaviour of the oxygen concentration over our full experimental range. An effective film thickness can still be defined, but the expression for it is so complex as to be valueless as it is then easier to solve the initial differential equation and not to bother about the 'short cut' of using an effective or fictitious film thickness.

- 5.3 Range of Applicability - The final point to be considered as a consequence of these results is their range of applicability: the temperature range of application is of particular importance.

Now, what we have established so far is that the solid surface reaction is first order at a temperature as low as 1000°C. This, however, was unexpected, being about 200° lower than the expected value of the 'higher critical temperature'. This was estimated, by assessment (7) of the available literature, at 1200°C. Below that, through the transition range down to 800°C, the reaction order was expected to drop progressively from unity to zero. The explanation for this apparent contradiction would appear to be a consequence of the influence of the

ambient gas velocity on the boundary layer thickness. The effect of ambient velocity is to promote such increased speed of mixing of the ambient gases that the thickness of the boundary layer, however defined, is progressively reduced. Initially, this must steepen the oxygen concentration gradient, with the result that both oxygen transfer, and therefore reaction rate, are increased. This increase can proceed just so far, up to the point that the rate of chemisorption exceeds the rate of reaction, and at that point the coverage of the solid surface by the chemisorbed film must increase; the surface reaction order then becomes fractional, and can drop progressively to zero as the ambient velocity also increases. This means that the transition range of temperature between the two extreme reaction conditions is velocity dependent. This dependence is shown very clearly by the single sphere experiments of Tu, Davis, and Hottel (12), but the analytical function relating the two is still unknown.

It would therefore seem that previously published experiments that were assessed as showing a first order reaction only down to 1200°C, cannot yet be directly correlated with the results of our experiments because the previous ones were carried out in flowing systems, whilst ours were in effectively quiescent systems. The increased film thickness that must have existed in our experiments can account qualitatively for the first order reaction down as low as 1000°C, but this inter-relation between temperature and velocity is now, in our opinion, the most outstanding problem of the combustion system requiring to be resolved by future work.

6. CONCLUSIONS

For coal particles inside the size range 350 microns to 2 m.m., burning in vitiated and enriched O₂ atmospheres (3% to 70%), at about 1000°C, under quiescent ambient conditions, the combustion behaviour was found to be as follows:

(1) Qualitative behaviour was, in general, similar to that observed previously with coal particles burning in air; for particles large enough, combustion proceeded in two sequential stages: (i) volatile evolution and combustion; followed by (ii) residue combustion.

(2) Particles below 1 m.m. tended to produce too small a quantity of volatiles for their combustion, because of low limit requirements. The frequency of this combustion failure tended to increase as the oxygen concentration was reduced. At 3% oxygen, even the residues failed to ignite. At high oxygen concentrations the particles ignited and burned satisfactorily, but they showed increasing tendency to decrepitate or explode.

(3) Quantitatively, only the residue combustion was examined in detail. Burning times of the residues (t_b) were found experimentally to obey the relation predicted from the Nusselt diffusion theory of reaction control:

$$t_b = m / \ln(1 - p_o)$$

where p_o is the ambient oxygen concentration; and m is a predictable constant.

(4) The results also showed good agreement with the following predicted relation between the constant m and the initial particle diameter d_0 :

$$m = M^2 d_0^2$$

where M is another predictable constant.

(5) The experimental value of the second constant M was also found to be in good agreement with the predicted value, as calculated from the relation

$$M^2 = [(C_F/100)/f] \sigma/3 \rho_0 D_0 (T/T_0)^{0.75}$$

where C_F is the fixed carbon of the coal; f is the swelling factor (of value 1.5 for bituminous coals); σ is the solid particle density; ρ_0 is the s.t.p. density of air; D_0 is the s.t.p. coefficient of oxygen diffusing through nitrogen; T is the absolute temperature and T_0 is the reference temperature of 273°K. The predicted and experimental values of M^2 were in fact identical, at 225; although this exact agreement was fortuitous it is still entirely satisfactory within the expected limits of error.

(6) The burning constant K in the Nusselt square-law equation

$$t_b = K d_0^2$$

was also calculated, being given by

$$K = M^2 / \ln(1 - p_0)$$

The value was 957 c.g.s. units, and this is in adequate agreement with values obtained previously for this same coal under similar (though not identical) experimental conditions.

(7) This general agreement with prediction therefore substantiates the primary assumption of the theoretical analysis: that the order of reaction at the solid particle surface with respect to oxygen concentration is unity. It also follows from the results that the rate of diffusion is the slow step that dominates the reaction rate, and that the importance of the chemisorption process is negligible under the conditions of experiment. There is background evidence from other previous experiments, however, indicating that this is true only for the fully quiescent system; and that, in a velocity field at these temperatures, the chemisorption process is likely to become significant, and increasingly so with increasing velocity. This is now the outstanding point requiring investigation in any subsequent work.

ACKNOWLEDGMENTS

The work described in this paper formed a part of a general program of research on Pulverized Fuel Firing, sponsored by the Electricity Supply Research Council of Great Britain. The work was carried out in the Department of Fuel Technology and Chemical Engineering, University of Sheffield, England. The authors are indebted to the ESRC for financial support of this work and for permission to publish this paper.

REFERENCES

1. Griffin, H. K., Adams, J. R. and Smith, D. F. Ind. Eng. Chem. 21(1929) 808.
2. Godbert, A. L. Fuel 9(1930) 57.
Godbert, A. L. and Wheeler, R. V. "Safety in Mines Research Board", Paper No. 73 H.M.S.O., London, 1932.
3. Orning, A. A. Trans. A.S.M.E. 64(1942) 497.
Omori, T. J. and Orning, A. A. - *ibid*- 72(1950) 591.
4. Essenhigh, R. H. and Thring, M. W. Proc. Conf. "Science in the Use of Coal", Sheffield, 1958; Paper 29 p. D21: Institute of Fuel, London, 1958.
5. Essenhigh, R. H. Paper No: 62-WA-35; to be presented at A.S.M.E. Winter Annual Meeting; Nov. 1962.
6. Frank-Kamenetskii, D. A. "Diffusion and Heat Exchange in Chemical Kinetics" Princeton University Press (Trans. 1955) Ch. II, pp. 64, 65.
7. Essenhigh, R. H. and Perry, M. G. Introductory Survey "Combustion and Gasification", Proc. Conf. "Science in the Use of Coal" Sheffield, 1958 p. D1: Institute of Fuel, London, 1958.
8. Essenhigh, R. H. and Fells, I. General Discussion on "The Physical Chemistry of Aerosols" Bristol, 1960; Paper No. 24, p. 208: Faraday Society, London, 1961.
9. Essenhigh, R. H. J. Inst. Fuel (Lond.) 34(1961) 239.
10. Nusselt, W. V.D.I. 68(1924) 124.
11. Fereday, F. and Flint, D. Fuel 29(1950) 283.
12. Tu, C. M., Davis, H. and Hottel, H. C. Ind. Eng. Chem. 26(1934) 749.

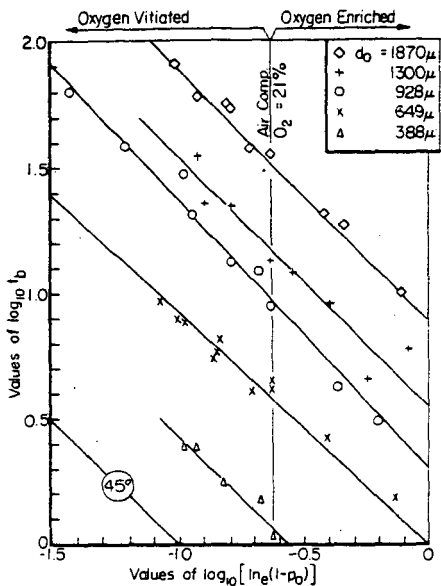


FIG. 1 - Double logarithmic plot of burning time, t_b , against the oxygen partial pressure function, $\ln_e(1-p_o)$.

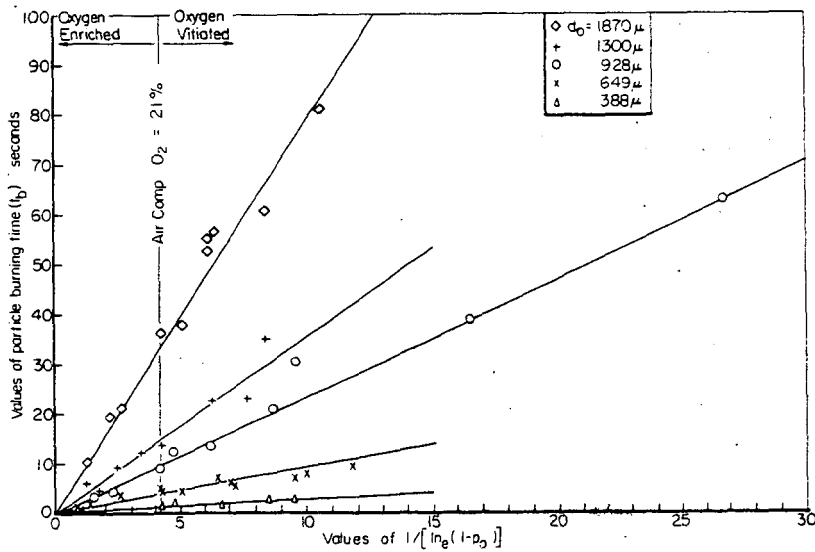


FIG. 2 - Linear plot of burning time, t_b , against the reciprocal of the oxygen partial pressure function: $\ln_e(1-p_o)$.

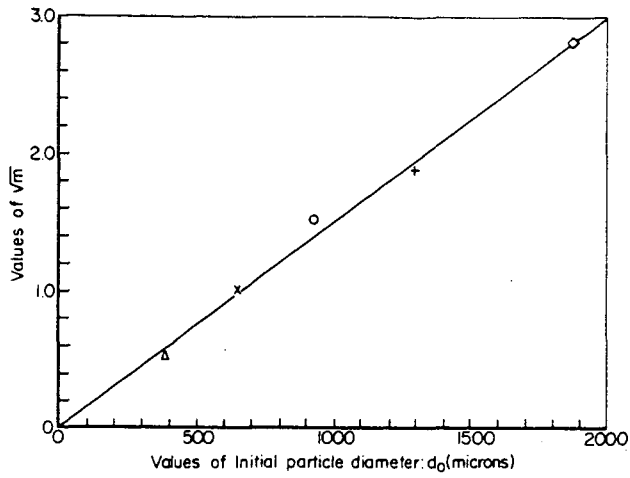


FIG. 3- Variation of square root of fig. 2 slopes (m) as a function of initial diameter of particle (d_0).

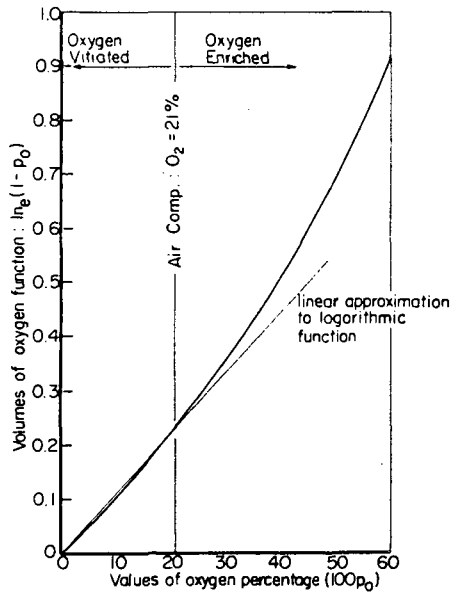


FIG. 4-Variation of oxygen function $\ln_e(1-p_0)$ with oxygen partial pressure p_0 .

The Theory of Gasification and its Application
to Graphite and Metallurgical Coke

by W. Peters and G.-W. Lask

Bergbau-Forschung GmbH, Essen-Kray

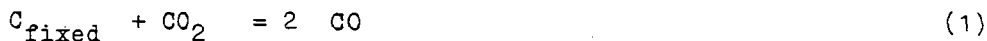
The theory of heterogeneous reactions^{1,2)} is applicable to the combustion and gasification of solid fuels. In connection herewith the passage of materials, i.e. the diffusion of the reacting gas through the boundary film and its penetration into the pores of the fuel, plays an important part, in dependency upon the temperature. A great number of measured values agree fairly well with the theoretical postulates.

For the determination of the reactivity, which varies in dependency upon the coking conditions, one preferred measuring method is prevailing today³⁾. The relation between the measured results and the coking conditions on the one side⁴⁾ and the suitability of the coke for metallurgical purposes on the other side⁵⁾ has been the object of a recent publication.

1. Theoretical bases of the Kinetics of the heterogeneous reactions in the gasification of coke

1.1. The rapidity constant of the chemical reaction

The gasification of fixed carbon with carbon dioxide (Boudouard's reaction) is a reaction of the first order⁶⁾. Thus, the speed of the reaction



is governed by the equation:

$$\frac{dx}{dt} = k \cdot O \cdot m \cdot c \quad (2)$$

where

- x = quantity of converted carbon (g)
- t = reaction time (sec)
- m = quantity of coke (g)
- O = sum of the external and internal surfaces ($\frac{\text{cm}^2}{\text{g}}$)
- c = concentration of CO_2 ($\frac{\text{g}}{\text{cm}^3}$)
- k = reaction speed constant ($\frac{\text{cm}^3}{\text{cm}^2 \text{sec}}$)

In the range of the technically interesting temperatures the back reaction, i.e. the decomposition of the carbon monoxide



does not play any part.

Equation (2) indicates the effective conversion in such cases where k is so small that the stream of gas can reach the reactive surface quickly enough. At sufficiently low temperatures this will always be the case; For Boudouard's reaction on industrial coke the upper temperature limit is situated at about 1100 °C.

When the reaction gas flows through a bed of coke (Fig. 1), formation of CO leads to a continuous decrease in the CO₂ concentration. Moreover, the speed of flow will increase, which is due to the increase of the number of molecules engaged in Boudouard's reaction. In these conditions, the quantity of CO₂ converted in the unit of time along a layer of infinitely small thickness is determined by the equation

$$\frac{dn}{dt} = k \cdot 0 \frac{m}{l} c(x) dx = -d[v(x) c(x)] \quad (4)$$

where n = C atoms transferred
 m = quantity of coke (g)
 l = height of the layer (cm)
 $c(x)$ = CO₂ concentration at point x (g/cm³)
 $v(x)$ = voluminal velocity at point x (cm³/sec)

Let us assume that the stream of CO₂ having a speed v_0 and a concentration c_0 penetrates into a coke layer of equal cross sectional area at any point; then the speed v_0 at any point of this layer is

$$v(x) = \frac{2v_0 \cdot c_0}{c_0 + c(x)} \quad (5)$$

Substitution of equation (5) into equation (4) and integration over x from zero to 1 leads to

$$2v_0 \cdot c_0 \int_0^1 \frac{1}{c(x)} \cdot d\left[\frac{c(x)}{c_0 + c(x)}\right] = - \int_0^1 k \cdot 0 \cdot \frac{m}{l} dx \quad (6)$$

After integration between the limits indicated equation (6) adopts the following form:

$$2 \ln \frac{2c_1/c_0}{1 + c_1/c_0} + \frac{1 - c_1/c_0}{1 + c_1/c_0} = - \frac{k \cdot 0 \cdot m}{v_0} \quad (7)$$

where c_1 = the concentration of CO₂ in the outgoing gas (g/cm³)

Often the differentiation plays a great part in the experimental determination of the reaction speed. m , c_0 and v_0 can be fixed in such a way that the required apparatuses do not become too expensive. c_1 can be determined by gas analysis; its value should range between 40 and 80 %. With lower CO₂ concentrations we come into a range where the concentration of CO inhibits Boudouard's reaction (10-13). Higher CO₂ concentration, by contrast, require a very high accuracy of analysis, as in

their range even great changes of the reaction speed entail only slight modifications of the CO_2 concentration.

With the experimental conditions as described and the values of CO_2 concentration found in the outgoing gas, the product $k \cdot O$ can be calculated quite simply. As, however, it is difficult to determine the surface of reaction O , k and O are combined to form the reaction speed constant k_m which is based upon the weight unit instead of the unit of surface:

$$k_m = k \cdot O \quad (8)$$

This value k_m is called "reactivity" in the following chapters; its dimension is $\text{cm}^3/\text{g sec}$.

If the method used for the determination of the reactivity involves direct weighing of the loss of weight of the coal, whilst the CO_2 concentration in the outgoing gas, c_1 , differs only slightly from its concentration c_0 when entering the reaction chamber, it is easier to use equation (2)⁰ in the form:

$$\frac{dx}{dt} = k' \cdot m \cdot c' \quad (9)$$

where k' = reaction speed constant ($1/\text{sec}$)
 c' = concentration of CO_2 (g/cm^3) under the existing conditions
 concentration of CO_2 (g/cm^3) under standard conditions

In this case the loss of weight during gasification is indicated by k' , and the following numerical relation exists between k_m and k' :

$$k' = 5,02 \cdot 10^{-4} k_m \quad (10)$$

1.2. Reactivity as a function of temperature

The dependence of the reactivity upon temperature is expressed in Arrhenius's formula:

$$k_m = H \cdot e^{-\frac{E}{RT}} \quad (11)$$

where H = the frequency factor ($\text{cm}^3/\text{g sec}$)
 E = activation energy (kcal/Mol.)
 R = gas constant (kcal/mol degree)
 T = the absolute temperature (degrees Kelvin)

By plotting $\log k_m$ or $\log k'$ against $\frac{1}{T}$, we obtain a straight line with the gradient $\frac{E}{R}$. From this gradient, the activation energy E can be de-

terminated. Figure 2 shows schematically the run of this straight line within range I.

1.3. The influence of diffusion upon the reaction speed constant and the energy of activation.

The validity of all the foregoing considerations is unrestricted only as long as the problems of molecular passage of materials during the gasification process do not yet come into play. With rising temperatures, however, the chemical reactivity will increase to such a degree that the diffusion of the gasifying agent in the carbon and towards the carbon, as the slowest step of a whole chain of physical and chemical reactions, becomes the dominant factor (1,2).

1.4. Pore diffusion

With rising temperature the reaction speed increases in conformity with equation

$$k = k_0 \cdot e^{-\frac{E}{RT}} \quad (12)$$

and the diffusion speed according to equation:

$$D = D_0 \cdot T^{1,8} \quad (13)$$

where D = diffusion speed (cm²/sec)
 D_0 = diffusion speed constant (cm²/sec)

As k rises much more sharply than D , the concentration of the gasifying agent in the pores of the fuel begins to decrease, beyond a certain temperature limit, as compared with its concentration in the ambient gas. This means that the conversion can utilize the internal surface only to a lesser degree, as expressed in equation

$$\frac{dx}{dt} = \left(\frac{dx}{dt} \right)_{\max} \cdot \eta \quad (14)$$

Beyond a zone of transition the utilization coefficient η is proportional^{to} the reciprocal value of the catalyser coefficient ρ (1,2).

$$\rho = L \cdot \sqrt{\frac{2k}{rD}} = \frac{1}{\eta} \quad (15)$$

where L = length of pores (cm)
 r = diameter of pores (cm)

For coke it is admissible to replace the length of pores by half the diameter of the lump $d/2$. Substitution of equations (14) and (15) into equation (2) leads to

$$\frac{1}{m} \frac{dx}{dt} = 0.5 c_0 \frac{1}{d} \sqrt{2 r D k} \quad (16)$$

As, according to equations (12) and (13), the reaction speed k rises much more rapidly than the diffusion speed D with the temperature,

$$\frac{dx}{dt} \propto e^{-\frac{E}{2RT}} \quad (17)$$

This is to say that in the case of pore diffusion the activation energy is reduced to half its value. In figure 2 this is schematically represented by the straight line within range II.

1.5. Boundary film diffusion

If the reaction speed continues to increase with rising temperature, the conversion is restricted to the external surface of the fuel. Around the piece of coke forms a boundary film through which the gasifying agent will diffuse towards the place of the reaction. Under these conditions the reaction speed mainly depends on this diffusion process which is governed by Fick's first law:

$$\frac{dx}{dt} = - D F \frac{dc}{d\delta} \quad (18)$$

where F = external surface of the coke (cm^2)
 δ = distance from the coke surface (cm)

In the boundary layer the concentration shows a linear decrease:

$$\frac{dc}{d\delta} = - \frac{c_0}{\delta} ; \quad c = \frac{c_0}{\delta} \delta \quad (19)$$

Substitution into equation (18) leads to

$$\frac{dx}{dt} = D \cdot F \cdot \frac{c_0}{\delta} \quad (20)$$

The determination of δ is an aerodynamic problem which can be solved as follows: The transfer of heat on surfaces is governed by the general law:

$$\frac{dq}{dt} = \alpha \cdot F \cdot \Delta T \quad (21)$$

where q = quantity of heat (cal)
 α = coefficient of heat transfer ($\text{cal}/\text{cm}^2 \text{ sec}^\circ\text{C}$)

On the other side the flow of heat in a layer can be expressed as follows:

$$\frac{dq}{dt} = \lambda \cdot F \cdot \frac{dT}{d\delta} \quad (22)$$

where λ = thermal conductivity (cal/cm sec °C)

According to equation (19), the temperature gradient $\frac{dT}{d\delta}$ is constant

as well as $\frac{dc}{d\delta}$; thus,

$$\frac{dq}{dt} = \lambda \cdot F \cdot \frac{\Delta T}{\delta} \quad (23)$$

Division of equation (23) by equation (21) leads to the next equation from which the thickness of the boundary layer δ can be determined.

$$1 = \frac{\lambda}{\alpha} \delta ; \quad \delta = \frac{\lambda}{\alpha} \quad (24)$$

From many measurements the ratio $\frac{\alpha}{\lambda}$ is known for pieces of coke in a

free stream of gas, as well as for coke grains in layers and fluidized beds; as a rule the following basis is assumed:

$$\bar{Nu} = b \cdot Re^a \quad (25)$$

where \bar{Nu} = Nusselt's number

$$\left(\frac{\alpha \cdot d}{\lambda} \right)$$

Re = Reynolds number

$$\left(\frac{w \cdot d}{\nu} \right)$$

d = coke diameter

a and b = constants which are independent of the conditions of flow (cm/sec)

ν = kinematic viscosity

By substituting into equation (24) the value of $\frac{\alpha}{\lambda}$ obtained from equation (25), we get the thickness of the boundary layer δ whose value is substituted into equation (20):

$$\frac{dx}{dt} = D \cdot F \cdot \frac{b \cdot c_0}{d} \cdot Re^a \quad (26)$$

With sufficient accuracy the kinematic viscosity ν can be assumed to be equal to the diffusion speed D , whose dependency upon the temperature is expressed by equation (13). Using a shape factor f , the external sur-

244.

face of the mass of coke (m) can be calculated from the equation

$$F = \frac{6 f m}{\rho d} \quad (27)$$

where F = shape factor
 ρ = apparent density of the piece of coke (g/cm^3)

To derive c_o from the standard concentration c_{No} , the temperature T and the pressure p have to be taken into account as usually:

$$c_o = c_{No} \frac{273 p}{T 760} \quad (28)$$

Taking into account equations (13), (27) and (28) we obtain from equation (26) the final formula:

$$\frac{1}{m} \frac{dx}{dt} = 2.16 f b D_o^{1-a} \frac{c_{No}^p}{\rho} d^{a-2} T^{0.8 - 1.8a} \quad (29)$$

In practice, the power a is about 0.5, so that the final formula in most cases reads as follows:

$$\frac{1}{m} \frac{dx}{dt} = 2.16 f b \sqrt{D_o} \frac{c_{No}^p}{\rho} \frac{1}{d \sqrt{d}} \frac{1}{T^{0.1}} \quad (30)$$

In the range of boundary film diffusion the dependency upon the temperature T is almost negligible, as appears from the horizontal stretch of the curve in range III (see fig. 2). The proportionality to $1/d^{1.5}$ reflects the great importance of the piece size in gasification processes at very high temperatures.

1.6. Dependency on the conditions of gasification

Practically, each range of reaction is characterized by a straight line in the Arrhenius diagram, the three straight sections being linked together by shorter or wider arches. If the conditions are changed, the straight lines are shifted, as will be shown in detail in the light of the three final equations, applicable to the three ranges, viz. (2), (19), and (30).

In the range of chemical reaction the particle size d is not influential upon the intensity of gasification. In the other ranges crushing of the coke leads to a higher intensity of gasification; in fact, in range II the way of diffusion up to the internal surface is reduced, whereas in range III the reactive external surface is enlarged. In the Arrhenius diagram (Fig. 3) the straight lines show a parallel upward displacement with decreasing particle size in the range II and III, whereas the transition zone between range I and II is shifted to the left, i.e. towards higher temperatures.

In ranges I and II the increase in the internal surface O entails a proportional intensification of gasification. In range II, where CO_2 is completely converted on the external surface, the internal surface does not play any part. In the Arrhenius diagram (Fig. 4) the straight lines show a parallel upward displacement with increasing surface O in ranges I and II, and the transition from range II to III is shifted to the right.

The speed is influential upon the decrease in CO_2 concentration during the passage through the layer of coke. Only for this reason, not directly the intensity of gasification is influenced by the speed of flow in ranges I and II. In range III, however, the speed of flow does influence the thickness of the adhering boundary layer. Here, a decrease in the boundary layer thickness results in a steeper gradient of concentration, in stronger boundary film diffusion and in a greater intensity of gasification (Fig. 5).

2. Measurements

2.1. Apparatuses

2.1.1. Gas-analytical method

For determining the reactivity of fine-grained coke we have used an apparatus (Fig. 6) which differs only slightly from that designed by Koppers and Jenkner (15-17). Recent experiments of Dahme and Junker (18) as well as of Hedden have confirmed the usefulness of this arrangement and have made it possible for conclusions to be drawn from the results with regard to the kinetics of reaction (19). The measuring method (20) may be briefly described as follows:

Analytically pure CO_2 flows at a speed of $2.5 \text{ cm}^3/\text{sec}$. through a reaction tube 20 mm in diameter. This tube is blown from quartz, the coke sample is resting upon a frit. In our tests the weight of the coke in the tube was 2.5. or 5 g. The gas flows downstream through the layer of coke and leaves the reaction zone through the frit. Through a pipe the outgoing gas flows into the analyser, viz. an azotometer, which has been adapted to the special purpose. In many cases an infra-red analyser was used. The oven is designed in such a way that the reaction temperature is reached after 10 minutes and the first measurement can be carried out after 15 minutes. The temperature is measured 10 mm above the frit with a platinum-rhodium couple.

2.1.2. Measurements on lumps of coke

For the determination of the intensity of gasification of lumpy coke up to temperatures of 1500°C an apparatus has been developed (see Fig. 7) which is not based on the principle of gas analysis but on the gravimetric determination of the loss of weight. The samples used in this method, are coke cylinders 40 mm high and 20 mm in diameter. A ceramic tube is suspended from a balance which records the time and the loss of weight. Through the tube a platinum-rhodium couple is introduced into the coke sample. This arrangement makes it possible to continuously observe the temperature of reaction in the coke sample during

weighing. Because of the endothermic reaction, this temperature differs from the temperature of the gas; at high temperatures the difference may reach values of some 50 °C. The throughput of gas is 400 l/h for each measurement. This means that the concentration of CO in the outgoing gas is only small and negligible in the calculation.

2.2. Measuring results

Our reactivity measurements were preceded by investigations intended to determine the influence of different factors upon the measuring accuracy.

2.2.1. Material used and sampling method

The electrode graphite used in our tests was ash-free, and thanks to its high graphitizing temperature it could be looked upon as a good primary material for the measurements intended. Microscopical determination of the pore volume and the pore structure, however, revealed significant differences from which an influence upon the reactivity was to be expected. In fact, the values found varied within the following limits:

Porosity:	19.3 to 29.3 %
Average pore size:	14 to 19 μ
Number of pores per mm:	12 to 16

The electrode graphite samples were received from the producer in form of cylinders 20 mm in diameter. For the tests they were cut to size, 40 mm long. The granular samples were obtained by grinding several cylinders.

Particularly careful sampling was required for the metallurgical coke which had been made in a semi-industrial coke oven at a heating flue temperature of 1300 °C; in fact, wide fluctuations in the properties of the individual pieces of coke have to be expected even if they come from the same charge. The coke was dry-quenched in an air-tight chamber; its ash content was 8.08 %. The sampling method was as follows: A representative sample was taken from about 150 kg of coke; this sample was crushed and screened into two fractions 3 - 2 mm and 1 - 0.5 mm. From the remaining coke long lumps were selected, extending from the wall of the coke oven up to its center, and well-preserved at both ends. Part of these lumps were cut into pieces so that the outer, the middle and the inner ends were separately available and could be ground and screened into the same fractions as the mean sample. From the remaining lumps cylindrical samples were prepared, by means of a 20 mm hollow drill, and these cylinders were grouped, according to their position in the big lumps. The number of utilizable cylinders was rather limited on account of the cracks and fissures in the coke.

2.2.2. Weight loss during high-temperature treatment in nitrogen.

It is well known that coke will lose weight in inert atmosphere at temperatures higher than the carbonizing temperature. It was necessary for us to determine the amount of this loss in order to estimate the weight of the error introduced into the gravimetric measurements. In

Fig. 8 the loss of weight is plotted against the time for different temperatures. Between 900 °C and 1500 °C the curves are similar. After a steep rise during the first 30 minutes they become flatter. The loss of weight reaches considerable values, e.g. 10 % at 1500 °C after 20 hours. The qualitative explanation of this phenomenon is very simple. Apart from after-carbonization at temperatures beyond the carbonization temperature, adsorbed gases are liberated, although to a lesser degree, volatile inorganic ash components are distilled, and oxides in the ash are reduced by the surrounding carbon, especially at high temperatures. A quantitative determination of these different concomitant phenomena, however, seems hardly possible.

2.2.3. Temperature difference between gas and coke

In the course of our preliminary tests we found out that the temperature of the coke which had been attained in nitrogen fell off when carbon dioxide was fed to the apparatus. This fact is due to the endothermic character of the gasification reaction which consumes more heat than the quantity supplied to the coke by radiation from the wall of the oven and, to a lesser degree, by convection. With decreasing temperature of the coke, the heat transfer is improved, and at a certain temperature difference radiation will be sufficient to make up for the heat consumed by the gasification reaction. Fig. 9 gives the results of measurements which show the difference of temperatures reigning in the ambient gas on the one side and in the core of the coke pieces on the other at different reaction temperatures.

Up to 1100 °C no perceptible difference is to be observed, as the heat required for the reaction at the given temperature is supplied by radiation. With rising temperature, however, the reaction speed increases rapidly and the heat consumption of the reaction will increase to such a degree that a considerable temperature difference does appear. Beyond 1400 °C the curve is flattening out which indicates that the reaction has reached range III where the gasification intensity becomes a function of the boundary film diffusion and is, according to equation (30), practically independent of the temperature.

2.2.4. Burn-off as a function of time

The burn-off in CO₂ as a function of time was determined on cylindrical samples, using only the gravimetric method. It was found that at the same temperature and after the same time the loss of weight of the graphite cylinders differed very much. This is to be explained by the large differences of the pore volume, as mentioned above. In range III where the internal structure of the graphite cylinders is no longer influential upon the gasification reaction, these differences disappear.

As expected, the differences of burn-off were still larger in the tests on coke cylinders. But here, as before, we could observe the trend that at high temperatures the burn-off after the same lapse of time was constant, no matter whether the samples had been taken from the middle of the chamber or from the wall of the oven. At lower temperatures it is always the samples taken from the middle of the chamber that show the highest loss of weight.

A comparison of the burn-off curves of graphite and coke leads to the result that for graphite the loss of weight per unit of time remains almost constant even after gasification of 50 % of the material. In case of coke, a slow-down of the loss of weight per unit of time with progressing combustion is clearly evident, at least up to 1200 °C. It is most of all the coke samples taken from the middle of the chamber that show this trend.

2.2.5. Reactivity of lumps between 900 and 1500 °C.

From the burn-off curves the reaction speed can be calculated using equation (9). In Fig. 10, the values calculated in this way have been marked on an Arrhenius diagram similar to that shown in the first part of this paper.

The lower curve represents the measurements made on graphite, the upper one on coke. The diagram shows the reaction speed at different stages of burn-off, ranging between 10 and 50 %. The lower section of the graphite curve, up to 1200 °C, is a straight line. From the gradient we can calculate the activation energy for the purely chemical reaction in range I; its value is 65 kcal/Mol. After a short arch the curve adopts again the form of a straight line starting at 1400 °C with a flat gradient. The activation energy in the range of pore diffusion, as calculated from the gradient of this second straight part, amounts to 34 kcal/Mol. This value agrees fairly well with the theoretical postulates according to equation (17), from which it is to be expected that the activation energy in this range should be 50 % of what it amounts to in range I. As for the conditions in the range of boundary film diffusion, the measurements made do not permit any conclusions to be drawn.

The upper curve of Fig. 10 shows the results of measurements made on coke. In the lower part the individual values found by this method are so widely dispersed that nothing can be said about the activation energy, but we come back to this question later on. It is interesting to note that this wide dispersion of the individual values disappears more and more. This proves that the chemical reactivity of the coke samples, taken from the different parts of the oven, differs very much. In fact, the lumps taken from the middle of the oven show a higher reactivity than those taken from the wall. This is to be explained by the fact that the final carbonization temperature reigned much longer near the wall of the oven which entails a higher degree of gas emission and a decrease in reactivity.

With rising temperature the wide dispersion of the values measured disappears; beyond 1350 °C all points are close together and differences caused by the position of the samples in the coke oven are no longer noticeable. The conclusion to be drawn from this observation is that with rising temperature the importance of the chemical properties decreases more and more, whereas structure and external surface become the dominating factors. This statement is confirmed by a comparison of the graphite and the coke curves which approach with rising temperature. In the pore diffusion range whose starting point for electrode graphite is about 100 °C higher than in the case of metallurgical coke, the ratio of the gasification intensities goes down to 1.6 at 1300 °C. At this temperature the internal structure of the coke becomes the decisive factor. Above 1300 °C the ratio of the gasification intensities of both materials is about 1.5 on the average, which corresponds to the difference.

of their apparent densities. It seems that the measurements were carried out not yet entirely within the limits of range III, i.e. the zone of pure boundary film diffusion.

2.2.6. Reactivity in dependency upon the position of the coke in the oven

In Fig. 11 we have reproduced the reactivity values of the fine-grained mean samples from the three zones of the oven as determined by the coincide gas-analytical method. It is understandable that the values obtained from these mean samples do not show the dispersion which was observed with the cylindrical samples. Here all the values measured coincide with the Arrhenius lines; this is true of the 3 to 2 mm as well as of the 1 to 0.5 mm size fraction. In both cases the reactivity increases from the wall of the oven towards the centre. In the preceding chapter it was already said that this is due to the final temperature of the coke, and to the length of time during which the final temperature has been effective. From the wall of the oven up to its centre line the reactivity increases by more than 100 %. The results obtained from the sample representing the whole of the charge do not agree with the mean value of the samples representing the three different zones of the coke oven. This leads to the conclusion that there is no linear relation between reactivity and the position of the coke in the oven. As the Arrhenius lines are parallel, the activation energy is the same for all measurements, irrespective of the position of the coke in the oven, namely 67 kcal/Mol.

2.2.7. Relation between reactivity and coke size

The theoretical considerations have made it clear that in the range of purely chemical reaction, i.e. range I, diffusion need not be taken into account. This is to say (Fig. 12) that the coke size does not matter, because below a certain temperature the gasifying agent (CO_2) will reach the whole reactive surface of the coke pieces, even of different diameter, without any perceptible decrease in concentration as compared with the ambient gas.

The experimental values confirm the conclusions reached on theoretical grounds. In Fig. 10 we have marked on the graphite curve the results obtained from both cylindrical samples and the granular samples 3 - 2mm. In the range of temperatures examined (1000 - 1100 °C) the values agree perfectly. For metallurgical coke Fig. 12 shows that the reactivity measured on lumps and on granular samples is the same up to 1050 °C. Above this temperature the cylindrical samples show the influence of the pore diffusion which, in the case of granular material would only appear after a further rise of temperature. These results, however, are only valid for coke originating from the chamber wall. Similar measurements on lumps from the centre of the oven led to a wider dispersion of the results so that it is not possible to draw exact conclusions from them.

In Fig. 11 we have also given the results of measurements made on granular coke of different size. Here the finer size fraction 1 - 0.5mm, does not show the same reactivity as the 3 - 2 mm fraction. This observation is no argument against the theory; it finds its explanation in the treatment after sampling. The finer fraction will always be composed

of unhomogeneous material. Crushing and grinding leads to a concentration of high-ash and weaker particles, and differences are unavoidable. Further investigations have shown that to all appearance the ash content is an important factor.

2.2.8. The influence of ash on reactivity.

In a large series of tests which are still going on, we are studying the influence of the ash content and the ash components on the reactivity of the coke. Very clean coal (ash content under 0.5 %) was coked with selected additions. It was found that Boudouard's reaction is accelerated by iron oxides and CaCO_3 , whereas SiO_2 will slightly inhibit the reaction. Very efficient is Na_2CO_3 . The following table shows the first results of reactivity tests made on very clean coke, with or without additions, at a temperature of 1050°C ; the coking temperature was 1150°C in all cases.

Material	Addition	k_m at 1050°C ($\text{cm}^3/\text{g sec}$)
Very pure coke	-	0.485
"	SiO_2	0.304
"	Fe_3O_4	0.825
"	CaCO_3	2.78
"	Na_2CO_3	7.55

For the time being we are not able to say whether the large differences between these values are due to catalytic or other influences.

Literature

- 1) Handbuch der Katalyse I, G.-M. Schwab, Wien, Springer-Verlag (1943)
- 2) Catalysis Vol. 2, Paul H. Emmett, Reinhold Publ. Co., New York (1955)
- 3) Placed to the Meeting of Experts on the Reactivity of Coke and semi-coke of the ECONOMIC COMMISSION FOR EUROPE COAL COMMITTEE (1962)
- 4) H. Echterhoff, K. G. Beck und W. Peters, Blast Furnace, Coke Oven, and Raw Materials Proceedings, Philadelphia, Vol. 20 (1961) S. 403-414.
- 5) W. Peters und H. Echterhoff, Blast Furnace, Coke Oven, and Raw Materials Proceedings, Philadelphia, Vol. 20 (1961) S. 158-170.
- 6) K. Hedden, Dissertation Göttingen (1954)
- 7) E. Wicke, K. Hedden, Z. Elektrochem. 57, 636/41 (1953)
- 8) E. Wicke, Fifth Symposium on Combustion, Univ. of Pittsburgh, 1954, Reinhold Publ. Co., New York, 1955, 245/52
- 9) K. Hedden, Brennstoff-Chem. 41, 193/224 (1960)
- 10) C. N. Hinshelwood, J. Gadsby, K. W. Sykes, Proc. Roy. Soc. (London) A 187, 129/51 (1946)
- 11) J. Gadsby u.a., Proc. Roy. Soc. (London) A 193, 357/76 (1948)
- 12) F. J. Lang, K. W. Sykes, Proc. Roy. Soc. (London) A 193, 377/99 (1948)
- 13) K. Hedden, E. Wicke, Proc. Third Conference on Carbon, Buffalo (1957)
- 14) W. Peters, G.-W. Lask, Brennstoff-Chem. 42, 84/90 (1961)
- 15) H. Koppers, A. Jenkner, Arch. Eisenhüttenw. 5, 543/547 (1931/32)
- 16) H. Koppers, A. Jenkner, Koppers-Mitt. 1, 15/16 (1922)
- 17) H. Koppers, VDI-Zeitschrift 66, 651 (1922)
- 18) A. Dahme, H. J. Junker, Brennstoff-Chem. 36, 193/224 (1955)
- 19) W. Peters, Glückauf 96, 997/1006 (1960)
- 20) W. Peters, G.-W. Lask, Brennstoff-Chem. 42, 323/328 (1961)

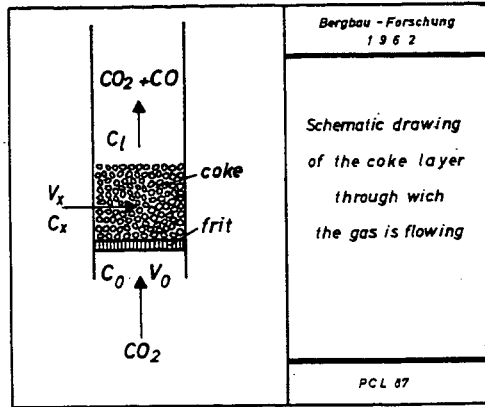


Figure 1

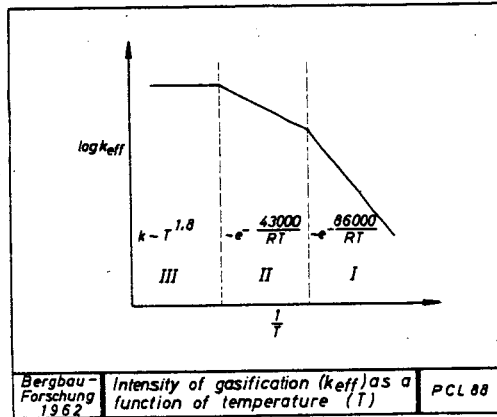


Figure 2

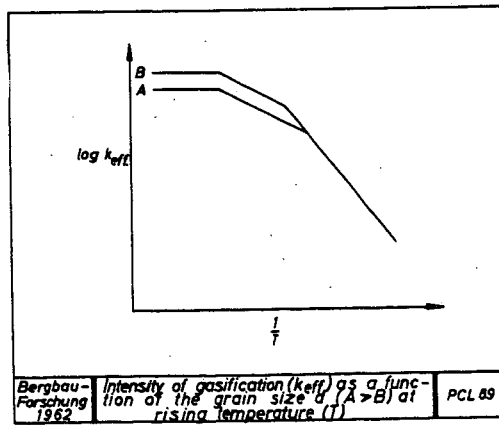


Figure 3

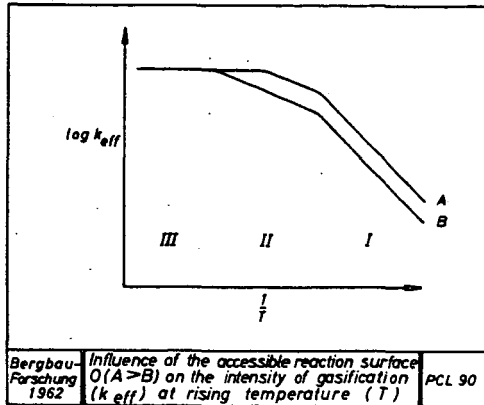


Figure 4

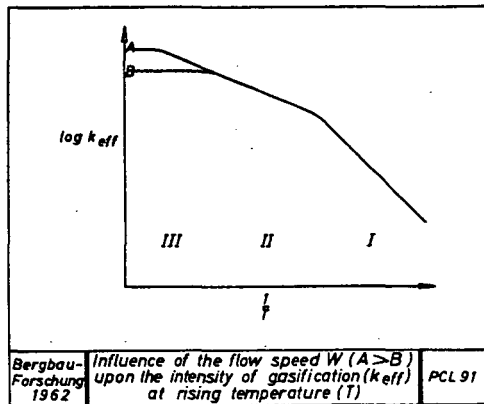


Figure 5

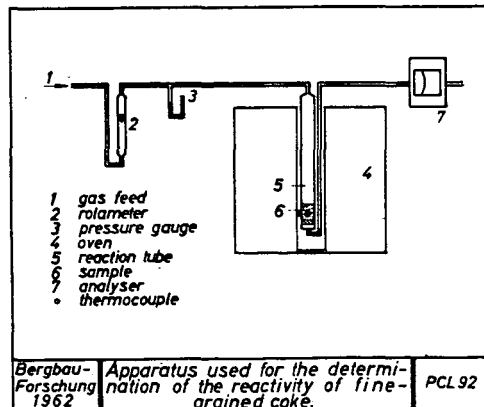


Figure 6

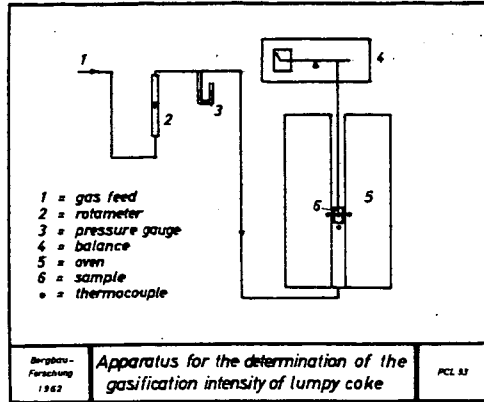


Figure 7

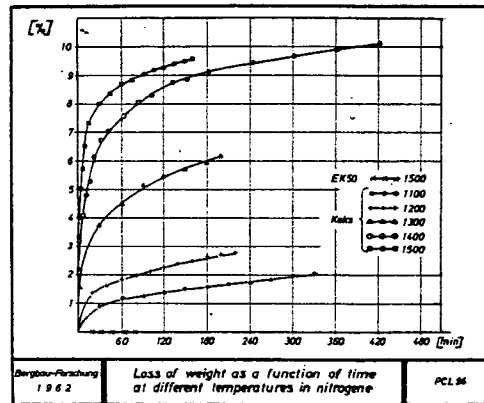


Figure 8

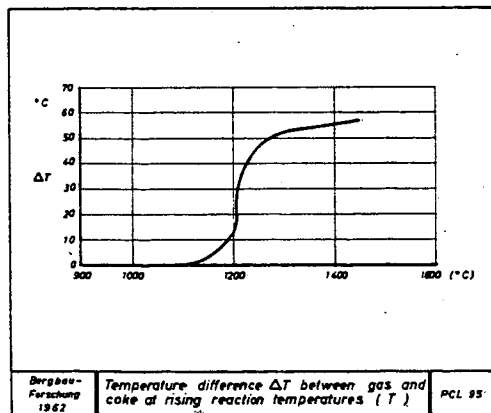


Figure 9

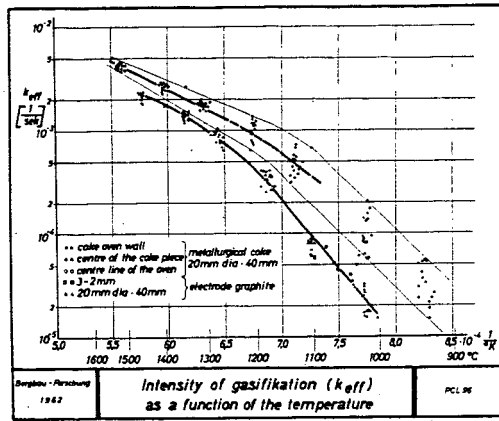


Figure 10

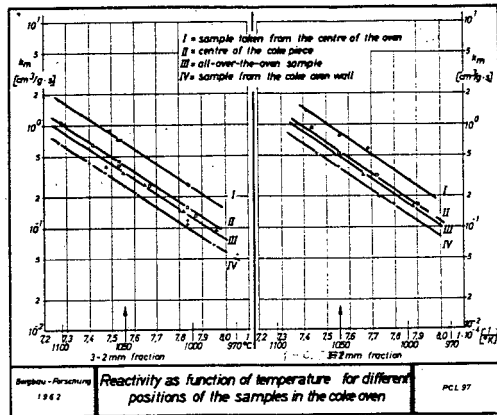


Figure 11

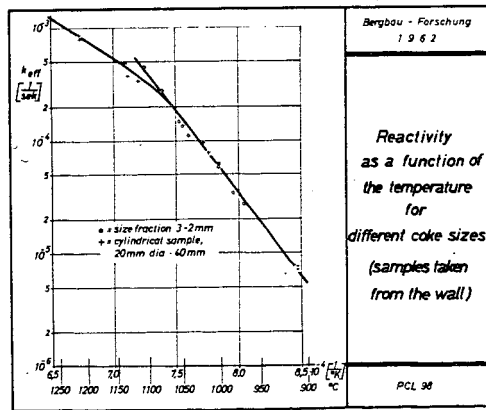


Figure 12

RELATION OF COKE STRUCTURE TO REACTIVITY

by

N. Schapiro and R. J. Gray
United States Steel Corporation
Applied Research Laboratory
Monroeville, Pa.

Introduction

The question of what criteria should be used to determine the relative quality of coke for blast-furnace use has never been satisfactorily nor completely answered. The size, strength,¹⁾* porosity, and reactivity of coke are certainly important properties that should be considered as criteria of coke quality. It is not within the scope of this paper to discuss the relative importance of the various properties that affect the performance of coke in the blast furnace; all these properties are, however, related to the structure of coke.

Previous investigations²⁻⁸⁾ have evaluated quantitatively the structural properties of coke in terms of its characteristics and behavior in specific uses. Also, qualitative observations,^{7,8)} have been made of differences in the optical properties of the wall material of cokes. These optical properties are related to the stages in crystallinity of the carbon from amorphous to graphitic forms. In carbon the crystal structure causes directional variations in the transmission or reflection of polarized light (anisotropism). Investigations conducted at the Applied Research Laboratory have shown that coke structure as well as the order of crystallinity of the carbon in the coke can be determined by reflectance measurements. When the polished surface of a piece of epoxy-impregnated coke is scanned with a reflectance-measuring microscope, areas representing the coke walls are high in reflectance compared with the filled pore areas of low reflectance. Also, the intensity of the reflectance from a wall is dependent on the rank of coal from which the particular coke was produced and on the temperature at which it was produced. Formerly, a manual method of traversing coke was used to obtain qualitative measurements of pore and wall areas. This time-consuming method required the continuous presence of the operator, and a constant speed could not be maintained. These difficulties were eliminated by the construction of the automatic traversing device, which permits the scanning of a specimen at a constant rate and thus makes possible quantitative measurements.

As part of a general program to investigate the various properties of coke that could be delineated by the use of this traversing device, studies were conducted to determine whether a significant correlation could be obtained with the instrument between coke structure as indicated by pore volume and the reactivity of coke. Reactivity was chosen as the parameter because various workers in the field⁹⁻¹²⁾ have reported it to be a function of surface area and/or porosity, both of which properties are concerned with structure.

Since coke-sample preparation is a rapid routine procedure and the reflectance-scanning microscope is automated, it may be possible to obtain much valuable information on the properties of cokes in a single operation.

Experimental

The laboratory cokes used in this study were prepared by carbonizing a variety of different-rank coals used in various coal blends in U. S. Steel operations. These coal samples were crushed to minus 8 mesh and placed in 1-1/4- by 1-1/2-inch stainless-steel cylinders, which were then put into a preheated (1850-F) electric furnace in an inert atmosphere. After the carbonized coals attained the temperature of the cylinder at 1850 F, they were soaked for an additional two hours and then cooled in nitrogen gas.

* See references

The cokes so produced were cut into halves, which were then impregnated with epoxy resin containing an opaque pigment. The low-reflecting resin filled the coke pores, providing contrast with the high-reflecting coke walls. The coke surface impregnated with the resin was then polished for microscopic examination.

The commercial cokes used in the study were obtained from U. S. Steel Corporation coke plants as complete fingers (one-half oven pieces) from one oven push. Fingers were selected because they represented the extremes in the time and temperature conditions under which the cokes were produced. From these fingers, portions representing the wall, the center, and the inner end were removed, impregnated, and polished in the manner described for the laboratory-produced cokes.

The individual coke specimens prepared for the microscope study were placed on the stage of the microscope and levelled optically to assure uniform focus throughout. The stage of the microscope is driven automatically and the number and length of traverses is automatically controlled. The x motion or principal direction of travel was set to move the specimen at the rate of 5 microns per second (18 mm per hour), and the y motion was set at 4.5 degrees. The instrument arrangement used in the automatic recording of coke microstructure is shown in Figure 1. A photomultiplier tube is attached to the monocular tube of the microscope and is used to sense reflectance differences. The microscope field of view exposed to the photomultiplier is a circular area with a diameter of 12 microns. The photomultiplier photometer is used in conjunction with a recorder that charts the reflectance differences. The chart moves at the speed of 0.85 mm per second (3,048 mm per hour). Thus each millimeter on the specimen surface is represented by 169.3 mm on the recorder chart. In this study the wall and pore areas and the relative height of the reflectance peaks are measured by counting the actual areas from the recorder graphs. This method is adequate to demonstrate the technique in this stage of development. However, for future work an integrator will be installed that will make this calculation automatically.

The measurement of the extent of reaction (weight loss) of the solid coke with CO_2 at a controlled temperature is defined as reactivity.* The conditions used for each determination were (1) temperature, 2,000 F; (2) atmosphere, 100 percent CO_2 at 2.5 liters per minute; (3) particle size, minus 4 plus 6 mesh; and (4) sample weight, 1.5 grams (± 0.0050 gram). A thermogravimetric unit was used to determine the reactivity of the coke samples. Each crushed coke sample was placed on a basket with an 80-mesh platinum screen bottom and suspended in the uniform-temperature zone of the platinum-rhodium-wound furnace. The platinum basket was suspended from the left pan of an Ainsworth balance. The balance sensed the changes at the conditions in the furnace, and a Bristol recorder connected to the balance recorded the weight change as a function of time. The weight loss was calculated on the dry, ash-free basis (daf) and corrected for the incremental loss of volatile matter. Because the initial portion of the weight loss-time curve, which is essentially linear, was considered to be the most significant, the weight loss in 30 minutes was used as a parameter of reactivity.

Results and Discussion

Photomicrographs of surface sections of the laboratory cokes prepared from four different ranks of coal used in various U. S. Steel coal blends for metallurgical-coke production are shown in Figure 2 to illustrate structural differences in the cokes; it can be observed that the coke produced from Sunnyside coal contains very thin walls and large pore area, whereas the cokes from higher-rank coals such as Pittsburgh and Pratt contain thicker walls and less pore area. However, cokes produced from Pocahontas No. 3 coals approach Sunnyside in pore volume. Photomicrographs of the various forms of carbons in these same coke

* The reactivity data used in this presentation were supplied by K. K. Kappmeyer of the U. S. Steel Applied Research Laboratory.

samples at higher magnification are shown in Figure 3 to indicate the relation of carbon forms in coke to the rank of the coal used in its preparation. The cokes from high-rank coals such as Pocahontas No. 3 under polarized reflected light show extreme anisotropic effects with the appearance of a sinuous structure and high reflectance. The cokes from lower-rank coal such as Sunnyside show carbon forms that are isotropic and have low reflectance.

In the laboratory cokes, the degree of anisotropism was used as a measure of the types of carbon present. Optically anisotropic substances transmit or reflect light in unequal velocities in different directions. Cokes displaying different degrees of anisotropism appear smooth, granular, or sinuous in polarized light. Therefore, the degree of anisotropism and the surface texture of the coke are used to identify the stage of coalification of the coal from which the coke was produced.

Since organic inerts do not become fluid during carbonization, they remain virtually isotropic in coals of all ranks. Thus the amount of organic inerts can be determined by the isotropism in cokes produced from coals of all ranks except the marginal-coking high-volatile coals. Figure 4 shows photomicrographs of inerts incorporated into the coke walls.

A graph of the reflectance and relative anisotropism of the principal carbon form from each of the seven laboratory cokes is shown in Figure 5. The samples are arranged in the order of increasing rank of the coals from which they were derived. The maximum and minimum reflectance of the subject material was measured by revolving the sample on a microscope stage through 360 degrees with the polarizer set at 45 degrees. The anisotropism of the carbon materials increases as the spread between the maximum and minimum reflectance increases as shown by the peaks and troughs. Thus, the reflectance measurements provide a quantitative determination of anisotropism. Furthermore, the graph shows that the maximum reflectance is proportional to the amount of anisotropism.

When polished surfaces of the various cokes are traversed at a constant rate with a continuously recording reflectance microscope, a pattern is obtained that shows the low-reflecting pore areas and the high-reflecting wall area. The intensity or magnitude of the reflectance is dependent upon the rank of the coal and carbonization conditions. Examples of the profiles obtained in traversing the coke surfaces of two cokes produced from high- and low-rank coals are shown in Figure 6. The approximate division between the wall and the pore area is displaced to the right of the vertical base line because of the occurrence of portions of both wall and pore area in the same field of view. These two profiles show the differences in structure and in the rank of the coals used to produce the cokes. The coke produced from Sunnyside coal has large pore areas, indicated by the large vertical spaces between the peaks. The reflectance is low, as indicated by the relatively short horizontal peaks. In contrast, the coke from Pocahontas No. 3 coal shows smaller but numerous pore areas, as indicated by the short vertical distance between the peaks. The reflectance is high, as indicated by the greater length of the horizontal peaks. The profiles thus obtained verify quantitatively the differences in structures observed in Figure 2 and the differences in the forms of carbon observed in Figure 3.

Since the objective of this phase of the program of characterizing coke was to establish whether relationship could be obtained between coke reactivity and the coke structure and carbon forms as obtained by reflectance measurements, seven samples of laboratory produced coke that had previously been tested for reactivity were analyzed for structure.

From the graphic profiles obtained, the pore volume of each of the cokes was calculated; and this value was then plotted against the rank of the coals used to produce the cokes. This plot is shown in Figure 7. The curve obtained was almost identical with the curve obtained by plotting the rank of the coals from which cokes were produced against the

reactivity of these same cokes as shown in Figure 8. Since both the reactivity of coke and the structure of coke are related in the same manner to coal rank, it was logical therefore to assume that the structure of coke, as defined by pore volume, would be related to the reactivity of the coke. The pore volume of these cokes was then plotted against the reactivity of the same cokes; the resulting curve is shown in Figure 9. This curve demonstrates that a strong relationship exists between the reactivity of coke and the structure of the coke as defined by pore volume, and that the reactivity is greatest in cokes from low-rank coals, least from medium-rank coals, and intermediate from high-rank coals.

This relationship between structure and reactivity was established on the basis of cokes produced from individual coals of different rank. To determine, therefore, whether the same relationship held for cokes produced from blends of different-rank coals (such as are normally used in making metallurgical coke), samples of U. S. Steel coke-plant cokes that are made from blends of two or more coals of different rank were analyzed. Photomicrographs of sections of the four cokes analyzed for structure are shown in Figure 10. Examination of these photographs indicates that plant coke A contains thin coke walls and large void areas and is similar to the coke from low-rank coals, which comprises 76 percent of the total coal blend at Plant A. In contrast, plant coke D shows thick cell walls and much less pore area. The carbon forms present in the commercial cokes are similar to those of the cokes made from individual coals making up the blends; they are shown in Figure 11.

Graphic profiles of these same four cokes obtained with the reflectance microscope are shown in Figure 12. Examination of these profiles indicates the difference in both structure and carbon forms of the various cokes. In general, the structure and carbon forms follow those of the cokes made from individual coals. For example, the cell structure of plant coke A is characterized primarily by thin walls and large pore area because of the large amount of low-rank coal in the blend.

When the reflectance is measured in a transect of a prepared coke surface, the carbons derived from the individual coals remain distinct so that the distribution, the size, and the structure of the individual carbon particles can be determined. In addition, the efficiency of the blending with reference to amount, size, distribution, and fusion characteristics of the individual carbon structures in the coke can be assessed.

Plotting the pore volume as obtained from the graphic profile against the reactivity of these same cokes, a relationship similar to that found for cokes from individual coals of different rank was obtained, see Figure 13. The data indicate that the cokes made from a preponderance of low-rank coals have the greatest pore volume and also the highest reactivity. Plant coke B exhibits both high reactivity and large pore volume because the coal blend consists of 40 percent low-volatile coal, which is of high rank and when used alone produces coke of relatively high reactivity. Plant coke C shows relatively low reactivity and smaller pore volume primarily because of the large amount of medium-volatile coal in the blend.

It is the opinion of the authors that an even better correlation would be obtained between pore volume and reactivity if the temperature at which the cokes were carbonized were taken into consideration. Plant coke D is carbonized at temperatures higher than those used at other U. S. Steel coke plants, whereas plant coke A is carbonized at the lowest temperatures. High final coke temperatures reduce reactivity, increase the reflectance of the coke walls, and may affect the relative proportion of the dense wall and more porous inner coke. For example, coke taken from the inner and outer portions of an oven at Plant D were analyzed for reactivity and pore volume. The inner oven coke, which is exposed to lower temperature and time at a given temperature than the cokes from the outer or wall portion of the oven, showed both higher reactivity and greater pore volume than the outer portion sample. The effects of temperature and time on coke structure thus appear significant and warrant further investigation.

Summary

This investigation has established a relationship between the reactivity property of coke and its structure as defined by pore volume. The structure and hence the reactivity of coke are dependent upon the rank of the coal from which the coke was produced. Low-rank coal produces coke having the highest pore volume and thus the greatest reactivity. As the coal rank increases, the pore volume and therefore the reactivity of the coke decreases to the minimum. High-rank coals produce coke of intermediate pore volume and reactivity. Blends of coals produce coke with pore volumes and reactivities dependent upon the rank and amount of the individual coals making up the blend.

The temperature and time also affect the pore volume and the reactivity of a particular coke. These effects will be studied and reported in the future.

References

1. C. G. Thibaut, "French Research on Coke in the Iron and Steel Industry," Institute de Recherches de la Siderurgie, 1957; pp. 1-13.
2. O. O. Malleis, "By-Product Coke Cell Structure," Industrial and Engineering Chemistry, Vol. 16, 1924; pp. 901-904.
3. H. J. Rose, "The Study of Coke Macrostructure," Fuel, Vol. 5, 1926; p. 58.
4. H. J. Rose, "Selection of Coals for the Manufacture of Coke," AIME Trans., Vol. 74, 1926; pp. 600-639.
5. H. Hoffman and F. Kuhlwein, "Rohstoffliche und verkokungstechnische Untersuchungen und Saarkohlen," Gluckauf, Vol. 71, 1934; pp. 625, 657.
6. J. Krajewski, "Microscopic Research on the Structures of Coke Produced from Various Polish Coals," Translated from Polish, Bulletin Instytutu Naukowo-Badawczego Przemyslu Weglowego, Report No. 37, 1948; pp. 1-25.
7. C. Abramski, "Zusammenhange zwischen Kohlenpetrographie and Verkokung," Troisième Congres Pour L'Avancement des Etudes de Stratigraphie et de Geologie du Carbonifere: Compte Rendu, Vol. 1, 1952; pp. 1-4.
8. C. Abramski and M. Th. Mackowsky, "Methoden und Ergebnisse der Angewandten Kokamikroskopie H. Freund, Handbuch der Mikroskopie in der Technik, Band II, Teil I, Umschau Verlag Frankfurt Am. Main, 1952; pp. 311-410.
9. Onusaitis and Yurevskaya, Zvest. Akad. Nauk USSR, Otdel, Tekh, Nauk 1949, 519.
10. Burden and Dove, Conf. on Sci. Use of Coal, Sheffield, 1958, E7-E13.
11. Zoja, Benuzsi, Cvei, Rev. Met. 57, 19 161, (1960).
12. Bastick, Comp. Rend. 240, 2524 (1955), Comp. Rend. 243, 1764 (1965), J. Chem. Phys. 58, 97 (1961).

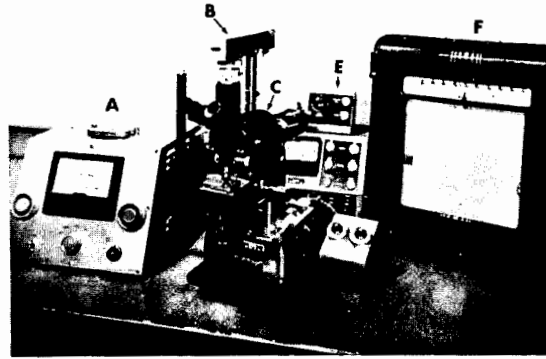


Figure 1. The equipment for automatic photometric scanning of coke specimens consists of a photometer (A), a photomultiplier sensing unit (B), an Ortholux microscope (C), an automatic stage-drive unit (D) and controls (E), and a strip-chart recorder (F).

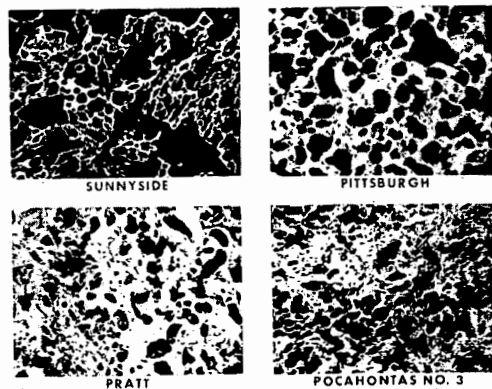


Figure 2. Coke from Sunnyside coal has very thin coke walls and much pore area, whereas coke from higher-rank coals such as Pittsburgh and Pratt has thicker walls and less pore area. Coke produced from the low-volatile Pocahontas No. 3 coal approaches that from the Sunnyside coal in that it contains much pore area. Surface sections of coke. Polarized reflected light, X50.

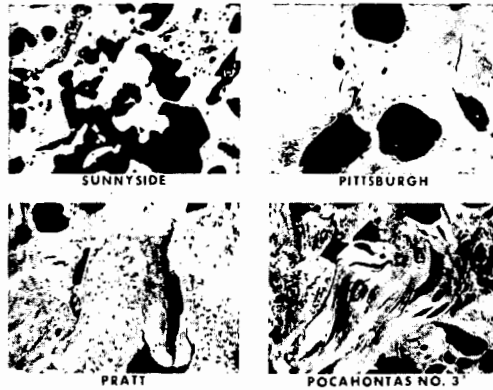


Figure 3. Sunnyside coke is low-reflecting and isotropic (smooth), whereas higher-rank coals such as Pittsburgh and Pratt produce cokes with high reflectance that show pin-point effects of anisotropism. The coke from the low-volatile Pocahontas No. 3 coal is highly reflectant and shows extreme ribbonlike anisotropism. Surface sections of coke. Polarized reflected light, X350.

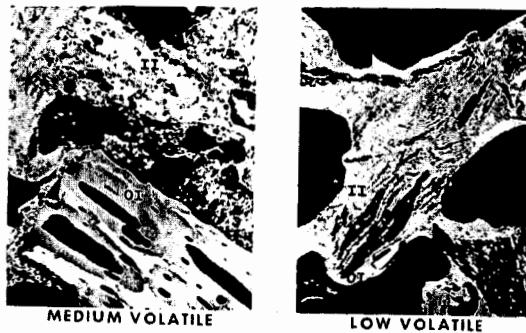


Figure 4. Organic inerts (OI) do not fuse during carbonization and remain virtually isotropic in coals of all ranks. Inorganic inerts (II) are easily recognizable in coke. Polarized reflected light, X350.

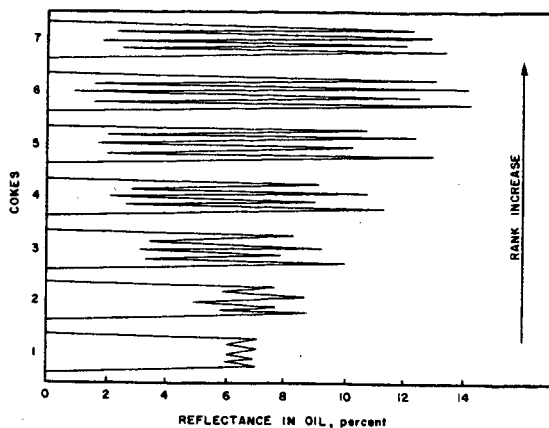


Figure 5. Reflectance in polarized light for one 360-degree revolution on a single carbon form in the following coke samples; arranged in order of increasing rank

1. Sunnyside	4. Mary Lee
2. Pittsburgh	5. Pratt
3. Pittsburgh	6. Pocahontas Nos. 3 & 4
7. Pocahontas No. 3	

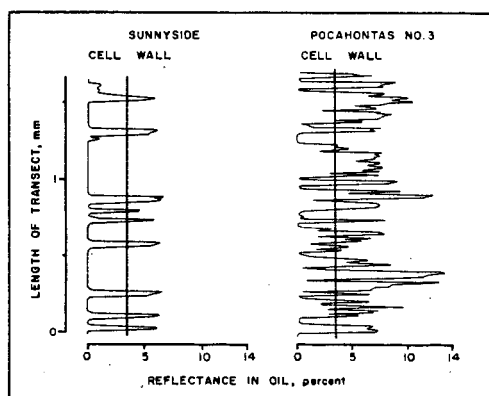


Figure 6. Graphic profile of indicated cokes showing (1) variations in reflectance of different carbon forms and (2) wall and pore areas.

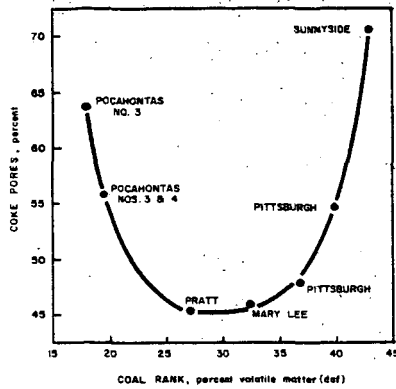


Figure 7. Relation of coke pores to the rank of the coal from which the coke was produced.

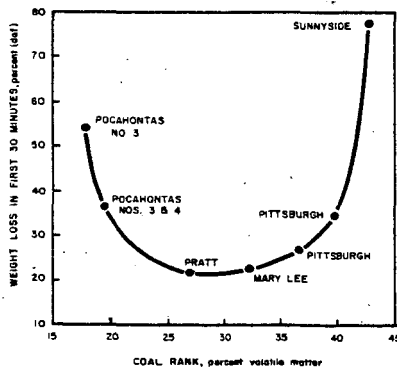


Figure 8. Relation of reactivity and coal rank for laboratory cokes.

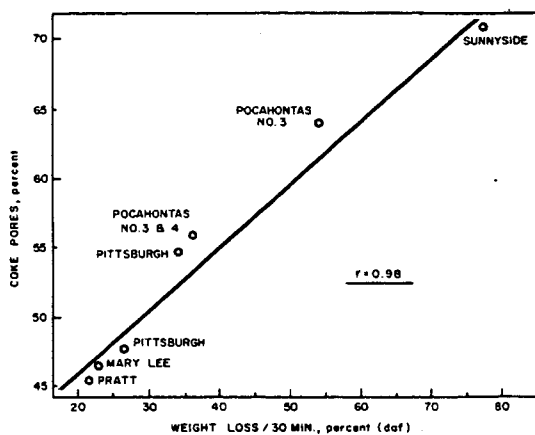


Figure 9. Relation of weight loss to coke pores at indicated conditions for laboratory cokes.

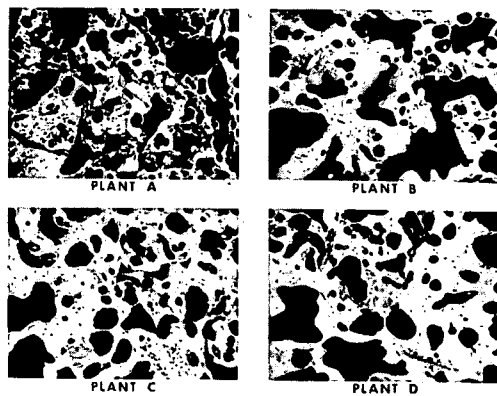


Figure 10. The coke from Plant A contains thin coke walls and much pore area, whereas the cokes from Plants B, C, and D show thickening coke walls and decreasing pore area. Polarized reflected light, X50.

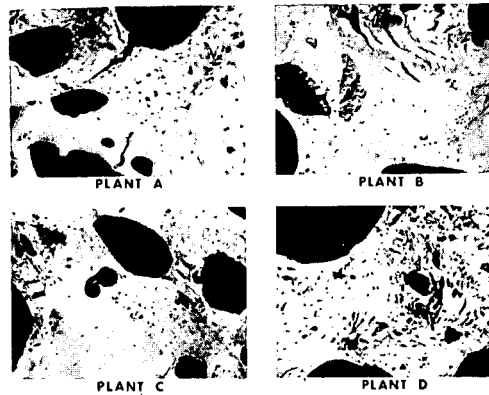


Figure 11. The plant cokes were produced from blends of either high- and low-volatile coals or high-, medium-, and low-volatile coals. The carbon forms representing the different coals are illustrated by the anisotropic effects. The coke from high-volatile coal is isotropic (smooth), the coke from medium-volatile coal shows pin-point anisotropism, and the coke from low-volatile coal shows ribbonlike anisotropism. Polarized reflected light, X350.

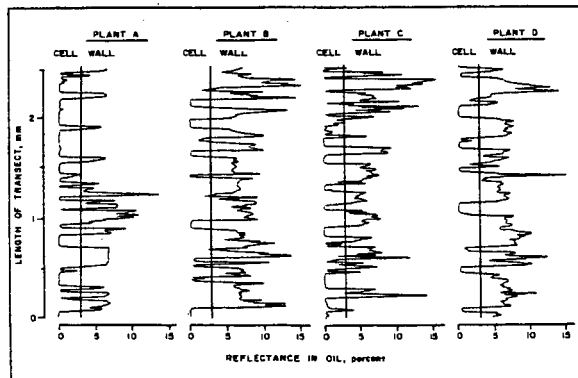


Figure 12. Graphic profiles of plant cokes showing (1) variations in reflectance due to different carbon forms and (2) wall and pore areas.

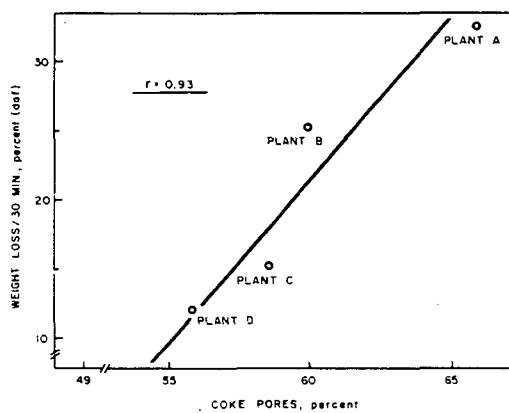


Figure 13. Relation of weight loss to coke pores at indicated conditions for plant cokes.